

# Durham E-Theses

---

## *Branes and applications in string theory and M-theory*

PICHET VANICHCHAPONGJAROEN

### How to cite:

---

VANICHCHAPONGJAROEN, PICHET (2014) Branes and applications in string theory and M-theory. Doctoral thesis, Durham University.

### Use policy

---

The full-text may be used and/or reproduced, and given to third parties in any format or medium, without prior permission or charge, for personal research or study, educational, or not-for-profit purposes provided that:

- a full bibliographic reference is made to the original source
- a <https://etheses.durham.ac.uk/id/eprint/10552/> is made to the metadata record in Durham E-Theses
- the full-text is not changed in any way

The full-text must not be sold in any format or medium without the formal permission of the copyright holders.

Please consult the [full Durham E-Theses policy](#) for further details.

# Branes and Applications in String Theory and M-theory

Pichet Vanichchaponjaroen

A Thesis presented for the degree of  
Doctor of Philosophy



Centre for Particle Theory  
Department of Mathematical Sciences  
University of Durham  
England

February 2014

*Dedicated to*

My Parents

# **Branes and Applications in String Theory and M-theory**

**Pichet Vanichchapongjaroen**

Submitted for the degree of Doctor of Philosophy

February 2014

## **Abstract**

This thesis discusses branes in string theory and M-theory. In chapter 1, we present background materials. In chapters 2 and 3, we discuss an application of a D3/D7 model in the framework of gauge/gravity duality, which uses the results of a gravity theory calculation to obtain informations about the corresponding gauge theory. Gauge/gravity duality is usually studied in a non-compact space. This thesis, however, focuses on the duality in a compact space. In chapter 2, we study a strongly coupled gauge theory in a compact space. We find that a homogeneous ground state is unstable at a sufficiently large isospin chemical potential. We then construct a new ground state which corresponds to a scalar meson condensate charged under a global  $SO(4)$  symmetry. In chapter 3, we discuss an on-going work. We study a strongly-coupled gauge theory living in a compact space with a generic value of quark mass at zero temperature in the presence of an external magnetic field. We are investigating the phase diagram of the external magnetic field and quark mass.

In chapter 4 and 5, we move to M-theory. In chapter 4, we construct a complete non-linear theory of a supersymmetric single M5-brane with a 3+3 splitting. The M5-brane lives in a general background of M-theory. The idea of our construction is to get equations of motion that agree with that obtained from the superembedding approach. In chapter 5, we consider a model which attempts to describe a theory on multiple M5-branes. Using this model, we construct self-dual string solutions which describes M2/M5 branes intersection. These solutions are supported by magnetic monopoles. For self-dual strings with large number of M2 and M5-branes, we obtain the required radius-distance relationship and energy.

# Declaration

The work in this thesis is based on research carried out at the Centre for Particle Theory, the Department of Mathematical Sciences, Durham, England. No part of this thesis has been submitted elsewhere for any other degree or qualification and it all my own work unless referenced to the contrary in the text.

Chapter 1 reviews published literatures. Chapters 2, 4, and 5 are based on works [1–4] by the author with collaborators. Chapter 3 is based on an on-going work by the author in collaboration with Suphakorn Chunlen, Kasper Peeters, and Marija Zamaklar.

**Copyright © 2014 by Pichet Vanichchajongjaroen.**

“The copyright of this thesis rests with the author. No quotations from it should be published without the author’s prior written consent and information derived from it should be acknowledged.”

# Acknowledgements

I would like to thank my supervisor, Dr. Marija Zamaklar, for her advices, suggestions, and discussions. I would also like to thank her for suggestions and comments on my thesis. I would like to thank Prof. Chong-Sun Chu for his advices, discussions, and encouragements. My thanks also go to Dr. Kasper Peeters and to Prof. Dmitri Sorokin for, on different occasions, their advices, suggestions, and discussions.

I would like to thank my collaborators: F for discussions and for showing me useful tips on Mathematica, and Sheng-Lan for comments, fun discussions, and for showing me useful calculation tricks which have been saving my time and efforts. I also thank to Gurdeep, Yang, and Alfonso for discussions.

My researches would have been less efficient if I had not obtained good basics. For this reason, I have been grateful to Prof. Mukund Rangamani for his advices on researches during my undergraduate. I also thank again to Prof. Chong-Sun Chu for his supervision during my master research.

I would also like to thank other staffs and students and to all other people for direct and indirect supports, inspirations, and motivations. Many people have been making my time in Durham enjoyable. I would like to thank these people especially P'Nim, P'Bank and P'Kae.

My family especially my mom, dad, and my brother have always been providing me with love and supports.

My PhD is supported by a Durham Doctoral Studentship and by a DPST Scholarship from the Royal Thai Government.

# Contents

<b>Abstract</b>	<b>iii</b>
<b>Declaration</b>	<b>iv</b>
<b>Acknowledgements</b>	<b>v</b>
<b>List of Figures</b>	<b>ix</b>
<b>List of Tables</b>	<b>xviii</b>
<b>1 Introduction</b>	<b>1</b>
1.1 Bosonic string theory . . . . .	2
1.2 Supersymmetrising strings . . . . .	5
1.3 D-branes . . . . .	11
1.3.1 Single D-brane . . . . .	11
1.3.2 Multiple D-branes . . . . .	15
1.3.3 D-branes as solutions of supergravity . . . . .	18
1.4 Development: gauge/gravity duality . . . . .	20
1.4.1 Original AdS/CFT correspondence . . . . .	20
1.4.2 Extension: finite temperature and finite size . . . . .	26
1.4.3 Further extension: adding flavour fields . . . . .	32
1.5 M-theory branes . . . . .	46
1.5.1 M2-branes . . . . .	48
1.5.2 M5-branes . . . . .	50
<b>2 Instability of <math>\mathcal{N} = 2</math> gauge theory in compact space with an isospin chemical potential</b>	<b>61</b>
2.1 Holography with a dual $S^3$ . . . . .	62

---

2.1.1	Brane embeddings in global $\text{AdS}_5 \times S^5$ and $\text{AdS}_5$ -Schwarzschild . . .	62
2.1.2	Chemical potentials and homogeneous solutions . . . . .	64
2.2	Perturbative analysis of the homogeneous vacuum at $T = 0$ . . . . .	66
2.2.1	Scalar fluctuations at zero temperature . . . . .	66
2.2.2	Vector fluctuations at zero temperature . . . . .	69
2.3	Perturbative analysis of the homogeneous vacuum at $T \neq 0$ . . . . .	73
2.4	The new ground states at zero and finite temperature . . . . .	77
2.4.1	The new ground state at zero temperature . . . . .	78
2.4.2	The new ground state at finite temperature . . . . .	83
2.5	Discussion and outlook . . . . .	86
<b>3</b>	<b>An <math>\mathcal{N} = 2</math> Gauge Theory in Compact Space at Zero Temperature with an External Magnetic Field</b>	<b>88</b>
3.1	Equations of motion on probe D7-branes . . . . .	89
3.2	Embedding at zero temperature in finite volume . . . . .	90
3.3	Equatorial embedding analysis . . . . .	98
3.3.1	Analytical discussion . . . . .	98
3.3.2	Numerical analysis: shooting from the boundary . . . . .	102
3.4	Full check by shooting from the boundary . . . . .	103
3.4.1	The case $m/R = 0.4, H_{ext} = 1$ . . . . .	105
3.4.2	The case $m/R = 0.4, H_{ext} = 2.5$ . . . . .	106
3.4.3	The case $m/R = 0.4, H_{ext} = 3$ . . . . .	107
3.5	Summary and discussions . . . . .	108
3.A	Gauge symmetry of embedding equations of motion . . . . .	110
3.B	Regularity of B-field . . . . .	112
<b>4</b>	<b>The M5-brane action revisited</b>	<b>114</b>
4.1	Notation and Conventions . . . . .	115
4.2	M5-brane actions . . . . .	116
4.2.1	Original M5-brane action . . . . .	116
4.2.2	New M5-brane action . . . . .	118
4.3	Derivation of the new M5-brane action . . . . .	120
4.3.1	Non-linear self-duality of the M5-brane in the superembedding ap- proach . . . . .	123
4.4	Comparison of the two M5-brane actions . . . . .	129

---

4.5	Relation to $M2$ -branes . . . . .	130
4.6	Discussions . . . . .	131
4.A	Exact check of the $M5$ -brane action non-linear self-duality from superembedding . . . . .	132
4.A.1	Matrix Notation . . . . .	133
4.A.2	Outline of computation . . . . .	133
<b>5</b>	<b>Non-Abelian Self-Dual String Solutions</b>	<b>136</b>
5.1	Review of the Non-Abelian Multiple 5-brane Theory . . . . .	137
5.2	Non-Abelian Self-Dual String Solution: Uncompactified Case . . . . .	139
5.2.1	Self-dual string solution in the Perry-Schwarz Theory . . . . .	139
5.2.2	Non-abelian Wu-Yang string solution . . . . .	146
5.3	Non-Abelian Self-Dual String Solution: Compactified Case . . . . .	150
5.4	Non-Abelian $SU(N_5)$ Self-Dual String Solution . . . . .	154
5.4.1	Generalised non-abelian Wu-Yang monopole . . . . .	154
5.4.2	Non-abelian self-dual string and the distance-radius relation . . . . .	156
5.5	Discussions . . . . .	160
<b>6</b>	<b>Conclusion</b>	<b>162</b>
	<b>Bibliography</b>	<b>164</b>

# List of Figures

1.1	A closed string worldsheet (left) and an open string worldsheet (right) in an $X^0 - X^1 - X^2$ slice of a spacetime. . . . .	4
1.2	A single $Dp$ -brane. This $Dp$ -brane stretches along $X^\mu$ directions, where $\mu = 0, 1, \dots, p$ . The directions $X^I, I = p + 1, \dots, 9$ are transverse to the $Dp$ -brane. Note that the $X^0$ direction is not shown in this figure. . . . .	11
1.3	A hyperplane transverse to a $Dp$ -brane. The $Dp$ -brane which is seen as a dot in this figure is surrounded by an $(8 - p)$ -sphere. . . . .	13
1.4	Two parallel but non-coincident $Dp$ -branes with strings stretching between them. . . . .	15
1.5	A sketch of the geometry of an extremal 3-brane solution. . . . .	20
1.6	A diagram showing a motivation of AdS/CFT correspondence. The equivalence between the two low energy interpretations of D3-branes suggests that an $\mathcal{N} = 4$ $SU(N_c)$ SYM theory in a four-dimensional Minkowski space is dual to a type IIB superstring theory in $AdS_5 \times S^5$ . . . . .	22
1.7	Illustrations of the space which is conformal to the global $AdS_5$ . $\tau$ is the time coordinate and is in the vertical direction. $\theta$ is the radial coordinate of the global $AdS_5$ , and is shown in the figure as the radial direction. The $\theta = 0$ axis corresponds to the AdS centre, while the cylinder's boundary $\theta = \pi/2$ corresponds to the AdS boundary. $\varphi$ is the $S^1$ representative of $S^3$ , and is shown as the angular direction. The picture on the left shows the full cylinder. The picture on the right shows the cylinder's vertical slice which passes through the $\theta = 0$ axis. $\theta$ is increasing from 0 to $\pi/2$ both to the left and to the right of the $\theta = 0$ axis. The values of $\varphi$ on the left and on the right of the $\theta = 0$ axis are $\varphi = \pi$ and $\varphi = 0$ , respectively. . . . .	28

- 1.8 Illustrations of the space which is conformal to the Poincaré  $AdS_5$ . This space is embedded into the space of figure 1.7. The picture on the left is taken from figure 2(b) of the reference [5]. It shows that the conformal space to the Poincaré  $AdS_5$  occupies a wedge-like region within the cylinder. Region I represents the Poincaré AdS boundary while Regions VIII-XVII represent the Poincaré horizon. Details of these and other regions are discussed in the reference [5]. The picture on the right shows the cylinder's vertical slice which passes through the  $\theta = 0$  axis.  $\theta$  is increasing from 0 to  $\pi/2$  both to the left and to the right of the  $\theta = 0$  axis. The values of  $\varphi$  on the left and on the right of the  $\theta = 0$  axis are  $\varphi = \pi$  and  $\varphi = 0$ , respectively. The light blue shaded region corresponds to the  $(t, r)$  subspace at  $x_1 = x_2 = x_3 = 0$  of the Poincaré  $AdS_5$ . . . . . 29
- 1.9 Illustrations of the space which is conformal to the global AdS-Schwarzschild.  $\tau$  is the time coordinate and is in the vertical direction.  $\theta$  is the radial coordinate of the global AdS-Schwarzschild, and is shown in the figure as the radial direction. The grey cylinder represents the black hole with horizon at  $\theta = \theta_H$ . The boundary  $\theta = \pi/2$  of the light blue cylinder corresponds to the AdS boundary.  $\varphi$  is the  $S^1$  representative of  $S^3$ , and is shown as the angular direction. The picture on the left shows the full cylinder. The picture on the right shows the cylinder's vertical slice which passes through the  $\theta = 0$  axis.  $\theta$  is increasing from 0 to  $\pi/2$  both to the left and to the right of the  $\theta = 0$  axis. The values of  $\varphi$  on the left and on the right of the  $\theta = 0$  axis are  $\varphi = \pi$  and  $\varphi = 0$ , respectively. . . . . 31
- 1.10 The D3/D7 system in a ten-dimensional flat spacetime. The D3-branes and the D7-branes are separated by the distance  $L$ . In this figure, the  $X^0$  direction is omitted. . . . . 33
- 1.11 An illustration of gauge/gravity duality from the D3/D7 model. On the gravity side (left) D7-branes wrap around  $AdS_5 \times S^3$  within  $AdS_5 \times S^5$ . The relevant degrees of freedom are from the closed strings propagating in the bulk and the  $7 - 7$  strings on D7-branes. The  $S^5$  is not shown in the figure. On the field theory side (right), the relevant degrees of freedom are from the  $3 - 3$  strings which correspond to the closed strings and the  $3 - 7$ , and  $7 - 3$  strings which correspond to the  $7 - 7$  strings on the gravity side. This figure is adapted from the figure 3.1 of the reference [6]. . . . . 34

1.12 Examples of D7-brane embeddings into the Poincaré  $AdS_5 \times S^5$  spacetime. These pictures show the D7-brane embeddings from the point of view of the six-dimensional flat space which is conformal to the transverse space to the D3-branes. The plot on the left shows the embeddings plotted in the  $\rho - L$  plane. The red curve is called the equatorial embedding, for which the D7-branes cover the whole  $AdS_5$  part. The blue curves are called the Minkowski embeddings, for which the D7-branes do not cover the whole  $AdS_5$  part. These two kinds of embeddings are visualised by the pictures on the right. In these pictures, the black dots represent the positions of the  $X^1 - X^2 - X^3$  hyperplanes. . . . . 37

1.13 Schematic diagrams showing D7-brane embeddings into the  $AdS_5$  part of the Poincaré  $AdS_5 \times S^5$  spacetime. The Poincaré  $AdS_5 \times S^5$  spacetime is represented by the slice of its conformal space (see figure 1.8). These pictures show that for the equatorial embedding, the D7-branes (grey-coloured) fill the whole  $AdS_5$  part, but for the Minkowski embedding, the D7-branes fill from the AdS boundary down to some point outside the Poincaré horizon. 38

1.14 A part of a D7-brane embedding which wraps an internal  $S^3 \subset S^5$ . The big sphere represents  $S^5$  while the red circle represents  $S^3$ . The internal angle  $\theta$  characterises the position of the wrapped  $S^3$ . . . . . 39

1.15 The internal angle  $\theta$  at each position  $r$  of the Poincaré  $AdS_5 \times S^5$ . The curves in this figure correspond to the curves presented in figure 1.12. This figure clearly shows the difference between the equatorial and Minkowski embeddings. The equatorial embedding reaches the AdS centre  $r = 0$ , and the internal angle  $\theta$  is always  $\theta = 0$  ( $S^3$  always wraps the equatorial of  $S^5$ ). On the other hand, the Minkowski embeddings have varying  $\theta$ , and they stop at some point at which  $\theta = \pi/2$  (which corresponds to the internal  $S^3$  shrinking to a point). . . . . 40

1.16 Examples of D7-brane embeddings into the global  $AdS_5 \times S^5$  spacetime. The red curves represent ball embeddings, the blue curves represent Minkowski embeddings, and the black dashed curve represents the critical embedding. The idea of this figure is from figure 1 in the reference [7]. . . . . 41

- 1.17 Various D7-brane embeddings in global  $AdS_5 \times S^5$ . The pictures are shown in the six-dimensional flat space conformal to the actual transverse space. Each blank sphere represents  $S^5$  with a radius  $R/2$  at the AdS centre. These spheres are artefacts of coordinate choice we use. . . . . 42
- 1.18 The internal angle  $\theta$  at each position  $r = (4u^2 - R^2)/(4u)$  of the global  $AdS_5 \times S^5$ . The curves in this figure correspond to the curves presented in figure 1.16. This figure clearly shows that while all the Ball embeddings reach the AdS centre  $r = 0$ , the Minkowski embeddings stop at some point at which  $\theta = \pi/2$  (which corresponds to the internal  $S^3$  shrinking to a point). The critical embedding interpolates between these two kinds of embeddings, and reaches the AdS centre  $r = 0$  when  $\theta = \pi/2$ . . . . . 43
- 1.19 Free energy (left) and condensate (right) versus quark mass. For each plot, the red curve presents the data from Ball embeddings, the blue curve from Minkowski embeddings, and the black dot from the equatorial embedding. These plots show the smooth phase transition between the Ball embedding phase and the Minkowski embedding phase. The reference [8] shows that the phase transition is of third order. . . . . 44
- 1.20 Various D7-brane embeddings in  $(AdS - Schwarzschild)_5 \times S^5$ . The pictures are shown in the six-dimensional flat space conformal to the actual transverse space. Each sphere represents the black hole. . . . . 45
- 1.21 Examples of string dualities. This web of dualities suggests how to obtain string theories and the eleven-dimensional supergravity from the M-theory. 47
- 2.1 Plots of the imaginary (left) and real (right) parts of the frequencies for the lowest lying uncharged scalar fluctuation (red), the vector fluctuation (blue) and the charged scalar fluctuation (green), at fixed temperature  $\pi TR = 2$ , as a function of the chemical potential. . . . . 76
- 2.2 Left is a plot of the real parts of the frequencies for the various modes (colours as in figure 2.1) as functions of the temperature at fixed value  $\mu R = 5$  of the chemical potential. The plot on the right shows the real parts of the frequencies as functions of both temperature and chemical potential. 77

- 2.3 Critical chemical potential as function of temperature, in two different dimensionless combinations. The figure on the right shows more clearly what happens in the  $TR \rightarrow \infty$  limit, which can be interpreted as the large radius limit at fixed temperature. . . . . 77
- 2.4 Profile of the fields  $A_0$  (left) and  $\eta$  (right) of the charged scalar condensate, evaluated at  $\mu R = 2.5$ . The boundary is at  $z = 0$  and the AdS centre is at  $z = 1$ . . . . . 80
- 2.5 The plot on the left shows the isospin density  $\rho R$  (blue) and scalar density  $\rho_\eta R$  (red) of the charged scalar condensate as functions of the isospin chemical potential. The plot on the right shows the scaled free energy as function of chemical potential. . . . . 81
- 2.6 Left: a plot of the functions  $A_0(z)$  (solid curve) and  $\psi(z)$  (dashed curve) for the vector solution. Right: plots of the functions  $A_0(z)$  (solid) and  $\Phi$  (dashed) for the scalar configuration, both evaluated at a fixed value of chemical potential  $\mu R = 4.5$ . . . . . 82
- 2.7 Plots of the densities  $\rho$  (blue) and  $\rho_\eta$  (red), as a function of the chemical potential  $\mu$ , at zero temperature, for the vector condensate (left) and scalar condensate (right). . . . . 83
- 2.8 Scaled free energy of the zero-temperature condensates as a function of the dimensionless chemical potential. The vector is plotted in blue, the scalar in red, the charged scalar green. The black line along the  $x$ -axis denotes the old ground state. . . . . 84
- 2.9 Left are plots of profile of the fields  $A_0$  (solid) and  $\eta$  (dashed) for the charged scalar, evaluated at  $\pi TR = 2.5$  and  $\mu R = 10.1$ . The boundary is at  $v = 1$  and horizon at  $v = 0$ . Right plot is for densities  $\rho$  (blue) and  $\rho_\eta$  (red), as function of chemical potential  $\mu$ , at fixed temperature  $\pi TR = 2.5$ . . . . . 85
- 2.10 Plots of solutions ( $A_0(z), \Phi(z)$ ), and ( $A_0(z), \psi(z)$ ) for the scalar and vector condensates respectively, at fixed temperature  $\pi TR = 2.5$  and chemical potential  $\mu R = 4.5$  (the curve for  $A_0$  is rather straight only because the plot is made for a chemical potential only slightly above the critical value). . . . . 86
- 2.11 Dependence of the charged scalar ground state densities on  $TR$  at fixed chemical potential  $\mu R = 4.005$ . . . . . 87

- 3.1 Plot of brane shapes for D7-branes embedding. The plots from left to right and top to bottom are at fixed external magnetic field  $H_{ext} = 0, 2, 4, 5$ , respectively. Each red curve is for Ball embedding where D7-branes reach AdS centre while each blue curve is for Minkowski embedding where D7-branes do not reach AdS centre. The horizontal and vertical axes are  $u\sqrt{1 - \chi^2}/R, u\chi/R$ . For some non-zero values of  $H_{ext}$ , there are forbidden values of bare quark mass. . . . . 96
- 3.2 Plot of brane shapes for D7 embedding in  $z$ -coordinates where  $z = R/(2u)$ . The plots from left to right and top to bottom are at fixed external magnetic field  $H_{ext} = 0, 2, 4, 5$ , respectively. Each red curve is for Ball embedding where D7-branes reach AdS centre while each blue curve is for Minkowski embedding where D7-branes do not reach AdS centre. The horizontal and vertical axes are  $z, \chi/(2z)$ . Quark mass of each embedding is proportional to the position of the brane on the vertical axis. The plots clearly show the development of mass gap. . . . . 98
- 3.3 Plot of possible values of  $H_{ext}$  and  $m$ . Different lines represent different initial condition of  $\chi(u)$ , while different points along each line represent different initial condition of  $H(u)$ . Red curves represent Ball embeddings while blue curves represent Minkowski embeddings. The left plot presents the raw data while the right plot shows the phase diagram. The quark mass is proportional to  $|m|$ , so the horizontal axis of the right plot has to be  $|m|$ . Given  $H_{ext}, |m|$ , we ask for a unique configuration. So if the line crosses, free energy of different configurations will need be compared. Furthermore, the phase diagram should not have a gap. So this phase diagram is quite subtle because of the presence of the mass gap. . . . . 99
- 3.4 The plots of  $H_{ext}$  versus  $H_{c2}$ . In these plots, we use the setting  $u_{ball}/R = 500001/1000000, u_{inf}/R = 10000$ . The right plot clearly shows that there is a maximal value of  $H_{ext}$ . . . . . 100
- 3.5 Left is the contour plot of the solution to (3.59). Right is the plot from the left with the result from the full numerical solution plotted in red. . . . . 101

- 3.6 The plot shows the  $(H_{ext}, M_{tz})$  parameter space. The blue line is associated with solutions which give B-field vanishing at the AdS centre. Brown dots are associated with solutions which give B-field non-vanishing at the AdS centre. The solutions associated with the blue line and brown dots have smooth profiles  $H(u)$ . Grey dots are associated with solutions that have  $|H'(u_{close})| > 10^{15}$  at some  $u_{close} > R/2$ ; this numerically indicates that  $H'(u)$  blows up at some point. . . . . 103
- 3.7 The contour plots showing the values of  $u_{close}/R$  in the  $(c_1, M_{tz})$  parameter space with fixed  $(m/R, H_{ext}) = (0.4, 1)$ . The left plot is the interpolation of the contour plot for the full range  $-10 \leq c_1/R^3 \leq 10, -10 \leq M_{tz}/R^2 \leq 10$ . The middle plot is the same as the left plot but with a smaller range focusing around the points with  $u_{close} = 0.5001R$  (the numerical value for  $u_{close} = R/2$ ). The sample points with  $u_{close} = 0.5001R$  are shown in black dots. The right plot is the colour bar encoding the values of  $u_{close}/R$ . Note that we use dark blue colour for  $u_{close}/R \geq 1$ . . . . . 106
- 3.8 The left plot shows the interpolation of black dots from figure 3.7. We define the affine parameter  $\alpha$  as the distance along the curve from a reference point which is shown to have  $\alpha = 0$ . The right plot shows the values of  $H_{c0} \equiv H(R/2)$  as a function of  $\alpha$ . The minimum value of  $|H_{c0}|$  which we found is 0.009 at  $\alpha = 0$ . A further investigation is required to see if we can get the point with  $H_{c0}$  closer to 0. . . . . 107
- 3.9 The contour plots showing the values of  $\chi(u_{close})$  in the  $(c_1, M_{tz})$  parameter space with fixed  $(m/R, H_{ext}) = (0.4, 1)$ . The left plot is the interpolation of the contour plot for the full range  $-10 \leq c_1/R^3 \leq 10, -10 \leq M_{tz}/R^2 \leq 10$ . The middle plot is the same as the left plot but with a smaller range focusing around the points with  $\chi(u_{close})$  closest to 1. The right plot is the colour bar encoding the values of  $\chi(u_{close})$ . The physical Minkowski embedding has  $\chi(u_{close}) \approx 1$ . However, the best result obtained from our sample points gives  $\chi(u_{close}) = 0.65$ . So it is highly unlikely that there is a Minkowski embedding for  $(m/R, H_{ext}) = (0.4, 1)$ . . . . . 108

- 3.10 The contour plots showing the values of  $u_{close}/R$  in the  $(c_1, M_{tz})$  parameter space with fixed  $(m/R, H_{ext}) = (0.4, 2.5)$ . The left plot is the interpolation of the contour plot for the full range  $-10 \leq c_1/R^3 \leq 10, -10 \leq M_{tz}/R^2 \leq 10$ . The middle plot is the same as the left plot but with a smaller range focusing around the points with  $u_{close} = 0.5001R$  (the numerical value for  $u_{close} = R/2$ ). The sample points with  $u_{close} = 0.5001R$  are shown in black dots. The right plot is the colour bar encoding the values of  $u_{close}/R$ . . . . 109
- 3.11 The left plot shows the interpolation of black dots from figure 3.10. We define the affine parameter  $\alpha$  as the angle from a reference axis. The right plot shows the values of  $H_{c0} \equiv H(R/2)$  as a function of  $\alpha$ . The interpolation suggests that it is unlikely to have  $H_{c0} = 0$ . . . . . 110
- 3.12 The contour plots showing the values of  $\chi(u_{close})$  in the  $(c_1, M_{tz})$  parameter space with fixed  $(m/R, H_{ext}) = (0.4, 2.5)$ . The left plot is the interpolation of the contour plot for the full range  $-10 \leq c_1/R^3 \leq 10, -10 \leq M_{tz}/R^2 \leq 10$ . The middle plot is the same as the top left plot but with a smaller range focusing around the points with  $\chi(u_{close})$  closest to 1. The right plot is the colour bar encoding the values of  $\chi(u_{close})$ . The physical Minkowski embedding has  $\chi(u_{close}) \approx 1$ . The best result obtained from our sample points gives  $\chi(u_{close}) = 0.967$ . Since this value is quite close to 1, we need a further investigation to see if there is a physical Minkowski embedding. . . 111
- 3.13 The contour plots showing the values of  $u_{close}/R$  in the  $(c_1, M_{tz})$  parameter space with fixed  $(m/R, H_{ext}) = (0.4, 3)$ . The left plot is the interpolation of the contour plot for the full range  $-10 \leq c_1/R^3 \leq 10, -10 \leq M_{tz}/R^2 \leq 10$ . The middle plot is the same as the left plot but with a smaller range focusing around the points with values closest to  $u_{close} = 0.5001R$ . From our data, there is no point with  $u_{close} = 0.5001R$ . The closest we get is  $0.546R$ . So it is quite unlikely that there is a Ball embedding. . . . . 112

- 3.14 The contour plots showing the values of  $\chi(u_{close})$  in the  $(c_1, M_{tz})$  parameter space with fixed  $(m/R, H_{ext}) = (0.4, 3)$ . The left plot is the interpolation of the contour plot for the full range  $-10 \leq c_1/R^3 \leq 10, -10 \leq M_{tz}/R^2 \leq 10$ . The middle plot is the same as the top left plot but with a smaller range focusing around the points with  $\chi(u_{close})$  closest to 1. The right plot is the colour bar encoding the values of  $\chi(u_{close})$ . The physical Minkowski embedding has  $\chi(u_{close}) \approx 1$ . The best result obtained from our sample points gives  $\chi(u_{close}) = 0.999$ . Since this value is very close to 1, it is highly likely that there is a physical Minkowski embedding. However, a further investigation is required to see if a physical Minkowski embedding really does exist. . . . . 113
- 5.1 An M2 brane ending on a system of two parallel M5-branes separated by a distance. . . . . 149
- 5.2 Scalar Profile. The red curve corresponds to  $R = 4$  and the blue one to  $R = 1$  . . . . . 154

# List of Tables

1.1	The D1/D3 brane intersection in a ten-dimensional flat spacetime. . . . .	17
1.2	The D3/D7 system in a ten-dimensional flat spacetime. . . . .	33

# Chapter 1

## Introduction

This thesis explores aspects of recent developments in string theory and M-theory, which are important theories of high energy physics. In particular, we focus on objects which are called branes. These objects are important in the development of non-perturbative aspects of string theory and M-theory.

In particle physics, the Standard Model has been very successful; its predictions about behaviours and interactions of subatomic particles are experimentally confirmed. Despite its successes, this model is far from being complete. For example, it does not incorporate the gravitational interaction, which, at a very high energy scale, should be combined with the other three already incorporated interactions — electromagnetic, weak, and strong.

In order to describe all these interactions, one needs to combine quantum mechanics with general relativity. String theory is the best candidate which achieves this. In this theory, the quantisation of a one-dimensional object, called a string, naturally gives rise to gravity. String theory also contains objects called D-branes, which are infinitely extended hypersurfaces. Theories on D-branes are gauge field theories, which shares some properties with the Standard Model.

Within the framework of the Standard Model, there is a theory called Quantum Chromodynamics (QCD) which describes the interaction between quarks and gluons. The study of this theory at strong coupling is important but difficult. A modern development of D-branes leads to a conjecture called AdS/CFT correspondence which states that a gravity theory is equivalent to a gauge theory. By studying the dual weakly-coupled gravity theories, it is possible to use AdS/CFT correspondence to explain some cousins of a strongly-coupled QCD. These cousins, however, are originally quite different from the real QCD. Generalisations of AdS/CFT correspondence can be done in many ways, and

the purposes are mainly to get as close to the real QCD as possible. We are particularly interested in the extension in which the QCD-like theory contains quarks. Furthermore, a finite-size effect is important in some phenomena, so we study the extension which explains also a finite-size system. The first part of this thesis concerns an application of AdS/CFT correspondence.

Another important development of string theory gives rise to M-theory, which can be thought of as more fundamental than string theory; in certain limits, string theory can be obtained from M-theory. In M-theory, there are also brane-like objects, which are called M-branes. These objects are still not fully understood, and there are still much to be done. The second part of this thesis is aimed to construct theories on M-branes.

Below, we review some basic backgrounds of string theory and M-theory. The rest of this chapter is mostly based on the books [9–12] and review articles [6, 13–16]

## 1.1 Bosonic string theory

String theory is a theory of a quantum string whose classical dynamics are described by a worldsheet in a  $D$ -dimensional spacetime. The theory is characterised by a string length  $l_s$  and a dimensionless coupling constant  $g_s$ . The string has the tension which is given by

$$T = \frac{1}{2\pi\alpha'}, \quad \text{where} \quad \alpha' = l_s^2. \quad (1.1)$$

Let  $X^M$  with  $M = 0, 1, 2, \dots, D - 1$  be spacetime coordinates, and let  $(\tau, \sigma)$  be the string worldsheet coordinates. It is convenient to denote  $(\tau, \sigma)$  collectively as  $(\sigma^\alpha)$ , where  $\alpha = 0, 1$  with  $\sigma^0 \equiv \tau, \sigma^1 \equiv \sigma$ . The embedding of the string worldsheet in the spacetime is described by a bosonic embedding function  $X^M(\tau, \sigma)$ . The action of the string is given by the Nambu-Goto action:

$$S = -T \int d\tau d\sigma \sqrt{-\det \left( g_{MN}(X) \frac{\partial X^M}{\partial \sigma^\alpha} \frac{\partial X^N}{\partial \sigma^\beta} \right)}, \quad (1.2)$$

where  $g_{MN}(X)$ , whose signature is given by  $\text{diag}(-1, 1, 1, \dots, 1)$ , is the metric of the spacetime.

The presence of a square root in the Nambu-Goto action will make the quantisation difficult. An alternative action called the Polyakov action is classically equivalent to the Nambu-Goto action. The Polyakov action does not contain a square root, but it introduces an auxiliary field  $h_{\alpha\beta}(\tau, \sigma)$  which is called a worldsheet metric. The Polyakov action is

given by

$$S = -\frac{1}{2}T \int d\tau d\sigma \sqrt{-h} h^{\alpha\beta} g_{MN}(X) \partial_\alpha X^M \partial_\beta X^N, \quad (1.3)$$

where

$$h = \det h_{\alpha\beta}, \quad h^{\alpha\beta} = (h^{-1})_{\alpha\beta}. \quad (1.4)$$

Let us consider the string in a flat spacetime, whose metric is given by  $g_{MN} = \eta_{MN} = \text{diag}(-1, 1, 1, \dots, 1)$ . The action can be simplified with the help of symmetries. We focus on the reparameterisation symmetry:

$$\sigma^\alpha \rightarrow \sigma'^\alpha(\sigma), \quad h_{\alpha\beta}(\sigma) = \frac{\partial \sigma'^\gamma}{\partial \sigma^\alpha} \frac{\partial \sigma'^\delta}{\partial \sigma^\beta} h_{\gamma\delta}(\sigma'), \quad X^M(\sigma) = X^M(\sigma'), \quad (1.5)$$

and the Weyl symmetry:

$$h_{\alpha\beta} \rightarrow e^{\varphi(\tau, \sigma)} h_{\alpha\beta}. \quad (1.6)$$

These symmetries leave the Polyakov action invariant. They are enough to fix the components of  $h_{\alpha\beta}$  so that the Polyakov action reduces to

$$S = \frac{T}{2} \int d\tau d\sigma \left( \frac{\partial X^M}{\partial \tau} \frac{\partial X_M}{\partial \tau} - \frac{\partial X^M}{\partial \sigma} \frac{\partial X_M}{\partial \sigma} \right). \quad (1.7)$$

The vanishing of the variation of this action with respect to  $X^M$  gives the equation of motion

$$\left( \frac{\partial^2}{\partial \tau^2} - \frac{\partial^2}{\partial \sigma^2} \right) X^M = 0, \quad (1.8)$$

as well as the vanishing of the boundary term:

$$\int d\tau \left( \frac{\partial X_M}{\partial \sigma} \delta X^M \Big|_{\sigma=\pi} - \frac{\partial X_M}{\partial \sigma} \delta X^M \Big|_{\sigma=0} \right) = 0, \quad (1.9)$$

where we have taken  $\sigma$  to be in the range  $\sigma \in [0, \pi]$ . There are also other conditions which are needed to be satisfied. They are

$$\frac{\partial X^M}{\partial \tau} \frac{\partial X_M}{\partial \sigma} = 0, \quad \frac{1}{2} \frac{\partial X^M}{\partial \tau} \frac{\partial X_M}{\partial \tau} + \frac{1}{2} \frac{\partial X^M}{\partial \sigma} \frac{\partial X_M}{\partial \sigma} = 0. \quad (1.10)$$

These conditions can be thought of as the equations of motion of  $h_{\alpha\beta}$ . Although we have fixed  $h_{\alpha\beta}$ , its equations of motion are not trivially satisfied.

Let us now discuss a classical string solution. To make the boundary term vanish, a string can be either closed or open. String worldsheets are illustrated in the figure 1.1. For a closed string, the embedding function is periodic in  $\sigma$ :  $X^M(\tau, \sigma) = X^M(\tau, \sigma + \pi)$ . For an open string, there are two types of endpoints that solve the boundary conditions. The first type is the Neumann boundary condition  $(\partial X^M / \partial \sigma)|_{0, \pi} = 0$  where the string endpoints are free to move. The second type is the Dirichlet boundary condition  $\delta X^M|_{0, \pi} = 0$  where

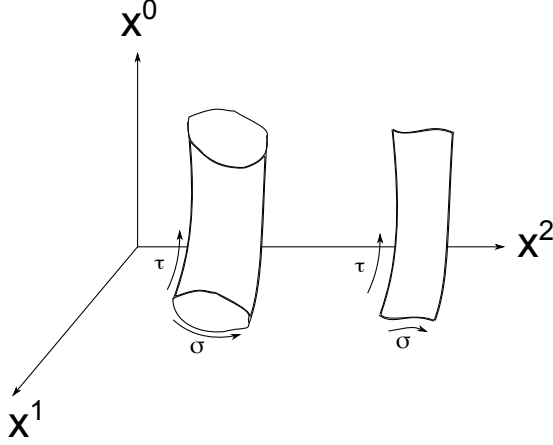


Figure 1.1: A closed string worldsheet (left) and an open string worldsheet (right) in an  $X^0 - X^1 - X^2$  slice of a spacetime.

the string endpoints are fixed. Open strings are in fact related to objects called D-branes. We postpone the discussion of open strings until we discuss D-branes.

For a closed string, the solution to the equations of motion is given in terms of a right-mover  $X_R^M$  and a left-mover  $X_L^M$ . That is

$$X^M(\tau, \sigma) = X_R^M(\tau - \sigma) + X_L^M(\tau + \sigma), \quad (1.11)$$

where

$$X_R^M = \frac{1}{2}x^M + \alpha' p^M(\tau - \sigma) + i\sqrt{\frac{\alpha'}{2}} \sum_{n \neq 0} \frac{1}{n} \alpha_n^M e^{-2in(\tau - \sigma)}, \quad (1.12)$$

$$X_L^M = \frac{1}{2}x^M + \alpha' p^M(\tau + \sigma) + i\sqrt{\frac{\alpha'}{2}} \sum_{n \neq 0} \frac{1}{n} \tilde{\alpha}_n^M e^{-2in(\tau + \sigma)}. \quad (1.13)$$

Note that this classical solution contains informations of the centre-of-mass position, total string momentum, and superpositions of oscillation modes.

Let us now mention some key steps to quantise a closed string. The Poisson brackets are computed classically. Then, they are promoted to commutators. The commutators of the oscillation modes are given by

$$[\alpha_m^M, \alpha_n^N] = [\tilde{\alpha}_m^M, \tilde{\alpha}_n^N] = m\eta^{MN} \delta_{m+n,0}, \quad [\alpha_m^M, \tilde{\alpha}_n^N] = 0. \quad (1.14)$$

Defining

$$\alpha_n^{N\dagger} = \alpha_{-n}^N, \quad \tilde{\alpha}_n^{N\dagger} = \tilde{\alpha}_{-n}^N, \quad n > 0, \quad (1.15)$$

we have

$$[\alpha_m^M, \alpha_n^{N\dagger}] = [\tilde{\alpha}_m^M, \tilde{\alpha}_n^{N\dagger}] = m\eta^{MN} \delta_{m,n}, \quad m, n > 0. \quad (1.16)$$

These commutation relations look like those of quantum harmonic oscillators. States can then be created by repeatedly acting on the vacuum state  $|0\rangle$  with creation operators  $\alpha_n^{N\dagger}, \tilde{\alpha}_n^{N\dagger}$ . Note however that when  $M = N = 0$ , this gives

$$[\alpha_m^0, \alpha_m^{0\dagger}] = [\tilde{\alpha}_m^0, \tilde{\alpha}_m^{0\dagger}] = -m. \quad (1.17)$$

These commutation relations are problematic because, for example, the state

$$\alpha_m^{0\dagger}|0\rangle \quad (1.18)$$

has a negative norm. Negative norm states are unphysical. A result of a further analysis states that in order to eliminate all the unphysical states, the number of spacetime dimensions should be fixed to  $D = 26$ . Furthermore, it states that the ground state is given by a vacuum state  $|0\rangle$  which is an eigenstate of a mass squared operator  $\mathcal{M}^2 = -p_M p^M$  with an eigenvalue  $-4/\alpha'$ . Therefore, the vacuum state describes a tachyon. States in the next level can be written as

$$\zeta_{\hat{M}\hat{N}} \alpha_1^{\hat{M}\dagger} \tilde{\alpha}_1^{\hat{N}\dagger} |0\rangle, \quad (1.19)$$

where  $\hat{M}, \hat{N} = 2, 3, \dots, 25$ . They are eigenstates of the mass squared operator with an eigenvalue  $\mathcal{M}^2 = 0$ . The traceless symmetric part of  $\zeta_{\hat{M}\hat{N}}$  corresponds to a graviton. The antisymmetric part corresponds a field called B-field. Finally, the trace part corresponds to a dilaton. Note that an exponential of the vacuum expectation value of the dilaton field is identified with the string coupling constant  $g_s$ . Therefore, the string coupling constant is actually not a free parameter.

Higher excited states of the closed string spectrum are massive. For example, a state  $\alpha_2^{\hat{M}\dagger} \tilde{\alpha}_2^{\hat{N}\dagger} |0\rangle$  has  $\mathcal{M}^2 = 4/\alpha'$ . In the main chapters of this thesis, these massive states are not relevant to us. If the closed string theory has an energy  $E \ll 1/\sqrt{\alpha'}$ , then the massive states can be discarded. This is because the energy  $E \ll 1/\sqrt{\alpha'}$  is not enough to excite the massive states, whose masses are of order  $1/\sqrt{\alpha'}$ .

The presence of the tachyon in the closed string spectrum poses a problem. It makes the theory unstable. Furthermore, this spectrum lacks fermions. It turns out that both of these problems can be solved by including the supersymmetry into the string theory.

## 1.2 Supersymmetrising strings

In order to supersymmetrise a string, it is natural to extend the string worldsheet coordinates to include fermionic coordinates. The approach which utilises this idea is called

the Ramond-Neveu-Schwarz (RNS) formalism [17,18]. In this approach, the worldsheet is now a superspace which contains the usual bosonic coordinates ( $\sigma^\alpha$ ) as well as fermionic coordinates

$$\theta_a = \begin{pmatrix} \theta_- \\ \theta_+ \end{pmatrix}_a. \quad (1.20)$$

Here,  $\theta$  is an example of a spinor. In this chapter, we use the indices  $a, b, c, \dots$  to represent components of spinors. A generic spin-1/2 fermion in a  $d$ -dimensional Lorentzian space (meaning, the space whose metric is of the signature  $\text{diag}(-1, 1, \dots, 1)$ ) is given by a Dirac spinor, which has  $2^{\lfloor d/2 \rfloor}$  complex components. Note that a worldsheet is a two-dimensional Lorentzian space, therefore a Dirac spinor on a worldsheet has two complex components. Sometimes it is possible to impose conditions which restrict the components of the spinor. There is a Majorana condition, which requires all the components of a spinor to be real. Also, there is a Weyl condition, which splits a Dirac spinor in an even dimensional Lorentzian space into two Weyl spinors. Hence, a Weyl spinor has  $2^{\lfloor d/2 \rfloor - 1}$  complex components. At the moment, a Majorana condition is of relevant to us. The spinor  $\theta$  is taken to be a Majorana spinor. This means that  $\theta_-$  and  $\theta_+$  are real. Note also that the components of  $\theta_a$  are Grassmannian. This means that they anticommute with each other:

$$\{\theta_a, \theta_b\} = 0. \quad (1.21)$$

Also  $\theta_a \theta_a = 0$  (no summation on  $a$ ). When describing a fermion, one needs gamma matrices  $\gamma_{ab}^\alpha$  which satisfy

$$\{\gamma^\alpha, \gamma^\beta\}_{ab} = 2\eta^{\alpha\beta} \delta_{ab}, \quad (1.22)$$

where  $\eta^{\alpha\beta} = \text{diag}(-1, 1)$ . In this case, the gamma matrices are taken to be

$$\gamma^0 = \begin{pmatrix} 0 & -1 \\ 1 & 0 \end{pmatrix}, \quad \gamma^1 = \begin{pmatrix} 0 & 1 \\ 1 & 0 \end{pmatrix}. \quad (1.23)$$

A conjugate of  $\theta$  is given by  $\bar{\theta} = i\theta^T \gamma^0$ . Note that, in fact, in two dimensions, both a Majorana and a Weyl condition can together be imposed. The spinor  $\theta$  is Majorana. So each of its components:  $\theta_-, \theta_+$  is a Majorana-Weyl spinor. Note also that in an even dimensional Lorentzian space, it is always possible to define a chirality operator whose eigenspinors are Weyl spinors. For our case, although  $\theta_-$  and  $\theta_+$  are Majorana-Weyl spinors, only the Weyl property is of relevance to the discussion of the chirality. A chirality operator is given by

$$\gamma^0 \gamma^1 = \begin{pmatrix} -1 & 0 \\ 0 & 1 \end{pmatrix}. \quad (1.24)$$

Each of the Weyl spinors is an eigenspinor of  $\gamma^0\gamma^1$  in the sense that

$$\gamma^0\gamma^1 \begin{pmatrix} \theta_- \\ 0 \end{pmatrix} = - \begin{pmatrix} \theta_- \\ 0 \end{pmatrix}, \quad \gamma^0\gamma^1 \begin{pmatrix} 0 \\ \theta_+ \end{pmatrix} = + \begin{pmatrix} 0 \\ \theta_+ \end{pmatrix}. \quad (1.25)$$

Therefore,  $\theta_-$  is said to have a negative chirality, while  $\theta_+$  is said to have a positive chirality. This discussion extends to higher even dimensions; it is always possible to construct a chirality operator, and each Weyl spinor either has a negative chirality or a positive chirality.

An embedding function, now being a function of the superspace, is called a superfield  $Y^M(\sigma^\alpha, \theta)$ . It can be Taylor-expanded in fermionic coordinates. This gives

$$Y^M(\sigma^\alpha, \theta) = X^M(\sigma^\alpha) + \bar{\theta}\psi^M(\sigma^\alpha) + \frac{1}{2}\bar{\theta}\theta B^M(\sigma^\alpha). \quad (1.26)$$

Note that due to the anticommutation relation, the series terminates at  $\bar{\theta}\theta$ . The fields  $X^M(\sigma^\alpha)$  and  $B^M(\sigma^\alpha)$  are bosonic, while the field  $\psi^M(\sigma^\alpha)$  is fermionic. One can construct an action which is invariant under a supersymmetry transformation

$$\delta\theta^a = \epsilon^a, \quad \delta\sigma^\alpha = \bar{\theta}\gamma^\alpha\epsilon, \quad (1.27)$$

under which the component fields transform as

$$\delta X^M = \bar{\epsilon}\psi^M, \quad \delta\psi^M = \gamma^\alpha\partial_\alpha X^M\epsilon + B^M\epsilon, \quad \delta B^M = \bar{\epsilon}\gamma^\alpha\partial_\alpha\psi^M. \quad (1.28)$$

Such an action can be written as

$$S = -\frac{T}{2} \int d\tau d\sigma (\partial_\alpha X^M \partial^\alpha X_M + \bar{\psi}^M \gamma^\alpha \partial_\alpha \psi_M - B_M B^M). \quad (1.29)$$

This is the action which is used to analyse a supersymmetric string (also known as superstring) in a flat spacetime. Note that the equation of motion for  $B^M$  of this action is given by  $B^M = 0$ . So only the fields  $X^M(\sigma^\alpha)$  and  $\psi^M(\sigma^\alpha)$  are relevant for our discussions.

To quantise a closed superstring, we follow the steps which are similar to the quantisation of a bosonic string. The boundary condition for  $X^M$  is exactly the same as its bosonic string counterpart. As for  $\psi^M$ , there are two possible choices of the boundary condition. The first choice is the Ramond, or R, boundary condition which requires  $\psi^M$  to be periodic in  $\sigma$ . The second choice is the Neveu-Schwarz, or NS, boundary condition which requires  $\psi^M$  to be antiperiodic in  $\sigma$ . Each of the left-mover and the right-mover can either be R or NS separately. When the two movers are combined, there are 4 possible cases: R-R, R-NS, NS-R, and NS-NS. Recall that in the case of a closed bosonic string, bosonic creation operators  $\alpha_n^{N\dagger}, \tilde{\alpha}_n^{N\dagger}$  are used to construct states. In the case of a closed

superstring, in addition to the bosonic creation operators, there are also fermionic creation operators. Together these operators are used to construct states.

The quantisation of a superstring requires the number of spacetime dimensions to be  $D = 10$ . The spectrum of a closed string originally contains tachyons. However, by using the GSO projection [19], the tachyons along with some other states are excluded from the spectrum. On each mover, the NS sector originally contains both bosons and fermions. The fermions are projected out by the GSO projection. For the R sector, every state is fermionic. Since these fermions live in the even dimensional spacetime, each of them can have either a positive or a negative chirality. After the GSO projection, all of the states of the R sector have the same chirality.

When the left-mover and the right-mover are combined, states in the NS-NS and the R-R sectors are bosonic while states in the R-NS and the NS-R are fermionic. There are two possibilities of combining the movers. R sector states from different movers can have either the opposite chirality or the same chirality. By this chirality consideration, there are two types of the string theory. They are respectively named as type IIA and type IIB. The massless spectrum of type IIA contains states coming from NS-NS, NS-R, R-NS and R-R sector as follows. The NS-NS sector contains a dilaton (a scalar), an antisymmetric 2-form gauge field, and a traceless symmetric rank-two tensor (a graviton). Each of the NS-R and R-NS sectors contains a gravitino (a spin-3/2 field) and a dilatino (a spin-1/2 field). The gravitinos in the different sectors have opposite chiralities. The R-R sector contains a 1-form gauge field and a 3-form gauge field. For type IIB, the NS-NS sector is the same as that of type IIA. However, the other sectors are different. The NS-R and R-NS sectors contain the same contents as their counterparts from type IIA, but the type IIB NS-R gravitino has the same chirality as the type IIB R-NS gravitino. In the R-R sector, the states are a 0-form gauge field, a 2-form gauge field and a 4-form gauge field. The 4-form gauge field has a self-dual field strength.

Let us make a small pause to explain how these massless fields look like. We have already explained how the fields from the NS-NS sector look like. So let us consider fields from the other sectors. A spin-1/2 field is represented by a spinor. A spin-3/2 field contains both a spinor index and a spacetime index. As for an  $n$ -form gauge field, it is represented by a differential  $n$ -form:

$$C^{(n)} = \frac{1}{n!} C_{M_1 M_2 \dots M_n}^{(n)} dX^{M_1} \wedge dX^{M_2} \wedge \dots \wedge dX^{M_n}. \quad (1.30)$$

Its  $(n + 1)$ -form field strength is given by

$$F^{(n+1)} = dC^{(n)}. \quad (1.31)$$

The dual of the  $(n + 1)$ -form field strength is a  $(D - n - 1)$ -form which is given by  $*(F^{(n+1)})$ , where  $*$  is a Hodge dual. The 4-form gauge field from the massless R-R sector has a self-dual field strength. Explicitly, its field strength satisfies

$$*\left(F^{(5)} - \frac{1}{2}C^{(2)} \wedge dB + \frac{1}{2}B \wedge F^{(3)}\right) = F^{(5)} - \frac{1}{2}C^{(2)} \wedge dB + \frac{1}{2}B \wedge F^{(3)}. \quad (1.32)$$

The massless spectrum of the closed string contains an equal number of bosonic and fermionic on-shell degrees of freedom. The equality suggests that the massless spectrum is obtained from a theory with spacetime supersymmetry. Since it is supersymmetric and contains a graviton, this theory is called a supergravity (SUGRA) theory. To study this theory, one constructs an action which is invariant under transformations. In particular, consider a local supersymmetry transformation on a gravitino  $\Psi_M$ . In a usual supersymmetry theory, an infinitesimal spinor  $\epsilon$  of a supersymmetry transformation is coordinate independent. However, in a supergravity theory, the spinor  $\epsilon$  becomes coordinate dependent. A typical form of a local supersymmetry transformation on a gravitino is given by  $\delta\Psi_M \sim \partial_M\epsilon + \dots$ . The massless spectrum of a closed superstring contains two gravitinos; therefore there are two  $\epsilon$ . A supersymmetric theory containing two  $\epsilon$  is called  $\mathcal{N} = 2$ . So the massless spectrum of a closed string gives an  $\mathcal{N} = 2$  supergravity theory. The name of the supergravity theory is related to the name of the associated superstring theory; type IIA and type IIB superstring theories give type IIA and type IIB supergravity theories. It is indeed possible to construct type IIA and type IIB supergravity theories (see, for example, a standard textbook [10]).

It can be shown, by counting states, that the number of bosonic degrees of freedom and the number of fermionic degrees of freedom in the closed string spectrum matches at each energy level. This suggests that the superstring theory has spacetime supersymmetry. An approach called the Green-Schwarz (GS) formalism [20] makes the spacetime supersymmetry manifest at the action level. This approach naturally supersymmetrises the Nambu-Goto action. A bosonic string worldsheet  $(\tau, \sigma)$  is embedded into a target superspace  $(X^M, \Theta^1, \Theta^2)$ . This means that the spacetime coordinates are extended to include fermionic coordinates  $\Theta^1, \Theta^2$ .

In this approach, the number of spacetime dimensions and the number of  $\epsilon$  are not specified *a priori*. Consistency conditions at classical level determine possible values of

$D$  and  $\mathcal{N}$ . We are particularly interested in the case of  $D = 10, \mathcal{N} = 2$ . Furthermore, let us consider a flat bosonic spacetime. In this case, the bosonic spacetime coordinates  $X^M$  transform as a vector in  $SO(1, 9)$ . So they give 8 on-shell bosonic degrees of freedom. However, the fermionic spacetime coordinates contain 16 on-shell degrees of freedom. This is because each of  $\Theta^1$  and  $\Theta^2$  is described by a Majorana-Weyl spinor. A Dirac spinor in ten dimensions has  $2^{\lfloor 10/2 \rfloor} = 32$  complex components. As discussed previously, Majorana and Weyl conditions reduce the number of components down to 16 real components. One also needs an on-shell condition which further reduces the number of components down to 8 real components. Therefore, the fermionic coordinates  $(\Theta^1, \Theta^2)$  have 16 fermionic on-shell degrees of freedom. To eliminate the mismatch between bosonic and fermionic degrees of freedom, an extra symmetry is needed. To obtain this extra symmetry, a new term is introduced into the action. As well as supersymmetry, the full action is invariant under a new symmetry called the  $\kappa$ -symmetry [21]. The  $\kappa$ -symmetry transformation provides a projector which projects out half the degrees of freedom of the fermionic spacetime coordinates.

One of the advantages of the GS formalism is that it can easily be generalised to the case of a curved target superspace. In this case, it is realised that the  $\kappa$ -symmetry requires background SUGRA fields to be on-shell [22]. Although it is very powerful at the classical level, the disadvantage of GS formalism is that it is very difficult to quantise.

Before we end this section, let us make a couple of remarks. The first remark is that there is a duality, called T-duality, which relates type IIA and type IIB superstring theories. For example, consider a type IIA superstring theory on a compactified spacetime which is  $\mathbb{R}^{1,8} \times S^1$  where the radius of  $S^1$  is given by  $R$ . This theory is dual to a type IIB superstring theory on a  $\mathbb{R}^{1,8} \times S^1$  spacetime where the radius of  $S^1$  is given by  $\alpha'/R$ .

The other remark concerns the construction of a superstring theory. We have discussed the RNS approach in which a supersymmetric worldsheet is embedded into a bosonic target space. We have also discussed the GS approach in which a bosonic worldsheet is embedded into a supersymmetric target space. It is therefore natural to ask if it is possible to supersymmetrise a string theory by embedding a supersymmetric worldsheet into a supersymmetric target space. This is indeed the case. This formalism, called the superembedding formalism, is constructed by the reference [23].

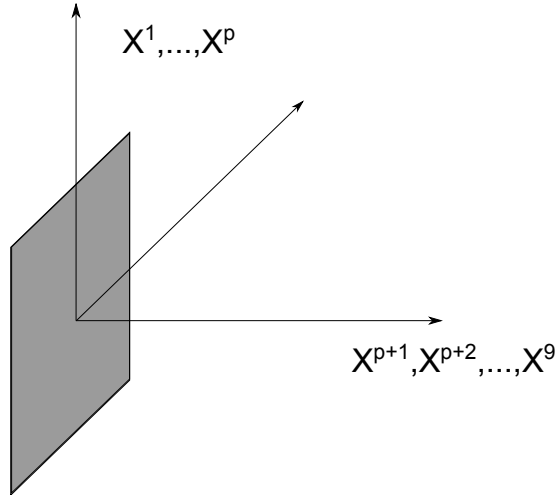


Figure 1.2: A single  $Dp$ -brane. This  $Dp$ -brane stretches along  $X^\mu$  directions, where  $\mu = 0, 1, \dots, p$ . The directions  $X^I, I = p + 1, \dots, 9$  are transverse to the  $Dp$ -brane. Note that the  $X^0$  direction is not shown in this figure.

## 1.3 D-branes

### 1.3.1 Single D-brane

Apart from strings, type IIA and type IIB superstring theories also contain objects called D-branes. The introduction of D-branes breaks symmetries of the underlying superstring theory. For example, D-branes in a flat spacetime break translational symmetry.

D-branes are extended hypersurfaces on which open strings end. In flat spacetime with Cartesian coordinates  $X^M, M = 0, 1, \dots, 9$ , using an appropriate frame of reference, a D-brane can be described as having coordinates  $X^\mu, \mu = 0, 1, \dots, p$  on its worldvolume, and  $X^I, I = p + 1, \dots, 9$  transverse to it. This D-brane is called a  $Dp$ -brane, where  $p$  denotes the number of spatial directions on the D-brane. A  $Dp$ -brane is illustrated in figure 1.2

D-branes couple to background fields which are created from a closed string spectrum. Let us restrict the discussions to the low energy limit, where the background fields are massless. We then focus on R-R gauge fields. Recall that in four dimensions, a gauge field is electrically or magnetically coupled to a point electric or magnetic charge. Consider a static electric or magnetic point charge in a four-dimensional flat spacetime written in terms of spherical coordinates

$$ds^2 = -dt^2 + dr^2 + r^2(d\theta^2 + \sin^2\theta d\phi^2). \quad (1.33)$$

The charge is located at the origin  $r = 0$ . In the case of an electric charge, the radial

direction of the electric field is given by

$$E_r = -\partial_r A_t = F_{tr}. \quad (1.34)$$

The electric charge is computed using the Gauss' law which instructs us to integrate the electric field over the sphere surrounding the electric charge:

$$\text{electric charge} = \int_{S^2} \vec{E} \cdot d\vec{S} = \int_{S^2} E_r r^2 \sin \theta d\theta d\phi = \int_{S^2} *F. \quad (1.35)$$

In the case of a magnetic charge, the radial direction of the magnetic field is given by

$$B_r = \frac{1}{r^2 \sin \theta} F_{\theta\phi}. \quad (1.36)$$

The magnetic charge is given by

$$\text{magnetic charge} = \int_{S^2} \vec{B} \cdot d\vec{S} = \int_{S^2} B_r r^2 \sin \theta d\theta d\phi = \int_{S^2} F. \quad (1.37)$$

The coupling of an R-R gauge field to a D-brane generalises this idea. Consider a  $Dp$ -brane which sources an R-R gauge field. There are  $9 - p$  directions which are transverse to the  $Dp$ -brane. These transverse directions are shown in figure 1.3. Let us decompose these directions into 1 radial direction and  $8 - p$  angular directions. These  $8 - p$  angular directions form an  $S^{8-p}$  which surrounds the  $Dp$ -brane. In order to compute the electric charge, one integrates  $*F$  over the asymptotic  $(8 - p)$ -sphere. That is

$$\text{electric charge} = \int_{S^{8-p}} *F. \quad (1.38)$$

This requires  $*F$  to be an  $(8 - p)$ -form, and hence  $F$  is a  $(p + 2)$ -form which is the field strength of a  $(p + 1)$ -form R-R gauge field. Similarly, in the case of magnetic charge, we have

$$\text{magnetic charge} = \int_{S^{8-p}} F. \quad (1.39)$$

Therefore,  $F$  is an  $(8 - p)$ -form which is the field strength of a  $(7 - p)$ -form R-R gauge field. In other words, if we set  $q = 6 - p$ , then a  $(q + 1)$ -form R-R gauge field is magnetically coupled to a  $D(6 - q)$ -brane.

So for  $p = -1, 0, 1, 2, 3$ , a  $(p + 1)$ -form R-R gauge field is electrically coupled to a  $Dp$ -brane and is magnetically coupled to a  $D(6 - p)$ -brane. In this sense, a  $D(6 - p)$ -brane is magnetic dual to a  $Dp$ -brane. In a special case where  $p = 3$ , a D3-brane actually carries both electric and magnetic charges. This corresponds to the fact that a D3-brane couples to a 4-form R-R gauge field which has a self-dual field strength.

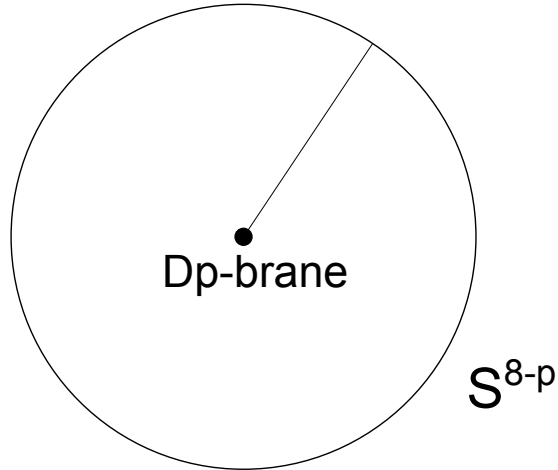


Figure 1.3: A hyperplane transverse to a  $Dp$ -brane. The  $Dp$ -brane which is seen as a dot in this figure is surrounded by an  $(8-p)$ -sphere.

$Dp$ -branes with  $p = -1, 0, 1, 2, 3$  carry electric charges while  $Dp$ -branes with  $p = 7, 6, 5, 4, 3$  carry magnetic charges.  $Dp$ -brane charges  $\mu_p$  are quantised according to Dirac-Teitelboim-Nepomechie charge quantisation condition [24–26] which is given by  $\mu_p \mu_{6-p} = 2\pi n$ ,  $n \in \mathbb{Z}$ . For D3-branes, each of them carries both electric and magnetic charges. Furthermore, the electric and magnetic charges have the same magnitude. The charge quantisation condition is modified [27, 28] to  $\mu_3 \mu'_3 + \mu'_3 \mu_3 = 2\pi n$ ,  $n \in \mathbb{Z}$ , where primed and unprimed notations denote charges of different D3-branes.

D-branes carrying charges are stable. In a type IIA superstring theory, stable D-branes are D0, D2, D4, D6 since R-R gauge fields are of odd-forms. In a type IIB superstring theory, stable D-branes are D(-1), D1, D3, D5, D7 since R-R gauge fields are of even-forms. By using T-duality, D8-branes can also be included into a type IIA superstring theory. Similarly, D9-branes can also be included into a type IIB superstring theory.

States on a stable  $Dp$ -brane can be obtained by quantising open strings which end on that  $Dp$ -brane. The lowest energy states are massless. The bosonic sector consists of  $9-p$  scalar fields and a gauge field. The total on-shell degrees of freedom of the bosonic sector is then  $(9-p) + (p-1) = 8$ . The fermionic sector consists of spinors which have 8 total on-shell degrees of freedom. The reason that degrees of freedom of fermions and bosons are the same is because the  $Dp$ -brane is supersymmetric.

A supersymmetric  $Dp$ -brane action can be obtained by using a similar approach to that of a superstring action. Although it is not known how to apply the RNS formalism (worldvolume supersymmetry), it is possible to apply the GS formalism (spacetime

supersymmetry). The action is given in the references [29–31].

Let us discuss some of the symmetries of a supersymmetric  $Dp$ -brane in a ten-dimensional flat spacetime. The  $Dp$ -brane is invariant under an  $SO(1, p)$  Lorentz symmetry. The  $9 - p$  scalar fields transform under an  $SO(9 - p)$  internal symmetry. The D-brane also has supersymmetry. There are two ten-dimensional Majorana-Weyl spinors  $\epsilon^1, \epsilon^2$  of supersymmetry transformation. Together these spinors have 32 independent real components. The  $\kappa$ -symmetry projects out half of this number. So there remains 16 independent real components. We thus say that this D-brane has 16 supercharges.

Let us now turn to a supersymmetric  $Dp$ -brane in a more general background. For applications in chapters 2 and 3, we are only interested in the bosonic part of a  $Dp$ -brane action. The bosonic part of background fields contains a metric  $G_{MN}$ , an NS-NS 2-form gauge field  $B_{MN}$ , a dilaton  $\Phi$  and R-R  $n$ -form gauge fields  $C^{(n)}$ . The bosonic part of worldvolume fields contains  $9 - p$  scalar fields encoded in an embedding function  $X^M(\xi^\mu)$ , and a gauge field  $A_\mu$  with field strength  $F_{\mu\nu} = \partial_\mu A_\nu - \partial_\nu A_\mu$ . The bosonic part of the worldvolume action is given by

$$S = S_{DBI} + S_{WZ}, \quad (1.40)$$

where the first part is the DBI action [32, 33]:

$$S_{DBI} = -T_{Dp} \int d^{p+1} \xi e^{-\Phi} \sqrt{-\det(g_{\mu\nu} + \mathcal{F}_{\mu\nu})}, \quad (1.41)$$

where

$$g_{\mu\nu} = P[G]_{\mu\nu} = \frac{\partial X^M}{\partial \xi^\mu} \frac{\partial X^N}{\partial \xi^\nu} G_{MN}, \quad (1.42)$$

$$\mathcal{F}_{\mu\nu} = 2\pi\alpha' F_{\mu\nu} + b_{\mu\nu}, \quad b_{\mu\nu} = P[B]_{\mu\nu} = \frac{\partial X^M}{\partial \xi^\mu} \frac{\partial X^N}{\partial \xi^\nu} B_{MN}, \quad (1.43)$$

$$\mu, \nu = 0, 1, \dots, p, \quad M, N = 0, 1, \dots, 9. \quad (1.44)$$

Here  $P[\dots]$  is a pull-back of a background field into the  $Dp$ -brane worldvolume. Note that we have made a shift in the dilaton field  $\Phi_{\text{original}} = \Phi + \log g_s$ , so the vacuum expectation value of  $\Phi$  is zero. We will adopt this convention throughout this thesis. The second part of the bosonic D-brane action is the Wess-Zumino (WZ) term

$$S_{WZ} = \mu_{Dp} \int \left( \sum_n P[C^{(n)}] \wedge e^{\mathcal{F}} \right)_{p+1}, \quad (1.45)$$

where the sum is over all background R-R gauge fields. The exponential is expressed formally as Taylor expansion with wedge product omitted. The  $(\dots)_{p+1}$  means that a  $(p + 1)$ -form should be extracted from the bracket.

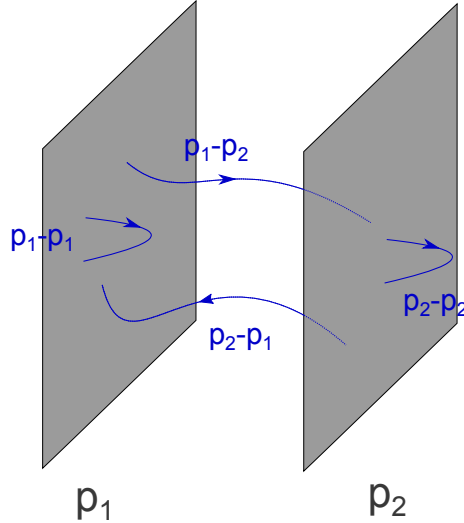


Figure 1.4: Two parallel but non-coincident D $p$ -branes with strings stretching between them.

In the D $p$ -brane worldvolume action,  $T_{Dp}$  is the D $p$ -brane tension which is given by

$$T_{Dp} = \frac{1}{(2\pi)^p g_s l_s^{p+1}}. \quad (1.46)$$

The quantity  $\mu_{Dp}$  is the D $p$ -brane charge<sup>1</sup>. Supersymmetry requires that

$$\mu_{Dp} = T_{Dp}. \quad (1.47)$$

We have discussed that a stable D $p$ -brane can be added into a type II superstring theory. It is also possible to add more than one D $p$ -brane and still get a stable configuration. There are several possible configurations. However, we will only state some configurations that are relevant to us.

### 1.3.2 Multiple D-branes

The first example of multiple D-branes that we will discuss is a set of  $N$  coincident D $p$ -branes. At low energy, the matter contents of this system is not simply  $N$  multiples of the contents from a single low-energy D $p$ -brane. Instead, the degrees of freedom get enhanced due to the coincidence of the D $p$ -branes.

This is easily seen from the open string point of view. Consider two parallel but non-coincident D $p$ -branes which are shown in figure 1.4. Let us label them as  $p_1$  and  $p_2$ . There are four types of open strings which stretch from these D $p$ -branes.

<sup>1</sup>The D $p$ -brane charge discussed here has a different normalisation from that discussed previously. Notice that the symbol  $\mu_{Dp}$  here is differed from the symbol  $\mu_p$  which is used previously.

- A  $p_1 - p_1$  string where both endpoints are on the  $p_1$ .
- A  $p_1 - p_2$  string where one endpoint is at the  $p_1$  while another is at the  $p_2$ .
- A  $p_2 - p_1$  string where one endpoint is at the  $p_2$  while another is at the  $p_1$ .
- A  $p_2 - p_2$  string where both endpoints are on the  $p_2$ .

Note that the strings are oriented, so it is necessary to distinguish between  $p_1 - p_2$  and  $p_2 - p_1$  strings. The spectrum of each of  $p_1 - p_1$  and  $p_2 - p_2$  strings contains massless states with matter contents the same as those discussed in the previous subsection. However, the spectrum of each of  $p_1 - p_2$  and  $p_2 - p_1$  strings generically contains no massless states. So these states are not relevant at low energy.

But when the two D-branes coincide, some states become massless. The field contents from each of  $p_1 - p_2$  and  $p_2 - p_1$  strings are the same as those from each of  $p_1 - p_1$  and  $p_2 - p_2$  strings. Note that even if the matter contents are the same, the strings are still distinguishable. The matter contents can in fact be realised as fields transforming in an adjoint representation of a  $U(2)$  gauge group. The internal degrees of freedom can collectively be represented by a  $2 \times 2$  matrix. Different strings are realised as different components of this matrix.

The discussion can be generalised to the case of  $N$  coincident  $Dp$ -branes. In this case, the massless fields transform under an adjoint representation of a  $U(N)$  gauge group. In fact, the  $U(N)$  gauge group can be decomposed as  $U(1) \times SU(N)$ . The  $U(1)$  part decouples from  $SU(N)$ . So  $N$  coincident  $Dp$ -branes contain massless fields which consist of 1 gauge field,  $9 - p$  scalar fields and fermionic superpartners. All these fields transform in an adjoint representation of an  $SU(N)$  gauge group.

The matter content suggests that, as in the case of a single  $Dp$ -brane, the coincident  $Dp$ -branes in a flat spacetime has 16 supercharges. However, the complete supersymmetric action is not known. In fact, it is already difficult to obtain a non-Abelian version of DBI action. Since the fields are non-Abelian, the ordering of the fields is important. For example, commutators that obviously vanish in single D-brane action have to be introduced at appropriate places in the coincident D-branes action. Attempts are carried out for example in [34–36]. The DBI action is obtained with the help of T-duality and is written using a symmetrised trace prescription. However, this action does not work beyond the fourth order in field strength [37–40]. Furthermore, the D-branes have to be in a static gauge, in which the embedding function is given by  $X^\mu = \xi^\mu, X^I = X^I(\xi^\mu)$ .

	$X^0$	$X^1$	$X^2$	$X^3$	$X^4$	$X^5$	$X^6$	$X^7$	$X^8$	$X^9$
$k$ D1-branes	•				•					
$N$ D3-branes	•	•	•	•						

Table 1.1: The D1/D3 brane intersection in a ten-dimensional flat spacetime.

This means that a subset of spacetime coordinates is identified with the worldvolume coordinates. Note that the non-Abelian WZ action can also be written down and is given by the reference [36].

Let us now consider  $N$  coincident D3-branes in a flat spacetime with all other background fields turned off. Up to the second order in field strength, the complete action can be obtained, and the worldvolume theory is an  $\mathcal{N} = 4$   $SU(N)$  super-Yang-Mills (SYM) theory in a four-dimensional flat spacetime. This theory is  $\mathcal{N} = 4$  because the 16 supercharges that the D3-branes possess are realised as forming 4 Weyl spinors in 4 dimensions. The matter content of this theory consists of a gauge field, four Weyl spinors, and six real scalars. These fields form a group called the  $\mathcal{N} = 4$  vector supermultiplet. Because of supersymmetry, all the fields in the supermultiplet transform in the adjoint representation of the gauge group, which in this case is  $SU(N)$ . Other properties of this theory will be discussed in section 1.4. For now, let us instead discuss other examples of multiple D-branes configurations.

Apart from multiple D-branes with 16 supercharges, it is also possible to construct systems that are still supersymmetric but has less amount of supersymmetry. We are interested in a particular case of D-brane intersections which has 8 supercharges.

Consider a stack of  $k$  coincident D1-branes and a stack of  $N$  coincident D3-branes in a ten-dimensional flat spacetime. The directions of D1-branes and D3-branes are given in table 1.1. The D3-branes are in  $X^0, X^1, X^2, X^3$  directions while the D1-branes are in  $X^0, X^4$  directions. The two stacks of D-branes intersect if they share the same position in  $X^5, X^6, \dots, X^9$  directions. For any value of  $k$  and  $N$ , the system has 8 supercharges.

More generally, intersecting D-branes have 8 supercharges if the total number of directions that only one stack of D-branes span is equal to 4 or 8. In the above example of the D1/D3 system, such directions are  $X^1, X^2, X^3, X^4$ , so there are 4 in total.

The D1/D3 system can be explained from the point of view of either D-branes stack. However, we are mainly interested in looking at D3-branes worldvolume. Although the action of multiple D3-branes has 16 supercharges, the solution which corresponds to the

D1/D3 brane intersection preserves only 8 supercharges. The solution is static, and in the case of  $k = 1, N = 2$ , it contains a non-Abelian gauge field and a scalar field transforming in an adjoint representation of an  $SU(2)$  gauge group. The solution is recognised as a non-Abelian 't Hooft-Polyakov monopole in the BPS limit. This non-Abelian monopole is smooth everywhere. Furthermore, it has  $SU(2)$  gauge symmetry at its core, but the gauge group is broken to  $U(1)$  asymptotically. We will give a further review of this solution in chapter 5.

### 1.3.3 D-branes as solutions of supergravity

We have been looking at low energy stable D-branes from the worldvolume perspective. Alternatively, D-branes can be viewed as solutions of type IIA/IIB supergravity theories. But before we discuss these solutions, let us first review how to obtain a trivial solution of the type IIA/IIB supergravity theories.

A solution of the type IIA/IIB supergravity theories can be obtained by solving equations of motion of the theories. A trivial solution is given by setting the metric flat:  $G_{MN} = \eta_{MN}$ , and turning off the other fields. This solution is simply a ten-dimensional flat spacetime. If we consider a local supersymmetry transformation of this solution, we see that

$$\delta\Psi_M^i(X) = \partial_M\epsilon^i(X), \quad i = 1, 2, \quad (1.48)$$

while local supersymmetry transformations of the other fields are trivially satisfied. In order to see if a solution preserves supersymmetry, one looks for  $\epsilon^i(X)$  which make local supersymmetry transformations vanish, and counts the total number of independent real components of these  $\epsilon^i(X)$ . In this trivial case, the vanishing of the local supersymmetry transformations implies that  $\partial_M\epsilon^i(X) = 0$ . Therefore,  $\epsilon^i$  are arbitrary constant spinors. Because each of the  $\epsilon^i$  is a ten-dimensional Majorana-Weyl spinor which has 16 independent real components, there are in total 32 independent real components from all the  $\epsilon^i$ . With this results, we say that the ten-dimensional flat spacetime preserves (all of the) 32 supercharges.

Let us now turn to solutions which correspond to D-branes. A solution called extremal  $p$ -brane solution is associated to a stack of  $N$  coincident stable  $Dp$ -branes in flat spacetime. Some of the symmetries of this solution are the same as that of D-branes. For example, this solution has  $SO(1, p) \times SO(9 - p)$  isometry, meaning that the metric is invariant under the group  $SO(1, p) \times SO(9 - p)$ . This group is identified with the Lorentz group  $SO(1, p)$  and the internal symmetry group  $SO(9 - p)$  of the  $Dp$ -branes. Furthermore, the extremal

$p$ -brane solution preserves 16 supercharges which is the same amount of supersymmetries that  $Dp$ -branes have.

An extremal 3-branes solution is of relevant to us. The non-vanishing fields are given by [41, 42]

$$\begin{aligned} ds^2 &= H^{-1/2}(-dt^2 + dx_1^2 + dx_2^2 + dx_3^2) + H^{1/2}(dr^2 + r^2 d\Omega_5^2), \\ F^{(5)} &= \pm(1 + *)dt dx_1 dx_2 dx_3 dH^{-1}, \end{aligned} \quad (1.49)$$

where

$$\begin{aligned} F^{(5)} &= dC^{(4)}, \\ H &= 1 + \frac{R^4}{r^4}, \quad R^4 = 4\pi g_s \alpha'^2 N, \end{aligned} \quad (1.50)$$

and  $d\Omega_5^2$  is a metric of a unit  $S^5$ . The sketch of the geometry of this solution is given in figure 1.5. Note that the  $\pm$  sign of  $F^{(5)}$  in fact only depends on orientation, so without loss of generality, we can choose either  $+$  or  $-$  sign. Note also that we have omitted the wedge product  $\wedge$  in the expression of  $F^{(5)}$ . The hyperplane  $t - x_1 - x_2 - x_3$  is interpreted as the D3-brane worldvolume while the other six directions are interpreted as transverse directions to the D3-branes. The electric and magnetic charges of the solution are given by integrating  $*F^{(5)}$  and  $F^{(5)}$  over the large  $S^5$  which surrounds the sources of the  $*F^{(5)}$  and  $F^{(5)}$  :

$$\int_{S^5} *F^{(5)} = \int_{S^5} F^{(5)} \propto N. \quad (1.52)$$

By using the charge quantisation condition, the quantity  $N$  is discrete. It can be interpreted as the number of D3-branes. This is because  $N$  D3-branes source the  $N$  units of the 5-form R-R charges. We will discuss more about the extremal 3-brane solution in section 1.4.

There are solutions called non-extremal black  $p$ -brane solutions [41], which break all the supersymmetry. These solutions contain outer and inner horizons. In the case where these horizons coincide the solution no longer has any horizon, and is identified with the extremal  $p$ -branes. Entropy of black  $p$ -branes can be obtained. In particular, the entropy of a near extremal black 3-brane solution is given by the reference [43]. The idea is to compute the area of the event horizon of the near extremal black 3-brane solution. This area is proportional to Bekenstein-Hawking entropy of the solution. The entropy scales as  $N^2$  which is identified with internal degrees of freedom of large  $N$  limit of  $SU(N)$  gauge group on the worldvolume of  $N$  coincident D3-branes.

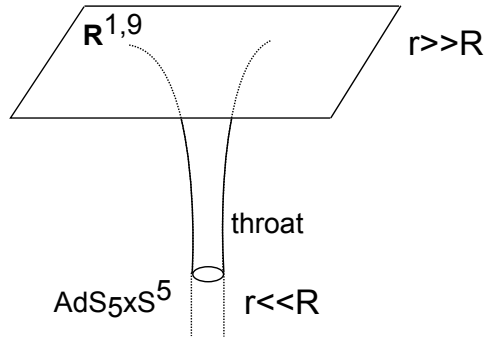


Figure 1.5: A sketch of the geometry of an extremal 3-brane solution.

## 1.4 Development: gauge/gravity duality

AdS/CFT correspondence [44] is a conjecture stating that a certain type of gauge theory is equivalent to a certain type of string theory. This correspondence and its generalisations are used to compute and describe physics of strongly coupled gauge theories which are tractable by only a few of other approaches.

### 1.4.1 Original AdS/CFT correspondence

Let us first motivate AdS/CFT correspondence in its original form. Consider a stack of  $N_c$  coincident D3-branes. We have seen in the previous section that there are two possible low-energy interpretations of the D-branes: either as an object on which open strings can end or as a solitonic solution of type IIB supergravity theory.

In the first low-energy interpretation of D3-branes, the action is of the form

$$S = S_{bulk} + S_{brane} + S_{int}. \quad (1.53)$$

$S_{bulk}$  describes the interactions between closed strings that propagate in the bulk. In the low energy limit where  $E \ll 1/\sqrt{\alpha'}$ , the closed strings become free. So gravitons, which are from spectrum of closed strings, are non-interacting. This gives rise to a flat spacetime. Similarly, the  $S_{int}$  part, which describes the interaction between closed and open strings, also vanishes in the low-energy limit. This implies that the D3-branes live in a ten-dimensional flat spacetime with other background fields turned off. As for  $S_{brane}$ , which is a worldvolume action on the D3-branes, its DBI part is reduced to YM in the low energy limit. Therefore it describes an  $\mathcal{N} = 4$   $SU(N_c)$  SYM theory in a four-dimensional Minkowski (flat Lorentzian) space.

Let us now consider the second low-energy interpretation. In the low-energy limit, type IIB superstring theory reduces to type IIB supergravity theory. The stack of D3-branes is then viewed as a supergravity solution which is given by the equation (1.49). Two limits of the metric are worth mentioning. The first limit is  $r \gg R$ , which is far away from the D3-branes. In this limit, the metric reduces to

$$ds^2 = -dt^2 + dx_1^2 + dx_2^2 + dx_3^2 + dr^2 + r^2 d\Omega_5^2, \quad (1.54)$$

which describes a ten-dimensional flat spacetime. The second limit is  $r \ll R$ , which is close to the D3-branes. This limit is also called the near-horizon limit. In this limit, the metric reduces to

$$ds^2 = \frac{r^2}{R^2}(-dt^2 + dx_1^2 + dx_2^2 + dx_3^2) + \frac{R^2}{r^2}(dr^2 + r^2 d\Omega_5^2), \quad (1.55)$$

which describes  $AdS_5 \times S^5$ . We say that the  $AdS_5$  part  $(t, x_1, x_2, x_3, r)$  of this metric is in the Poincaré coordinates. The full geometry of the equation (1.49) interpolates between a ten-dimensional flat spacetime and an infinite throat region with geometry  $AdS_5 \times S^5$ . In the low energy limit, only these two geometries are important. Consider closed string excitations in the full background geometry. The proper energy  $E_r$  of an object at a position  $r$  is observed by an observer at the asymptotic flat spacetime as

$$E = \frac{E_r}{\left(1 + \frac{R^4}{r^4}\right)^{1/4}}. \quad (1.56)$$

If the object gets closer to  $r = 0$ , its the energy as observed by an observer at infinity would appear to be lower. In the low energy limit  $E \ll 1/\sqrt{\alpha'}$ , the proper energy of a closed string near  $r = 0$  can become very large. As a result, the full spectrum of the quantised closed string should be considered. This gives a type IIB superstring theory in  $AdS_5 \times S^5$ . From the point of view of an observer at infinity, there are two kinds of low energy excitations: any excitation from the region which is very close to  $r = 0$  or low energy excitations in the asymptotic region  $r \gg R$ . These two kinds of excitations decouple from each other. An excitation near  $r = 0$  cannot escape to the asymptotic region  $r \gg R$ , while an excitation in the asymptotic region  $r \gg R$  cannot be captured by the branes which are very small when compared to the wavelength of the excitation.

Therefore, to a good approximation, this second low-energy interpretation describes two decoupled systems: type IIB superstring theory in  $AdS_5 \times S^5$  and a system of free closed strings in flat spacetime.

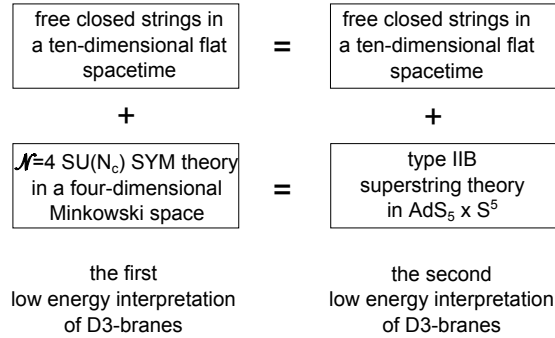


Figure 1.6: A diagram showing a motivation of AdS/CFT correspondence. The equivalence between the two low energy interpretations of D3-branes suggests that an  $\mathcal{N} = 4$   $SU(N_c)$  SYM theory in a four-dimensional Minkowski space is dual to a type IIB superstring theory in  $AdS_5 \times S^5$ .

In each of the low energy descriptions, there are two decoupled systems. Both descriptions have, in common, a system of free closed strings in a ten-dimensional flat spacetime. It is then natural to assume that the rest are equivalent. This means that an  $\mathcal{N} = 4$   $SU(N_c)$  SYM theory in a four-dimensional Minkowski space is expected to be equivalent (dual) to a type IIB superstring theory in  $AdS_5 \times S^5$ . The equivalence is called AdS/CFT correspondence. We summarise the results of the motivation in figure 1.6. Note that the background in which the type IIB superstring theory lives is in fact given by the full solution (1.49). We, however, usually mention only the metric.

The  $\mathcal{N} = 4$   $SU(N_c)$  SYM theory in a four-dimensional Minkowski space is invariant under a group called the conformal group which consists of four translations, six Lorentz generators, one scale transformation and four special conformal transformations. These fifteen generators form an  $SO(2, 4)$  algebra. The conformal invariance of this theory remains at the quantum level. Because of this property, this theory is called a conformal field theory (CFT). The implied invariance under the scaling transformation implies that this theory has no dimensionful scale. Since this theory has no length scale, it is characterised by dimensionless quantities which are a dimensionless coupling constant  $g_{YM}$  and a number  $N_c$  from the  $SU(N_c)$  gauge group.

For our purpose, AdS/CFT correspondence will be useful for studying the SYM theory at large  $N_c$  and strong coupling. As  $N_c \rightarrow \infty$ , the coupling of the SYM theory is better described by the 't Hooft coupling  $\lambda = g_{YM}^2 N_c$ . Therefore, by strong coupling, we mean  $\lambda \rightarrow \infty$ . In particular, consider the limit where  $g_{YM} \rightarrow 0, N_c \rightarrow \infty$  but  $\lambda$  is kept fixed. Then take the limit  $\lambda \rightarrow \infty$ .

When the SYM theory is in this strong coupling limit, the dual superstring theory in  $AdS_5 \times S^5$  becomes tractable. This can be seen by relating the dimensionless constants between the two theories. The dimensionless constants of the SYM theory are  $g_{YM}$  and  $N_c$  while the dimensionless constants of the string theory are  $g_s$  and  $R/\sqrt{\alpha'}$ . The relationships are

$$g_s = \frac{1}{2\pi} g_{YM}^2, \quad \frac{R^4}{\alpha'^2} = 2g_{YM}^2 N_c = 2\lambda. \quad (1.57)$$

Therefore, the limits in the field theory translates to  $g_s \rightarrow 0$  and  $R^4/\alpha'^2 \rightarrow \infty$ . In these limits the string theory reduces to classical supergravity.

Our discussions of AdS/CFT correspondence and its applications will be based on this limit. This means that we consider the case where  $\mathcal{N} = 4$   $SU(N_c)$  SYM theory in a four-dimensional Minkowski space at large  $N_c$  and strong coupling is dual to a classical type IIB supergravity in  $AdS_5 \times S^5$ . We will call the former as the field theory side while the latter as the gravity side.

We can also motivate the correspondence between the two theories by discussing symmetries. The field theory is invariant under the  $SO(2,4)$  conformal group. Furthermore, it is also invariant under a group called the R-symmetry group, which, in this case, is  $SU(4)_R$ . Recall that the matter content of this theory consists of a gauge field, four Weyl spinors, and six real scalars. The field theory's matter content transforms in this R-symmetry group as follows. The gauge field transforms in  $\mathbf{1}$ , the fermions in  $\mathbf{4}$  and the scalars in  $\mathbf{6}$  of the R-symmetry group. This means that the R-symmetry rotates each type of the fields among themselves. The conformal symmetry and R-symmetry are bosonic; that is, the generators of these symmetries transform bosons to bosons and fermions to fermions. The field theory also has fermionic symmetries, whose generators transform bosons to fermions and vice versa. This theory has 16 supercharges. Additionally, there are 16 real superconformal charges which are needed to ensure the closure of the algebra of the bosonic and fermionic symmetries. These bosonic and fermionic symmetries all together combine into a superconformal group  $SU(2, 2|4)$ .

This symmetry group can also be realised from the gravity side. The  $AdS_5$  part,  $(t, x_1, x_2, x_3, r)$ , of the equation (1.55) is by definition the solution of the embedding of the hypersurface

$$X_0^2 + X_5^2 - \sum_{n=1}^4 X_n^2 = R^2, \quad (1.58)$$

into an  $\mathbb{R}^{2,4}$  space with metric

$$ds^2 = -dX_0^2 - dX_5^2 + \sum_{n=1}^4 dX_n^2. \quad (1.59)$$

This solution is given by

$$\begin{aligned} X_0 &= \frac{R^2}{2r} + \frac{r}{2R^2} \left( R^2 + \sum_{j=1}^3 x_j x_j - t^2 \right), & X_5 &= \frac{r}{R} t, \\ X_i &= \frac{r}{R} x_i \quad (i = 1, 2, 3), \\ X_4 &= \frac{R^2}{2r} - \frac{r}{2R^2} \left( R^2 - \sum_{j=1}^3 x_j x_j + t^2 \right). \end{aligned} \quad (1.60)$$

Both the ambient metric (equation (1.59)) and the constraint (equation (1.58)) are invariant under the rotation group  $SO(2, 4)$ . Therefore, the  $AdS_5$  part has an isometry group  $SO(2, 4)$ . The  $S^5$  part of the metric (1.55) has an isometry group  $SO(6) \cong SU(4)$ . The fermionic symmetries are coming from preserved supercharges. Although the background (1.49) preserves only half the supersymmetry, its near-horizon limit  $r \ll R$  preserves all the supersymmetry. In other words,  $AdS_5 \times S^5$  has 32 supercharges. When combining the bosonic and fermionic symmetries, the full symmetry group of the gravity side is  $SU(2, 2|4)$  which is the same as the symmetry group of the field theory side.

Note that in fact the  $SU(2, 2|4)$  symmetry of the field theory side is a global symmetry while the  $SU(2, 2|4)$  symmetry of the gravity side is a gauge symmetry. This is an example of a correspondence between global symmetries of the field theory side and gauge symmetries of the gravity side.

Consider the  $AdS_5$  part of the metric (1.55). The  $r$  coordinate ranges from 0 to  $\infty$ . The  $G_{tt} = -r^2/R^2$  component of the metric is zero at  $r = 0$ , so there is a horizon at  $r = 0$ . We call this horizon as the Poincaré horizon. Another point of interest of this  $AdS_5$  is its boundary, which will be described in terms of the conformal boundary. A metric  $d\tilde{s}^2$  is conformally equivalent to a metric  $ds^2(X)$  if  $d\tilde{s}^2 = k^2(X)ds^2(X)$  for a function  $k(X)$ . Let us multiply the  $AdS_5$  part of the metric (1.55) by  $R^2/r^2$ , and then take the limit  $r \rightarrow \infty$ . We obtain

$$d\tilde{s}^2 \rightarrow -dt^2 + dx_1^2 + dx_2^2 + dx_3^2. \quad (1.61)$$

This is the conformal boundary of the Poincaré  $AdS_5$ . This conformal boundary is a four-dimensional Minkowski spacetime which can be identified with spacetime in which the field theory lives. In this way, the field theory side of the AdS/CFT correspondence can be thought of as living on the boundary of the gravity theory. This is also true in the

generalised version of AdS/CFT correspondence where the conformal boundary of the gravity side is no longer flat but the field theory still lives on this boundary.

Important quantities in a quantum field theory can be obtained by studying correlation functions, all of which are encoded in a generating functional. It is usually difficult to compute a generating functional of a generic quantum field theory. However, in the framework of AdS/CFT correspondence the calculations are much simpler. A generating functional of the field theory side can be obtained [45, 46] by computing a partition function in the dual gravity theory. More explicitly,

$$\langle e^{\int d^4x \phi_0(x) \mathcal{O}(x)} \rangle_{CFT} = Z_{SUGRA} \Big|_{\phi(x, \infty) = \phi_0(x)}, \quad (1.62)$$

where the left-hand side describes the generating functional of the field theory while the right-hand side describes the partition function in the gravity side. On the gravity side, one solves the equation of motion for the field  $\phi(x, r)$ , where  $x$  is a collective name for  $(t, x_1, x_2, x_3)$ . Then one computes the on-shell supergravity action, which in turn can be used to obtain the on-shell supergravity partition function  $Z_{SUGRA}$  and then evaluates at the boundary  $r \rightarrow \infty$ . This gives, via AdS/CFT correspondence, the generating functional of the field theory side. The field  $\phi_0(x)$  is identified with a source of the field theory operator  $\mathcal{O}(x)$ .

As an example, consider a massive scalar field in  $AdS_5$  which can be thought of as coming from a Kaluza-Klein (KK) reduction on  $S^5$  of the scalar field in the full  $AdS_5 \times S^5$  spacetime. This means that the scalar field  $\phi_{10D}(x, r, \Omega_5)$  in  $AdS_5 \times S^5$  is given by

$$\phi_{10D}(x, r, \Omega_5) = \sum_l \phi_l(x, r) Y_l(\Omega_5), \quad (1.63)$$

where  $Y_l(\Omega_5)$  is a spherical harmonics on  $S^5$  with a collection  $l$  of quantum numbers. The equation of motion is given by

$$\frac{\partial_r (r^5 \partial_r \phi)}{r^5} + \frac{R^4}{r^4} \left( -\frac{\partial^2}{\partial t^2} + \frac{\partial^2}{\partial \vec{x}^2} \right) \phi - \frac{m^2 R^2}{r^2} \phi = 0, \quad (1.64)$$

where  $\vec{x} = (x_1, x_2, x_3)$ . Note that  $m^2$  depends on quantum numbers of the spherical harmonics on  $S^5$ . Note also that we have omitted the index  $l$ . The asymptotic form of the solution of the above equation of motion is given by

$$\phi \rightarrow \frac{\phi_0(x)}{r^{4-\Delta}} + \frac{\phi_1(x)}{r^\Delta}, \quad (1.65)$$

where  $\Delta = 2 + \sqrt{4 + m^2 R^2}$ . Note that if  $m^2$  is considered arbitrary, this solution holds as long as  $m^2 R^2 \geq -4$ . This is an example of Breitenlohner-Freedman (BF) bound [47, 48].

From the asymptotic form, one can identify  $\phi_0(x)$  as a source of the corresponding operator  $\mathcal{O}(x)$  in the field theory, and identify  $\phi_1(x)$  as a vacuum expectation value (VEV) of the operator. Note that the VEV can also be obtained by a functional derivative of  $Z_{SUGRA}$ . In some cases, the on-shell supergravity action is infinite, so regularisations and renormalisations are needed to be applied before computing the action and  $Z_{SUGRA}$ .

Although there is still no concrete proof, it is widely believed that AdS/CFT correspondence can be extended. In the extended version, the field theory side does not need to be CFT, and the gravity side does not need to be AdS. We call this extended framework as gauge/gravity duality. It is often the case that several motivations of a given proposed duality are sufficient to start the investigation.

In our case, we want to extend the original AdS/CFT correspondence to study the field theory at finite temperature, finite volume, and containing flavour fields. Such models are in fact already available in the literatures. Let us discuss the cases that are relevant to us.

#### 1.4.2 Extension: finite temperature and finite size

So far, we have considered the field theory side which is at zero temperature and lives in an infinite space. We will also be interested in studying the field theory at finite temperature and lives in a compact space. This generalisation can be done simply by compactifying the Wick rotated time direction and making  $AdS_5$  to be in global coordinates.

Let us put the field theory in a compact space. This is equivalent to studying the gravity side with a metric

$$ds^2 = - \left( 1 + \frac{r^2}{R^2} \right) dt^2 + \frac{dr^2}{1 + \frac{r^2}{R^2}} + r^2 d\bar{\Omega}_3^2 + R^2 d\Omega_5^2. \quad (1.66)$$

We call this metric as the global  $AdS_5 \times S^5$  and call the  $AdS_5$  part  $(t, \bar{\Omega}_3, r)$  of this metric as the global  $AdS_5$ . Recall that the Poincaré  $AdS_5$  has the Poincaré horizon. On the contrary, the global  $AdS_5$  is smooth everywhere. The point  $r = 0$  in which the radius of the three-sphere shrinks to zero is called the AdS centre. Another difference between the Poincaré  $AdS_5$  and the global  $AdS_5$  is that while the boundary of the Poincaré  $AdS_5$  is  $\mathbb{R}^{1,3}$ , the boundary of the global  $AdS_5$  is  $\mathbb{R} \times S^3$ . The boundary of the global  $AdS_5$  is at  $r \rightarrow \infty$ . In order to obtain this boundary, we multiply the global  $AdS_5$  metric by  $1/(1 + r^2/R^2)$ , and then take the limit  $r \rightarrow \infty$ . This gives the boundary metric  $ds_{\text{boundary}}^2 = -dt^2 + R^2 d\bar{\Omega}_3^2$ . As in the case of the Poincaré  $AdS_5$ , the global  $AdS_5$  satisfies the equations (1.58) and (1.59). However, the Poincaré  $AdS_5$  covers only a part of the global  $AdS_5$ .

The temperature  $T$  can be added into the global  $AdS_5 \times S^5$  by Wick rotating the time

coordinate  $t \rightarrow \tau = it$ , then compactifying it on a circle  $\tau \sim \tau + \beta$ , and finally identifying the period with the inverse temperature  $\beta = 1/T$ . This temperature is identified with the temperature on the field theory side. The global  $AdS_5 \times S^5$  at finite temperature is valid for  $T \leq T_{HP} = 3/(2R)$ . For our application, if  $T < T_{HP}$ , the results will not depend on  $T$ . So whenever we consider  $T < T_{HP}$ , we will simply focus on zero temperature.

In the case  $T \geq T_{HP}$ , another metric is thermodynamically preferred. It is obtained [49] simply by introducing a black hole. The metric is given by

$$ds^2 = -\frac{2\rho_H^2}{uR^2} \frac{1-u^2}{1-\frac{uR^2}{4\rho_H^2}} dt^2 + \frac{2\rho_H^2}{u} \left(1 - \frac{uR^2}{4\rho_H^2}\right) d\Omega_3^2 + \frac{R^2}{4u^2(1-u^2)} du^2 + R^2 d\Omega_5^2. \quad (1.67)$$

This metric has an event horizon at  $u = 1$ , and a boundary at  $u = 0$ . The temperature whose inverse is identified with the period of the Wick rotated time coordinate which makes the near-horizon metric contain no conical singularity is called the Hawking temperature. For this metric, the Hawking temperature is given by

$$T = \frac{\sqrt{2}\rho_H}{\pi R^2 \sqrt{1 - \frac{R^2}{4\rho_H^2}}}, \quad (1.68)$$

which is identified with the temperature of the dual field theory. We will call this metric as  $(AdS - Schwarzschild)_5 \times S^5$  in the global coordinates, and call its AdS part as the global AdS-Schwarzschild.

In the  $TR \rightarrow \infty$  limit, the metric becomes

$$ds^2 = \frac{2\rho_H^2}{uR^2} (-(1-u^2)dt^2 + d\vec{x}^2) + \frac{R^2}{4u^2(1-u^2)} du^2 + R^2 d\Omega_5^2. \quad (1.69)$$

This metric has an event horizon at  $u = 1$ , and a boundary at  $u = 0$ . The Hawking temperature is

$$T = \frac{\sqrt{2}\rho_H}{\pi R^2}. \quad (1.70)$$

We will call this metric as  $(AdS - Schwarzschild)_5 \times S^5$  in the Poincaré coordinates, and call its AdS part as the Poincaré AdS-Schwarzschild. Before taking the  $TR \rightarrow \infty$  limit,  $R$  is the radius of the  $S^3$  in which the field theory lives. So one may interpret that in the  $TR \rightarrow \infty$  limit the dual field theory is at finite temperature and lives in the infinite-volume space. Alternatively, one can say that the field theory is at infinite temperature and lives in the finite-volume space. We will often adopt the former point of view.

Let us now try to visualise the  $AdS_5$  part of these spacetimes. We start with the global  $AdS_5$  metric.

$$ds^2 = -\left(1 + \frac{r^2}{R^2}\right) dt^2 + \frac{dr^2}{1 + \frac{r^2}{R^2}} + r^2 d\Omega_3^2 \quad (1.71)$$

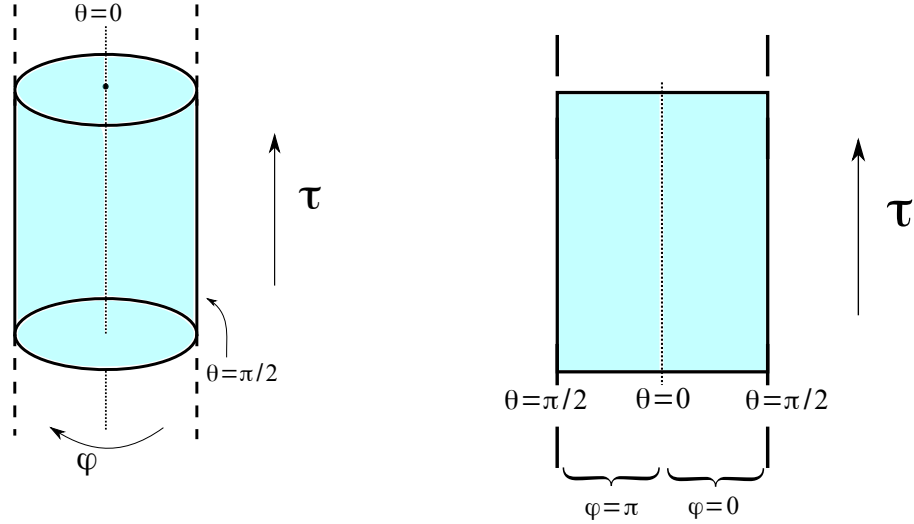


Figure 1.7: Illustrations of the space which is conformal to the global  $AdS_5$ .  $\tau$  is the time coordinate and is in the vertical direction.  $\theta$  is the radial coordinate of the global  $AdS_5$ , and is shown in the figure as the radial direction. The  $\theta = 0$  axis corresponds to the AdS centre, while the cylinder's boundary  $\theta = \pi/2$  corresponds to the AdS boundary.  $\varphi$  is the  $S^1$  representative of  $S^3$ , and is shown as the angular direction. The picture on the left shows the full cylinder. The picture on the right shows the cylinder's vertical slice which passes through the  $\theta = 0$  axis.  $\theta$  is increasing from 0 to  $\pi/2$  both to the left and to the right of the  $\theta = 0$  axis. The values of  $\varphi$  on the left and on the right of the  $\theta = 0$  axis are  $\varphi = \pi$  and  $\varphi = 0$ , respectively.

After the coordinate transformation:  $t = R\tau$ ,  $r = R \tan \theta$ , the metric becomes

$$ds^2 = \frac{R^2}{\cos^2 \theta} (-d\tau^2 + d\theta^2 + \sin^2 \theta d\Omega_3^2) \equiv \frac{R^2}{\cos^2 \theta} ds'^2. \quad (1.72)$$

Instead of visualising  $ds^2$ , it is simpler to visualise  $ds'^2$ . The range of  $\tau$  is  $-\infty < \tau < \infty$ , and the range of  $\theta$  is  $0 \leq \theta \leq \pi/2$ . For illustration propose, let us view  $S^3$  simply as  $S^1$ , that is, we replace  $d\Omega_3^2$  with  $d\varphi^2$ , where  $\varphi$  is in the range  $0 \leq \varphi < 2\pi$ . The AdS centre is at  $\theta = 0$ , while the AdS boundary is at  $\theta = \pi/2$ . We visualise this conformal space of global  $AdS_5$  in figure 1.7. We draw it in the cylindrical coordinate system in which  $\theta$  is the radial direction,  $\varphi$  is the angular direction, and  $\tau$  is the vertical direction. In the same figure, we also present the vertical slice which passes through the  $\theta = 0$  axis of this space.

Let us now turn to the Poincaré  $AdS_5$  metric

$$ds^2 = \frac{r^2}{R^2} (-dt^2 + dx_1^2 + dx_2^2 + dx_3^2) + \frac{R^2}{r^2} dr^2. \quad (1.73)$$

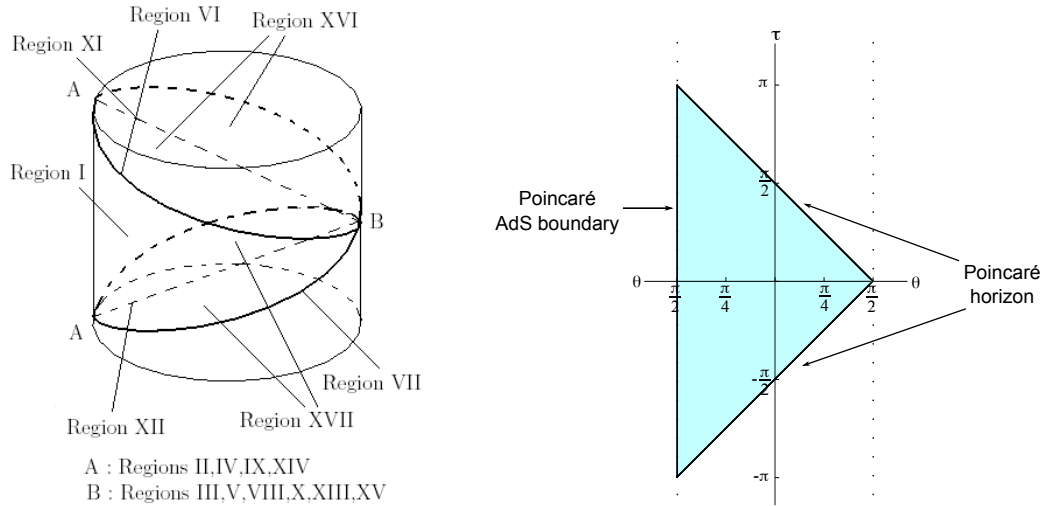


Figure 1.8: Illustrations of the space which is conformal to the Poincaré  $AdS_5$ . This space is embedded into the space of figure 1.7. The picture on the left is taken from figure 2(b) of the reference [5]. It shows that the conformal space to the Poincaré  $AdS_5$  occupies a wedge-like region within the cylinder. Region I represents the Poincaré AdS boundary while Regions VIII-XVII represent the Poincaré horizon. Details of these and other regions are discussed in the reference [5]. The picture on the right shows the cylinder's vertical slice which passes through the  $\theta = 0$  axis.  $\theta$  is increasing from 0 to  $\pi/2$  both to the left and to the right of the  $\theta = 0$  axis. The values of  $\varphi$  on the left and on the right of the  $\theta = 0$  axis are  $\varphi = \pi$  and  $\varphi = 0$ , respectively. The light blue shaded region corresponds to the  $(t, r)$  subspace at  $x_1 = x_2 = x_3 = 0$  of the Poincaré  $AdS_5$ .

Again, we want to visualise the space associated with the metric  $ds'^2$  which is defined via

$$ds^2 = \frac{R^2}{\cos^2 \theta} ds'^2, \quad (1.74)$$

where  $\theta$  here is the same as  $\theta$  in the metric (1.72). Since the Poincaré  $AdS_5$  is a part of the global  $AdS_5$ , it is possible to find the relationship between the coordinates  $(t, r, x_1, x_2, x_3)$  of the Poincaré  $AdS_5$  and the coordinates  $(\tau, \theta, \Omega_3)$  of the metric (1.72). The reference [5] thoroughly studied this relationship and show explicitly how the Poincaré  $AdS_5$  is contained within the global  $AdS_5$ . We reproduce their results in figure 1.8. This figure shows that the conformal space of the Poincaré  $AdS_5$  occupies a wedge-like region within the cylinder of the conformal space of the global  $AdS_5$ . The same figure also shows the vertical slice which passes through the  $\theta = 0$  axis. The resulting triangular region shows the  $(t, r)$  subspace at  $x_1 = x_2 = x_3 = 0$  of the Poincaré  $AdS_5$ .

Let us now visualise the global AdS-Schwarzschild. The metric is given by

$$ds^2 = -\frac{2\rho_H^2}{uR^2} \frac{1-u^2}{1-\frac{uR^2}{4\rho_H^2}} dt^2 + \frac{2\rho_H^2}{u} \left(1 - \frac{uR^2}{4\rho_H^2}\right) d\Omega_3^2 + \frac{R^2}{4u^2(1-u^2)} du^2. \quad (1.75)$$

It is useful to make the coordinate transformation

$$t = R\tau, \quad u = \frac{4\rho_H^2}{R^2} \frac{1}{(1+2\tan^2\theta)}. \quad (1.76)$$

This gives

$$ds^2 = \frac{R^2}{\cos^2\theta} \left( -g(\theta)dt^2 + \frac{d\theta^2}{g(\theta)} + \sin^2\theta d\Omega_3^2 \right) \equiv \frac{R^2}{\cos^2\theta} ds'^2, \quad (1.77)$$

where

$$g(\theta) = 1 - \frac{1}{4} \left( \frac{16\rho_H^4}{R^4} - 1 \right) \frac{\cos^4\theta}{\sin^2\theta}. \quad (1.78)$$

Since the metric (1.77) is put in the similar form as that of the metric (1.72), we can visualise the global AdS-Schwarzschild by following the steps similarly to those outlined in the case of the global  $AdS_5$ . The only difference is that  $\theta$  here is in the range  $\theta_H < \theta \leq \pi/2$ , where

$$\theta_H = \tan^{-1} \left( \frac{1}{\sqrt{2}} \sqrt{\frac{4\rho_H^2}{R^2} - 1} \right). \quad (1.79)$$

We show the conformal space of the global AdS-Schwarzschild and its slice in figure 1.9. In the figure, the black hole is depicted as a cylinder whose boundary at  $\theta = \theta_H$  corresponds to the black hole horizon. The value of  $\theta_H$  is increased as the temperature of the black hole increases.

Given the gravity theory on each of the  $AdS_5 \times S^5$  spacetimes, let us now try to see to what field theory this gravity theory corresponds. The motivation of the duality can be done by following the low energy limit discussion. The only metric that can be motivated in this way is (1.69). It can be realised (see for example [50]) as a near-horizon limit of a non-extremal black 3-brane solution which is a solution of type IIB supergravity theory.

Unlike the extremal 3-branes, the non-extremal black 3-brane solutions do not preserve supersymmetry. So we may expect that the worldvolume theory on the corresponding 3-brane in string theory also does not have supersymmetry. However, the matter content should be the same<sup>2</sup> as that of  $\mathcal{N} = 4$   $SU(N_c)$  SYM theory in a four-dimensional Minkowski space. Although supersymmetry is broken, we will sometimes call the theory as if it has  $\mathcal{N} = 4$ . This is just to remind us of the matter content. Note also that temperature introduces a scale. So the field theory is no longer conformal.

---

<sup>2</sup>Strictly speaking, the reference [49] states that in this case the supersymmetry is broken such that scalars and fermions gain mass and are ignored from the discussion.

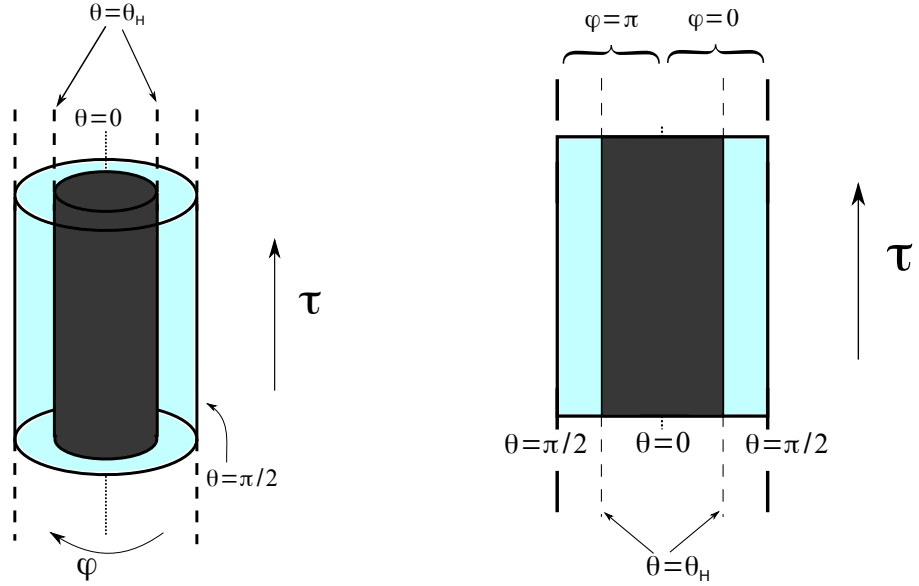


Figure 1.9: Illustrations of the space which is conformal to the global AdS-Schwarzschild.  $\tau$  is the time coordinate and is in the vertical direction.  $\theta$  is the radial coordinate of the global AdS-Schwarzschild, and is shown in the figure as the radial direction. The grey cylinder represents the black hole with horizon at  $\theta = \theta_H$ . The boundary  $\theta = \pi/2$  of the light blue cylinder corresponds to the AdS boundary.  $\varphi$  is the  $S^1$  representative of  $S^3$ , and is shown as the angular direction. The picture on the left shows the full cylinder. The picture on the right shows the cylinder's vertical slice which passes through the  $\theta = 0$  axis.  $\theta$  is increasing from 0 to  $\pi/2$  both to the left and to the right of the  $\theta = 0$  axis. The values of  $\varphi$  on the left and on the right of the  $\theta = 0$  axis are  $\varphi = \pi$  and  $\varphi = 0$ , respectively.

This motivates the correspondence between an  $\mathcal{N} = 4$   $SU(N_c)$  SYM theory with large  $N_c, \lambda$  in a four-dimensional Minkowski spacetime at finite temperature and type IIB supergravity theory in  $(AdS - Schwarzschild)_5 \times S^5$  in the Poincaré coordinates. In fact, the metric (1.69) is a part of the type IIB supergravity solution

$$\begin{aligned}
 ds^2 &= \frac{2\rho_H^2}{uR^2} (-(1-u^2)dt^2 + d\vec{x}^2) + \frac{R^2}{4u^2(1-u^2)} du^2 + R^2 d\Omega_5^2, \\
 F_5 &= \frac{4}{R} (1 + *) \left( \frac{2\rho_H^4}{R^3 u^3} dt dx_1 dx_2 dx_3 du \right) = \frac{4}{R} (1 + *) \text{Vol}(AdS_5),
 \end{aligned} \tag{1.80}$$

where  $\text{Vol}(AdS_5)$  is the volume form of the AdS part of the metric.

Let us now consider the other cases. The metrics (1.66) and (1.67) cannot be realised as coming from near-horizon limit of a certain solution of type IIB supergravity theory. However, we simply believe that the duality still applies. So in the case of (1.66) we say that an  $\mathcal{N} = 4$   $SU(N_c)$  SYM theory with large  $N_c, \lambda$  in  $\mathbb{R} \times S^3$  is equivalent to type IIB

supergravity theory in global  $AdS_5 \times S^5$  where the full background is given by

$$ds^2 = - \left( 1 + \frac{r^2}{R^2} \right) dt^2 + \frac{dr^2}{1 + \frac{r^2}{R^2}} + r^2 d\Omega_3^2 + R^2 d\Omega_5^2, \quad (1.81)$$

$$F_5 = \frac{4}{R} (1 + *) r^3 dt dr \text{Vol}(S^3) = \frac{4}{R} (1 + *) \text{Vol}(AdS_5),$$

where  $\text{Vol}(S^3)$  is a volume form of the unit  $S^3$ . This background is a solution of type IIB supergravity theory, but it is not a near-horizon limit of any known solution of type IIB supergravity theory. This solution has the isometries  $SO(2, 4)$  and  $SO(6)$  and preserves the full supersymmetry. So, the dual field theory should still have the same symmetry as its infinite volume counterpart. However, the generators of the conformal group  $SO(2, 4)$  are modified<sup>3</sup> in such a way that the conformal group no longer contains a scaling symmetry. This agrees with the fact that the theory now has a dimensionful scale which is the radius  $R$  of  $S^3$ .

Similarly, for the case of (1.67) we say that there is a correspondence between an  $\mathcal{N} = 4$   $SU(N_c)$  SYM theory with large  $N_c, \lambda$  in  $\mathbb{R} \times S^3$  at finite temperature and type IIB supergravity theory in global  $(AdS - Schwarzschild)_5 \times S^5$  where the full background is given by

$$ds^2 = - \frac{2\rho_H^2}{uR^2} \frac{1 - u^2}{1 - \frac{uR^2}{4\rho_H^2}} dt^2 + \frac{2\rho_H^2}{u} \left( 1 - \frac{uR^2}{4\rho_H^2} \right) d\Omega_3^2 + \frac{R^2}{4u^2(1 - u^2)} du^2 + R^2 d\Omega_5^2 \quad (1.82)$$

$$F_5 = \frac{4}{R} \left( \frac{2\rho_H^4}{u^3} \left( 1 - \frac{uR^2}{4\rho_H^2} \right) dt \text{Vol}(S^3) du \right) = \frac{4}{R} (1 + *) \text{Vol}(AdS_5),$$

which is a solution of type IIB supergravity theory.

### 1.4.3 Further extension: adding flavour fields

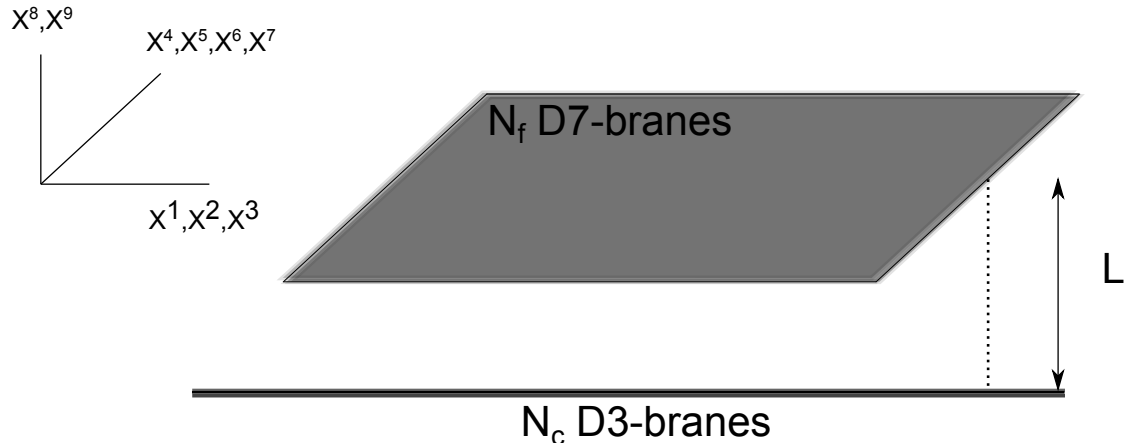
We have discussed the extension of AdS/CFT correspondence to the case where the field theory is at finite temperature and/or living in the compact space. We are now interested in making the field theory more resemblance to the real QCD. There are several directions to do this. However, we will only focus on a model called the D3/D7 model. This model is not the most efficient<sup>4</sup>, but it is relatively simple to compute, and its results can be used to give some insights into QCD-like systems.

<sup>3</sup>See for example [51] for generators of the conformal group  $SO(2, 4)$  on  $\mathbb{R} \times S^3$ .

<sup>4</sup>A more efficient model, called the Sakai-Sugimoto model [52, 53], describes a QCD-like system with  $N_f$  massless flavour fields having  $SU(N_f) \times SU(N_f)$  flavour group that is spontaneously broken down to  $SU(N_f)$ . This behaviour is in a close resemblance to the real QCD. The efficiency of Sakai-Sugimoto model is realised for example in the computation of meson masses which is in a reasonable agreement with experiments.

	$X^0$	$X^1$	$X^2$	$X^3$	$X^4$	$X^5$	$X^6$	$X^7$	$X^8$	$X^9$
$N_c$ D3-branes	•	•	•	•						
$N_f$ D7-branes	•	•	•	•	•	•	•	•		

Table 1.2: The D3/D7 system in a ten-dimensional flat spacetime.

Figure 1.10: The D3/D7 system in a ten-dimensional flat spacetime. The D3-branes and the D7-branes are separated by the distance  $L$ . In this figure, the  $X^0$  direction is omitted.

The matter content in the  $\mathcal{N} = 4$   $SU(N_c)$  SYM theory transforms in the adjoint representation of the gauge group. To move towards QCD, the D3/D7 model introduces multiplets which transform in a fundamental representation of the gauge group while still preserving as many supersymmetries as possible.

In the D3/D7 model, we consider a stack of  $N_c$  coincident D3-branes, and a stack of  $N_f$  coincident D7-branes. For simplicity, let us consider the case of a flat spacetime with coordinates  $X^M$ ,  $M = 0, 1, 2, \dots, 9$ . The D3-branes cover  $X^0, X^1, X^2, X^3$  while the D7-branes cover  $X^0, X^1, \dots, X^7$ . These two types of D-branes do not necessarily coincide; the stack of D7-branes can be separated from the stack of D3-branes. The setting is shown in table 1.2 and figure 1.10.

As in the case of the original AdS/CFT correspondence, here it is also possible to discuss the low energy limit. We consider a probe limit where  $N_f \ll N_c$ . In this case, the gravity side consists of closed strings and open 7–7 strings. The strings and branes live in  $AdS_5 \times S^5$  spacetime. In this probe limit D7-branes do not back-react on the background geometry. The field theory side of the correspondence contains open 3–3, 3–7, and 7–3 strings. The 3–3 strings give, as usual, the  $\mathcal{N} = 4$  vector supermultiplet. The

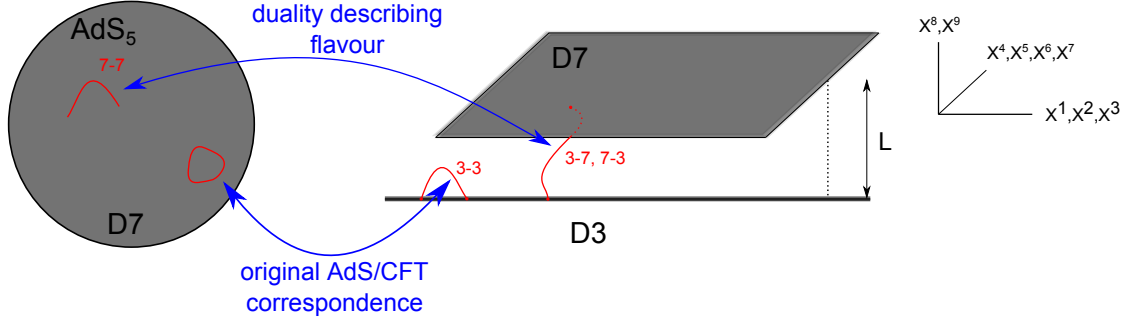


Figure 1.11: An illustration of gauge/gravity duality from the D3/D7 model. On the gravity side (left) D7-branes wrap around  $AdS_5 \times S^3$  within  $AdS_5 \times S^5$ . The relevant degrees of freedom are from the closed strings propagating in the bulk and the 7 – 7 strings on D7-branes. The  $S^5$  is not shown in the figure. On the field theory side (right), the relevant degrees of freedom are from the 3 – 3 strings which correspond to the closed strings and the 3 – 7, and 7 – 3 strings which correspond to the 7 – 7 strings on the gravity side. This figure is adapted from the figure 3.1 of the reference [6]

3 – 7 and 7 – 3 strings give  $N_f$  copies of the  $\mathcal{N} = 2$  hypermultiplets transforming in a fundamental representation of the  $SU(N_c)$  gauge group. An  $\mathcal{N} = 2$  hypermultiplet contains a Dirac spinor and two complex scalars. The R-symmetry group of the  $\mathcal{N} = 2$  hypermultiplet is given by  $SU(2)_R$ . The spinor transforms in  $\mathbf{1}$  while the scalars transform in  $\mathbf{2}$  of this R-symmetry group. Since the  $\mathcal{N} = 2$  hypermultiplets are introduced, the full supersymmetry of the theory is reduced to  $\mathcal{N} = 2$ . Because of supersymmetry, every field in the hypermultiplets has the same mass. If the D3-branes coincide with the D7-branes, then the hypermultiplets are massless. However, if the D7-branes are separated by the distance  $L$  from the D3-branes, then the hypermultiplets gain the mass  $m_q = L/(2\pi\alpha')$ .

Having motivated the correspondence, we present the statement. On the field theory side, there is an  $\mathcal{N} = 2$  SYM theory in a four-dimensional spacetime. The matter contents are from an  $\mathcal{N} = 4$  supermultiplet transforming in an adjoint representation of the  $SU(N_c)$  gauge group and from  $\mathcal{N} = 2$  hypermultiplets having  $SU(N_f)$  flavour symmetry and transforming in a fundamental representation of the  $SU(N_c)$  gauge group. On the gravity side, there is a stack of  $N_f$  D7-branes wrapping  $AdS_5 \times S^3$  within  $AdS_5 \times S^5$  spacetime. The correspondence is shown in figure 1.11.

Massless hypermultiplets on the field theory side corresponds to  $N_f$  D7-branes wrapping the whole of  $AdS_5$  and an equatorial  $S^3 \subset S^5$ . An embedding which gives massive hypermultiplets is more complicated. It is determined by minimising the area of the D7-

branes. Then the hypermultiplet mass is determined from how far the asymptotics of the D7-branes are from the origin of the  $X^8 - X^9$  plane.

Let us now discuss embeddings into each type of spacetimes and how to draw field theory informations from these embeddings.

### Low temperature $T \leq T_{HP}$ systems in an infinite space

For the  $AdS_5 \times S^5$  in the Poincaré coordinates, the part of the metric on the six-dimensional transverse space to the D3-branes is given by

$$\frac{R^2}{r^2}(dr^2 + r^2 d\Omega_5^2). \quad (1.83)$$

This part of metric is conformal to

$$dr^2 + r^2 d\Omega_5^2, \quad (1.84)$$

which is a six-dimensional flat metric. When visualising the six-dimensional transverse space to the D3-branes, it is often convenient to instead visualise the six-dimensional flat space which is conformal to the actual transverse space. We adopt this view point for the case of  $AdS_5 \times S^5$  in the Poincaré coordinates considered here and for the subsequent cases of the other  $AdS_5 \times S^5$  spacetimes. Let us express the metric part (1.84) into Cartesian coordinates. We can write

$$r^2 = (X^4)^2 + (X^5)^2 + (X^6)^2 + (X^7)^2 + (X^8)^2 + (X^9)^2, \quad (1.85)$$

as well as the relationships between  $\Omega_5$  and  $(X^4, X^5, \dots, X^9)$ . The full metric is then given by

$$ds^2 = \frac{r^2}{R^2}(-dt^2 + d\vec{x}^2) + \frac{R^2}{r^2}((dX^4)^2 + (dX^5)^2 + (dX^6)^2 + (dX^7)^2 + (dX^8)^2 + (dX^9)^2). \quad (1.86)$$

To describe the embedding of D7-branes, let us define

$$\rho^2 = (X^4)^2 + (X^5)^2 + (X^6)^2 + (X^7)^2, \quad (1.87)$$

$$L^2 = (X^8)^2 + (X^9)^2, \quad (1.88)$$

as well as the coordinates  $\Omega_3$  and  $\phi$ . The coordinates  $\rho$  and  $\Omega_3$  are polar coordinates of the hypersurface  $X^4 - X^5 - X^6 - X^7$  while  $L$  and  $\phi$  are polar coordinates of the hypersurface  $X^8 - X^9$ . The coordinates  $\Omega_3$  describe the  $S^3 \subset S^5$  which the D7-branes wrap. The coordinate transformation  $(t, \vec{x}, X^4, \dots, X^9) \rightarrow (t, \vec{x}, \rho, \Omega_3, L, \phi)$  gives

$$ds^2 = \frac{\rho^2 + L^2}{R^2}(-dt^2 + d\vec{x}^2) + \frac{R^2}{\rho^2 + L^2}(dL^2 + d\rho^2 + L^2 d\phi^2 + \rho^2 d\Omega_3^2). \quad (1.89)$$

Let us consider the D7-brane embedding which is given by  $(t, \vec{x}, \rho, \Omega_3) = (t, \vec{x}, \rho, \Omega_3)$  and  $L = L(\rho), \phi = 0$ . The equation which determines the embedding is given by

$$L''(\rho) + \frac{3}{\rho}L'(\rho) + L'(\rho)^3 = 0, \quad (1.90)$$

which is subject to the boundary conditions at the AdS boundary  $\rho \rightarrow \infty$  and at  $\rho = 0$ . Instead of solving this boundary value problem, it is more convenient to use a method called the shooting method to transform this problem into an initial value problem. In this case, let us consider the initial condition at  $\rho = 0$ . Numerically, it is not possible to impose the condition exactly at  $\rho = 0$ ; we need to make an expansion near  $\rho = 0$ . This gives

$$L(\rho) = L_0 + O(\rho^3). \quad (1.91)$$

Then we are instructed to solve the differential equation subject to this initial condition near  $\rho = 0$ , and match the solution with the asymptotic behaviour near  $\rho \rightarrow \infty$ :

$$L(\rho) = m + \frac{c}{\rho^2} + O\left(\frac{1}{\rho^3}\right). \quad (1.92)$$

The value of  $m$  is proportional to the dual field theory's  $\mathcal{N} = 2$  hypermultiplet mass, which we will simply call the quark mass. Since  $m$  is the distance between the D3- and D7-branes, the quantisation of the string stretching between these branes gives rise to the quark mass  $m_q = m/(2\pi\alpha')$ . The asymptotic expansion also determines the VEV of a quark bilinear operator  $\langle q\bar{q} \rangle$ , which in this case is proportional to the coefficient  $c$  of the sub-leading term.

Various embeddings are shown in figure 1.12. There are two kinds of embeddings which we will call the equatorial embedding and the Minkowski embedding. This figure visualises these embeddings by showing that while the equatorial embedding reaches all the way to the Poincaré horizon, the Minkowski embedding stops at some point above the Poincaré horizon. If we consider the  $AdS_5$  part, then we see that the equatorial embedding covers the whole  $AdS_5$  but the Minkowski embedding does not. These behaviours are visualised in figure 1.13. At each position on the  $AdS_5$  part of the D7-brane embedding, the D7-branes wrap an internal  $S^3 \subset S^5$ . This wrapping is shown in figure 1.14. It is characterised by an angle  $\theta$  which is given by

$$\theta = \tan^{-1}\left(\frac{L}{\rho}\right). \quad (1.93)$$

For example, for  $\theta = 0$ , the brane wraps the equatorial  $S^3$  of the  $S^5$  while for  $\theta = \pi/2$ , the  $S^3$  shrinks to a point at the pole of the  $S^5$ . In figure 1.15, we show the angle  $\theta$  for various D7-brane embeddings. The plot shows that the equatorial embedding wraps the

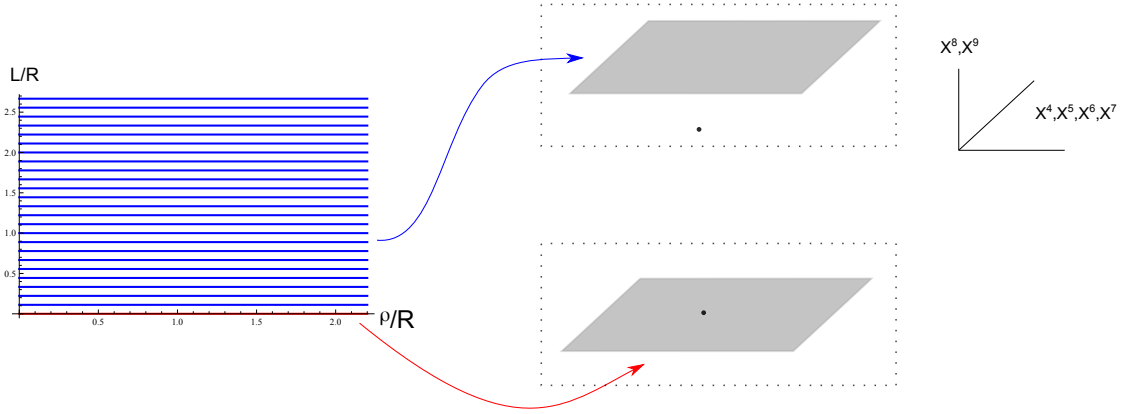


Figure 1.12: Examples of D7-brane embeddings into the Poincaré  $AdS_5 \times S^5$  spacetime. These pictures show the D7-brane embeddings from the point of view of the six-dimensional flat space which is conformal to the transverse space to the D3-branes. The plot on the left shows the embeddings plotted in the  $\rho - L$  plane. The red curve is called the equatorial embedding, for which the D7-branes cover the whole  $AdS_5$  part. The blue curves are called the Minkowski embeddings, for which the D7-branes do not cover the whole  $AdS_5$  part. These two kinds of embeddings are visualised by the pictures on the right. In these pictures, the black dots represent the positions of the  $X^1 - X^2 - X^3$  hyperplanes.

equatorial  $S^3$  of the  $S^5$  at every position  $r$ . The behaviours for the Minkowski embeddings are clearly different from this. Asymptotically as  $r \rightarrow \infty$ , a Minkowski embedding wraps the equatorial  $S^3$  of the  $S^5$ . However, as  $r$  is lowered, the  $S^3$  is shrinking, and at  $r = r_0 > 0$ , the  $S^3$  shrinks to a point. The value  $r_0$  is the shortest distance between this Minkowski embedding and the Poincaré horizon.

Having discussed the geometry of the embeddings, let us now discuss the asymptotic behaviour. The equatorial embedding has  $m = 0$  and  $c = 0$  while the Minkowski embeddings have  $m > 0$  and  $c = 0$ . Note that every embedding has  $c = 0$ . This behaviour, however will no longer be true when we discuss the embedding at finite temperature and/or finite space.

#### Low temperature $T \leq T_{HP}$ systems in a finite space

Let us now consider the embedding in global  $AdS_5 \times S^5$ . We need to change the radial coordinate to  $u$  which satisfies

$$\frac{dr^2}{1 + \frac{r^2}{R^2}} = R^2 \frac{du^2}{u^2}. \quad (1.94)$$

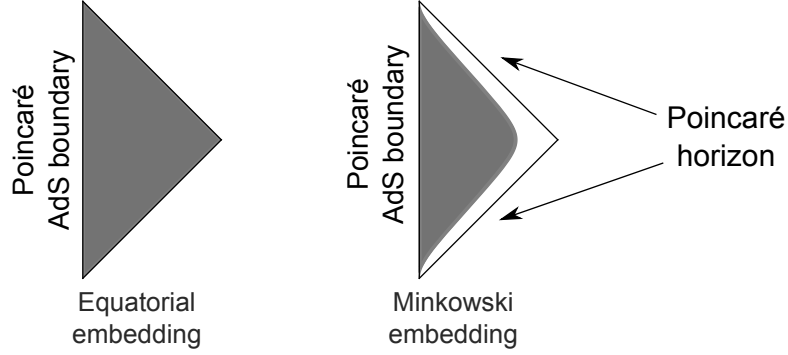


Figure 1.13: Schematic diagrams showing D7-brane embeddings into the  $AdS_5$  part of the Poincaré  $AdS_5 \times S^5$  spacetime. The Poincaré  $AdS_5 \times S^5$  spacetime is represented by the slice of its conformal space (see figure 1.8). These pictures show that for the equatorial embedding, the D7-branes (grey-coloured) fill the whole  $AdS_5$  part, but for the Minkowski embedding, the D7-branes fill from the AdS boundary down to some point outside the Poincaré horizon.

We choose [7]

$$u = \frac{r + \sqrt{r^2 + R^2}}{2}. \quad (1.95)$$

The AdS centre is now at  $u = R/2$  while the AdS boundary is at  $u \rightarrow \infty$ . In this coordinate system, the six-dimensional transverse space is conformal to the flat space with metric

$$du^2 + u^2 d\Omega_5^2. \quad (1.96)$$

At the AdS centre, the  $S^5$  in this space has the radius  $R/2$ . This  $S^5$  is just an artefact of this coordinate choice. Let us now describe the embeddings. Instead of  $(\rho, L)$ , it is more convenient to use  $(u, \chi = \sin \theta)$ . So the metric is now given by

$$ds^2 = -\frac{u^2}{R^2} \left(1 + \frac{R^2}{4u^2}\right)^2 dt^2 + u^2 \left(1 - \frac{R^2}{4u^2}\right)^2 d\bar{\Omega}_3^2 + \frac{R^2}{u^2} du^2 + R^2 \frac{d\chi^2}{1 - \chi^2} + R^2 \chi^2 d\phi^2 + R^2 (1 - \chi^2) d\Omega_3^2. \quad (1.97)$$

The equation which determines embeddings is given by

$$\chi''(u) + \frac{3R^2 \chi(u)}{u^2} + \frac{4u(R^4 + 4R^2 u^2 + 16u^4) \chi'(u)^3}{R(16u^4 - R^4)(1 - \chi(u)^2)} + \frac{(3R^5 + 16R^3 u^2 + 80R u^4) \chi'(u)}{16u^5 - R^4 u} + \frac{4\chi(u) \chi'(u)^2}{1 - \chi(u)^2} = 0. \quad (1.98)$$

Near the AdS centre, there are two main types of embeddings. Let us call them the Ball embedding and the Minkowski embedding. A Ball embedding has the expansion

$$\chi(u) = \chi_{\text{ball}} - \frac{3}{2R^2} \left(u - \frac{R}{2}\right)^2 \chi_{\text{ball}} + O((u - R/2)^3), \quad (1.99)$$

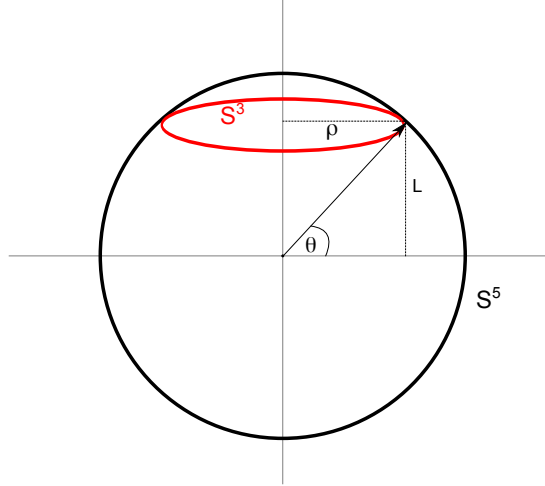


Figure 1.14: A part of a D7-brane embedding which wraps an internal  $S^3 \subset S^5$ . The big sphere represents  $S^5$  while the red circle represents  $S^3$ . The internal angle  $\theta$  characterises the position of the wrapped  $S^3$ .

where  $0 \leq \chi_{\text{ball}} \leq 1$ . For a Minkowski embedding, as in the case of its counterpart in Poincaré  $AdS_5 \times S^5$ , it does not reach the AdS centre. Instead, it ends at some point  $u = u_{\text{Mink}} > R/2$ . The expansion near  $u = u_{\text{Mink}}$  is given by

$$\begin{aligned} \chi(u) = & 1 + \frac{R^4 - 16u_{\text{Mink}}^4}{R^4 u_{\text{Mink}} + 4R^2 u_{\text{Mink}}^3 + 16u_{\text{Mink}}^5} (u - u_{\text{Mink}}) \\ & - \frac{2(68R^4 u_{\text{Mink}}^2 - 16R^2 u_{\text{Mink}}^4 - 384u_{\text{Mink}}^6 + 5R^6)}{3(4R^2 u_{\text{Mink}}^2 + 16u_{\text{Mink}}^4 + R^4)^2} (u - u_{\text{Mink}})^2 + O((u - u_{\text{Mink}})^3). \end{aligned} \quad (1.100)$$

There is in fact another type of embedding which is called the critical embedding. It satisfies the initial conditions of both the Ball and Minkowski embeddings. The expansion near  $u = R/2$  is given by

$$\chi(u) = 1 - \frac{2}{R^2} \left(u - \frac{R}{2}\right)^2 + \frac{4}{R^3} \left(u - \frac{R}{2}\right)^3 + O((u - R/2)^4). \quad (1.101)$$

Every type of embeddings has the same AdS boundary condition which is given by

$$\chi(u) = \frac{m}{u} + \frac{c_1}{u^3} - \frac{mR^2}{2u^3} \log \frac{u}{R} + O(u^{-4}). \quad (1.102)$$

We present the embeddings in figures 1.16, 1.17, and 1.18. There exists a Ball embedding which satisfies  $\chi = 0$ . As in the case of Poincaré  $AdS_5 \times S^5$ , this Ball embedding always wraps around the equatorial  $S^3 \subset S^5$ . So we call this embedding as the equatorial embedding.

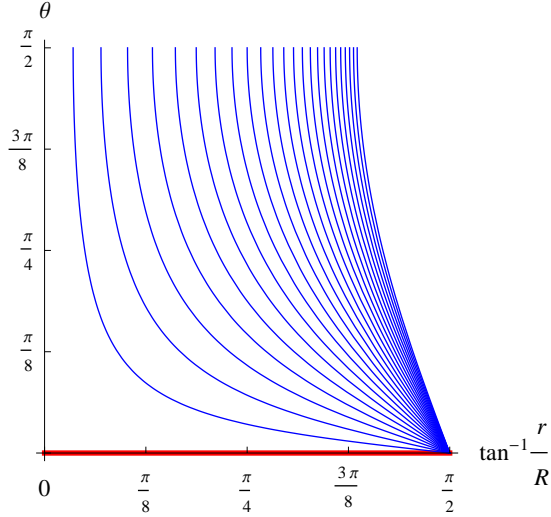


Figure 1.15: The internal angle  $\theta$  at each position  $r$  of the Poincaré  $AdS_5 \times S^5$ . The curves in this figure correspond to the curves presented in figure 1.12. This figure clearly shows the difference between the equatorial and Minkowski embeddings. The equatorial embedding reaches the AdS centre  $r = 0$ , and the internal angle  $\theta$  is always  $\theta = 0$  ( $S^3$  always wraps the equatorial of  $S^5$ ). On the other hand, the Minkowski embeddings have varying  $\theta$ , and they stop at some point at which  $\theta = \pi/2$  (which corresponds to the internal  $S^3$  shrinking to a point).

Out of possible embeddings, only the critical embedding is irregular; it contains conical singularities. Consider an induced metric of a D7-brane embedding:

$$ds^2 = -\frac{u^2}{R^2} \left(1 + \frac{R^2}{4u^2}\right)^2 dt^2 + u^2 \left(1 - \frac{R^2}{4u^2}\right)^2 d\bar{\Omega}_3^2 + \left(\frac{R^2}{u^2} + \frac{R^2 \chi'(u)^2}{1 - \chi(u)^2}\right) du^2 + R^2(1 - \chi(u)^2) d\Omega_3^2. \quad (1.103)$$

Let us expand this metric near  $u = R/2$  of the critical embedding. In order to do this, we make a change of coordinate  $u = R/2 + \xi/(2\sqrt{2})$ . This gives

$$ds^2 \approx -dt^2 + \frac{\xi^2}{2} d\bar{\Omega}_3^2 + d\xi^2 + \frac{\xi^2}{2} d\Omega_3^2, \quad (1.104)$$

which shows conical singularities at both external  $S^3$  (whose metric is  $d\bar{\Omega}_3^2$ ) and internal  $S^3$  (whose metric is  $d\Omega_3^2$ ); if there were to be no conical singularity, the numerical coefficients in front of  $\xi^2 d\bar{\Omega}_3^2$  and  $\xi^2 d\Omega_3^2$  should have been 1 instead of 1/2. On the contrary, the other embeddings are smooth everywhere. Each of them could potentially become singular at the position where the  $S^3$  shrinks to a point. At the AdS centre of a Ball embedding, the

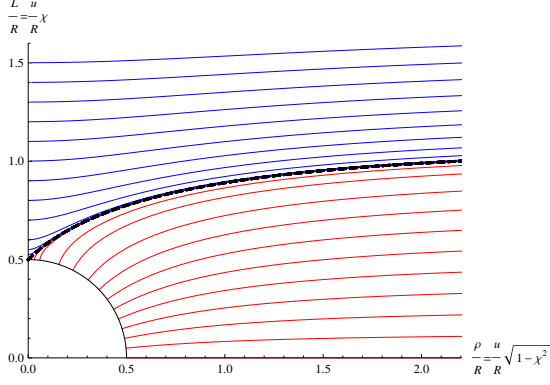


Figure 1.16: Examples of D7-brane embeddings into the global  $AdS_5 \times S^5$  spacetime. The red curves represent ball embeddings, the blue curves represent Minkowski embeddings, and the black dashed curve represents the critical embedding. The idea of this figure is from figure 1 in the reference [7].

external  $S^3$  shrinks to a point. The expansion around this point gives

$$ds^2 \approx -dt^2 + \xi^2 d\bar{\Omega}_3^2 + d\xi^2 + R^2(1 - \chi_{\text{ball}}^2) d\Omega_3^2, \quad (1.105)$$

where  $\xi = 2u - R$ . Clearly, there is no conical singularity. Similarly, at the tip of a Minkowski embedding, the internal  $S^3$  shrinks to a point. The expansion around this point gives

$$ds^2 \approx -\frac{(4u_{\text{Mink}}^2 + R^2)^2}{16R^2 u_{\text{Mink}}^2} dt^2 + \frac{(4u_{\text{Mink}}^2 - R^2)^2}{16u_{\text{Mink}}^2} d\bar{\Omega}_3^2 + d\xi^2 + \xi^2 d\Omega_3^2, \quad (1.106)$$

where

$$\xi^2 = \frac{2R^2(u - u_{\text{Mink}})(16u_{\text{Mink}}^4 - R^4)}{u_{\text{Mink}}(4R^2u_{\text{Mink}}^2 + 16u_{\text{Mink}}^4 + R^4)}. \quad (1.107)$$

Again, there is no conical singularity.

The on-shell action of the D7-branes is given by

$$S_{D7} = -T_{D7} N_f R^7 \int d\Omega_3 d\bar{\Omega}_3 dt du \frac{u^4}{R^4} \left(1 + \frac{R^2}{4u^2}\right) \left(1 - \frac{R^2}{4u^2}\right)^3 \left(\frac{1}{u^2} + \frac{\chi'^2}{1 - \chi^2}\right)^{1/2} (1 - \chi^2)^{3/2}. \quad (1.108)$$

The free energy of the embedding is given by  $-S_{D7}$ . However, this value is not finite; a regularisation is needed to be performed before computing the free energy. We follow the discussions outlined in the references [54, 55]. Let us define

$$\begin{aligned} S_0 &= -\frac{S_{D7}}{T_{D7} N_f R^7 \int d\Omega_3 d\bar{\Omega}_3 dt} \\ &= \int_{R/2}^{\infty} du \frac{u^4}{R^4} \left(1 + \frac{R^2}{4u^2}\right) \left(1 - \frac{R^2}{4u^2}\right)^3 \left(\frac{1}{u^2} + \frac{\chi'^2}{1 - \chi^2}\right)^{1/2} (1 - \chi^2)^{3/2} \end{aligned} \quad (1.109)$$

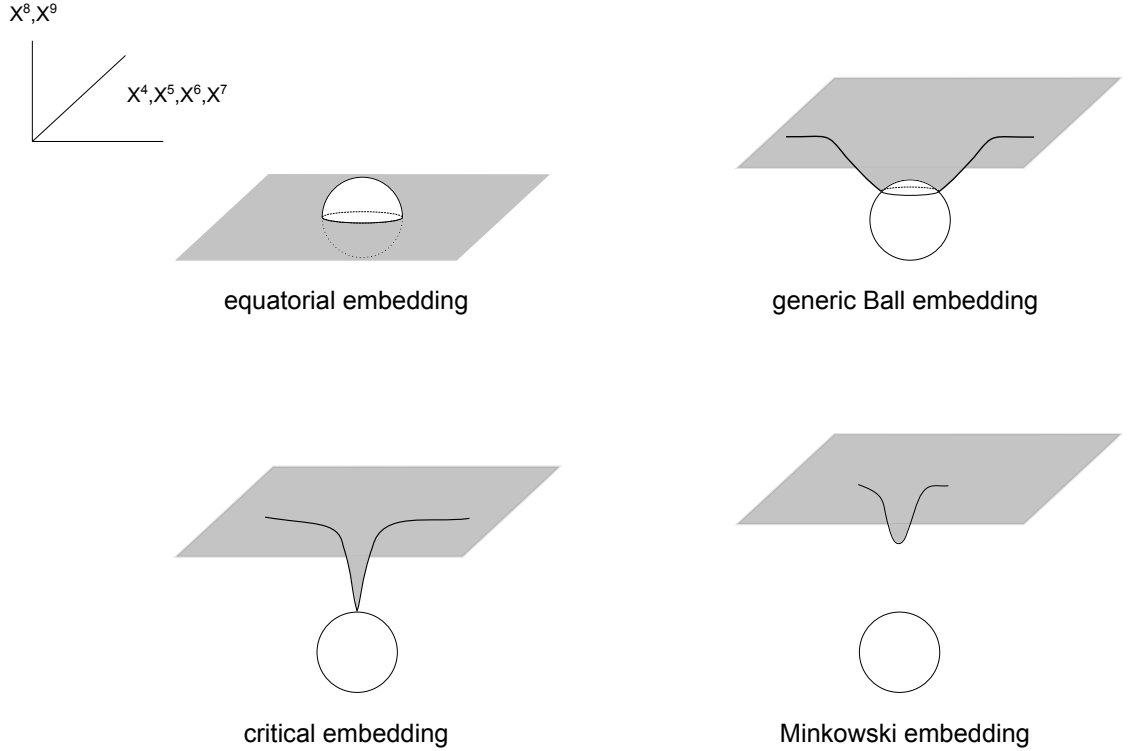


Figure 1.17: Various D7-brane embeddings in global  $AdS_5 \times S^5$ . The pictures are shown in the six-dimensional flat space conformal to the actual transverse space. Each blank sphere represents  $S^5$  with a radius  $R/2$  at the AdS centre. These spheres are artefacts of coordinate choice we use.

The divergence of this action is due to the behaviour near the AdS boundary. To fix this problem, the integral over  $u$  should be from  $R/2$  to  $R/(2\epsilon)$  for a small  $\epsilon$ . Consider the  $AdS_5$  part. The hypersurface perpendicular to the  $u$  direction at  $u = R/(2\epsilon)$  has a metric

$$ds_\gamma^2 = \gamma_{\mu\nu} dx^\mu dx^\nu = -\frac{(1+\epsilon^2)^2}{4\epsilon^2} dt^2 + \frac{R^2(1-\epsilon^2)^2}{4\epsilon^2} d\bar{\Omega}_3^2. \quad (1.110)$$

The Ricci scalar  $R_\gamma$  is given by

$$R_\gamma = \frac{6}{R^2} \frac{4\epsilon^2}{(1-\epsilon^2)^2}. \quad (1.111)$$

The counter-terms are given by

$$L_1 = -\frac{1}{4} \frac{\sqrt{-\gamma}}{R^6 \sin \bar{\theta} \cos \bar{\theta}} = -\frac{1}{64\epsilon^4} (1+\epsilon^2)(1-\epsilon^2)^3, \quad (1.112)$$

$$L_2 = \frac{1}{48} \frac{\sqrt{-\gamma} R_\gamma}{R^4 \sin \bar{\theta} \cos \bar{\theta}} = \frac{(1-\epsilon^4)}{32\epsilon^2}, \quad (1.113)$$

$$L_4 = \frac{1}{2} \frac{\sqrt{-\gamma} \chi_\epsilon^2}{R^6 \sin \bar{\theta} \cos \bar{\theta}} = \frac{1}{32\epsilon^4} (1+\epsilon^2)(1-\epsilon^2)^3 \chi_\epsilon^2, \quad (1.114)$$

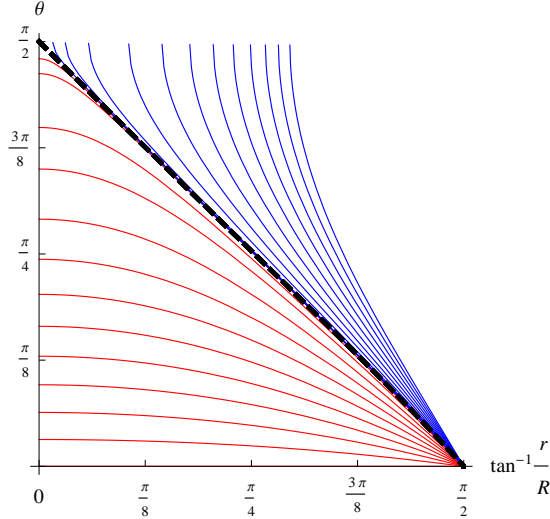


Figure 1.18: The internal angle  $\theta$  at each position  $r = (4u^2 - R^2)/(4u)$  of the global  $AdS_5 \times S^5$ . The curves in this figure correspond to the curves presented in figure 1.16. This figure clearly shows that while all the Ball embeddings reach the AdS centre  $r = 0$ , the Minkowski embeddings stop at some point at which  $\theta = \pi/2$  (which corresponds to the internal  $S^3$  shrinking to a point). The critical embedding interpolates between these two kinds of embeddings, and reaches the AdS centre  $r = 0$  when  $\theta = \pi/2$ .

$$L_5 = \frac{1}{24} \frac{\sqrt{-\gamma} R_\gamma}{R^4 \sin \bar{\theta} \cos \bar{\theta}} \log(\chi_\epsilon^2) \chi_\epsilon^2 = \frac{(1 - \epsilon^4)}{16\epsilon^2} \log(\chi_\epsilon^2) \chi_\epsilon^2, \quad (1.115)$$

$$L_f = -\frac{1}{4} \frac{\sqrt{-\gamma}}{R^6 \sin \bar{\theta} \cos \bar{\theta}} \chi_\epsilon^4 = -\frac{1}{64\epsilon^4} (1 + \epsilon^2)(1 - \epsilon^2)^3 \chi_\epsilon^4, \quad (1.116)$$

where

$$\chi_\epsilon \equiv \chi \left( \frac{R}{2\epsilon} \right). \quad (1.117)$$

The subtracted action is given by

$$S_{\text{sub}} = S_0 + L_1 + L_2 + L_4 + L_5 + L_f. \quad (1.118)$$

The scaled free energy is given by

$$F = \lim_{\epsilon \rightarrow 0} S_{\text{sub}}, \quad (1.119)$$

and the condensate is proportional to

$$c = -\lim_{\epsilon \rightarrow 0} \frac{R^6}{16\epsilon^3} \frac{R^3}{\sqrt{-\gamma}} \sin \bar{\theta} \cos \bar{\theta} \frac{\delta S_{\text{sub}}}{\delta \chi_\epsilon} = c_1 - \frac{mR^2}{2} \log \left( \frac{m}{R} \right). \quad (1.120)$$

These quantities are plotted in figure 1.19. They are not multivalued for any given quark mass. This implies that the phase transition between the Ball embeddings and the Minkowski embeddings is continuous. The reference [8] shows that the phase transition is of third order.

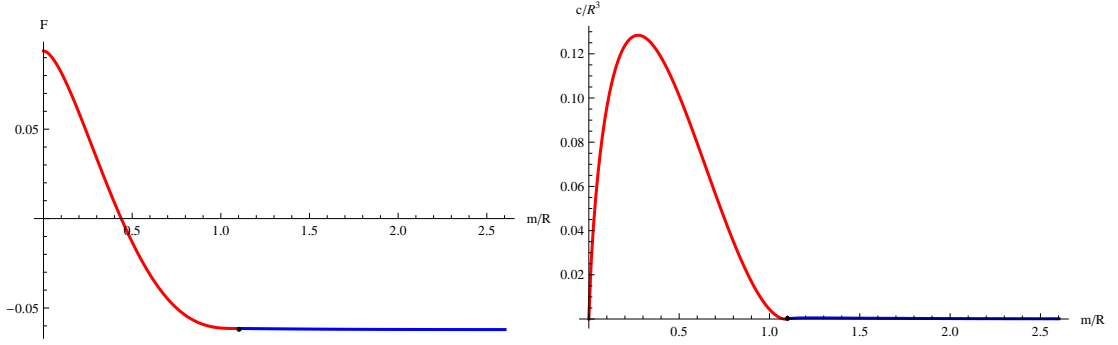


Figure 1.19: Free energy (left) and condensate (right) versus quark mass. For each plot, the red curve presents the data from Ball embeddings, the blue curve from Minkowski embeddings, and the black dot from the equatorial embedding. These plots show the smooth phase transition between the Ball embedding phase and the Minkowski embedding phase. The reference [8] shows that the phase transition is of third order.

### High temperature $T \geq T_{HP}$ systems

Let us now briefly discuss the embeddings into an  $(AdS - Schwarzschild)_5 \times S^5$  spacetime. For our purposes, the discussions in the cases of infinite and finite volume are similar, so we consider them together. The embeddings are shown in figure 1.20. There are two main kinds of embeddings: the Black Hole embeddings for which the branes pierce through the event horizon, and the Minkowski embeddings for which the branes close off before reaching the horizon. These two types are separated by the critical embedding. Within the class of the Black Hole embeddings, there exists the equatorial embedding for which the branes always wrap around the equatorial  $S^3 \subset S^5$ . In this thesis, for the systems with  $T \geq T_{HP}$ , we only consider the equatorial embedding.

### Mesonic excitations

Having discussed the embeddings, we are now interested in describing mesons on the field theory side. This corresponds to studying certain fluctuations of D7 worldvolume fields transforming in an adjoint representation of the  $SU(N_f)$  gauge group.

The meson mass spectrum can be obtained by studying normal modes of the corresponding fields on gravity side. This means that one needs to require the fields to be regular everywhere and to vanish at the AdS boundary. The frequency of a field which satisfies this condition tells us about the value of the meson mass in the dual field theory. For the case of finite temperature, the mesons are not stable, and cannot be described in

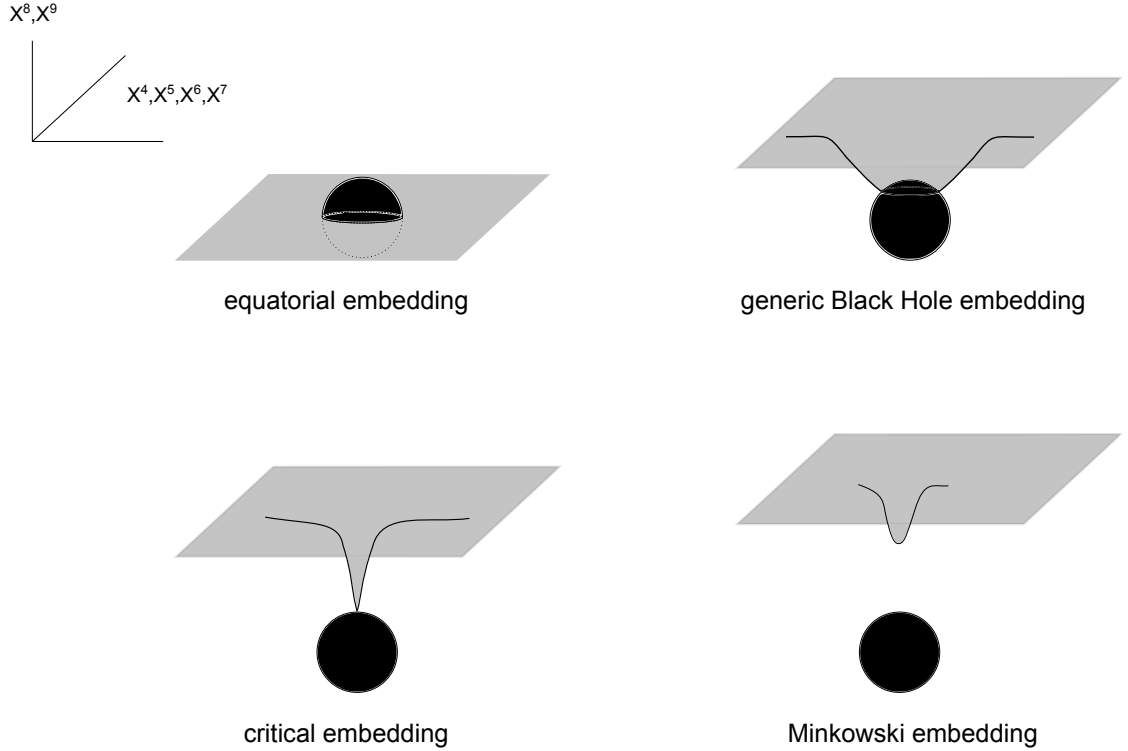


Figure 1.20: Various D7-brane embeddings in  $(AdS - Schwarzschild)_5 \times S^5$ . The pictures are shown in the six-dimensional flat space conformal to the actual transverse space. Each sphere represents the black hole.

terms of normal modes. Instead, one has to determine both the mass and the decay rate. These informations are encoded in complex frequencies which can be determined from the quasi-normal modes (QNM) of the corresponding fields on the gravity side. In this case, one demands the fields to be ingoing waves near the black hole horizon, and to vanish at the AdS boundary.

In our study, we will limit ourselves to the case of  $N_f = 2$ . The  $SU(2)$  flavour symmetry is historically called isospin symmetry. It appears in a QCD Lagrangian if up and down quarks are of the same mass and there is no other quark flavours. The up and down quarks are eigenstates of  $\tau_3 \equiv \sigma_3/2$  with eigenvalues  $1/2$  and  $-1/2$  respectively. Here,  $\sigma_3$  is the third component of the Pauli spin matrices. The flavour fields in our case can be described in a similar way.

Initially, there are equal numbers of the ‘up’ and ‘down’ flavours. We want to introduce the imbalance of the numbers. This can be done by introducing an isospin chemical potential. On the gravity side, this is equivalent to introducing a gauge field  $A_0^{(3)}$  on D7-branes. The subscript 0 means that the field is in the time direction while the superscript

(3) means that it is in the  $\tau_3$  direction of the gauge group.

After turning on the isospin chemical potential, the mass spectrum of mesonic excitations will be changed. When the isospin chemical potential reaches a certain value, we expect that the system is unstable. In the finite temperature case, the instability is demonstrated when an oscillation of a field corresponding to a meson keeps growing over time. In other words, its complex frequency has a positive imaginary part. In the zero temperature case, it is more difficult to determine the instability. A potential situation is when a meson has a zero frequency. If the isospin chemical potential is increased further, then there is a possibility that the meson can develop a frequency with a positive imaginary part.

When the old system is unstable, a new system is developed. In other words, the system undergoes a phase transition. In our case, mesons are condensed in the new system. The order parameter of the phase transition is given by VEV of the mesons.

In chapter 2 and 3, we will demonstrate how to use gauge/gravity duality to describe and investigate instabilities of  $\mathcal{N} = 2$  systems living in a compact space.

## 1.5 M-theory branes

The discussions so far have covered some aspects of superstring theory and its applications. There is another direction which we want to cover. This concerns M-theory, and will be discussed in the rest of this chapter and in chapters 4 and 5.

There are 5 types of consistent superstring theories. They are called type I, type IIA, type IIB, heterotic  $E_8 \times E_8$ , and heterotic  $SO(32)$ . We discussed type IIA and IIB superstring theories in the previous sections. The type I superstring theory can be obtained from the type IIB superstring theory by requiring that strings are unoriented. This means that one projects out the states which are not invariant under the worldsheet parity operation:  $\sigma^1 \rightarrow -\sigma^1$ . This operation exchanges the left- and right-moving oscillation modes of a closed string, so for example, only one of the two gravitinos survives this projection. This will imply that the type I superstring theory has  $\mathcal{N} = 1$ . In addition to the unoriented closed string, the theory also contains unoriented open strings. The heterotic theories are obtained by combining the left-movers of 26-dimensional bosonic strings with the right-movers of 10-dimensional superstrings. The heterotic theories also have  $\mathcal{N} = 1$  supersymmetry.

Different types of superstring theories are related by dualities. For example, T-duality

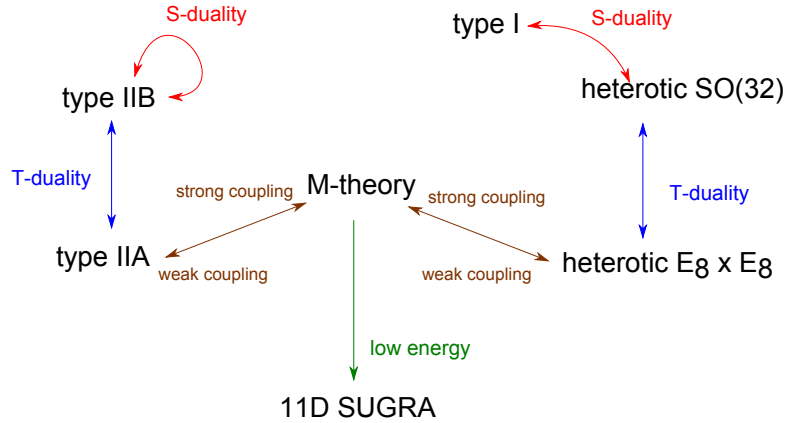


Figure 1.21: Examples of string dualities. This web of dualities suggests how to obtain string theories and the eleven-dimensional supergravity from the M-theory.

relates type IIA to type IIB, and relates heterotic  $E_8 \times E_8$  to heterotic  $SO(32)$ . Another duality called S-duality relates one theory at weak coupling to another theory at strong coupling. For example, type I is related to heterotic  $SO(32)$  while type IIB is related to itself. A type IIA superstring theory at a strong coupling has an extra dimension which is a circle of radius  $g_s l_s$ . So the strong coupling  $g_s \rightarrow \infty$  theory has eleven dimensions. This theory is called M-theory, and was discovered in the reference [56]. Additionally, a strong coupling heterotic  $E_8 \times E_8$  theory has an extra dimension as a line interval of size  $g_s l_s$ . The eleven dimensional strong coupling  $g_s \rightarrow \infty$  theory obtained this way is again M-theory. Furthermore, the low energy limit of M-theory is given by an eleven-dimensional supergravity theory [57]. Examples of these string dualities are shown in figure 1.21.

M-theory does not have any strings or any perturbative objects, so its matter contents cannot be obtained from the same approach as that of string theories. Nevertheless, since the low energy limit of M-theory is an eleven-dimensional supergravity theory, whose Lagrangian is known [58], the matter content of low-energy M-theory is just the matter content of an eleven-dimensional supergravity theory. The bosonic part contains a graviton (44 degrees of freedom) and a 3-form gauge field (84 degrees of freedom) while the fermionic part has a gravitino (128 degrees of freedom). All of these fields are massless.

As in the case of string theory, there are objects charged under a form field. In the case of M-theory, these objects are called M-branes. Since there is only one type of form fields, the types of M-branes are limited. There are M2-branes which are electrically coupled to the 3-form gauge field and M5-branes which are magnetically coupled to the 3-form gauge field.

Recall that in type IIA and IIB supergravity theories, there are extremal  $p$ -brane solutions which are associated to multiple  $Dp$ -branes of type IIA and IIB superstring theories. In the eleven-dimensional supergravity theory, the solutions associated to M2-branes and M5-branes can be obtained. The entropies of these solutions can also be computed. They scale as  $N^{3/2}$  and  $N^3$  for M2-branes and M5-branes respectively, where  $N$  is the number of coincident M-branes. These entropy scalings are clearly differed from the case of D-branes whose entropy scalings  $N^2$  are associated to internal degrees of freedom of Yang-Mills theories. One is not familiar with the  $N^{3/2}$  and  $N^3$  scalings of internal degrees of freedom. From this point of view, it is a puzzle to determine a non-Abelian theory to which the stack of multiple M-branes is related. Fortunately, the case of coincident M2-branes is already known. However, there is still no known complete low-energy worldvolume Lagrangian for M5-branes.

The matter content on M-brane worldvolumes can be obtained by considering the symmetries which are broken by the associated supergravity solution. For each broken symmetry, there is a massless field called the Goldstone mode. These fields form the matter content of the associated M-branes. For an M2-brane, there are 8 scalar fields in the bosonic sector and 8 on-shell fermionic degrees of freedom in the fermionic sector. For an M5-brane, the bosonic sector consists of 5 scalar fields and a 2-form gauge field with a self-dual field strength. The 2-form gauge field has 3 on-shell degrees of freedom. The fermionic sector contains 8 on-shell fermionic degrees of freedom which are given by 2 (symplectic) Majorana spinors.

### 1.5.1 M2-branes

The low-energy description of the theory on a single M2-brane is known. It was first obtained by the GS formalism [59] and later by the superembedding approach [23]. The extension to the case of multiple M2-branes is non-trivial because there is no 1-form gauge field in the matter content. Nevertheless, a 1-form gauge field can be introduced as long as it does not have any degree of freedom. In this case, the gauge field is technically the Chern-Simons gauge field.

The maximally supersymmetric  $\mathcal{N} = 8$  multiple M2-brane theory is given by the Bagger-Lambert-Gustavsson (or BLG) model [60–63]. This model uses a 3-bracket  $[\cdot, \cdot, \cdot]$  which is a generalisation of a commutator  $[\cdot, \cdot]$ . Let  $T^a$  be a generator of the 3-bracket algebra. The commutation relation is given by

$$[T^a, T^b, T^c] = f^{abc}{}_d T^d, \quad (1.121)$$

where  $f$  is totally anti-symmetric in the upper indices  $a, b, c$ . The metric is given by

$$h^{ab} = \text{tr}(T^a, T^b). \quad (1.122)$$

It is used to raise and lower the indices, for example  $f^{abcd} = f^{abc}{}_e h^{ed}$ . The 3-bracket is used to define the derivative:

$$\delta_{A,B}X \equiv [A, B, X]. \quad (1.123)$$

The derivative on the 3-bracket has the property:

$$\delta_{A,B}[X, Y, Z] = [\delta_{A,B}X, Y, Z] + [X, \delta_{A,B}Y, Z] + [X, Y, \delta_{A,B}Z], \quad (1.124)$$

and the trace should be invariant:

$$0 = \delta_{A,B}\text{tr}(X, Y) = \text{tr}(\delta_{A,B}X, Y) + \text{tr}(X, \delta_{A,B}Y). \quad (1.125)$$

These conditions give the fundamental identity

$$\begin{aligned} [T^a, T^b, [T^c, T^d, T^e]] &= [[T^a, T^b, T^c], T^d, T^e] + [T^c, [T^a, T^b, T^d], T^e] \\ &+ [T^c, T^d, [T^a, T^b, T^e]], \end{aligned} \quad (1.126)$$

as well as

$$\text{tr}([T^a, T^b, T^c], T^d) + \text{tr}(T^c, [T^a, T^b, T^d]) = 0. \quad (1.127)$$

The appearance of the 3-bracket in the BLG model is seen for example in the scalar potential which is of the form  $\text{tr}([X^I, X^J, X^K], [X^I, X^J, X^K])$ , where  $I, J, K = 1, 2, \dots, 8$ . The BLG model can be well-defined as long as one can find a 3-algebra which satisfies the above properties. It is shown [64,65] that the only non-trivial finite-dimensional 3-algebra with positive definite metric  $h^{ab}$  is given by

$$f^{abcd} \propto \epsilon^{abcd}, \quad h^{ab} \propto \delta^{ab}, \quad a, b, c, d \in \{1, 2, 3, 4\}. \quad (1.128)$$

This algebra is called  $\mathcal{A}_4$ . The BLG Lagrangian with  $\mathcal{A}_4$  describes 2 coincident M2-branes. If one relaxes the requirement that the 3-algebra is to be finite-dimensional, one can have the Nambu-Poisson bracket. On a three-dimensional manifold  $N_3$  with coordinates  $\{y^1, y^2, y^3\}$ , the Nambu-Poisson bracket is locally given by (here  $y$  is the collective name for  $\{y^1, y^2, y^3\}$ )

$$\{f^1(y), f^2(y), f^3(y)\}_{NP} \equiv \epsilon_{ijk} \frac{\partial f^1(y)}{\partial y^i} \frac{\partial f^2(y)}{\partial y^j} \frac{\partial f^3(y)}{\partial y^k}, \quad i, j, k \in \{1, 2, 3\}. \quad (1.129)$$

Let  $\chi^a(y)$  with  $a = 1, 2, \dots$  be a basis of functions on  $N_3$ . The commutation relation and the trace are given by

$$\{\chi^a(y), \chi^b(y), \chi^c(y)\}_{NP} = f^{abc}{}_d \chi^d(y), \quad (1.130)$$

and

$$\text{tr}(f^1, f^2) = \int_{N_3} d^3y \mu(y) f^1(y) f^2(y), \quad (1.131)$$

where  $\mu(y)$  is chosen to ensure that the trace is invariant under the derivative

$$\delta_{A,B} X \equiv \{A, B, X\}_{NP}. \quad (1.132)$$

The representation of the Nambu-Poisson bracket is given for example by the reference [66]. The BLG Lagrangian with the Nambu-Poisson bracket describes an infinite number of coincident M2-branes.

We have mentioned above that theories on maximally supersymmetric  $N$  coincident M2-branes can be constructed as long as  $N = 1, 2, \infty$ . In order to describe different numbers of  $N$ , one needs to relax some conditions.

If one relaxes the condition that the theory should be maximally supersymmetric, then one can have an alternative model. This is called the Aharony-Bergman-Jafferis-Maldacena (or ABJM) model [67]. The ABJM Lagrangian also uses a Chern-Simons gauge field and a 3-bracket. However, the 3-bracket here is less restrictive and allows one to describe any number  $N$  of coincident M2-branes. The ABJM theory has  $\mathcal{N} = 6$  supersymmetry for a generic case. The reference [68] shows that the ABJM theory gives the desired  $N^{3/2}$  scaling of degrees of freedom.

### 1.5.2 M5-branes

The low energy description of a single M5-brane is expected to be a  $(2, 0)$  superconformal field theory. The first description was obtained by the superembedding approach [69], which gives equations of motion of the fields on the M5-brane. We will be mainly interested in the equation of motion of the 2-form gauge field  $B$ . If we ignore all other fields, then this equation contains two kinds of 3-form fields. The first one is a field strength  $H = dB$  of the 2-form gauge field while the second one is an auxiliary field  $h$ . The auxiliary field is not a field strength of any 2-form fields but it is self-dual  $h = *h$ . Let the Greek indices label the directions on the M5-brane. The duals of  $H$  and  $h$  are given by

$$\tilde{H}^{\mu\nu\rho} = (*H)^{\mu\nu\rho} = \frac{1}{3!} \epsilon^{\mu\nu\rho\lambda\tau\sigma} H_{\lambda\tau\sigma}, \quad (1.133)$$

$$\tilde{h}^{\mu\nu\rho} = (*h)^{\mu\nu\rho} = \frac{1}{3!} \epsilon^{\mu\nu\rho\lambda\tau\sigma} h_{\lambda\tau\sigma} = h^{\mu\nu\rho}, \quad (1.134)$$

where  $\epsilon^{012345} = 1$ , and the indices are raised and lowered by the Minkowski metric. The equation of motion

$$\frac{1}{4} H_{\mu\nu\rho} = m_{\mu}^{-1\lambda} h_{\lambda\nu\rho} \quad (1.135)$$

algebraically relates the two kinds of the 3-form fields. Here  $m_\mu^{-1\lambda}$  is the inverse matrix of

$$m_\mu^\lambda = \delta_\mu^\lambda - 2k_\mu^\lambda, \quad (1.136)$$

where  $k_\mu^\lambda = h_{\mu\nu\rho}h^{\lambda\nu\rho}$ .

Let us now discuss how to construct the action which will give the equations of motion (1.135). Such an action with manifest Lorentz invariance cannot be constructed without introducing an auxiliary field. To get some insights into why this is not possible, let us consider a naive attempt. Quadratically, the action should give the equation of motion  $H_{\mu\nu\rho} = \tilde{H}_{\mu\nu\rho}$ . We require the action to be invariant under the gauge transformation  $\delta B = d\Upsilon$ . All possible gauge invariant quadratic terms in the Lagrangian are

$$H^{\mu\nu\rho}H_{\mu\nu\rho}, \quad \tilde{H}^{\mu\nu\rho}\tilde{H}_{\mu\nu\rho}, \quad H^{\mu\nu\rho}\tilde{H}_{\mu\nu\rho}. \quad (1.137)$$

However, the first term and the second term are not linearly independent to each other while the third term is a total derivative:

$$H^{\mu\nu\rho}\tilde{H}_{\mu\nu\rho} = \partial^\mu(3B^{\nu\rho}\tilde{H}_{\mu\nu\rho}). \quad (1.138)$$

So at the quadratic level, the Lagrangian is of the form

$$\mathcal{L}_{\text{quadratic}} \propto H^{\mu\nu\rho}H_{\mu\nu\rho}, \quad (1.139)$$

which fails to give the linearised self-duality condition  $H_{\mu\nu\rho} = \tilde{H}_{\mu\nu\rho}$ .

Let us now discuss the attempts which will lead to the correct result. One way to do this is by dropping the requirement that the action should be manifestly Lorentz invariant. One makes the 1+5 splitting [70,71] in which one direction is split from the six-dimensional manifold. One can either split the time-like direction or the space-like direction. Let us focus on the latter case and label the separated direction as  $x^5$ , and the other directions as  $x^{\hat{a}}$ ,  $\hat{a} = 0, 1, 2, 3, 4$ . Let us first consider the quadratic level, for which the action is given by

$$S = \frac{1}{2} \int d^6x \left( \tilde{H}^{\hat{a}\hat{b}5}H_{\hat{a}\hat{b}5} - \tilde{H}^{\hat{a}\hat{b}5}\tilde{H}_{\hat{a}\hat{b}5} \right). \quad (1.140)$$

The equation of motion is given by

$$\epsilon^{\hat{a}\hat{b}\hat{c}\hat{d}\hat{e}5}\partial_{\hat{c}}(H_{\hat{d}\hat{e}5} - \tilde{H}_{\hat{d}\hat{e}5}) = 0, \quad (1.141)$$

which gives general solutions

$$H_{\hat{d}\hat{e}5} - \tilde{H}_{\hat{d}\hat{e}5} = -2\partial_{[\hat{d}}\Phi_{e]}. \quad (1.142)$$

The gauge transformation

$$\delta_{\Phi} B_{5\hat{a}} = \Phi_{\hat{a}}, \quad \delta_{\Phi} B_{\hat{a}\hat{b}} = 0 \quad (1.143)$$

leaves the action invariant. This transformation  $B \rightarrow B + \delta_{\Phi} B$  is therefore the symmetry of the theory and can be used to gauge transform the equation (1.142) to give

$$H_{\hat{a}\hat{e}\hat{5}} - \tilde{H}_{\hat{a}\hat{e}\hat{5}} = 0, \quad (1.144)$$

which is, as required, equivalent to  $H_{\mu\nu\rho} = \tilde{H}_{\mu\nu\rho}$ . As well as giving the linearised self-duality condition, the quadratic action should also be Lorentz invariant. The Lorentz transformation  $x^{\mu} \rightarrow \Lambda^{\mu}_{\nu} x^{\nu} = -\Lambda_{\nu}^{\mu} x^{\nu}$  on the B-field is given by

$$B_{\mu\nu}(x^{\tau}) \rightarrow \Lambda_{\mu}^{\rho} \Lambda_{\nu}^{\sigma} B_{\rho\sigma}(\Lambda_{\lambda}^{\tau} x^{\lambda}). \quad (1.145)$$

Infinitesimally  $\Lambda_{\mu}^{\rho} \approx \delta_{\mu}^{\rho} + \lambda_{\mu}^{\rho}$  the Lorentz transformation is

$$\delta B_{\mu\nu} = \lambda_{\sigma}^{\rho} x^{\sigma} \partial_{\rho} B_{\mu\nu} + \lambda_{\nu}^{\rho} B_{\mu\rho} + \lambda_{\mu}^{\rho} B_{\rho\nu}. \quad (1.146)$$

The component  $B_{\hat{a}\hat{5}}$  enters the quadratic action only through the total derivative. Therefore, it is convenient to use the gauge transformation  $\delta B = d\Upsilon$  to choose the gauge in which  $B_{\hat{a}\hat{5}} = 0$ . The only relevant Lorentz transformation is then

$$\delta B_{\hat{a}\hat{b}} = 2\lambda_{[\hat{b}}^{\hat{c}} B_{\hat{a}]\hat{c}} - \lambda^{\hat{c}}_{\hat{d}} x^{\hat{d}} \partial_{\hat{c}} B_{\hat{a}\hat{b}} + \lambda^{\hat{c}} x_{\hat{c}} \partial_{\hat{5}} B_{\hat{a}\hat{b}} - \lambda^{\hat{c}} x^{\hat{5}} \partial_{\hat{c}} B_{\hat{a}\hat{b}}, \quad (1.147)$$

where  $\lambda^{\hat{c}} \equiv \lambda^{\hat{c}}_5$ . The quadratic action is not invariant under this transformation, but rather under the modified Lorentz transformation

$$\delta B_{\hat{a}\hat{b}} = 2\lambda_{[\hat{b}}^{\hat{c}} B_{\hat{a}]\hat{c}} - \lambda^{\hat{c}}_{\hat{d}} x^{\hat{d}} \partial_{\hat{c}} B_{\hat{a}\hat{b}} + \lambda^{\hat{c}} x_{\hat{c}} \tilde{H}_{\hat{a}\hat{b}\hat{5}} - \lambda^{\hat{c}} x^{\hat{5}} \partial_{\hat{c}} B_{\hat{a}\hat{b}}, \quad (1.148)$$

which is equivalent to the usual one at the level of equations of motion. The quadratic action is manifestly invariant under the Lorentz transformation in the five-dimensional part  $\{x^{\hat{a}}\}$ . Therefore, we only need to check the part of the transformation which mixes  $x^{\hat{a}}$  with  $x^{\hat{5}}$ . The relevant transformation parameters of this part are given by  $\lambda^{\hat{c}}$ . So, it is sufficient to show that the transformation

$$\delta B_{\hat{a}\hat{b}} = \lambda^{\hat{c}} x_{\hat{c}} \tilde{H}_{\hat{a}\hat{b}\hat{5}} - \lambda^{\hat{c}} x^{\hat{5}} \partial_{\hat{c}} B_{\hat{a}\hat{b}}, \quad \delta B_{\hat{a}\hat{5}} = 0 \quad (1.149)$$

leaves the action invariant. As is explicitly shown in the reference [71], this is indeed the case.

Having made sure that the quadratic action (1.140) is desirable, let us now consider the full non-linear action [71]:

$$S = \int d^6 x \left( \frac{1}{4} \tilde{H}^{\hat{a}\hat{b}} H_{\hat{a}\hat{b}} + L \right), \quad (1.150)$$

where

$$L \equiv \sqrt{\det(\delta_{\hat{a}}^{\hat{b}} + i\tilde{H}_{\hat{a}}^{\hat{b}})} = \sqrt{1 + \frac{1}{2}\text{tr}\tilde{H}^2 - \frac{1}{4}\text{tr}\tilde{H}^4 + \frac{1}{8}(\text{tr}\tilde{H}^2)^2}. \quad (1.151)$$

Here we define

$$H_{\hat{a}\hat{b}} \equiv H_{\hat{a}\hat{b}5}, \quad \tilde{H}_{\hat{a}\hat{b}} \equiv \tilde{H}_{\hat{a}\hat{b}5}. \quad (1.152)$$

The quantities  $H_{\hat{a}}^{\hat{b}}, \tilde{H}_{\hat{a}}^{\hat{b}}$  are  $5 \times 5$  antisymmetric matrices. The trace and determinant of these matrices are denoted as  $\text{tr}$  and  $\det$ . The full non-linear action also has the symmetry (1.143). It is invariant under the modified Lorentz transformation for which the relevant part is

$$\delta B_{\hat{a}\hat{b}} = \lambda^{\hat{c}} x_{\hat{c}} \mathcal{V}_{\hat{a}\hat{b}} - \lambda^{\hat{c}} x^5 \partial_{\hat{c}} B_{\hat{a}\hat{b}}. \quad (1.153)$$

The check is shown in the reference [71]. After an appropriate gauge fixing, the equation of motion of the non-linear action is given by

$$H_{\hat{a}\hat{b}} = \mathcal{V}_{\hat{a}\hat{b}}, \quad (1.154)$$

where

$$\mathcal{V}_{\hat{a}\hat{b}} \equiv -\frac{\partial L}{\partial \tilde{H}^{\hat{a}\hat{b}}} = \frac{\left(1 + \frac{1}{2}\text{tr}\tilde{H}^2\right) \tilde{H}_{\hat{a}\hat{b}} - \tilde{H}_{\hat{a}\hat{b}}^3}{\sqrt{1 + \frac{1}{2}\text{tr}\tilde{H}^2 - \frac{1}{4}\text{tr}\tilde{H}^4 + \frac{1}{8}(\text{tr}\tilde{H}^2)^2}}. \quad (1.155)$$

The reference [72] shows that the equations (1.154) and (1.135) are equivalent. To get some insights into the derivation, let us show the key steps which follow the reference [72] very closely. The equation (1.135) gives

$$\frac{1}{4}H_{\hat{a}\hat{b}} = Q^{-1}((1 + 2\text{tr}h^2)h_{\hat{a}\hat{b}} - 8h_{\hat{a}\hat{b}}^3), \quad (1.156)$$

$$\frac{1}{4}\tilde{H}_{\hat{a}\hat{b}} = Q^{-1}((1 - 2\text{tr}h^2)h_{\hat{a}\hat{b}} + 8h_{\hat{a}\hat{b}}^3), \quad (1.157)$$

$$Q = 1 + 4(\text{tr}h^2)^2 - 16\text{tr}h^4, \quad (1.158)$$

where  $h$  is the matrix form of  $h_{\hat{a}}^{\hat{b}} \equiv h_{\hat{a}}^{\hat{b}5}$ . It is also convenient to denote the matrix forms of  $H_{\hat{a}}^{\hat{b}}, \tilde{H}_{\hat{a}}^{\hat{b}}$  as  $H, \tilde{H}$ . In most steps of the derivation, one needs to repeatedly use the Cayley-Hamilton formula for the  $5 \times 5$  antisymmetric matrix  $X$ :

$$X^5 = \frac{1}{4} \left( \text{tr}X^4 - \frac{1}{2}(\text{tr}X^2)^2 \right) X + \frac{1}{2}(\text{tr}X^2)X^3. \quad (1.159)$$

This formula implies that, without loss of generality,  $h$  can be written in the form

$$h = a\tilde{H} + b\tilde{H}^3, \quad (1.160)$$

where  $a, b$  are scalar functions. It is also convenient to express  $h$  in the form

$$h = (x + yh^2)\tilde{H}, \quad (1.161)$$

where  $x, y$  are scalar functions. By using the equation (1.157), applying the Cayley-Hamilton formula (1.159), and then comparing the coefficients of  $h$  and  $h^3$ , one gets

$$h = (1 + 2\text{tr}h^2 - 8h^2)\frac{\tilde{H}}{4}. \quad (1.162)$$

By substituting  $h$  from the equation (1.160) into the equation (1.162), using the equation (1.159), and then comparing the coefficients of  $\tilde{H}$  and  $\tilde{H}^3$ , one gets two equations for the unknown variables  $a$  and  $b$ . There are two possible solutions, but we choose the one for which its leading order is  $h = \tilde{H}/4$ . The required solution gives

$$h = \tilde{H} \frac{(\text{tr}\tilde{H}^2(-4 + 4L) - 4\text{tr}\tilde{H}^4)}{4((\text{tr}\tilde{H}^2)^2 - 4\text{tr}\tilde{H}^4)} - \frac{\tilde{H}^3}{4 + 4L + \text{tr}\tilde{H}^2}. \quad (1.163)$$

As a check, by making an auxiliary scaling  $h \rightarrow \alpha h, H \rightarrow \alpha H, \tilde{H} \rightarrow \alpha \tilde{H}$ , and expanding near  $\alpha = 0$ , the equation (1.163) becomes  $\alpha h = \alpha \tilde{H}/4 + O(\alpha^2)$ . By substituting the equation (1.163) into the equation (1.156), one arrives at the result (1.154).

Having shown that the action (1.150) agrees with the equations of motion from the superembedding approach, let us now review the extension of this action. The idea is to use the GS formalism, that is, to include the other fields and get a supersymmetric action in which the worldvolume fields couple to an eleven-dimensional background. One can either keep using the 1 + 5 splitting [73, 74] or try to complete the GS formalism after making the action manifestly Lorentz invariant [75, 76]. Let us review the latter case, which is of relevance to us. In order to keep the manifest Lorentz invariance, the references [75, 77] introduce an auxiliary field  $a(x)$  which can be seen as projecting out one direction. The quantities

$$H_{\mu\nu} = H_{\mu\nu\rho} \frac{\partial^\rho a}{\sqrt{\partial_\sigma a \partial^\sigma a}}, \quad \tilde{H}_{\mu\nu} = \tilde{H}_{\mu\nu\rho} \frac{\partial^\rho a}{\sqrt{\partial_\sigma a \partial^\sigma a}} \quad (1.164)$$

will appear in the action. The quantity  $\partial_\rho a$  can either be space-like or time-like, but for definiteness, we choose it to be space-like. By simply choosing  $a(x) = x^5$ , one can see that the equation (1.164) reduces to the equation (1.152). Let us keep  $a(x)$  arbitrary and write down the action:

$$S = 2 \int_{\mathcal{M}_6} d^6x \left[ \sqrt{\det(\delta_\mu^\nu + i\tilde{H}_\mu^\nu)} + \frac{1}{4(\partial a)^2} \partial_\lambda a \tilde{H}^{\lambda\mu\nu} H_{\mu\nu\rho} \partial^\rho a \right]. \quad (1.165)$$

Here, the symmetry which ensures that the equation of motion is the non-linear self-duality condition is given by

$$\delta B_{\mu\nu} = 2\partial_{[\mu} a \Phi_{\nu]}(x), \quad \delta a(x) = 0. \quad (1.166)$$

In an appropriate gauge, the equation of motion of  $B_{\mu\nu}$  is

$$H_{\mu\nu} = \mathcal{V}_{\mu\nu}(\tilde{H}), \quad \mathcal{V}^{\mu\nu}(\tilde{H}) \equiv -\frac{\partial\sqrt{\det(\delta_{\mu}^{\nu} + i\tilde{H}_{\mu}^{\nu})}}{\partial\tilde{H}_{\mu\nu}}, \quad (1.167)$$

while the equation of motion of  $a(x)$  is the consequence of the equations of motion of the B-field. There is an extra symmetry (called the PST symmetry)

$$\delta a = \varphi(x), \quad \delta B_{\mu\nu} = \frac{\varphi(x)}{\sqrt{(\partial a)^2}}(H_{\mu\nu} - \mathcal{V}_{\mu\nu}), \quad (1.168)$$

which ensures that  $a(x)$  is auxiliary. One can see that after gauge fixing, this covariant formulation gives the non-covariant one. It is possible to choose the gauge in which  $a(x) = x^5$ . In this gauge, the action (1.165) reduces to the action (1.150), and the equation (1.166) reduces to the equation (1.143). Furthermore, by fixing the gauge, one can obtain the non-covariant modified Lorentz transformation. One first chooses the gauge  $a(x) = x^5$ , then makes the gauge transformation which is a combination of the PST symmetry and the Lorentz transformation to ensure that one still has the gauge  $a(x) = x^5$ . By using this gauge choice and fixing  $B_{\hat{a}5} = 0$ , one gets the modified Lorentz transformation whose relevant part is given by the equation (1.153).

One can naturally promote the action (1.165) to the one which fully describes an M5-brane coupled to a general eleven-dimensional supergravity background. This involves working with curved metrics as well as supersymmetry, so before writing down the action, let us review some essential materials.

The eleven-dimensional target space has the coordinates  $Z^{\mathcal{M}} = (X^M, \theta)$ , where  $X^M$  are eleven bosonic coordinates and  $\theta$  are 32 real fermionic coordinates. Here  $M = 0, 1, \dots, 10$ , and we omit the fermion index. When a theory involves a fermion in a curved space, it is necessary to define a flat space on which the gamma matrices can be kept constant. This flat space is called the tangent frame. The map between the bosonic part of the target space and the bosonic part of the tangent frame is given by the vielbein  $e_M^A(X)$ , where  $A = 0, 1, \dots, 10$  is the index on the tangent frame. The tangent frame also contains the fermionic part, whose indices represented by the beginning of Greek alphabet:  $\alpha, \beta, \dots \in \{1, \dots, 32\}$ .

As we have discussed previously, the field content of the eleven-dimensional supergravity theory consists of a graviton  $e_M^A(X)$ , a gravitino  $\psi_M^\alpha(X)$ , and a 3-form gauge field  $C_{MNP}(X)$ . The superfields which encode these supergravity fields are respectively given by a tangent-space vector supervielbein  $E^A(Z) = dZ^{\mathcal{M}}E_{\mathcal{M}}^A(Z)$ , a Majorana-spinor supervielbein  $E^\alpha(Z) = dZ^{\mathcal{M}}E_{\mathcal{M}}^\alpha(Z)$ , and the 3-form gauge superfield  $C_3(Z) =$

$\frac{1}{3!}dZ^{\mathcal{M}_1}dZ^{\mathcal{M}_2}dZ^{\mathcal{M}_3}C_{\mathcal{M}_3\mathcal{M}_2\mathcal{M}_1}$ . It will be convenient to also define the  $C_6(Z)$  dual of the  $C_3(Z)$ . Note that the index ordering of differential forms here is in the opposite order to those given in the definition (1.30). The convention here is usually applied when supersymmetry and superfields are involved.

Let us now show essential equations of motion of the background supergravity theory. The vector supervielbein satisfies the following essential torsion constraint

$$T^A = DE^A = dE^A + E^B\Omega_B{}^A = -iE^\alpha\Gamma_{\alpha\beta}^A E^\beta, \quad (1.169)$$

where  $\Omega_B{}^A(Z)$  is the one-form spin connection in  $D = 11$ ,  $\Gamma_{\alpha\beta}^A = \Gamma_{\beta\alpha}^A$  are real symmetric gamma matrices and the external differential acts from the right. The field strengths of  $C_3(Z)$  and  $C_6(Z)$  are constrained as follows

$$\begin{aligned} dC_3 &= -\frac{i}{2}E^A E^B E^\alpha E^\beta (\Gamma_{BA})_{\alpha\beta} + \frac{1}{4!}E^A E^B E^C E^D F_{DCBA}^{(4)}(Z), \\ dC_6 - C_3 dC_3 &= \frac{2i}{5!}E^{A_1} \dots E^{A_5} E^\alpha E^\beta (\Gamma_{A_5\dots A_1})_{\alpha\beta} + \frac{1}{7!}E^{A_1} \dots E^{A_7} F_{A_7\dots A_1}^{(7)}(Z), \\ F^{(7)A_1\dots A_7} &= \frac{1}{4!}\epsilon^{A_1\dots A_{11}} F_{A_8\dots A_{11}}^{(4)}, \quad \epsilon^{0\dots 10} = -\epsilon_{0\dots 10} = 1. \end{aligned} \quad (1.170)$$

Here  $\Gamma_{A_1 A_2 \dots A_n} = \Gamma_{[A_1} \Gamma_{A_2} \dots \Gamma_{A_n]}$ .

Let us now show the fields on the M5-brane worldvolume. The induced metric on the worldvolume is constructed with the pull-backs of the vector supervielbeins  $E^A(Z)$

$$g_{\mu\nu}(x) = E_\mu^A E_\nu^B \eta_{AB}, \quad E_\mu^A = \partial_\mu Z^N E_N^A(Z(x)). \quad (1.171)$$

The generalised field strengths of the B-field  $B_2(x) = \frac{1}{2}dx^\mu dx^\nu B_{\nu\mu}(x)$  is

$$H_3 = dB_2 + C_3, \quad (1.172)$$

where  $C_3(Z(x))$  is the pull-back on the M5-brane worldvolume of the 3-form gauge field. To ensure the  $6d$  worldvolume covariance of the M5-brane action one uses a normalised gradient of the auxiliary scalar field  $a(x)$  which can be chosen to be time-like or space-like. For definiteness, we show the space-like case:

$$v_\mu(x) = \frac{\partial_\mu a}{\sqrt{\partial_\nu a g^{\nu\lambda}(x) \partial_\lambda a}}, \quad v_\mu v^\mu = 1. \quad (1.173)$$

The projector of rank one

$$P_\mu{}^\nu(x) = \frac{\partial_\mu a \partial^\nu a}{(\partial a)^2}, \quad PP = P, \quad (\partial a)^2 \equiv \partial_\nu a g^{\nu\lambda} \partial_\lambda a = \partial_\nu a \partial^\nu a, \quad (1.174)$$

singles out one worldvolume direction from the six, i.e. makes the 1+5 covariant splitting of the  $6d$  worldvolume directions.

Let us now present the M5-brane action [74–76] in a generic eleven-dimensional supergravity background:

$$S = +2 \int_{\mathcal{M}_6} d^6x \left[ \sqrt{-\det(g_{\mu\nu} + i\tilde{H}_{\mu\nu})} + \frac{\sqrt{-g}}{4(\partial a)^2} \partial_\lambda a \tilde{H}^{\lambda\mu\nu} H_{\mu\nu\rho} \partial^\rho a \right] - \int_{\mathcal{M}_6} (C_6 + H_3 \wedge C_3), \quad (1.175)$$

with

$$\tilde{H}^{\rho\mu\nu} \equiv \frac{1}{6\sqrt{-g}} \epsilon^{\rho\mu\nu\lambda\sigma\tau} H_{\lambda\sigma\tau}, \quad \tilde{H}_{\mu\nu} \equiv \frac{\partial^\rho a}{\sqrt{(\partial a)^2}} \tilde{H}_{\rho\mu\nu}, \quad g = \det g_{\mu\nu}, \quad (1.176)$$

where  $\epsilon^{0\dots 5} = -\epsilon_{0\dots 5} = 1$ .

In addition to the gauge symmetry  $\delta B_2 = d\Upsilon$ , the action (1.175) has also the following two local gauge symmetries :

$$\delta B_{\mu\nu} = 2\partial_{[\mu} a \Phi_{\nu]}(x), \quad \delta a(x) = 0, \quad (1.177)$$

as well as

$$\delta a = \varphi(x), \quad \delta B_{\mu\nu} = \frac{\varphi(x)}{\sqrt{(\partial a)^2}} (H_{\mu\nu} - \mathcal{V}_{\mu\nu}), \quad (1.178)$$

where

$$\mathcal{V}^{\mu\nu}(\tilde{H}) \equiv -\frac{\partial \sqrt{\det(\delta_\mu^\nu + i\tilde{H}_{\mu\nu})}}{\partial \tilde{H}_{\mu\nu}}, \quad H_{\mu\nu} \equiv H_{\mu\nu\rho} \frac{\partial^\rho a(x)}{\sqrt{(\partial a)^2}}, \quad (1.179)$$

with  $\varphi(x)$  and  $\Phi_\mu(x)$  being arbitrary local functions on the worldvolume. The first symmetry (1.177) ensures that the equation of motion of  $B_2$  reduces to the non-linear self-duality condition

$$H_{\mu\nu} = \mathcal{V}_{\mu\nu}(\tilde{H}), \quad (1.180)$$

while the second symmetry (1.178) is responsible for the auxiliary nature of the scalar field  $a(x)$  and the  $6d$  covariance of the action.

The action (1.175) is invariant under the supersymmetry transformation of the form

$$\begin{aligned} \delta_\epsilon E^A &= 0, & \delta_\epsilon C^{(3)} &= id(\bar{\epsilon}\Delta^2), \\ \delta_\epsilon B &= -i\bar{\epsilon}\Delta^2, & \delta_\epsilon C^{(6)} &= 2id(\bar{\epsilon}\Delta^5) - i(\bar{\epsilon}\Delta^2) \wedge dC^{(3)}. \end{aligned} \quad (1.181)$$

It is also invariant under the local fermionic kappa-symmetry transformations with the parameter  $\kappa^\alpha(x)$

$$\begin{aligned} i_\kappa E^\alpha &\equiv \delta_\kappa Z^\mathcal{M} E_{\mathcal{M}}^\alpha = \frac{1}{2}(1 + \bar{\Gamma})^{\alpha\beta} \kappa^\beta, & i_\kappa E^A &\equiv \delta_\kappa Z^\mathcal{M} E_{\mathcal{M}}^A = 0, \\ \delta_\kappa g_{\mu\nu} &= -4iE_{(\mu}^\alpha (\Gamma_{\nu)})_{\alpha\beta} i_\kappa E^\beta, & \delta_\kappa H^{(3)} &= i_\kappa dC^{(3)}, & \delta_\kappa a(x) &= 0, \end{aligned} \quad (1.182)$$

where  $(1 + \bar{\Gamma})/2$  is the projector of rank 16 with  $\bar{\Gamma}$  having the following form

$$\begin{aligned}\sqrt{\det(\delta_\mu^\nu + i\tilde{H}_\mu{}^\nu)} \bar{\Gamma} &= \gamma^{(6)} - \frac{1}{2} \Gamma^{\mu\nu\lambda} P_\mu{}^\rho \tilde{H}_{\nu\lambda\rho} - \frac{1}{16\sqrt{-g}} \epsilon^{\mu_1\cdots\mu_6} \tilde{H}_{\mu_1\mu_2\lambda} \tilde{H}_{\mu_3\mu_4\rho} P^{\lambda\rho} \Gamma_{\mu_5\mu_6}, \\ \bar{\Gamma}^2 &= 1, \quad \text{tr}\bar{\Gamma} = 0,\end{aligned}\tag{1.183}$$

where

$$\Gamma_\mu = E_\mu{}^A \Gamma_A, \quad \gamma^{(6)} = \frac{1}{6!\sqrt{-g}} \epsilon^{\mu_1\cdots\mu_6} \Gamma_{\mu_1\cdots\mu_6}.\tag{1.184}$$

When compared with the other symmetries, the kappa-symmetry is relatively difficult to check. So let us give a brief review of its proof. Let us decompose the action (1.165) as

$$S = S_0 + S_2 + S_{WZ},\tag{1.185}$$

where

$$\begin{aligned}S_0 &= 2 \int_{\mathcal{M}_6} d^6x \frac{\sqrt{-g}}{4(\partial a)^2} \partial_\lambda a \tilde{H}^{\lambda\mu\nu} H_{\mu\nu\rho} \partial^\rho a, \\ S_2 &= 2 \int_{\mathcal{M}_6} d^6x \sqrt{-\det(g_{\mu\nu} + i\tilde{H}_{\mu\nu})} \equiv 2 \int_{\mathcal{M}_6} d^6x \sqrt{-g} \mathcal{L}, \\ S_{WZ} &= - \int_{\mathcal{M}_6} (C_6 + H_3 \wedge C_3).\end{aligned}\tag{1.186}$$

Their kappa-symmetry transformations are found to be of the form

$$\begin{aligned}\delta S_0 &= -2i\sqrt{-g} E_\mu^\alpha (J_0^\mu)_{\alpha\beta} i_\kappa E^\beta, \\ \delta S_2 &= -2i\sqrt{-g} E_\mu^\alpha (J_2^\mu)_{\alpha\beta} i_\kappa E^\beta, \\ \delta S_{WZ} &= -2i\sqrt{-g} E_\mu^\alpha (J_{WZ}^\mu)_{\alpha\beta} i_\kappa E^\beta,\end{aligned}\tag{1.187}$$

where (with fermion indices suppressed)

$$\begin{aligned}J_0^\mu &= \left( -\frac{1}{2} \frac{v^{(\mu} \epsilon^{\nu_1)\nu_2\nu_3\nu_4\nu_5\nu_6} v_{\nu_2} \tilde{H}_{\nu_3\nu_4} \tilde{H}_{\nu_5\nu_6}}{\sqrt{-g}} \right) \Gamma_{\nu_1} + \left( -\frac{1}{2} \tilde{H}^{\mu\nu_1\nu_2} + 3\tilde{H}^{[\mu\nu_1} v^{\nu_2]} \right) \Gamma_{\nu_1\nu_2}, \\ J_2^\mu &= (2g^{\mu\nu} \mathcal{L} - \text{tr}(\mathcal{V}\tilde{H})\Pi^{\mu\nu} + 2(\mathcal{V}\tilde{H})^{(\mu\nu)}) \Gamma_\nu - \left( \frac{1}{2} \mathcal{V}_{\nu_3\nu_4} v_{\nu_5} \frac{\epsilon^{\nu_3\nu_4\nu_5\mu\nu_1\nu_2}}{\sqrt{-g}} \right) \Gamma_{\nu_1\nu_2}, \\ J_{WZ}^\mu &= \left( \frac{1}{2} \tilde{H}^{\mu\nu_1\nu_2} \Gamma_{\nu_1\nu_2} - 2\Gamma^\mu \bar{\gamma} \right),\end{aligned}\tag{1.188}$$

where  $\Pi^{\mu\nu} = g^{\mu\nu} - P^{\mu\nu}$ . To determine  $\bar{\Gamma}$ , one requires

$$\mathcal{L} J_2^\mu = -\mathcal{L} (J_0^\mu + J_{WZ}^\mu) \bar{\Gamma},\tag{1.189}$$

with

$$\bar{\Gamma}^2 = 1, \quad \text{tr}\bar{\Gamma} = 0.\tag{1.190}$$

If this is true, one will have (with fermion indices suppressed)

$$\begin{aligned}
\delta S &= -2i\sqrt{-g}E_\mu(J_0^\mu + J_{WZ}^\mu)(1 - \bar{\Gamma})i_\kappa E \\
&= -i\sqrt{-g}E_\mu(J_0^\mu + J_{WZ}^\mu)(1 - \bar{\Gamma})(1 + \bar{\Gamma})\kappa \\
&= -i\sqrt{-g}E_\mu(J_0^\mu + J_{WZ}^\mu)(1 - \bar{\Gamma}^2)\kappa \\
&= 0.
\end{aligned} \tag{1.191}$$

If one contracts the equation (1.189) with  $\Gamma_\mu$ , then one gets  $\bar{\Gamma}$  which is given by the equation (1.183). The  $\bar{\Gamma}$  obtained this way indeed satisfies the equation (1.189).

It is also possible to construct the M5-brane action by using a different splitting. We are particularly interested in the so called 3 + 3 splitting. Recall that in the 1 + 5 splitting, the manifest  $SO(1, 5)$   $6d$  Lorentz symmetry is broken to  $SO(1, 4)$ . In the 3 + 3 splitting, the manifest  $6d$  Lorentz symmetry is broken to  $SO(1, 2) \times SO(3)$ . The 3 + 3 splitting is motivated from the construction [66, 78] in which a 5-brane action based on the BLG action is obtained. To see whether this 5-brane action would be related to the original M5-brane action, the reference [2] constructs a full non-linear M5-brane action with a 3 + 3 splitting. We discuss this full action in chapter 4.

Having discussed single M5-brane actions, let us now turn to coincident M5-branes. The worldvolume description of coincident M5-branes is very subtle. There have been various attempts, for example in references [3, 4, 79–97], to describe the worldvolume theory. However, it is still no known complete description.

We are mainly interested in the model [87]. This model describes a non-Abelian 2-form field with a self-dual field strength. We have mentioned above that in order to include a non-dynamical gauge field in the case of coincident M2-branes, one needs the Chern-Simons gauge field. In the case of M5-branes, however, the Chern-Simons gauge fields are dynamical. A non-dynamical 1-form gauge field is instead obtained from boundary values of the 2-form. We are interested in studying the solutions of this model in which the relevant equation of motion is given by

$$\tilde{H}_{\mu\nu} = \partial_5 B_{\mu\nu}, \quad \mu, \nu \in \{0, 1, \dots, 4\}, \tag{1.192}$$

where

$$\tilde{H}_{\mu\nu} = \frac{1}{6}\epsilon_{\mu\nu\delta\rho\sigma\tau}H^{\rho\sigma\tau}, \quad H_{\mu\nu\lambda} = 3D_{[\mu}B_{\nu\lambda]} = 3[\partial_{[\mu} + A_{[\mu}, B_{\nu\lambda]}]. \tag{1.193}$$

The auxiliary gauge field is determined by the equation:

$$F_{\mu\nu} = \partial_\mu A_\nu - \partial_\nu A_\mu + [A_\mu, A_\nu] = c \int dx_5 \tilde{H}_{\mu\nu}. \tag{1.194}$$

---

Solitonic solutions of this model are obtained in [3, 4, 97]. In chapter 5, we will explain the solutions [3, 4] which describe M2/M5 intersections as viewed from the worldvolume of M5-branes.

## Chapter 2

# Instability of $\mathcal{N} = 2$ gauge theory in compact space with an isospin chemical potential

This chapter is largely based on [1]. We use a D3/D7 model to study, via gauge/gravity duality, a strongly coupled  $\mathcal{N} = 2$  gauge theory in compact space with an isospin chemical potential. We show an instability of an old ground state and show the presence of a new ground state.

In section 2.1, we first briefly review D3/D7 system in global coordinates at finite and at zero temperature. We consider the set up which corresponds to turning on an isospin chemical potential in a homogeneous ground state of a strongly coupled  $\mathcal{N} = 2$  gauge field theory on  $\mathbb{R} \times S^3$  having massless flavour fields. In section 2.2 and 2.3, we discuss the fluctuation of scalar fields and gauge fields on the D7-branes worldvolume in the homogeneous ground state. The study is performed respectively at zero temperature and at finite temperature. In order to study stabilities of the system, the spectrum of each fluctuation field is analysed. For each field, an isospin chemical potential has a critical value beyond which the ground state becomes unstable or just potentially unstable. These instabilities are clarified in section 2.4 where a new ground state, which has a finite vacuum expectation value for a mesonic operator, for each field can be constructed when the isospin chemical potential is higher than its corresponding critical value. By comparing free energy of different ground states, the state having the lowest free energy is identified as the true new ground state. We end this chapter with section 2.5 which gives a discussion and an outlook on this project.

From our findings, there are two features worth mentioning. The first is that the particles which condense first are *not* vector excitations ('rho mesons'), but rather scalar particles charged under the global symmetry group.<sup>1</sup> The second feature is that the thermal pole masses of some of the mesons can cross as the dimensionless ratio is varied.<sup>2</sup> This crossing behaviour is also the case for the condensate formation. In our model the crossing does not involve the lightest particle, but in other models the situation may not be so simple, and it would be interesting to investigate this further.

## 2.1 Holography with a dual $S^3$

### 2.1.1 Brane embeddings in global $\text{AdS}_5 \times S^5$ and $\text{AdS}_5$ -Schwarzschild

In this section we will briefly review some properties of the global  $\text{AdS}_5 \times S^5$  and  $\text{AdS}_5$ -Schwarzschild spaces as well as various embeddings of D7-probe branes in these geometries [55]. String theory in global  $\text{AdS}_5 \times S^5$  space is believed to be dual to the  $\mathcal{N} = 4$  SYM theory at zero temperature, which lives at the boundary of this space, which is an  $S^3 \times \mathbb{R}$ . Turning on the temperature makes the time direction (both in the gauge and gravity sides) compact, with the radius being inversely proportional to the gauge theory temperature.

The metric of the global  $\text{AdS}_5$  spaces (both at zero and finite temperature) is given by

$$ds^2 = \left(1 + \frac{r^2}{R^2}\right) d\tau^2 + \frac{dr^2}{1 + \frac{r^2}{R^2}} + r^2 d\Omega_3^2 + R^2 d\Omega_5^2, \quad (2.1)$$

where the origin of the AdS space is at  $r = 0$ , the boundary is at  $r \rightarrow \infty$ , and  $R$  is the AdS radius. The Euclideanised time direction  $\tau$  is periodic with period  $R_\tau$ . Since the theory is conformal, it implies that only the ratio of the thermal circle  $\tau$  and the size of the boundary sphere on which dual theory is living,  $R/R_\tau$ , is physically observable, i.e. unchanged by the conformal symmetry of the theory.

As the temperature of the thermal AdS space is increased, a first order Hawking-Page phase transition takes place and global AdS-Schwarzschild space replaces the thermal AdS space as the proper ground state of the system [49]. The metric of the global AdS-

---

<sup>1</sup>This could perhaps have been expected from the analysis of the meson spectrum of [7], which finds that these  $SO(4)$  charged scalar mesons are the lightest, but their work does not discuss the effect of a chemical potential, and the qualitative argument based on only a comparison of the mass may in any case not be the complete story.

<sup>2</sup>This crossing behaviour is somewhat reminiscent of the mixing of states observed in [98].

Schwarzschild black hole is given by

$$ds^2 = - \left( 1 + \frac{r^2}{R^2} - \frac{M^2}{r^2} \right) dt^2 + \frac{dr^2}{1 + \frac{r^2}{R^2} - \frac{M^2}{r^2}} + r^2 d\Omega_3^2 + R^2 d\Omega_5^2, \quad (2.2)$$

where  $M^2 = 8G_N m_{\text{bh}} / (3\pi)$  and  $m_{\text{bh}}$  is the mass of the black hole, while its temperature is given by

$$T = \frac{1}{4\pi} \left( \frac{2r_0}{R^2} + \frac{2M^2}{r_0^3} \right), \quad (2.3)$$

where

$$r_0^2 = R^2 \left( \frac{-1 + \sqrt{1 + 4M^2/R^2}}{2} \right). \quad (2.4)$$

The dimensionless ratio  $R/R_\tau$  is proportional to  $TR$ , and we will later on expand our results for large values of this parameter, interpreting this limit as one at finite temperature and large volume [8, 55], so that a comparison with results in the Poincaré patch can be made.

Introducing D7-probe branes in this geometry corresponds, in the holographic language, to adding flavour hypermultiplets to  $\mathcal{N} = 4$  SYM on the sphere  $S^3$ . A study of various D-brane probes, in particular D7-probe branes, in these geometries was performed in [8, 55]. However, in this chapter we are only interested in the embedding where D7-branes ‘coincides with D3-branes’. This corresponds to adding massless hypermultiplets.

In this chapter, instead of using the coordinates (2.1), it will be useful to use another set of coordinates given by

$$ds^2 = - \frac{u^2}{R^2} \left( 1 + \frac{R^2}{4u^2} \right)^2 dt^2 + u^2 \left( 1 - \frac{R^2}{4u^2} \right)^2 d\bar{\Omega}_3^2 + \frac{R^2}{u^2} (du^2 + u^2 d\Omega_5^2), \quad (2.5)$$

which is related to (2.1) via the coordinate change

$$u = \frac{1}{2}(r + \sqrt{r^2 + R^2}). \quad (2.6)$$

In these coordinates the origin of the AdS space is at  $u = R/2$ , while the boundary is an  $S^3$  at  $u \rightarrow \infty$ . We will also use

$$ds^2 = - \frac{1}{4z^2} (1 + z^2)^2 dt^2 + \frac{R^2}{4z^2} (1 - z^2)^2 d\bar{\Omega}_3^2 + R^2 \frac{dz^2}{z^2} + R^2 d\Omega^2, \quad (2.7)$$

which is related to the previous coordinates by  $z = R/(2u)$ . Let us also note that in the  $z$  coordinate the origin of AdS space is at  $z = 1$ , while the boundary is at  $z = 0$ .

Similarly for the system at finite temperature in addition to metric (2.2) we will also use  $(u, t)$  coordinates,

$$ds^2 = - \frac{2\rho_H^2}{uR^2} \frac{F(u)}{W(u)} dt^2 + 2\frac{\rho_H^2}{u} W(u) d\bar{\Omega}_3^2 + \frac{R^2}{4u^2 F(u)} du^2 + R^2 d\Omega_5^2, \quad (2.8)$$

where

$$F(u) = 1 - u^2, \quad \frac{\rho_H^4}{R^4} = \frac{1}{16} + \frac{M^2}{4R^2}, \quad W(u) = 1 - \frac{uR^2}{4\rho_H^2}. \quad (2.9)$$

Note here that the variable  $u$  is dimensionless and ranges from  $u \in [0, 1]$ , where the horizon is at  $u = 1$ , and the boundary is at  $u = 0$ . The Hawking temperature of this black hole is

$$T = \frac{\sqrt{2}\rho_H}{\pi R^2 \sqrt{1 - \frac{R^2}{4\rho_H^2}}}. \quad (2.10)$$

For numerical investigation it turns out that another form of the metric at finite  $T$  will also be useful.<sup>3</sup> If we change coordinates as

$$v = \frac{1 - u}{1 - \frac{uR^2}{4\rho_H^2}} \quad \Lambda = \frac{8\rho_H^2}{4\rho_H^2 + R^2}, \quad (2.11)$$

then the metric becomes

$$ds^2 = -\frac{v(\Lambda - v)}{(1 - v)(2 - \Lambda)} dt^2 + \frac{\Lambda - 1}{(2 - \Lambda)(1 - v)} R^2 d\bar{\Omega}_3^2 + \frac{\Lambda - 1}{4(1 - v)^2 v(\Lambda - v)} R^2 dv^2 + R^2 d\Omega_5^2, \quad (2.12)$$

where

$$d\bar{\Omega}_3^2 = d\bar{\theta}^2 + \sin^2 \bar{\theta} d\bar{\phi}^2 + \cos^2 \bar{\theta} d\bar{\psi}^2. \quad (2.13)$$

In these coordinates  $v = 0$  is the horizon while  $v = 1$  is the boundary, and  $\Lambda$  is function of the temperature given by

$$\Lambda = \frac{4(\pi TR)^2}{3(\pi TR)^2 - \sqrt{(\pi TR)^2(-2 + (\pi TR)^2)}}. \quad (2.14)$$

### 2.1.2 Chemical potentials and homogeneous solutions

In this section we will construct solutions which correspond to adding a chemical potential associated to the global  $SU(2)$  flavour symmetry. This symmetry originates from the fact that we are considering two coinciding D7-probe branes. In addition to the  $SU(2)$  symmetry, our systems also exhibits another global  $SO(4)$  symmetry associated to the residual global isometry of the system of probes. In principle one could also consider switching on a chemical potential which is associated to this symmetry group, as it was done in e.g. [99]. However, our prime interest will be the physically more relevant  $SU(2)$  group, which has direct analogue with the  $SU(2)$  flavour symmetry group in the Sakai-Sugimoto model [98].

---

<sup>3</sup>This is related to the fact that the solutions at vanishing bare quark mass can be related to Heun functions in these coordinates.

In order to turn on a chemical potential corresponding to this global  $SU(2)$  “isospin” symmetry, let us consider two coincident D7-branes, which for simplicity have equatorial embedding  $\theta = 0$ , so that the induced metric on the D7-branes is

$$ds^2 = -\frac{u^2}{R^2} \left(1 + \frac{R^2}{4u^2}\right)^2 dt^2 + \frac{R^2}{u^2} du^2 + u^2 \left(1 - \frac{R^2}{4u^2}\right)^2 d\bar{\Omega}_3^2 + R^2 d\Omega_3^2. \quad (2.15)$$

In other words, the D7-probes fill out the full  $\text{AdS}_5$  space, as well as a maximal  $S^3 \in S^5$ . We should note that there are two  $S^3$  factors present on the world-volume of the brane, one  $\bar{\Omega}_3$  which is dual to the boundary  $S^3$  and another one  $S^3$  in  $S^5$ , which is part of the global symmetry group.

In order to turn on a chemical potential we need to turn on the  $A_0$  component of the gauge field, such that it satisfies the boundary condition

$$A_0(x, z \rightarrow 0) \rightarrow \mu_I \tau^3, \quad (2.16)$$

where  $\tau^3 = \sigma^3/2$  with  $\sigma^3$  being the third Pauli spin matrices (and we will define  $\tau^1$  and  $\tau^2$  in the similar way). As a first guess for finding the ground state of the system in the presence of this chemical potential, we consider the homogeneous ansatz

$$A = A_0^{(3)}(u) \tau^3 dt, \quad (2.17)$$

so that the DBI action becomes

$$S = -T_{D7} 8\pi^4 R^3 \int dz \sqrt{-g(z)} \left[ 1 + \frac{\pi^2 R^4}{2\lambda} \left( \partial_z A_0^{(3)}(z) \right)^2 g^{tt}(z) g^{zz}(z) \right]^{1/2}. \quad (2.18)$$

The equation of motion for the field  $A_0(z)$  can be integrated once, yielding

$$\partial_z (A_0^{(3)}(z) R) = \frac{4cz(1+z^2)}{\sqrt{(1-z^2)^6 + 32\frac{c^2\pi^2}{\lambda} z^6}}, \quad (2.19)$$

where  $c$  is an integration constant. We are looking for a physical configuration which is smooth and differentiable everywhere. Specifically, we require that the field  $A_0$  and its derivatives are smooth at the origin of AdS space. However, by expanding the right hand side of the above equation near the origin of AdS space one sees that the radial derivative of the  $A_0$  field is non-vanishing. In other words, it is not possible to obtain any nontrivial (different from a constant solution) homogeneous solution which is smooth at the origin. This observation persists also for the Yang-Mills truncation of the DBI action, and it also holds in the Poincaré limit (see [100]). Hence as the starting configuration for our fluctuation analysis we will use a homogeneous solution with non-zero isospin potential, given by

$$A_0 = a_0 \tau^3, \quad a_0 = \text{const.} \quad (2.20)$$

This solution implies that at zero temperature, the homogeneous background does not lead to generation of an isospin density.

Above the Hawking-Page transition, the situation is similar. The homogeneous ansatz yields a first order differential equation,

$$\partial_u A_0^{(3)}(u) \left(1 - \frac{uR^2}{4\rho_H^2}\right)^2 = a_0, \quad (2.21)$$

where  $a_0$  is an integration constant. This is solved by

$$A_0^{(3)}(u) = \frac{\mu_I(1-u)}{1 - \frac{uR^2}{4\rho_H^2}}, \quad (2.22)$$

where we have imposed the boundary condition that  $A_0(u \rightarrow 0) = \mu_I$  at the boundary, and also required vanishing of  $A_0$  at the horizon of the black hole in AdS space. In contrast to the low temperature situation, we see that there is now a non-vanishing isospin density present, even for this homogeneous system.

## 2.2 Perturbative analysis of the homogeneous vacuum at $T = 0$

While the homogeneous and isotropic solution which was discussed in the previous section is a legitimate solution to the equations of motion, we expect that for large enough values of the chemical potential this configuration will become unstable and “decay” into another, presumably non-homogeneous or non-isotropic ground state. Our expectations are based on a similar analysis which was previously performed for the Sakai-Sugimoto model in [98]. A major difference, however, with respect to the analysis of that paper is that we are now dealing with a field theory on a *compact* space. In the present section we will discuss the perturbative stability analysis at  $T = 0$ , which from a technical perspective largely follows the meson spectrum analysis of [7]; we recall some elements of that construction for completeness and in order to be able to compare with the finite temperature analysis which is to follow in section 2.3.

### 2.2.1 Scalar fluctuations at zero temperature

We will start the perturbative analysis of the homogeneous solution (2.20) by considering scalar perturbations. By scalars we here mean scalars in the dual theory that are also scalars from the point of view of the D7-probe, i.e. gauge theory scalar fields which are

uncharged under the  $SO(4)$ . Some of the scalars in the dual gauge theory originate from the components of the gauge field on the D7-probe and will be analysed in the next section. Our starting point is the flat (i.e. maximal) D7-probe embedding with the world-volume field (2.20) turned on. The induced metric on the world-volume was written in (2.15). Since the D7-probe brane is filling out the full  $AdS_5$  space and wrapping a maximal  $S^3$  in  $S^5$ , there are only two transverse scalars to the brane world-volume, and they are within the  $S^5$ . To see which scalars these are, let us write the metric on  $S^5$  as

$$ds_5^2 = \frac{1}{1 - \frac{w_1^2 + w_2^2}{R^2}} \left( dw_1^2 + dw_2^2 - \left( \frac{w_2}{R} dw_1 - \frac{w_1}{R} dw_2 \right)^2 \right) + \left( 1 - \frac{w_1^2 + w_2^2}{R^2} \right) d\Omega_3^2. \quad (2.23)$$

Note that the metric significantly simplifies for  $w_1 = 0, w_2 = w$ . It can easily be checked from the equations of motion that it is indeed consistent to set one of the  $w_1, w_2$  to zero.<sup>4</sup> We expect that the first instability will appear already for the lowest lying (S-wave) mode on the dual gauge theory sphere  $\bar{S}^3$ , which is also a singlet on  $S^3 \in S^5$ . Therefore, when looking for the instabilities in the system, we will look at the fluctuation which is a function of only the time and  $u$ -coordinates. Let us define the fluctuation variable as

$$\Psi(t, u) = \frac{\delta w_2(t, u)}{2\pi\alpha'}. \quad (2.24)$$

The induced metric on the D7-brane becomes

$$ds^2 = -\frac{u^2}{R^2} \left( 1 + \frac{R^2}{4u^2} \right)^2 dt^2 + u^2 \left( 1 - \frac{R^2}{4u^2} \right)^2 d\bar{\Omega}_3^2 + \frac{R^2}{u^2} du^2 + R^2 \left( 1 - (2\pi\alpha')^2 \frac{\Psi(t, u)^2}{R^2} \right) d\Omega_3^2 + (2\pi\alpha')^2 \left( \frac{\partial \Psi(t, u)}{\partial t} dt + \frac{\partial \Psi(t, u)}{\partial u} du \right)^2. \quad (2.25)$$

We next need to write down the action for the scalar fluctuation to leading order in  $\alpha'$ . A subtle point here is that all scalars are in the adjoint representation of the  $SU(2)$  group on the world-volume of two D7-branes. The approach we adopt here to write the action, is to first treat all scalars as *abelian* and derive the action for the fluctuation by linearising the DBI action. In the last step we then promote all fields to be in the adjoint representation by introducing an overall trace in front of the action (for more on this and other approaches, see e.g. [36, 101]).

---

<sup>4</sup>The fluctuation in the other direction leads to the same spectrum, so we will not comment on it any further (though we should emphasise that this is a property of the equatorial embedding not shared by non-zero bare quark mass embeddings).

Following these steps we end up with the action governing the scalar fluctuations,

$$S = -T_{D7} \frac{4\pi^6 R^4}{\lambda} \int du dt u^3 \left(1 + \frac{R^2}{4u^2}\right) \left(1 - \frac{R^2}{4u^2}\right)^3 \times \left[ -\frac{R^2}{2} \left(\frac{4u}{4u^2 + R^2}\right)^2 D_t \Psi^{(a)} D_t \Psi^{(a)} + \frac{u^2}{2R^2} \partial_u \Psi^{(a)} \partial_u \Psi^{(a)} - \frac{3}{2} \frac{\Psi^{(a)} \Psi^{(a)}}{R^2} \right]. \quad (2.26)$$

Since we expect that an instability will appear in the gauge direction orthogonal to the background field  $A_0$ , we make the ansatz for the fluctuation field to be

$$\Psi(t, u) = e^{-i\omega t} \left( \Psi_\omega^{(1)}(u) \tau^1 + \Psi_\omega^{(2)}(u) \tau^2 \right), \quad (2.27)$$

where we have focused on one Fourier mode.

The equations of motion for the components  $\Psi_\omega^{(1)}$  and  $\Psi_\omega^{(2)}$  are coupled, but can be decoupled by changing variables as

$$\Psi_\omega^{(\pm)}(u) = \Psi_\omega^{(1)}(u) \pm i \Psi_\omega^{(2)}(u). \quad (2.28)$$

The equations of motion for the components  $\Psi^{(\pm)}$  are

$$\frac{\partial_u (\sqrt{-g} g^{uu} \partial_u \Psi_\omega^{(\pm)})}{\sqrt{-g} g^{uu}} - \frac{g^{tt}}{g^{uu}} \left( \omega \pm A_0^{(3)} \right)^2 \Psi_\omega^{(\pm)} + \frac{3}{R^2 g^{uu}} \Psi_\omega^{(\pm)} = 0, \quad (2.29)$$

which for the specific metric on the D7-brane world-volume become

$$\partial_u^2 \Psi_\omega^{(\pm)} + \frac{\partial_u \left( u^5 \left(1 + \frac{R^2}{4u^2}\right) \left(1 - \frac{R^2}{4u^2}\right)^3 \right)}{u^5 \left(1 + \frac{R^2}{4u^2}\right) \left(1 - \frac{R^2}{4u^2}\right)^3} \partial_u \Psi_\omega^{(\pm)} + \left[ \frac{R^4}{u^4 \left(1 + \frac{R^2}{4u^2}\right)^2} (\omega \pm \mu)^2 + \frac{3}{u^2} \right] \Psi_\omega^{(\pm)} = 0. \quad (2.30)$$

These equations can be solved by reducing them to Schrödinger form. A very similar equation has been analysed in [7] for the determination of the mesonic spectrum on the world-volume of a probe  $D7$  brane at  $T = 0$ , in global AdS space. Following steps similar to those in [7], and focusing on modes which are constant both on the  $S^3 \in S^5$  and on the gauge theory  $\bar{S}^3$ , we obtain for the spectrum of fluctuations

$$(\mu + \omega)R = \pm(3 + 2n) \quad n = 0, 1, 2, \dots \quad (2.31)$$

Here  $n$  is the main quantum number. We see that the key effect of the non-vanishing chemical potential is to shift the frequency  $\omega \rightarrow \omega + \mu$ . Because of this we see that for large enough chemical potential  $\mu > \mu_{\text{crit}} = 3/R$ , the frequency of the lowest lying mode becomes zero, signalling that the homogeneous solution potentially becomes unstable at this value of the chemical potential, and a condensate of the scalar might form.

### 2.2.2 Vector fluctuations at zero temperature

Following the perturbative analysis in the scalar sector, we now turn our attention to vectors. We again expect unstable modes, but would like to know whether or not they occur before the instability of the scalar sector. An analysis of the vector mode spectrum was performed in infinite volume limit (on the Poincaré patch) in [102] and then later extended to non-zero chemical potential in [101, 103, 104]. At finite volume and vanishing temperature and chemical potential the spectrum can be found in [7]. The upshot of the analysis of [102] is that the lowest lying supermultiplet consists of two transverse scalars describing the transverse fluctuations of the D7-brane in the  $S^5$ , one scalar which originates from the vector component in the internal  $S^3 \in S^5$  wrapped by the D7-brane, and gauge components in the non-compact directions of  $\text{AdS}_5$ . As one moves to the compact case, i.e. global AdS space [7], the states from this supermultiplet get reorganised (split) so that the lightest state in the compact space is the scalar which originates from the component of the gauge field in the direction of the internal  $S^3 \in S^5$ . The vector components in the direction of the dual sphere as well as the transverse scalars both have larger masses. We now want to see how the fluctuations from the vector sector are shifted upon introducing a chemical potential.

#### The gauge theory vector fluctuations

Let us start with the vector components in the direction of the sphere  $\bar{S}^3$  of the dual gauge theory. These fluctuations are dual to the vector excitations in the gauge theory. Similarly to what we did for scalars, we start by writing the fluctuations as

$$A = A_0^{(3)}(u)\tau^3 dt + Ra_i^{(1)}(t, u, \bar{\Omega}_3)\tau^1 d\bar{\theta}^i + Ra_i^{(2)}(t, u, \bar{\Omega}_3)\tau^2 d\bar{\theta}^i, \quad (2.32)$$

where  $i = (1, 2, 3)$  are indices on the dual  $\bar{S}^3$ , and as for scalars we fluctuate in the gauge directions orthogonal to  $A_0^{(3)}$ . Since we know that the lowest lying vector is a singlet on  $S^3$  we do not have to consider excitations which depend on the coordinates of the internal sphere.<sup>5</sup>

---

<sup>5</sup>In the language of [7] we consider type II fluctuations, with type I fluctuations to be considered in the next subsection. Looking ahead, it turns out that type III fluctuations condense after type I fluctuations and we will not consider them in detail here.

Next, we linearise the Yang-Mills action on the world-volume of the D7-probe,

$$S = -T_{D7}\pi^2 \frac{R^4}{2\lambda} \int d^8\xi \sqrt{-g} \left[ (\partial_u A_0^{(3)})^2 g^{tt} g^{uu} + R^2 \left( ((D_t a_i)^{(a)})^2 g^{tt} g^{ii} + (\partial_u a_i^{(a)})^2 g^{uu} g^{ii} \right) + R^2 (f_{ij}^a)^2 g^{ii} g^{jj} \right], \quad (2.33)$$

where

$$(D_t a_i)^{(a)} = \partial_t a_i^{(a)} - \epsilon^{abc} A_0^{(b)} a_i^{(c)}, \quad f_{ij}^a = (\partial_i a_j^{(a)} - \partial_j a_i^{(a)}). \quad (2.34)$$

Here,  $g_{ij}$  is the metric on  $\bar{S}^3$ . The equations of motion for the fluctuations  $a_i^{(a)}$  are given by

$$\begin{aligned} \sqrt{-g} \epsilon^{abc} A_0^{(c)} D_t a_i^{(b)} g^{tt} g^{ii} + \sqrt{-g} \partial_t \left( D_t a_i^{(a)} \right) g^{tt} g^{ii} + \partial_u \left( \sqrt{-g} \partial_u a_i^{(a)} g^{uu} g^{ii} \right) \\ + \sum_j \left( \sqrt{-g} \left( \partial_j a_i^{(a)} - \partial_i a_j^{(a)} \right) g^{jj} g^{ii} \right) = 0, \end{aligned} \quad (2.35)$$

In order to solve this equation let us Fourier transform in the time direction. In order to decouple the equations for the fluctuations  $a_i^{(1)}$  and  $a_i^{(2)}$  we introduce a new pair of variables

$$\bar{X}_i^{(\pm)}(u, \omega, \bar{\Omega}_3) = e^{-i\omega t} \left( a_i^{(1)}(u, \omega, \bar{\Omega}_3) \pm i a_i^{(2)}(u, \omega, \bar{\Omega}_3) \right). \quad (2.36)$$

This finally yields the fluctuation equations

$$\begin{aligned} \partial_u \left( \sqrt{-g} g^{uu} g^{ii} \partial_u \bar{X}_i^{(\pm)} \right) + \sum_j \partial_j \left( \sqrt{-g} g^{jj} g^{ii} \left( \partial_j \bar{X}_i^{(\pm)} - \partial_i \bar{X}_j^{(\pm)} \right) \right) \\ - \sqrt{-g} g^{tt} g^{ii} \left( \omega \pm A_0^{(3)} \right)^2 \bar{X}_i^{(\pm)} = 0, \end{aligned} \quad (2.37)$$

which are equivalent to

$$D^u \left( \partial_u \bar{X}_i^{(\pm)} \right) + \nabla^j \left( \partial_j \bar{X}_i^{(\pm)} - \partial_i \bar{X}_j^{(\pm)} \right) - g^{tt} \left( \omega \pm A_0^{(3)} \right)^2 \bar{X}_i^{(\pm)} = 0. \quad (2.38)$$

In order to solve these equations, we make a factorised ansatz for  $\bar{X}_i$ , as a product of radial and angular functions, and expand the angular part  $\bar{X}_i^{\bar{\Omega}_3}(\bar{\Omega}_3)$  on  $\bar{S}^3$  in terms of vector spherical harmonics. In general, the fluctuations could also depend on a direction on internal sphere  $S^3$ . However, as mentioned before, we will focus only on singlets under the global  $SO(4)$  symmetry group. Also, while there exists three type of vector spherical harmonics on  $\bar{S}^3$ , it has been argued in [7, 102], that for fluctuations of the vector field which are taking place in  $\bar{S}^3 \in \text{AdS}_5$ , only  $Y_i^{l,\pm}$  which transform in  $\left( \left( \frac{l\mp 1}{2}, \frac{l\pm 1}{2} \right) \right)$ ,  $l \geq 1$  irreducible representations of  $SO(4)$  are relevant. Hence we expand the fluctuations as

$$\bar{X}_i^{(\pm)}(u, \omega, \bar{\Omega}_3) = \sum_{\bar{l}, s=\pm} \bar{\Phi}_{\omega, \bar{l}, s}^{(\pm)}(u) Y_i^{\bar{l}, s}, \quad (2.39)$$

where the index  $(\pm)$  refers to the two linear combinations of modes as defined in (2.36), and the  $\pm$  index refers to the value of the index  $s$  labelling the vector spherical harmonics.

The spherical harmonics satisfy the identities

$$\begin{aligned}\nabla_i \nabla^i Y_j^{l,\pm} - R_j^k Y_k^{l,\pm} &= -(l+1)^2 Y_j^{l,\pm}, \\ \epsilon^{ijk} \nabla_j Y_k^{l,\pm} &= \pm(l+1) Y_{l,\pm}^i, \\ \nabla^i Y_i^{l,\pm} &= 0,\end{aligned}\tag{2.40}$$

Using these identities the equation for the vector fluctuations can be rewritten as

$$\begin{aligned}\bar{\Phi}_{\omega,\bar{l},s}^{(\pm)''}(u) + \frac{\partial_u \left( \sqrt{-g(u)} g^{uu}(u) P(u) \right)}{\left( \sqrt{-g(u)} g^{uu}(u) P(u) \right)} \bar{\Phi}_{\omega,\bar{l},s}^{(\pm)'}(u) \\ - \frac{1}{g^{uu}(u)} \left[ g^{tt}(u) \left( \omega \pm A_0^{(3)}(u) \right)^2 + (\bar{l}+1)^2 P(u) \right] \bar{\Phi}_{\omega,\bar{l},s}^{(\pm)}(u) = 0,\end{aligned}\tag{2.41}$$

where the  $\pm$  sign in front of  $A_0$  in the equation is correlated with the  $(\pm)$  sign on the  $\bar{\Phi}^{(\pm)}$  and  $P(u)$  is the inverse of the  $u$ -dependent part of the the metric factor in front of  $d\bar{\Omega}_3^2$ . We should note that this equation is independent of the quantum number  $s = \pm 1$ , which will be different when we start looking at the vector fluctuations in the direction of the internal sphere. In the case of zero temperature the fluctuation equation becomes (see also [7])

$$\begin{aligned}\bar{\Phi}_{\omega,\bar{l}}^{(\pm)''}(u) + \frac{\partial_u \left( u^3 \left( 1 + \frac{R^2}{4u^2} \right) \left( 1 - \frac{R^2}{4u^2} \right) \right)}{u^3 \left( 1 + \frac{R^2}{4u^2} \right) \left( 1 - \frac{R^2}{4u^2} \right)} \bar{\Phi}_{\omega,\bar{l}}^{(\pm)'}(u) \\ + \left[ \frac{R^4}{u^4 \left( 1 + \frac{R^2}{4u^2} \right)^2} (\omega \pm \mu)^2 - \frac{R^2}{u^4 \left( 1 - \frac{R^2}{4u^2} \right)^2} (\bar{l}+1)^2 \right] \bar{\Phi}_{\omega,\bar{l}}^{(\pm)}(u) = 0.\end{aligned}\tag{2.42}$$

This equation is very similar to (2.30), and can again be cast in Schrödinger form. We then find that the spectrum of vector fluctuations for the  $\bar{l}$ -th spherical harmonics is given by

$$(\omega \pm \mu)R = (3 + \bar{l} + 2n) \quad n = 0, 1, 2, 3, \dots \quad \bar{l} = 1, 2, 3, \dots,\tag{2.43}$$

Here  $n$  is again the main quantum number, and  $\bar{l}$  is an  $SO(4)$  quantum number corresponding to the sphere  $\bar{S}^3 \in \text{AdS}_5$ . We see that the result is again the same as the one in [7] if we consider  $SO(4)$  singlets (i.e. set  $l = 0$ ), except that the chemical potential shifts the frequency  $\omega \rightarrow \omega \pm \mu$ .

From equation (2.43) we see that for a critical value of the chemical potential given by  $\mu_{\text{crit}} = 4/R$ , the lowest lying mode  $\bar{l} = 1$  will become massless. Therefore, we expect

that when the chemical potential is larger than this value, the system potentially becomes unstable.

### The charged scalar fluctuations

Let us now consider fluctuations of the vector field in the direction of the internal  $S^3 \in S^5$ , which are dual to an  $SO(4)$  charged scalar field in the gauge theory. Since the WZW term in the action is now non-zero, when considering fluctuations, we have to modify the action from (2.33) by adding the term

$$S_{WZW} = \frac{T_{D7}\pi^2 R^4}{\lambda} \int \text{Tr}(C \wedge F \wedge F), \quad dC = \frac{4}{R}(1 + *)\text{Vol}(\text{AdS}_5). \quad (2.44)$$

Similarly as before, we make an ansatz as in (2.32) except that the index  $i$  is now taking values in the internal  $S^3$ . In addition, we will also allow the fluctuations to depend on both  $S^3$  and  $\bar{S}^3$  variables. In order to decouple the equations of motion we redefine variables as in (2.36) and make a factorised ansatz

$$X_i^{(\pm)}(u, \omega, \Omega_3, \bar{\Omega}_3) = e^{-i\omega t} \Phi^{(\pm)}(u) \bar{Y}^{\bar{l}}(\bar{\Omega}_3) Y_i^{l,s}(\Omega_3), \quad (2.45)$$

where the index  $(\pm)$  refers to the sign in the linear combination (2.36),  $i$  denotes the index in the direction of the internal  $S^3$ , and the index  $s = \pm 1$ . Also to shorten the notation we have suppressed indices on the functions  $\Phi^{(\pm)}$ , which should really also carry indices  $(\omega, s, \bar{l}, l)$ .

Following the same procedure as for scalars and the other gauge components we arrive at the equation for the fluctuations (see also [7])

$$\begin{aligned} \partial_u^2 \Phi^{(\pm)} + \frac{\partial_u(u^5 (1 + \frac{R^2}{4u^2}) (1 - \frac{R^2}{4u^2})^3)}{u^5 (1 + \frac{R^2}{4u^2}) (1 - \frac{R^2}{4u^2})^3} \partial_u \Phi^{(\pm)} + \frac{R^2}{u^4 (1 + \frac{R^2}{4u^2})^2} (\omega \pm \mu)^2 \Phi^{(\pm)} \\ - \left[ (l+1)^2 + \bar{l}(\bar{l}+2) \frac{R^2}{u^2 (1 - \frac{R^2}{4u^2})^2} + 4s(l+1) \right] \frac{1}{u^2} \Phi^{(\pm)} = 0, \end{aligned} \quad (2.46)$$

where the sign in the  $(\omega \pm \mu)$  is the same as for  $\Phi^{(\pm)}$ . We should note that this equation explicitly depends on the quantum number  $s$ , which is labelling the vector harmonics on  $S^3$ . This is in contrast to the previous case for the equation for vector fluctuations on  $\bar{S}^3$ .

Putting equation (2.46) in Schrödinger form, like we did for the other fluctuations, we

obtain for the spectrum

$$(\omega \pm \mu)R = 3 + 2s + l + 2n + \bar{l} \quad \text{where}$$

$$\bar{l} = 0, 1, 2, \dots \quad l = 1, 2, 3, \dots \quad n = 0, 1, 2, \dots \quad s = \pm 1. \quad (2.47)$$

This is the same as (4.31) of [7] except for the shift  $\omega \rightarrow \omega + \mu$ . Let us also note that the lowest lying excitation carries quantum numbers  $(\bar{l} = 0, l = 1, s = -1, n = 0)$ , and this mode will reach zero frequency when  $\mu > \mu_{\text{crit}} = 2/R$ .<sup>6</sup>

## 2.3 Perturbative analysis of the homogeneous vacuum at $T \neq 0$

In the previous section we have observed that the homogeneous isotropic ground state at non-zero chemical potential and zero temperature was unstable under both scalar and vector fluctuations. We would now like to see how is this modified once the temperature is turned on, paying particular attention to the order in which the instabilities set in as a function of temperature.

We should emphasise that in contrast to the zero temperature case, where all fluctuations have real frequency  $\omega$  (corresponding to stable mesonic scalar and vector particles), at finite temperature (above the Hawking-Page transition), even in the absence of chemical potential all fluctuation frequencies have a non-vanishing imaginary part. When the chemical potential is zero the imaginary part of these frequencies are negative, corresponding to the fact that these excitations are decaying in time, i.e. that they describe *quasi-stable* particles. However, as the chemical potential is turned on, if there is indeed an instability present, we expect that the negative imaginary part of the frequencies will become positive, i.e. that a decaying excitation would become an exponentially growing mode, which signals an instability. In what follows, we will therefore focus on studying the imaginary part of the quasi-normal modes of the system.

We start our analysis by looking at the scalar fluctuations, and repeat the procedure similar to that at zero temperature. Again, we use the metric on the  $S^5$  as in (2.23), keeping only the transverse scalar  $\Psi(t, u)$  nonzero (see equation (2.24)) and making it depend only on time and the radial direction  $u$ . As argued before, such excitation is

---

<sup>6</sup>The fact that this excitation has the lowest mass at  $\mu = 0$  was also observed in [7], but no attempt was made to study its condensation under the influence of a chemical potential.

consistent with the full equations of motion, and should correspond to the lowest energy mode, an S-wave on  $\bar{S}^3$ . The induced metric on the D7-brane world-volume is then

$$ds^2 = -\frac{2\rho_H^2 F(u)}{uR^2 W(u)} dt^2 + 2\frac{\rho_H^2}{u} W(u) d\bar{\Omega}_3^2 + \frac{R^2}{4u^2 F(u)} du^2 + R^2 \left( 1 - \frac{\Psi(t, u)^2}{R^2} \right) d\Omega_3^2 + \left( \frac{\partial \Psi(t, u)}{\partial t} dt + \frac{\partial \Psi(t, u)}{\partial u} du \right)^2, \quad (2.48)$$

where

$$F(u) = 1 - u^2, \quad W(u) = 1 - \frac{uR^2}{4\rho_H^2}. \quad (2.49)$$

As before, we Fourier transform the scalar  $\Psi(t, u)$  and make the ansatz that it is pointing in the direction orthogonal to the  $A_0^{(3)}\tau^3$  in colour space,

$$\Psi(t, u) = \int \frac{d\omega}{2\pi} e^{-i\omega t} (\Psi_\omega^{(1)}(u)\tau^1 + \Psi_\omega^{(2)}(u)\tau^2). \quad (2.50)$$

We then again change variables as

$$\Psi_\omega^{(\pm)}(u) = \Psi_\omega^{(1)}(u) \pm i\Psi_\omega^{(2)}(u), \quad (2.51)$$

so that the equations for the  $\Psi^{(\pm)}$  fluctuations decouple and are given by<sup>7</sup>

$$\frac{\partial_u \left( \frac{W(u)F(u)}{u} \partial_u \Psi_\omega^{(\pm)}(u) \right)}{\frac{W(u)F(u)}{u}} + \frac{R^4 W(u)}{8u\rho_H^2 F(u)^2} \left( \omega \pm A_0^{(3)}(u) \right)^2 \Psi_\omega^{(\pm)}(u) + \frac{3}{4u^2 F(u)} \Psi_\omega^{(\pm)}(u) = 0. \quad (2.52)$$

We solve the fluctuation equation by imposing that the modes satisfy an incoming boundary condition at horizon,

$$\Psi_\omega^{(\pm)}(u) \Big|_{u \approx 1} = (1 - u)^{-i\omega/(4\pi T)} (1 + O(1 - u)). \quad (2.53)$$

The equations for the vector fluctuations are derived in a similar way. Let us first consider the vector fluctuations which are dual to vectors. We take them to be singlets under the global  $SO(4)$  ( $l = 0$ ), and orthogonal to the isospin chemical potential in the gauge group as we did at zero temperature, see (2.32). Following steps similar to those at zero temperature, instead of  $a_i^{(1)}, a_i^{(2)}$ , we introduce a new pair of variables  $X_i^{(\pm)}$ , as in

<sup>7</sup>Note that at  $T = 0$ , the equations only depend on  $\omega - \mu$ , and hence the critical chemical potential coincides with the frequency of the lightest mode. At  $T > 0$  the  $A_0^{(3)}$  component is no longer a constant, and obtaining the critical chemical potential is more complicated (physical states are no longer straight lines in the  $\omega, \mu$  plane).

(2.36) and Fourier expand it in spherical harmonics as in (2.39). Hence, we arrive at the equations of motion for these fluctuations

$$\partial_u^2 \bar{\Phi}_\omega^{(\pm)s, \bar{l}} + \frac{\partial_u F(u) \partial_u \bar{\Phi}_\omega^{(\pm)s, \bar{l}}}{F(u)} - (\bar{l} + 1)^2 \frac{R^2}{8\rho_H^2 W(u) F(u) u} \bar{\Phi}_\omega^{(\pm)s, \bar{l}} + \frac{R^4 W(u)}{8u\rho_H^2 F(u)^2} (\omega \pm A_0^{(3)})^2 \bar{\Phi}_\omega^{(\pm)s, \bar{l}} = 0. \quad (2.54)$$

As for scalars, we impose incoming boundary conditions at the black hole horizon

$$\bar{\Phi}_\omega^{(\pm)s, \bar{l}} \Big|_{u \approx 1} = (1 - u)^{-i\omega/(4\pi T)} (1 + O(1 - u)). \quad (2.55)$$

Finally, we turn to the vector fluctuations dual to the charged scalars. Following similar steps as we did at zero temperature we arrive at the equations governing these fluctuations (see equation (2.46))

$$\frac{\partial_u \left( \frac{W(u)F(u)}{u} \partial_u \Phi^{(\pm)} \right)}{\frac{W(u)F(u)}{u}} - (l + 1)^2 \frac{1}{4u^2 F(u)} \Phi^{(\pm)} - \bar{l}(\bar{l} + 2) \frac{R^2}{8\rho_H^2 W(u) F(u) u} \Phi^{(\pm)} - \frac{s(l + 1)}{u^2 F(u)} \Phi^{(\pm)} + \frac{R^4 W(u)}{8u\rho_H^2 F(u)^2} (\omega \pm A_0^{(3)})^2 \Phi^{(\pm)} = 0. \quad (2.56)$$

where we have again suppressed the indices  $(\omega, \bar{l}, l, s)$  on the functions  $\Phi$  and we impose incoming boundary conditions at the horizon of the black hole

$$\Phi^{(\pm)} \Big|_{u \approx 1} = (1 - u)^{-i\omega/(4\pi T)} (1 + O(1 - u)). \quad (2.57)$$

In order to solve the fluctuation equations (2.52), (2.54) and (2.56), we use a shooting technique, in which we start from the horizon and look for modes that decay at infinity i.e. we look for the modes that describe normalisable excitations. These boundary conditions will be satisfied only for a discrete set of frequencies. We plot the imaginary parts of those frequencies for the scalar and two vectors, for fixed temperature and various values of the chemical potential  $\mu$ , in figure 2.1.

We see that as the value of the chemical potential is increased, the imaginary parts of the frequencies, which were initially all negative, become less and less negative and approach zero. When the chemical potential exceeds a critical value, the imaginary parts become positive one by one, signalling the presence of unstable modes in the system. Similarly, the real parts of the frequencies are decreasing to zero as the chemical potential grows, signalling again the onset of an instability. For a particular value of the temperature presented on the left plot in the figure 2.1, we see that the vector dual to the gauge theory

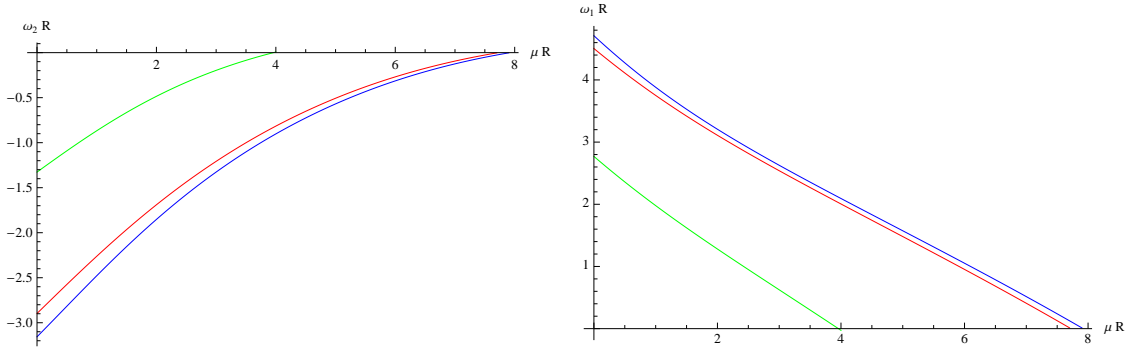


Figure 2.1: Plots of the imaginary (left) and real (right) parts of the frequencies for the lowest lying uncharged scalar fluctuation (red), the vector fluctuation (blue) and the charged scalar fluctuation (green), at fixed temperature  $\pi TR = 2$ , as a function of the chemical potential.

charged scalar remains the lightest in the spectrum and condenses first, followed by the transverse scalar and finally the vector.

In general, one would expect that particles condense roughly when the chemical potential become of the order of their mass. It is thus of interest to look at the behaviour of the masses<sup>8</sup> as a function of temperature. Figure 2.2 shows the result of this analysis. We here observe another interesting phenomenon, namely that there is a crossover point at some critical value of the temperature, above which the lightest vector becomes lighter than the transverse scalar. This suggests that above the crossover temperature, the lightest vector would condense before the lightest transverse scalar, if it had not been for the  $SO(4)$  charged scalar that condenses even earlier. One can indeed see that the corresponding imaginary parts cross as well, approximately at this point, see figure 2.3.

For large  $TR$ , the results read

$$\begin{aligned}
 \text{charged scalar :} \quad & \mu_{\text{crit}}R \approx 2.00\pi TR - \frac{2.00 \times 0.05}{4\pi TR} + \dots, \\
 \text{vector :} \quad & \mu_{\text{crit}}R \approx 4.00\pi TR - \frac{4.00 \times 0.05}{4\pi TR} + \dots, \\
 \text{uncharged scalar :} \quad & \mu_{\text{crit}}R \approx 4.16\pi TR - \frac{4.16 \times 1.00}{4\pi TR} + \dots.
 \end{aligned} \tag{2.58}$$

The leading order terms should agree with those obtained in the Poincaré patch, though to our knowledge only the one for the vector has been computed in the literature [101, 104, 105]. The result for the critical chemical potential of [101, 104] (when extrapolated to

<sup>8</sup>We use pole masses here for convenience as they are easy to obtain from the quasi-normal mode analysis, and the intuition we want to verify is anyhow qualitative.

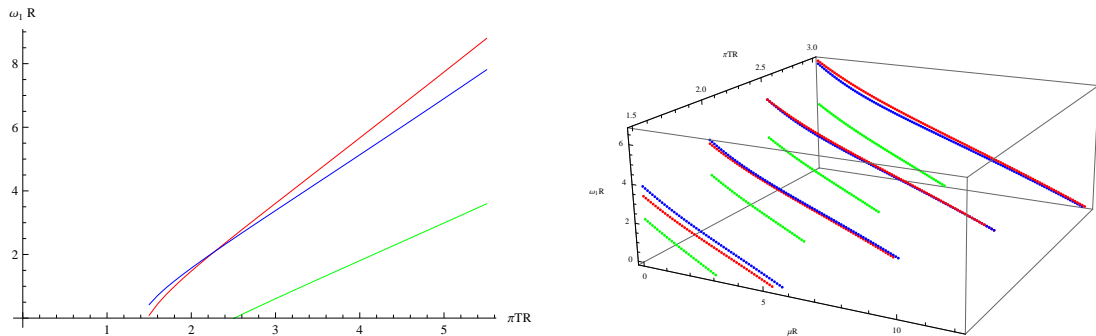


Figure 2.2: Left is a plot of the real parts of the frequencies for the various modes (colours as in figure 2.1) as functions of the temperature at fixed value  $\mu R = 5$  of the chemical potential. The plot on the right shows the real parts of the frequencies as functions of both temperature and chemical potential.

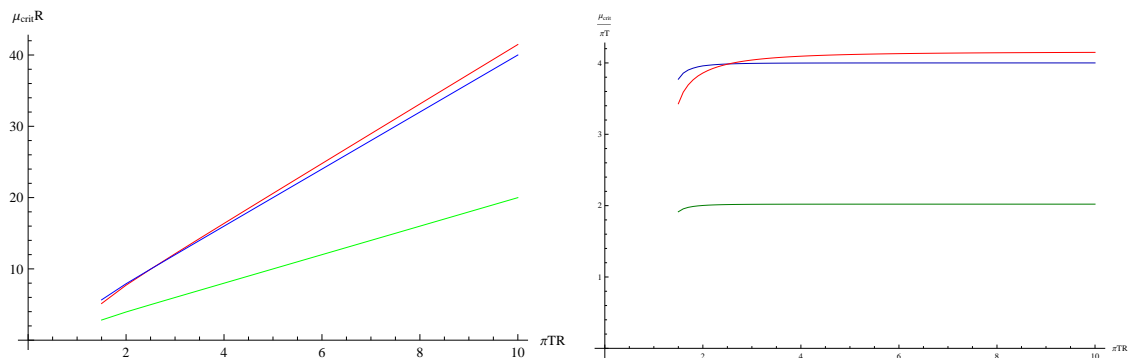


Figure 2.3: Critical chemical potential as function of temperature, in two different dimensionless combinations. The figure on the right shows more clearly what happens in the  $TR \rightarrow \infty$  limit, which can be interpreted as the large radius limit at fixed temperature.

zero bare quark mass) seems to be somewhat larger than ours, which may be due to the fact that we have used a Yang-Mills truncation rather than the full DBI action.

## 2.4 The new ground states at zero and finite temperature

In the previous two sections we have seen that for large enough chemical potential the homogeneous ground state on  $\bar{S}^3 \in \text{AdS}_5$  becomes unstable under both scalar and various components of vector fluctuations. This is happening both at zero and non-zero temperature. In particular we observe that, at zero temperature, vector fluctuations in the direction of the internal  $S^3 \in S^5$  are the first to become unstable. As the temperature is increased, these vector components remain the first to become unstable. On the other

hand, the ordering in which the other components of the vector fluctuations and the scalar fluctuations become unstable is dependent on the temperature, as there is a ‘crossover’ temperature above which all vector components first become unstable.

Our previous analysis was done in perturbation theory, i.e. at the linearised level. So we would now like to see if the instabilities which we have found are present in the full non-linear theory, and to explore the new ground state in which the system settles for large enough values of the chemical potential.

### 2.4.1 The new ground state at zero temperature

In section 2.2.2 we have observed that as the chemical potential is turned on, when its value reaches  $\mu \geq 2/R$ , the lowest lying mode of the vector component in the internal  $S^3$ , becomes massless, signalling the onset of possible instability in the system. We have also seen that for even larger values of the chemical potential, the scalar becomes massless at  $\mu \geq 3/R$  and the other components of the vector develop an instability for  $\mu \geq 4/R$ .

To see whether the appearance of these massless modes indeed signals a real instability, we will now turn to the full non-linear theory and try to explicitly construct the new ground state to which the system would evolve as a consequence of the instability. As the perturbative analysis suggests that vector components in the internal  $S^3$  direction are first to condense, we will start the analysis of the new ground state by turning on only those components. We will later, for comparison, also analyse possible ground states due to condensation of the other fluctuations, and verify that those always have higher energy than the scalar condensate.

When writing down an ansatz for the scalar condensate ground state, we will use the fact that in perturbation theory, the first unstable mode is an  $\bar{l} = 0, l = 1, n = 0, s = -1$  wave (where  $\bar{l}$  labels modes in the  $\bar{S}^3$  and  $l$  labels modes in the  $S^3 \in S^5$ ). As far as the  $A_0$  component is concerned, at linearised level one cannot see the back-reaction of the scalar on the background value of this field, so in principle one cannot say if in the new ground state the  $A_0$  component will start to depend on the angular coordinates or not.

As a simplest attempt we take  $A_0$  to remain homogeneous, i.e. independent of the  $\bar{S}^3$  angular coordinates. With this ansatz, potential problems in the equations of motion could originate from expression of the form “ $A_\alpha A_\beta g_{S^3}^{\alpha\beta}$ ”, which are now turned on due to the non-vanishing vector field in the direction of the internal sphere  $S^3$ . Since these terms will typically produce spherical harmonics of higher  $l$ -number we would need to balance them in the equations of motion. However, we expect that the ground state would originate from

condensation of only the lowest harmonic, so that higher  $l$ -harmonics are not needed. It is possible to reconcile these two observations if the “ $A_\alpha A_\beta g_{S^3}^{\alpha\beta}$ ” expression is independent of the angular coordinates. This can indeed be achieved for a particular linear combination of spherical harmonics given by

$$Y_\alpha = \frac{ik_0}{K} Y_\alpha^{1,0,0,-1} + \frac{(k_1 + ik_2)}{K} Y_\alpha^{1,0,-1,-1} + \frac{(k_1 - ik_2)}{K} Y_\alpha^{1,0,1,-1}$$

where  $K \equiv \sqrt{k_0^2 + 2(k_1^2 + k_2^2)}$ , (2.59)

and  $k_0, k_1, k_2$  are three arbitrary real numbers which are not simultaneously vanishing, and  $(l, m_1, m_2, s)$  are the quantum numbers of the spherical harmonics. We should note here that value of these quantum numbers will be taken to be the same as those of the lowest lying excitation we have previously found in the perturbative analysis. Explicitly, the spherical harmonics are given by

$$\begin{aligned} Y^{1,0,0,-1} &= -i \sin^2 \theta d\phi - i \cos^2 \theta d\psi \\ Y^{1,0,1,-1} &= \frac{e^{i(\psi+\phi)}}{\sqrt{2}} d\theta + \frac{i \sin \theta \cos \theta e^{i(\psi+\phi)}}{\sqrt{2}} (d\phi - d\psi) \\ Y^{1,0,-1,-1} &= \frac{e^{-i(\psi+\phi)}}{\sqrt{2}} d\theta - \frac{i \sin \theta \cos \theta e^{-i(\psi+\phi)}}{\sqrt{2}} (d\phi - d\psi), \end{aligned} \quad (2.60)$$

where  $\theta, \phi, \psi$  are Euler coordinates on  $S^3 \in S^5$ ,

$$ds_{S^3}^2 = d\theta^2 + \sin^2 \theta d\phi^2 + \cos^2 \theta d\psi^2. \quad (2.61)$$

It is also useful to keep in mind that

$$(Y_i^{l,m_1,m_2,s})^* = -(-1)^{m_1-m_2} Y_i^{l,-m_1,-m_2,s}. \quad (2.62)$$

Our ansatz for the new ground state is

$$A_0 = A_0^{(3)}(u)\tau^3, \quad A_\alpha = R\eta(u)Y_\alpha(\Omega_3)\tau^1 \quad (2.63)$$

Plugging this into equations of motion, and using identities (2.40) we get an equation for  $A_0(u)$

$$\frac{\partial_u \left( (\partial_u A_0^{(3)}) u^3 \left(1 - \frac{R^2}{4u^2}\right)^3 / \left(1 + \frac{R^2}{4u^2}\right) \right)}{u^3 \left(1 - \frac{R^2}{4u^2}\right)^3 / \left(1 + \frac{R^2}{4u^2}\right)} - \frac{R^2}{u^2} (\eta(u))^2 A_0^{(3)}(u) = 0, \quad (2.64)$$

and an equation for the function  $\eta(u)$

$$\frac{\partial_u \left( \partial_u \eta(u) u^5 \left(1 + \frac{R^2}{4u^2}\right) \left(1 - \frac{R^2}{4u^2}\right)^3 \right)}{u^5 \left(1 + \frac{R^2}{4u^2}\right) \left(1 - \frac{R^2}{4u^2}\right)^3} + \frac{R^4}{u^4 \left(1 + \frac{R^2}{4u^2}\right)^2} (A_0^{(3)}(u))^2 \eta(u) + \frac{4}{u^2} \eta(u) = 0. \quad (2.65)$$

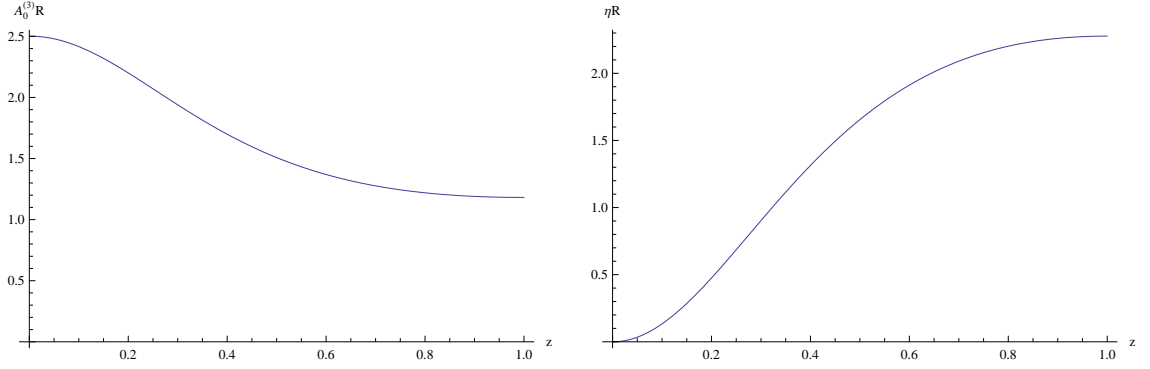


Figure 2.4: Profile of the fields  $A_0$  (left) and  $\eta$  (right) of the charged scalar condensate, evaluated at  $\mu R = 2.5$ . The boundary is at  $z = 0$  and the AdS centre is at  $z = 1$ .

Note that these are independent of the parameter  $K$ , which only appears in the angular part of the equations of motion, which is automatically satisfied for our ansatz.

Equations (2.64), and (2.65) are written in the non-compact coordinate  $u$  for which the AdS centre is at  $u = R/2$  and the boundary is at  $u = \infty$ . However, for numerical considerations it is more convenient to perform a coordinate change to compact coordinates  $z = R/(2u)$ , so that the AdS origin is at  $z = 1$ , and the boundary at  $z = 0$ . The equations of motion then are given by

$$\begin{aligned} \partial_z^2 A_0^{(3)}(z) + \frac{1 + 8z^2 + 3z^4}{z^5 - z} \partial_z A_0^{(3)}(z) - \frac{R^2}{z^2} \eta(z)^2 A_0^{(3)}(z) &= 0, \\ \partial_z^2 \eta(z) + \frac{3 + 4z^2 + 5z^4}{z^5 - z} \partial_z \eta(z) + \left( \frac{4}{z^2} + \frac{4R^2}{(1 + z^2)^2} A_0^{(3)}(z)^2 \right) \eta(z) &= 0. \end{aligned} \quad (2.66)$$

We are interested in the solutions of these equations that are regular everywhere, and in particular at the origin of AdS space. This removes half of the solutions, as can be seen by looking at the  $z \rightarrow 1$  limit of the above equations. Namely, assuming that  $A_0$  and  $\eta$  are regular at the AdS origin, it is easy to see that the above equations reduce to the conditions that the first derivatives of  $A_0$  and  $\eta$  are vanishing at the origin. Hence, the general regular solution will be parametrised by two parameters  $a, b$ . We then solve the equations of motion by shooting from the AdS origin, and look for the solutions at the boundary such that  $\eta$  is normalisable, while  $A_0$  is not. This normalisability condition further reduces the number of parameters by one. Hence in the expansion near infinity

$$A_0^{(3)} = \mu - \rho z^2 + \dots, \quad A_\alpha^{(1)} = R \rho_\eta Y_\alpha z^2 + \dots. \quad (2.67)$$

both the densities  $\rho$  and  $\rho_\eta$  are functions of the chemical potential  $\mu$ .

We plot the radial profile of the functions  $A_0(z)$  and  $\eta(z)$  for one particular solution

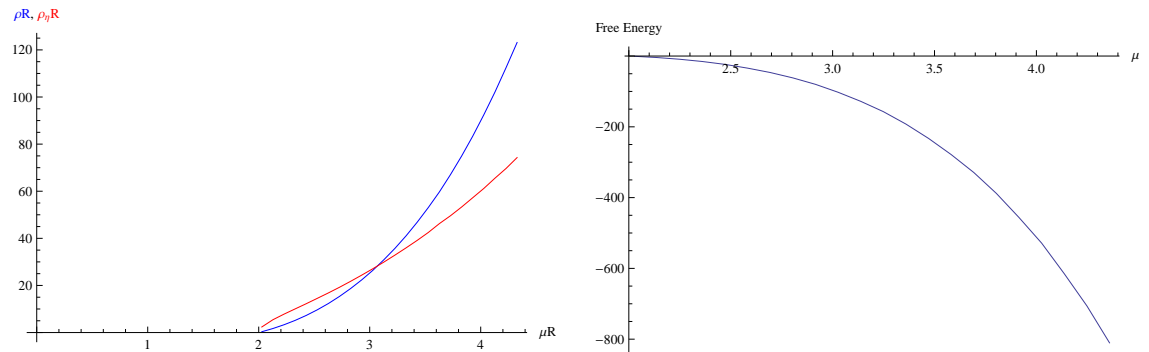


Figure 2.5: The plot on the left shows the isospin density  $\rho R$  (blue) and scalar density  $\rho_\eta R$  (red) of the charged scalar condensate as functions of the isospin chemical potential. The plot on the right shows the scaled free energy as function of chemical potential.

in figure 2.4. As required, we see that the solution is regular everywhere, and approaches the origin of AdS with vanishing derivative, so that no cusp is present. We also study various solutions for different values of chemical potential, see figure 2.5. The shooting procedure shows that there is a critical value of the chemical potential  $\mu_{\text{crit}} \sim 2/R$  below which there is no nontrivial solution present. Above  $\mu = \mu_{\text{crit}}$  a nontrivial condensate of scalar particles forms, and in the neighbourhood of  $\mu_{\text{crit}}$ , this condensate is to a good approximation given by

$$\rho_\eta = \begin{cases} 0 & \text{for } \mu < \mu_{\text{crit}} \\ \sqrt{\mu - \mu_{\text{crit}}} & \text{for } \mu > \mu_{\text{crit}}. \end{cases} \quad (2.68)$$

We have also evaluated the free energy for various values of the chemical potential (see figure 2.5), and observed that it is less than the (vanishing) free energy of the trivial configuration, which is in agreement with the statement that this is the ground state.

In summary, our analysis shows that for large enough value of the chemical potential, this system undergoes a second order phase transition in which the homogeneous isotropic solution is replaced with a non-isotropic one. The order parameter in this transition is the density  $\rho_\eta$ , and the critical exponent is the same as in the Landau-Ginsburg theory with positive quartic potential.

In order to complete the picture, and to show that (as expected from the perturbative analysis) the charged scalar condensate is always the one with the lowest energy, we will now construct condensates of the transverse scalar and the vector, and show that their energies are always higher than the one of the charged scalar. When constructing the transverse scalar ground state we recall that perturbative analysis suggested that the

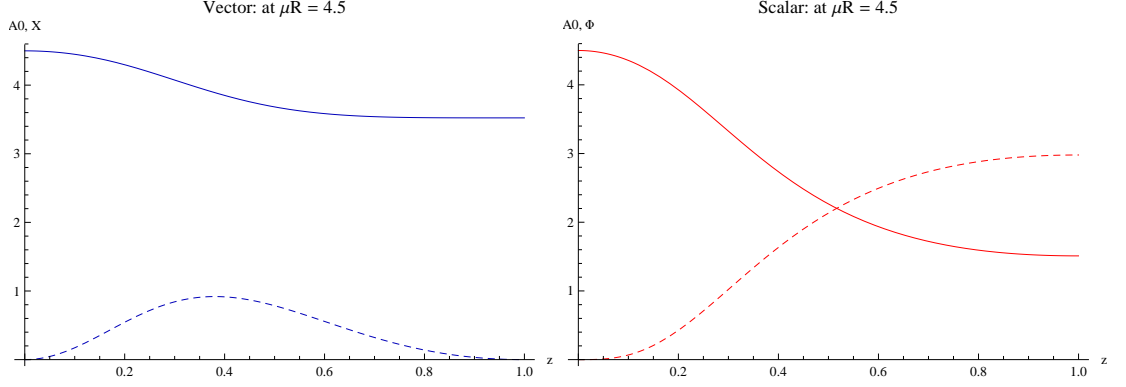


Figure 2.6: Left: a plot of the functions  $A_0(z)$  (solid curve) and  $\psi(z)$  (dashed curve) for the vector solution. Right: plots of the functions  $A_0(z)$  (solid) and  $\Phi$  (dashed) for the scalar configuration, both evaluated at a fixed value of chemical potential  $\mu R = 4.5$ .

s-wave is the first excitation of the scalar which becomes massless. Hence we make a homogeneous (i.e. only  $u$ -dependent) ansatz as follows

$$A = A_0^{(3)}(u)\tau^3 dt, \quad \Phi = \Phi^{(1)}(u)\tau^1, \quad (2.69)$$

where the vector  $A_0$  is present to account for the non-vanishing chemical potential, while all other vector components are zero. The equations of motion for the fields  $(A_0, \Phi)$  are given by

$$\begin{aligned} \partial_z^2 A_0^{(3)}(z) + \frac{1 + 8z^2 + 3z^4}{z^5 - z} \partial_z A_0^{(3)}(z) - \frac{R^2}{z^2} \Phi(z)^2 A_0^{(3)}(z) &= 0, \\ \partial_z^2 \Phi(z) + \frac{3 + 4z^2 + 5z^4}{z^5 - z} \partial_z \Phi(z) + \left( \frac{3}{z^2} + \frac{4R^2}{(1 + z^2)^2} A_0^{(3)}(z)^2 \right) \Phi(z) &= 0. \end{aligned} \quad (2.70)$$

Similarly, when constructing the ground state originating from vector condensation, we start with an ansatz which is similar to that of the vector component dual to a charged scalar, i.e. we write

$$A_0 = A_0^{(3)}(u)\tau^3, \quad A_{\bar{\alpha}} = \psi(u)Y_{\bar{\alpha}}(\bar{\Omega}_3)\tau^1, \quad (2.71)$$

where  $Y_{\bar{\alpha}}$  is as in (2.63), except that the index  $\bar{\alpha} = 1, 2, 3$  now refers to the  $\bar{S}^3 \in \text{AdS}_5$ . The equations of motion then become

$$\begin{aligned} \partial_z^2 A_0^{(3)}(z) + \frac{1 + 8z^2 + 3z^4}{z^5 - z} \partial_z A_0^{(3)}(z) - \frac{4}{(1 - z^2)^2} \psi(z)^2 A_0^{(3)}(z) &= 0, \\ \partial_z^2 \psi(z) + \frac{1 + 3z^4}{z^5 - z} \partial_z \psi(z) + \left( \frac{4R^2}{(1 + z^2)^2} A_0^{(3)}(z)^2 - \frac{16}{(1 - z^2)^2} \right) \psi(z) &= 0. \end{aligned} \quad (2.72)$$

We should emphasise here that this equation is derived from an ansatz which uses spherical harmonics with  $\bar{l} = 1, s = -1$ , similar to the ansatz we used when we constructed the state

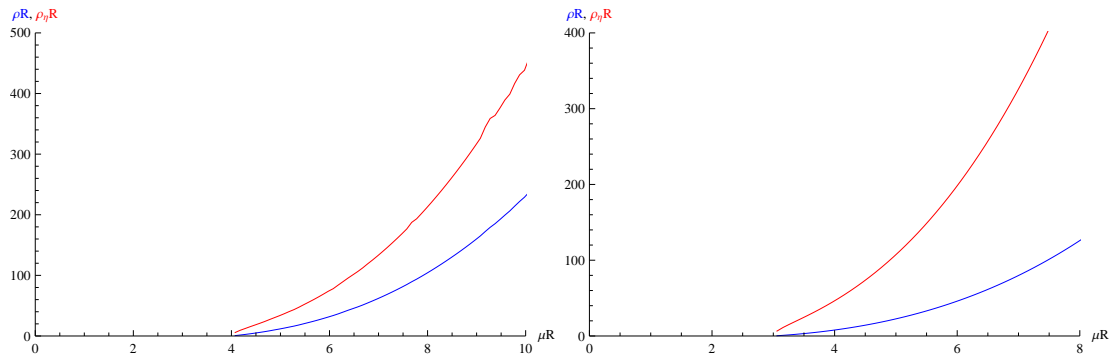


Figure 2.7: Plots of the densities  $\rho$  (blue) and  $\rho_\eta$  (red), as a function of the chemical potential  $\mu$ , at zero temperature, for the vector condensate (left) and scalar condensate (right).

for the vector dual to a charged scalar. However, we have also seen in the perturbative analysis that vector fluctuations in the direction of  $\bar{S}^3 \in \text{AdS}_5$  are insensitive to the quantum number  $s$ , unlike the fluctuation in direction of  $S^3 \in S^5$ . Therefore, it should also be possible to construct an alternative state with spherical harmonics with  $\bar{l} = 1, s = 1$ . This is indeed the case, and the free energy of this state is the same as for the state with  $\bar{l} = 1, s = -1$ .

Equations (2.70) and (2.72) are solved in the same fashion as equation (2.66), that is by the shooting method and imposing that the solution is regular everywhere and in particular at the origin of  $\text{AdS}_5$ . The solutions for the radial functions  $(A_0, \Phi)$  for the scalar configuration and  $(A_0, \psi)$  for the vector are plotted in figure 2.6. We also plot the densities for both configurations (defined analogous to (2.67)) as functions of the chemical potential, see figure 2.7.

In order to compare various configurations we plot the free energies for all three states, see figure 2.8. As expected from the perturbative analysis, we see that the state which originates from a condensation of the vector components which are dual to a charged scalar has the lowest free energy. We also see that as the chemical potential is increased, the difference between the free energies of the other two states and the true ground state becomes larger.

#### 2.4.2 The new ground state at finite temperature

So far we have seen that at zero temperature, the ground state originates from the condensation of vector components which are dual to a charged scalar, exactly as perturbation

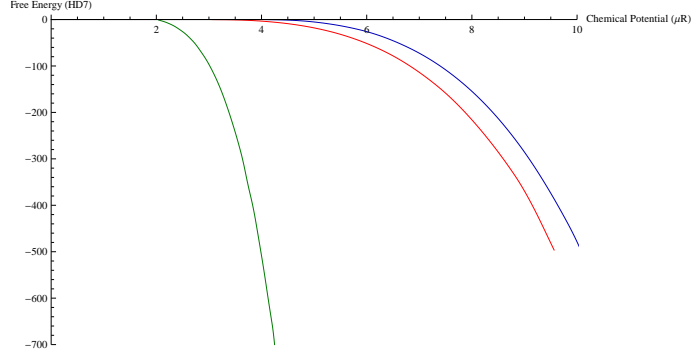


Figure 2.8: Scaled free energy of the zero-temperature condensates as a function of the dimensionless chemical potential. The vector is plotted in blue, the scalar in red, the charged scalar green. The black line along the  $x$ -axis denotes the old ground state.

theory suggested. We now want to see what is happening with this new ground state as the temperature is turned on. We start by making the same ansatz as at zero temperature, see (2.63). The equations of motion in the coordinates (2.12) are given by

$$\partial_v^2 A_0^{(3)}(v) - \frac{\Lambda - 1}{4(\Lambda - v)(1 - v)^2 v} R^2 \eta(v)^2 A_0^{(3)}(v) = 0, \quad (2.73)$$

together with

$$\begin{aligned} \partial_v^2 \eta(v) + \left( \frac{1}{1 - v} + \frac{1}{v} - \frac{1}{\Lambda - v} \right) \partial_v \eta(v) \\ + \frac{\Lambda - 1}{(\Lambda - v)(1 - v)^2 v} \left( 1 + \frac{(2 - \Lambda)(1 - v)R^2}{4(\Lambda - v)v} A_0^{(3)}(v)^2 \right) \eta(v) = 0. \end{aligned} \quad (2.74)$$

We are interested in finding regular solutions to these equations. It is easy to see that the solutions which are regular are parametrised by two free parameters. A general, perturbative expansion of the solution near the black hole horizon which is regular is given by

$$\begin{aligned} A_0^{(3)}(v) &= av + \frac{ab^2(\Lambda - 1)}{8\Lambda R^2} v^2 + O(v^3), \\ \eta(v) &= b - \frac{(\Lambda - 1)b}{\Lambda} v - \frac{12b(\Lambda - 1) + (2 - \Lambda)(\Lambda - 1)a^2 R}{16\Lambda^2} v^2 + O(v^3), \end{aligned} \quad (2.75)$$

i.e. a regular solution is parametrised by two real numbers  $a, b$ . We also see that the general regular solution for  $A_0$  vanishes at the horizon, as required by global regularity. We solve this system of equations again using a shooting method with two free parameters. As at zero temperature, we require in addition that the solution for  $\eta$  is normalisable at infinity, or explicitly

$$A_0^{(3)}(v) = \mu - \rho(1 - v) + O((1 - v)^2), \quad \eta(v) = \rho_\eta(1 - v) + O((1 - v)^2). \quad (2.76)$$

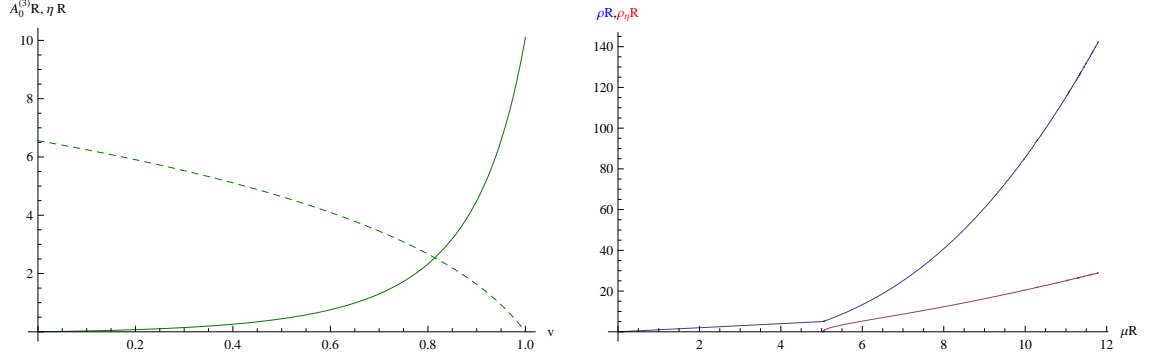


Figure 2.9: Left are plots of profile of the fields  $A_0$  (solid) and  $\eta$  (dashed) for the charged scalar, evaluated at  $\pi TR = 2.5$  and  $\mu R = 10.1$ . The boundary is at  $v = 1$  and horizon at  $v = 0$ . Right plot is for densities  $\rho$  (blue) and  $\rho_\eta$  (red), as function of chemical potential  $\mu$ , at fixed temperature  $\pi TR = 2.5$ .

This is possible only for a particular pair of parameters  $a, b$ , or in other words both densities  $\rho, \rho_\eta$  are functions of the chemical potential. An example of the radial profiles for a regular solution is plotted in figure 2.9. We also plot both densities as a function of chemical potential (see right plot on figure 2.9). We observe that, just as at zero temperature, the densities increase as the chemical potential is increased.

As for zero temperature, we should make sure that possible alternative states which appear due to condensation of other unstable particles have a larger free energy (as suggested by perturbation theory). We start with the scalar ground state. We make the same ansatz for the ground state, as we did at the zero temperature, see (2.69). The equations of motion in the coordinates (2.12) are given by

$$\begin{aligned}
\partial_v^2 A_0^{(3)}(v) - \frac{\Lambda - 1}{4(\Lambda - v)(1 - v)^2 v} \chi(v)^2 R^2 A_0^{(3)}(v) &= 0, \\
\partial_v^2 \chi(v) + \left( \frac{1}{1 - v} + \frac{1}{v} - \frac{1}{\Lambda - v} \right) \partial_v \chi(v) & \\
+ \frac{\Lambda - 1}{(\Lambda - v)(1 - v)^2 v} \left( 1 + \frac{(2 - \Lambda)(1 - v)R^2}{4(\Lambda - v)v} A_0^{(3)}(v)^2 \right) \chi(v) &= 0.
\end{aligned} \tag{2.77}$$

Similarly, the ground state originating from the vectors is derived starting with the ansatz

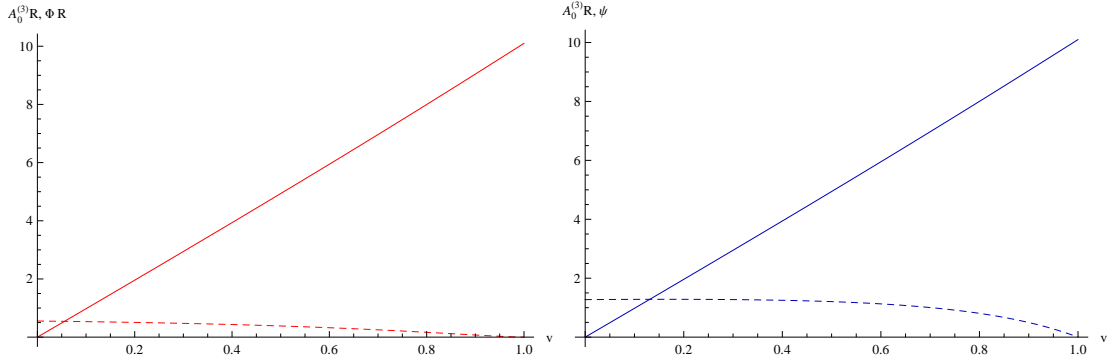


Figure 2.10: Plots of solutions  $(A_0(z), \Phi(z))$ , and  $(A_0(z), \psi(z))$  for the scalar and vector condensates respectively, at fixed temperature  $\pi T R = 2.5$  and chemical potential  $\mu R = 4.5$  (the curve for  $A_0$  is rather straight only because the plot is made for a chemical potential only slightly above the critical value).

(2.71). The equations of motion are given by

$$\begin{aligned} \partial_v^2 A_0^{(3)}(v) - \frac{2 - \Lambda}{4(\Lambda - v)(1 - v)v} \psi(v)^2 A_0^{(3)}(v) &= 0, \\ \partial_v^2 \psi(v) + \left( \frac{1}{v} - \frac{1}{\Lambda - v} \right) \partial_v \psi(v) & \\ - \frac{2 - \Lambda}{(\Lambda - v)(1 - v)v} \left( 1 - \frac{(\Lambda - 1)R^2}{4(\Lambda - v)v} A_0^{(3)}(v)^2 \right) \psi(v) &= 0. \end{aligned} \quad (2.78)$$

As before we consider only regular solutions to the equations (2.77) and (2.78) and require that the solutions are normalisable. Sample solutions for rather arbitrary values of the temperature and chemical potential are plotted in figure 2.10. We have also evaluated the densities for these solutions, and find a qualitatively similar dependence on the chemical potential as before. We have also verified that indeed the charge scalar always has a lower free energy than the condensate of the other particles, as predicted by perturbation theory.

Finally, we present in figure 2.11 the dependence of the charged scalar condensate densities on the temperature, for fixed chemical potential. This shows how increasing the temperature ‘melts’ the condensate.

## 2.5 Discussion and outlook

In this chapter we have analysed the stability of the homogeneous isotropic phase of conformal  $\mathcal{N} = 2$  super-Yang-Mills theory on a three sphere in the presence of an isospin chemical potential. We have found that for sufficiently large chemical potential, the theory

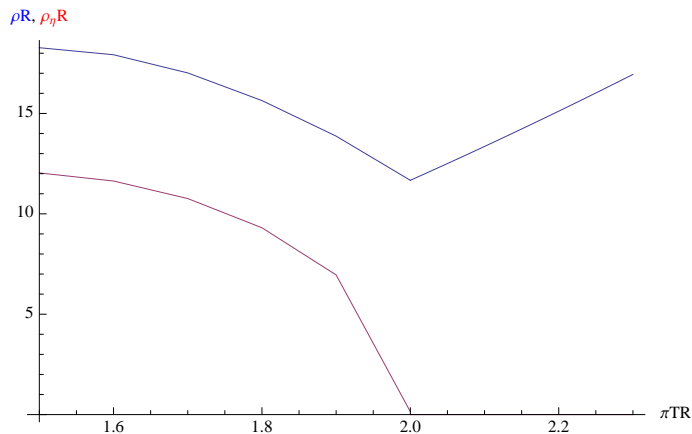


Figure 2.11: Dependence of the charged scalar ground state densities on  $TR$  at fixed chemical potential  $\mu R = 4.005$ .

exhibits unstable vector and scalar modes, as well as an unstable vector mode which is dual to an  $SO(4)$  charged scalar in the dual gauge theory. The latter modes turn out to condense first. We have verified this explicitly by constructing the condensate and showing that it has the lowest energy. The new ground state is anisotropic in the directions of the internal three sphere within the five sphere, but isotropic on the gauge theory sphere. Therefore, the new ground state breaks the global  $SO(4)$  symmetry.

Since the anisotropy of the system originates from the compactness of the internal three sphere, this anisotropy persists if we take the limit towards a non-compact system, i.e. the limit in which the radius of the sphere on which the dual gauge theory lives is taken to be very large (at fixed temperature).

We have observed that the spectrum of fluctuations of the more massive vector and scalar mesons crosses as a function of  $TR$ . This does not influence the formation of the dual charged scalar condensate, but it conceivably plays a role for larger values of the chemical potential. In particular, by doing a fluctuation analysis around the dual charged scalar condensate, one expects by analogy to the results of [98] that at some point new instabilities will set in, corresponding to the more massive particles condensing as well. An analysis of this type has appeared for example in [101, 103, 106, 107]. However, all of these references show that the new ground state is always stable. It would be interesting to see whether our case would turn out otherwise.

## Chapter 3

# An $\mathcal{N} = 2$ Gauge Theory in Compact Space at Zero Temperature with an External Magnetic Field

An influence of external magnetic field on a strongly coupled system is an interesting problem to study. For example, it is found [108, 109] that external magnetic field breaks chiral symmetry of a QCD system. This effect is known as magnetic catalysis. For a review, see [110].

In the context of gauge/gravity duality, this effect is studied in the reference [111]. This reference studies the D3/D7 model at zero temperature in Poincaré coordinates with a constant B-field added into the background geometry. This constant B-field plays a role of constant external magnetic field in the dual field theory. As well as studying magnetic catalysis, which centres around massless quarks, this reference also studies the system in the case of massive quarks. In principle, their model can be used to describe the system at any value of quark mass and external magnetic field.

A natural extension to this model is to discuss finite-size effect. This can be done by using global coordinates. The field theory side then lives on  $\mathbb{R} \times S^3$ . Since the space is compact, it is not possible to define a constant B-field. The reference [112] studies this set-up and suggests that in order for the B-field to not back-react on the background metric, the B-field has to be pure gauge. Unfortunately, as later suggested by our study, the D7-branes cannot be embedded into the background suggested by the reference [112],

and hence this choice of B-field is wrong. We found a more proper choice of B-field in which the D7-branes are allowed to be embedded. The discussion of this particular model is the subject of this chapter. This is based on an on-going work with Suphakorn Chunlen, Kasper Peeters, and Marija Zamaklar.

The introduction of the B-field seems to induce a quark mass gap in which there is no known embedding which produces these forbidden values of quark mass. The mass gap separates Ball and Minkowski embeddings.

### 3.1 Equations of motion on probe D7-branes

In some places in the previous chapter, we show the derivation of equations of motion by substituting an ansatz into an action and then vary the action. While this method is quick, it is not always correct. The safest way is to vary the action to get equations of motion, and then substitute the ansatz into the equations of motion.

In fact, as pointed out in the reference [113], the quick method was widely used around ten years ago. It turns out it is still used nowadays. There is no problem with the quick method as long as it can be shown that the solutions obtained from this method actually solves the equations of motion of the model.

In the case at hand, the model is non-linear and lives in a compact space. It is tempting to use the quick method and guess a natural-looking ansatz to avoid complications. Unfortunately this does not work. Instead, the way to tackle this problem is to obtain the equations of motion from the first principle. The form of the equations will give us an idea of what ansatz is to use.

The full equations of motion for probe branes are given in the reference [113]. Here, we rederive the equations of motion for the case of D7-branes. For the system we study, it is sufficient to consider only the DBI action. In the background with a constant dilaton, the DBI action is given by

$$S_{DBI} = -T_{D7} \int d^8\sigma \sqrt{-\det(e_{ab} + 2\pi\alpha' F_{ab})}, \quad (3.1)$$

where  $e_{ab} = E_{\mu\nu} \partial_a x^\mu \partial_b x^\nu$  with  $E_{\mu\nu} = G_{\mu\nu} + B_{\mu\nu}$ . Spacetime coordinates are denoted by  $x^\mu$  while worldsheet coordinates are denoted by  $\sigma^a$ . The equations of motion for embedding function  $x^\lambda(\sigma)$  and for gauge field  $A_b(\sigma)$  are respectively given by

$$\partial_b \left( \sqrt{-\mathcal{E}} \mathcal{E}^{ba} E_{\nu\lambda} \frac{\partial x^\nu}{\partial \sigma^a} \right) + \partial_a \left( \sqrt{-\mathcal{E}} \mathcal{E}^{ba} E_{\lambda\nu} \frac{\partial x^\nu}{\partial \sigma^b} \right) - \sqrt{-\mathcal{E}} \mathcal{E}^{ba} \partial_\lambda E_{\mu\nu} \frac{\partial x^\mu}{\partial \sigma^a} \frac{\partial x^\nu}{\partial \sigma^b} = 0, \quad (3.2)$$

$$\partial_a (\sqrt{-\mathcal{E}} (\mathcal{E}^{ab} - \mathcal{E}^{ba})) = 0, \quad (3.3)$$

where  $\mathcal{E}^{ab}$  and  $\mathcal{E}$  are inverse and determinant of  $\mathcal{E}_{ab} = e_{ab} + 2\pi\alpha' F_{ab}$ , respectively. Note that even if gauge field is not turned on, the left-hand side of the equation (3.3) is not trivially zero. With a given embedding ansatz, this equation essentially constrains the form of background B-field. Note that as a consistency check, it can be shown that equations (3.2) and (3.3) are invariant under gauge transformations that relate  $B$  and  $F$ . We discuss this gauge symmetry in appendix 3.A.

### 3.2 Embedding at zero temperature in finite volume

On  $\mathbb{R}^3$ , one is normally interested in studying a constant magnetic field. Here, we would like to see what happens if the system is put on  $S^3$ . However, on  $S^3$  it is not clear what it means to have a constant magnetic field. A possible way to get as close as possible to the concept of a constant magnetic field is to utilise the symmetry of  $S^3$ . An attempt given in [112] is to use local tetrads. Consider the background whose metric is given by

$$ds^2 = -\frac{u^2}{R^2} \left(1 + \frac{R^2}{4u^2}\right)^2 dt^2 + u^2 \left(1 - \frac{R^2}{4u^2}\right)^2 d\bar{\Omega}_3^2 + \frac{R^2}{u^2} (du^2 + u^2 d\Omega_5^2), \quad (3.4)$$

where

$$d\bar{\Omega}_3^2 = d\bar{\theta}^2 + \sin^2 \bar{\theta} d\bar{\phi}^2 + \cos^2 \bar{\theta} d\bar{\psi}^2, \quad d\Omega_5^2 = d\theta_3^2 + \sin^2 \theta_3 d\phi_3^2 + \cos^2 \theta_3 d\Omega_3^2. \quad (3.5)$$

Local tetrads are given by

$$e^{(1)} = R d\bar{\theta}, \quad e^{(2)} = R \sin \bar{\theta} d\bar{\phi}, \quad e^{(3)} = R \cos \bar{\theta} d\bar{\psi}. \quad (3.6)$$

They are used to define a pure gauge B-field

$$B = H e^{(1)} \wedge e^{(2)} = H R^2 \sin \bar{\theta} d\bar{\theta} d\bar{\phi} = d(-H R^2 \cos \bar{\theta} d\bar{\phi}). \quad (3.7)$$

The embedding is given by

$$\{t, u, \bar{\theta}, \bar{\phi}, \bar{\psi}, \theta, \phi, \psi, \theta_3, \phi_3\} \rightarrow \{t, u, \bar{\theta}, \bar{\phi}, \bar{\psi}, \theta, \phi, \psi\} \quad (3.8)$$

with

$$\{t, u, \bar{\theta}, \bar{\phi}, \bar{\psi}, \theta, \phi, \psi\} = \{t, u, \bar{\theta}, \bar{\phi}, \bar{\psi}, \theta, \phi, \psi\}, \quad \theta_3 = \theta_3(u), \quad \phi_3 = 0. \quad (3.9)$$

The worldvolume gauge field is not turned on.

We now show that their ansatz does not satisfy the equation (3.3). We split the inverse matrix  $\mathcal{E}^{ab}$  into two parts as follows

$$\mathcal{E}^{ab} = S^{ab} + J^{ab}, \quad (3.10)$$

where  $S^{ab}$  is a symmetric part while  $J^{ab}$  is an antisymmetric part. We substitute the ansatz into the equation (3.3). For this purpose, it is useful to compute  $J^{ab}$ . The non-zero components of  $J^{ab}$  are

$$J^{\bar{\theta}\bar{\phi}} = -\frac{HR^2}{\sin\bar{\theta}\left(H^2R^4 + \left(u - \frac{R^2}{4u}\right)^4\right)} = -J^{\bar{\phi}\bar{\theta}}. \quad (3.11)$$

The left-hand side of the non-zero component of (3.3) is then

$$\begin{aligned} \partial_a(\sqrt{-\mathcal{E}}(\mathcal{E}^{a\bar{\phi}} - \mathcal{E}^{\bar{\phi}a})) &= \partial_{\bar{\theta}}(\sqrt{-\mathcal{E}}(\mathcal{E}^{\bar{\theta}\bar{\phi}} - \mathcal{E}^{\bar{\phi}\bar{\theta}})) \\ &= -\frac{2HR^2}{H^2R^4 + \left(u - \frac{R^2}{4u}\right)^4} \partial_{\bar{\theta}}\left(\frac{\sqrt{-\mathcal{E}}}{\sin\bar{\theta}}\right) \\ &= \frac{2HR^5u}{\sqrt{H^2R^4 + \left(u - \frac{R^2}{4u}\right)^4}} \sin\bar{\theta} \sin\theta \cos\theta \cos^3(\theta_3(u)) \times \\ &\quad \times \left(1 - \frac{R^4}{16u^4}\right) \sqrt{1 + u^2\theta_3'(u)^2} \\ &\neq 0. \end{aligned} \quad (3.12)$$

So the gauge field equation of motion (3.3) is not satisfied.

Let us now propose another attempt. Consider background metric (3.4), and the background B-field

$$B = \frac{1}{2}H'(u)R^2(\sin^2\bar{\theta}dud\bar{\phi} + \cos^2\bar{\theta}dud\bar{\psi}) + H(u)R^2\sin\bar{\theta}\cos\bar{\theta}(d\bar{\theta}d\bar{\phi} - d\bar{\theta}d\bar{\psi}). \quad (3.13)$$

It can be shown that  $B = d\Lambda$ , where

$$\Lambda = \frac{1}{2}H(u)R^2(\sin^2\bar{\theta}d\bar{\phi} + \cos^2\bar{\theta}d\bar{\psi}). \quad (3.14)$$

To discuss the embedding, let us make a change of coordinates:

$$\chi = \sin\theta_3 \cos\phi_3, \quad \kappa = \sin\theta_3 \sin\phi_3. \quad (3.15)$$

The metric becomes

$$\begin{aligned} ds^2 &= -\frac{u^2}{R^2}\left(1 + \frac{R^2}{4u^2}\right)^2 dt^2 + u^2\left(1 - \frac{R^2}{4u^2}\right)^2 (d\bar{\theta}^2 + \sin^2\bar{\theta}d\bar{\phi}^2 + \cos^2\bar{\theta}d\bar{\psi}^2) \\ &\quad + \frac{R^2}{u^2}du^2 + \frac{R^2}{1 - \chi^2 - \kappa^2} (d\chi^2 + d\kappa^2 - (\kappa d\chi - \chi d\kappa)^2) \\ &\quad + R^2(1 - \chi^2 - \kappa^2)(d\theta^2 + \sin^2\theta d\phi^2 + \cos^2\theta d\psi^2). \end{aligned} \quad (3.16)$$

Note that with this choice of coordinates,  $\chi, \kappa \in [-1, 1]$ . Let us use the embedding

$$\{t, u, \bar{\theta}, \bar{\phi}, \bar{\psi}, \theta, \phi, \psi, \chi, \kappa\} \rightarrow \{t, u, \bar{\theta}, \bar{\phi}, \bar{\psi}, \theta, \phi, \psi\} \quad (3.17)$$

with

$$\{t, u, \bar{\theta}, \bar{\phi}, \bar{\psi}, \theta, \phi, \psi\} = \{t, u, \bar{\theta}, \bar{\phi}, \bar{\psi}, \theta, \phi, \psi\}, \quad \chi = \chi(u), \quad \kappa = 0. \quad (3.18)$$

We do not turn on worldvolume gauge field here. With the embedding ansatz, two equations can be obtained from (3.2), (3.3). They are given by

$$\begin{aligned} 0 = \chi''(u) &+ \frac{3\chi(u) \left(4R^2 u^4 H'(u)^2 + (R^2 - 4u^2)^2\right)}{(R^2 u - 4u^3)^2} - \frac{4\chi(u)\chi'(u)^2}{\chi(u)^2 - 1} \\ &+ \frac{\left(256R^8 u^4 H(u)^2 + 12288R^4 u^8 H(u)^2 + (R^2 - 4u^2)^4 (3R^4 + 16R^2 u^2 + 80u^4)\right) \chi'(u)}{u(4u^2 - R^2)(R^2 + 4u^2) \left(256R^4 u^4 H(u)^2 + (R^2 - 4u^2)^4\right)} \\ &+ \frac{\left(1024R^6 u^8 H(u)^2 + 4(R^2 - 4u^2)^2 (3R^6 u^4 + 8R^4 u^6 + 48R^2 u^8)\right) H'(u)^2 \chi'(u)}{u(4u^2 - R^2)(R^2 + 4u^2) \left(256R^4 u^4 H(u)^2 + (R^2 - 4u^2)^4\right)} \\ &+ \frac{4u \left(128R^4 u^4 H(u)^2 (R^4 + 16u^4) + (R^2 - 4u^2)^4 (R^4 + 4R^2 u^2 + 16u^4)\right) \chi'(u)^3}{(R^2 - 4u^2)(R^2 + 4u^2)(\chi(u)^2 - 1) \left(256R^4 u^4 H(u)^2 + (R^2 - 4u^2)^4\right)} \end{aligned} \quad (3.19)$$

$$\begin{aligned} 0 = H''(u) &- \frac{256R^4 u^4 H(u) H'(u)^2}{256R^4 u^4 H(u)^2 + (R^2 - 4u^2)^4} \\ &- \frac{4R^2 u^3 \left(256R^4 u^4 H(u)^2 + (R^2 - 4u^2)^2 (3R^4 + 8R^2 u^2 + 48u^4)\right) H'(u)^3}{(R^2 - 4u^2)(R^2 + 4u^2) \left(256R^4 u^4 H(u)^2 + (R^2 - 4u^2)^4\right)} \\ &+ \frac{64H(u) (R^3 - 4Ru^2)^2 (u^2 \chi'(u)^2 - \chi(u)^2 + 1)}{(\chi(u)^2 - 1) \left(256R^4 u^4 H(u)^2 + (R^2 - 4u^2)^4\right)} \\ &+ \frac{\left((R^2 - 4u^2)^4 (R^4 + 48u^4) - 256R^4 u^4 H(u)^2 (R^4 + 16R^2 u^2 - 16u^4)\right) H'(u)}{u(4u^2 - R^2)(R^2 + 4u^2) \left(256R^4 u^4 H(u)^2 + (R^2 - 4u^2)^4\right)} \\ &+ \frac{4u \left(128R^4 u^4 H(u)^2 (R^4 + 16u^4) + (R^2 - 4u^2)^4 (R^4 + 4R^2 u^2 + 16u^4)\right) H'(u) \chi'(u)^2}{(R^2 - 4u^2)(R^2 + 4u^2)(\chi(u)^2 - 1) \left(256R^4 u^4 H(u)^2 + (R^2 - 4u^2)^4\right)} \end{aligned} \quad (3.20)$$

Equivalently, these two equations can also be obtained by first putting the ansatz into the action, and then vary the action with respect to  $H(u)$ ,  $\chi(u)$ . For reference, the substituted action is

$$\begin{aligned} S = -T_{D7} \frac{R^6}{2} \int d^8 \sigma \sin \theta \cos \theta \sin \bar{\theta} \cos \bar{\theta} \frac{u}{R} \left(1 + \frac{R^2}{4u^2}\right) \sqrt{\left(\frac{u^4}{R^4} \left(1 - \frac{R^2}{4u^2}\right)^4 + H(u)^2\right)} \times \\ \sqrt{\left((1 - \chi(u)^2) \left(4 \left(1 - \frac{R^2}{4u^2}\right)^2 + H'(u)^2 R^2\right) + 4u^2 \left(1 - \frac{R^2}{4u^2}\right)^2 \chi'(u)^2\right) (1 - \chi(u)^2)}. \end{aligned} \quad (3.21)$$

We note that  $H(u) = H$ , for a constant  $H$  is not a solution of the equation of motion. In general, we need to numerically solve for  $\chi(u)$  and  $H(u)$ .

Before showing how to solve the equations of motion, let us try to see why our choice of ansatz is natural. From the ansatz (3.13), the norm  $B_{\mu\nu}B^{\mu\nu}$  of B-field is angular independent. This property is desirable because it is quite analogous to the case of a constant B-field in  $\mathbb{R}^3$ . Moreover, the constant B-field preserves  $SO(2)$  subset of the  $SO(3)$  rotational symmetry of  $\mathbb{R}^3$ . So by analogy, we should expect that our B-field ansatz preserves a certain amount of  $SO(4)$  rotational symmetry of  $S^3$ . To see if this is the case, let us adopt the criteria which is shown in the reference [114]. This criteria is used in order to check if a given gauge field is spherically symmetric. For a basis  $\{\xi_m\}$  of a vector field generating rotations, the gauge field  $A$  is spherically symmetric if it satisfies

$$\mathcal{L}_{\xi_m} A = d\alpha_m. \quad (3.22)$$

This implies

$$i_{\xi_m} F = d\Psi_m, \quad (3.23)$$

where  $i_{\xi_m}$  is an interior product by  $\xi_m$ . So for any  $\xi_m$ , if there exists  $\Psi_m$ , then our gauge field is spherically symmetric. In our case, we should expect that our B-field is preserved under a subset of this basis. We may use the gauge transformation discussed in the appendix 3.A to replace  $F$  with  $B$ . So essentially, we want to compute  $i_{\xi_m} B$ , and see if there is  $\Psi_m$  which satisfies

$$i_{\xi_m} B = d\Psi_m. \quad (3.24)$$

The generators of rotations on  $S^3$  are given by

$$R_1 = -\frac{i}{2} (\cos(\bar{\phi} + \bar{\psi})\partial_{\bar{\theta}} - \cot \bar{\theta} \sin(\bar{\phi} + \bar{\psi})\partial_{\bar{\phi}} + \sin(\bar{\phi} + \bar{\psi}) \tan \bar{\theta} \partial_{\bar{\psi}}), \quad (3.25)$$

$$R_2 = -\frac{i}{2} (\sin(\bar{\phi} + \bar{\psi})\partial_{\bar{\theta}} + \cot \bar{\theta} \cos(\bar{\phi} + \bar{\psi})\partial_{\bar{\phi}} - \cos(\bar{\phi} + \bar{\psi}) \tan \bar{\theta} \partial_{\bar{\psi}}), \quad (3.26)$$

$$R_3 = -\frac{i}{2} (\partial_{\bar{\psi}} + \partial_{\bar{\phi}}), \quad (3.27)$$

$$L_1 = -\frac{i}{2} (-\cos(\bar{\phi} - \bar{\psi})\partial_{\bar{\theta}} + \cot \bar{\theta} \sin(\bar{\phi} - \bar{\psi})\partial_{\bar{\phi}} + \sin(\bar{\phi} - \bar{\psi}) \tan \bar{\theta} \partial_{\bar{\psi}}), \quad (3.28)$$

$$L_2 = -\frac{i}{2} (\sin(\bar{\phi} - \bar{\psi})\partial_{\bar{\theta}} + \cot \bar{\theta} \cos(\bar{\phi} - \bar{\psi})\partial_{\bar{\phi}} + \cos(\bar{\phi} - \bar{\psi}) \tan \bar{\theta} \partial_{\bar{\psi}}), \quad (3.29)$$

$$L_3 = -\frac{i}{2} (\partial_{\bar{\psi}} - \partial_{\bar{\phi}}), \quad (3.30)$$

where

$$[R_i, R_j] = i\epsilon_{ijk} R_k, \quad [L_i, L_j] = i\epsilon_{ijk} L_k, \quad [R_i, L_j] = 0. \quad (3.31)$$

So

$$\Psi_{R1} = (\text{no solution}), \quad \Psi_{R2} = (\text{no solution}), \quad \Psi_{R3} = \frac{i}{4}H(u)R^2, \quad (3.32)$$

$$\begin{aligned} \Psi_{L1} &= \frac{i}{4}H(u)R^2 \sin(2\bar{\theta}) \sin(\bar{\phi} - \bar{\psi}), & \Psi_{L2} &= \frac{i}{4}H(u)R^2 \sin(2\bar{\theta}) \cos(\bar{\phi} - \bar{\psi}), \\ \Psi_{L3} &= \frac{i}{4}H(u)R^2 \cos(2\bar{\theta}). \end{aligned} \quad (3.33)$$

This means that our B-field is symmetric under  $SO(3) \times SO(2) \subset SO(3) \times SO(3) \cong SO(4)$ .

Let us now turn to the ansatz of the transverse scalar. The equations (3.2) and (3.3) are non-linear. So without making the full use of the symmetry of the system, it is quite unlikely to find the solution. We assume that the scalar  $\chi$  is preserved under the same set of the generators which preserves B-field. This means that

$$R_3\chi = L_1\chi = L_2\chi = L_3\chi = 0. \quad (3.34)$$

This requirement implies

$$\chi = \chi(u). \quad (3.35)$$

So based on symmetry alone, our ansatz is natural. Let us try to see if it is possible to have a more general ansatz. For simplicity, we want the norm of the B-field ansatz to still be angular independent. This can be achieved by using the B-field of the form  $B = d\Lambda$  with  $\Lambda = H(u)Y(\bar{\theta}, \bar{\phi}, \bar{\psi})$ , where  $Y(\bar{\theta}, \bar{\phi}, \bar{\psi})$  is a linear combination of vector spherical harmonics of either mode  $\bar{l} = 1, \bar{s} = 1$  or mode  $\bar{l} = 1, \bar{s} = -1$ . Combining this with the embedding ansatz (3.18), we can indeed obtain the equations of motion (3.19) and (3.20). Finally, in order to see if there is an even more general ansatz, we will need some further insights. At the moment, it is not clear whether this is the case. So we will simply use the ansatz (3.13) and (3.18) which are based on symmetry considerations, but keep in mind that we might be missing a non-trivial ansatz.

Let us now proceed to solve the equations of motion (3.19) and (3.20). We use the shooting method by starting from the position closest to AdS centre and shoot to AdS boundary. Different kinds of embeddings are distinguished by different initial conditions. We expand near  $u = u_{ini}$ , where  $u_{ini} = R/2$  for Ball embeddings, and  $u_{ini} = u_{Mink} > R/2$  for Minkowski embeddings. Since the equations of motion (3.19) and (3.20) are symmetric under  $\chi(u) \leftrightarrow -\chi(u), H(u) \leftrightarrow -H(u)$ , we can take, without loss of generality,  $\chi(u_{ini}) \geq 0, H(u_{ini}) \geq 0$ . For Ball embedding, the expansion near  $u = u_{ini}$  is given by

$$\chi(u) = \chi_{ball} - \frac{3}{32R^2} \left( -\frac{R}{2} + u \right)^2 (16 + H_{c2}^2) \chi_{ball} + O((u - R/2)^3), \quad (3.36)$$

$$H(u) = \frac{H_{c2}}{R^2} \left(-\frac{R}{2} + u\right)^2 - 2\frac{H_{c2}}{R^3} \left(-\frac{R}{2} + u\right)^3 + O((u - R/2)^4). \quad (3.37)$$

For Minkowski embedding, we have

$$\chi(u) = 1 + \chi_{M1}(u - u_{Mink}) + \chi_{M2}(u - u_{Mink})^2 + O((u - u_{Mink})^3), \quad (3.38)$$

$$H(u) = H_M + H_{M1}(u - u_{Mink}) + H_{M2}(u - u_{Mink})^2 + O((u - u_{Mink})^3), \quad (3.39)$$

where  $\chi_{M1}, \chi_{M2}, H_{M1}, H_{M2}$  are long expressions of  $u_{Mink}, H_M$ . By counting parameters, regularity requirements demand that a Ball embedding has two free parameters remaining while a Minkowski embedding has one free parameter remaining. Note in particular that in order to avoid B-field singularity at the AdS centre, we require  $H(u) \rightarrow 0$  as  $u \rightarrow R/2$ . We show this regularity requirement explicitly in the appendix 3.B.

We solve the equations of motion (3.19) and (3.20) subject to the above initial conditions, then match the solution with the expansion near the AdS boundary:

$$\chi(u) = \frac{m}{u} + \frac{c_1}{u^3} - \frac{mR^2}{2u^3} \log \frac{u}{R} + O(u^{-4}), \quad (3.40)$$

$$H(u) = H_{ext} + \frac{M_{tz}}{u^2} - \frac{2H_{ext}R^2}{u^2} \log \frac{u}{R} + O(u^{-3}). \quad (3.41)$$

The quantity  $m$  is proportional to the bare quark mass  $m_q = |m|/(2\pi\alpha')$  while  $H_{ext}$  are proportional to the value of external magnetic field. As for the vacuum expectation value, we need to properly renormalise the on-shell actions. Again, we follow the procedure discussed in the references [54,55]. We have also outlined this procedure in chapter 1. We start from

$$S_0 = -\frac{S}{R^7 T_{D7} \int dt d\Omega_3 d\Omega_3}. \quad (3.42)$$

We integrate  $u/R$  from  $1/2$  up to  $1/(2\epsilon)$  and add counter terms which are given by

$$L_1 = -\frac{1}{64\epsilon^4} (1 + \epsilon^2)(1 - \epsilon^2)^3, \quad (3.43)$$

$$L_2 = \frac{(1 - \epsilon^4)}{32\epsilon^2}, \quad (3.44)$$

$$L_4 = \frac{1}{32\epsilon^4} (1 + \epsilon^2)(1 - \epsilon^2)^3 \chi_\epsilon^2, \quad (3.45)$$

$$L_5 = \frac{(1 - \epsilon^4)}{16\epsilon^2} \log(\chi_\epsilon^2) \chi_\epsilon^2, \quad (3.46)$$

$$L_f = -\frac{1}{64\epsilon^4} (1 + \epsilon^2)(1 - \epsilon^2)^3 \chi_\epsilon^4, \quad (3.47)$$

$$L_H = -\frac{(1 + \epsilon^2) H_\epsilon^2 \log(2\epsilon)}{2(1 - \epsilon^2)}. \quad (3.48)$$

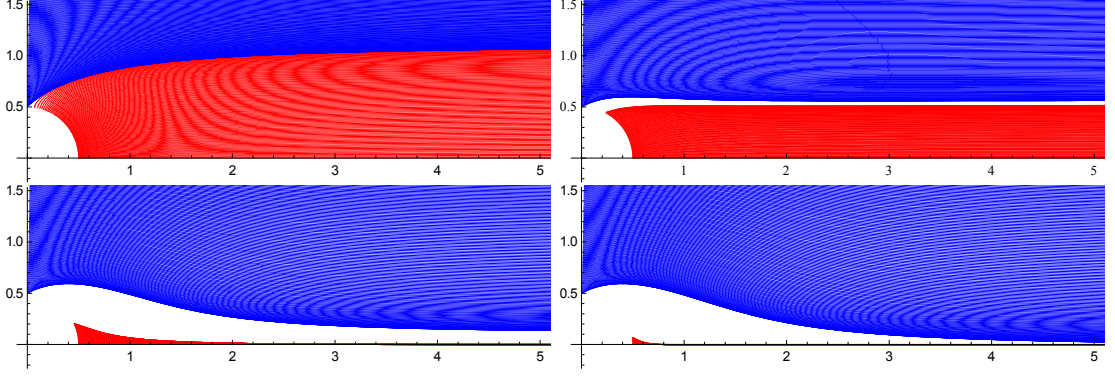


Figure 3.1: Plot of brane shapes for D7-branes embedding. The plots from left to right and top to bottom are at fixed external magnetic field  $H_{ext} = 0, 2, 4, 5$ , respectively. Each red curve is for Ball embedding where D7-branes reach AdS centre while each blue curve is for Minkowski embedding where D7-branes do not reach AdS centre. The horizontal and vertical axes are  $u\sqrt{1-\chi^2}/R, u\chi/R$ . For some non-zero values of  $H_{ext}$ , there are forbidden values of bare quark mass.

where

$$\chi_\epsilon \equiv \chi \left( \frac{R}{2\epsilon} \right), \quad H_\epsilon \equiv H \left( \frac{R}{2\epsilon} \right). \quad (3.49)$$

The subtracted action is given by

$$S_{\text{sub}} = S_0 + L_1 + L_2 + L_4 + L_5 + L_f + L_H. \quad (3.50)$$

The resulting vacuum expectation values are given by

$$c = -R^3 \lim_{\epsilon \rightarrow 0} \epsilon \frac{\delta S_{\text{sub}}}{\delta \chi_\epsilon} = c_1 - \frac{mR^2}{2} \log \left( \frac{m}{R} \right), \quad (3.51)$$

$$M = -2R^2 \lim_{\epsilon \rightarrow 0} \frac{\delta S_{\text{sub}}}{\delta H_\epsilon} = M_{tz} + H_{ext} R^2. \quad (3.52)$$

Here  $c$  is proportional to a vacuum expectation value of a quark bilinear operator, while  $M$  can be interpreted as an induced current.

In the figure 3.1, we show the brane shape at various fixed  $H_{ext}$ . Let us first discuss the top left plot which corresponds to  $H_{ext} = 0$ . As we have mentioned in chapter 1, this case is studied in the references [8, 55]. The brane shape plot is visualised in the reference [7]. In the plot, the horizontal and vertical axes are  $u\sqrt{1-\chi^2}/R, u\chi/R$ . The AdS centre is at  $u = R/2$ , and is shown in the plot as an arc of radius  $1/2$  centred at the origin. The horizontal axis represents the origin of the  $X^8 - X^9$  plane<sup>1</sup> while the vertical axis shows the

<sup>1</sup>As discussed in chapter 1, the  $X^8 - X^9$  plane is the flat plane which is conformal to the transverse plane to D7-branes.

distance away from the origin of the  $X^8 - X^9$  plane. Therefore, the quark mass can be read off from the value of the vertical axis when the horizontal axis approaches infinity. The red curves represent Ball embeddings while the blue curves represent Minkowski embeddings. As mentioned in the previous chapter, the phase transition between these embeddings is of third order [8].

Let us now discuss the other plots of figure 3.1. For a given  $H_{ext}$  in the range  $0 < H_{ext} \lesssim 4.8$ , there is a “mass gap”. This is the region in which some values of bare quark mass are excluded. This is under investigation. The mass gap closes off at  $H_{ext} \approx 4.8$ . The development of the mass gap can be viewed as follows. From the point of view at the AdS centre, more and more Ball embeddings disappear as  $H_{ext}$  is increased. This potentially leaves the quark mass gap between the Ball and Minkowski embeddings. Furthermore, although the presence of the B-field generically reduces the value of quark mass for each embedding, the quark mass of the Minkowski embedding is decreased too slowly that the lowest quark mass obtained from the Minkowski embeddings is still greater than the highest quark mass obtained from the Ball embeddings. This leaves a mass gap between the Ball and Minkowski embeddings.

It is not visually clear from the figure 3.1 that there is actually a mass gap. So let us present an alternative plot. In figure 3.2, we make the similar plots to those of the figure 3.1, but we use the  $z$ -coordinate:  $z = R/(2u)$ , and change the horizontal and vertical axes to  $z, \chi/(2z)$ . For each curve in these plots, the quark mass can be read off from the value at the vertical axis. So the figure 3.2 clearly visualises the mass gap.

In figure 3.3, we plot possible values of  $H_{ext}$  and  $m$ . Note that since the bare quark mass is given by  $m_q = |m|/(2\pi\alpha')$ , it is more appropriate to investigate the phase diagram from the right plot. At some places in the plot, lines from different configurations are crossed. At these places, the free energy will need to be compared. We however, postpone this calculation until we understand the more important issue which is the presence of the mass gap in the phase diagram.

We have mentioned above that the disappearance of Ball embeddings is partly responsible for the presence of the mass gap. We want to make sure that the disappearance is not due to a numerical mistake, therefore we will cross check the analysis by an analytical calculation. The analysis will be possible in the simplest case which is the case of the equatorial embedding. In this special case, the disappearance is due to the fact that there is a maximum value of  $H_{ext}$  which can be obtained from the analysis. The disappearance of other Ball embeddings are because of similar reasons.

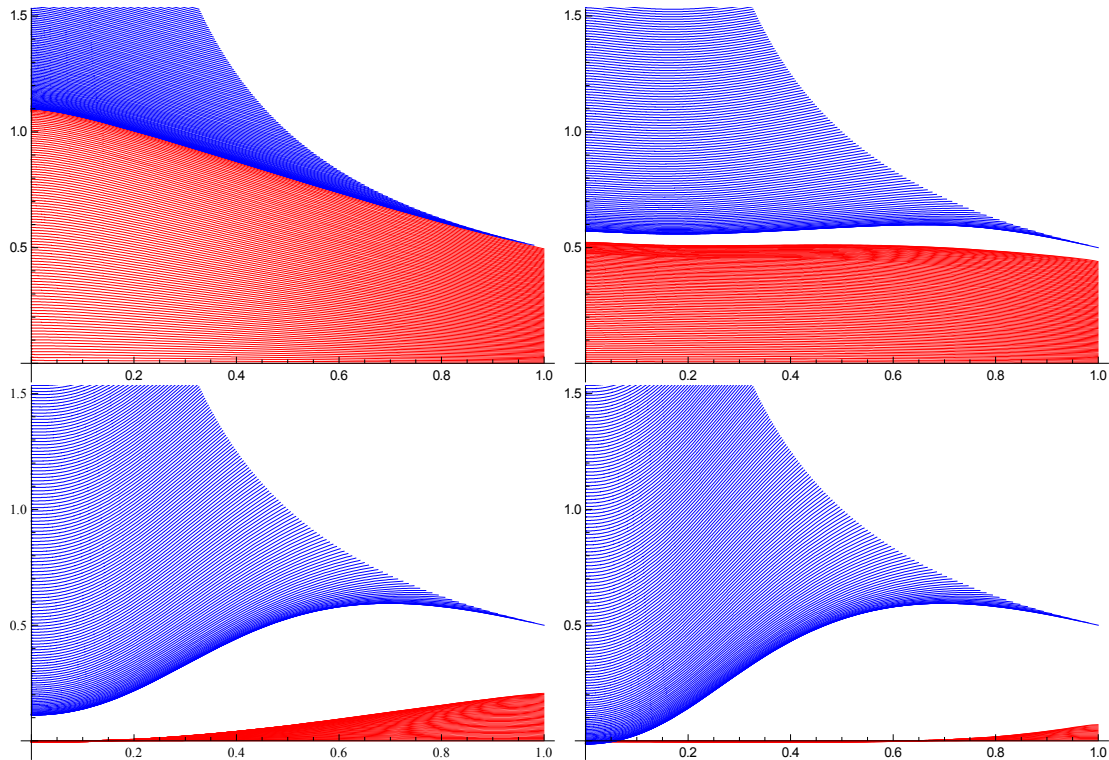


Figure 3.2: Plot of brane shapes for D7 embedding in  $z$ -coordinates where  $z = R/(2u)$ . The plots from left to right and top to bottom are at fixed external magnetic field  $H_{ext} = 0, 2, 4, 5$ , respectively. Each red curve is for Ball embedding where D7-branes reach AdS centre while each blue curve is for Minkowski embedding where D7-branes do not reach AdS centre. The horizontal and vertical axes are  $z, \chi/(2z)$ . Quark mass of each embedding is proportional to the position of the brane on the vertical axis. The plots clearly show the development of mass gap.

### 3.3 Equatorial embedding analysis

#### 3.3.1 Analytical discussion

Before analysing the equatorial embedding analytically, let us first numerically demonstrate the saturation of the external magnetic field. For the equatorial embedding, we have  $\chi(u) = 0$ . This makes the equation (3.19) trivially satisfied while the equation (3.20)

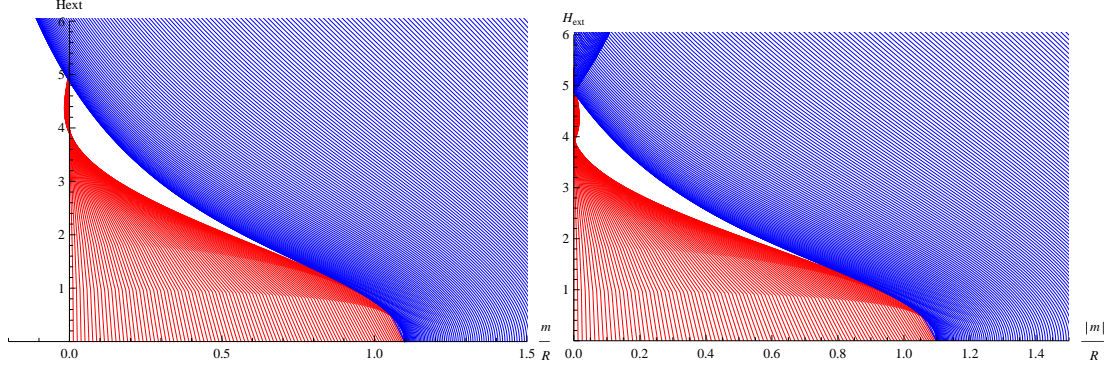


Figure 3.3: Plot of possible values of  $H_{ext}$  and  $m$ . Different lines represent different initial condition of  $\chi(u)$ , while different points along each line represent different initial condition of  $H(u)$ . Red curves represent Ball embeddings while blue curves represent Minkowski embeddings. The left plot presents the raw data while the right plot shows the phase diagram. The quark mass is proportional to  $|m|$ , so the horizontal axis of the right plot has to be  $|m|$ . Given  $H_{ext}, |m|$ , we ask for a unique configuration. So if the line crosses, free energy of different configurations will need to be compared. Furthermore, the phase diagram should not have a gap. So this phase diagram is quite subtle because of the presence of the mass gap.

is reduced to

$$\begin{aligned}
H''(u) &- \frac{R^4 H(u) H'(u)^2}{R^4 H(u)^2 + \left(u - \frac{R^2}{4u}\right)^4} - \frac{64H(u) (R^3 - 4Ru^2)^2}{256R^4 u^4 H(u)^2 + (R^2 - 4u^2)^4} \\
&- \frac{2(R^2 + 4u^2)(R^2 - 4u^2)^3 H'(u)}{256R^4 u^5 H(u)^2 + u(R^2 - 4u^2)^4} - \frac{(R^4 + 16R^2 u^2 - 16u^4) H'(u)}{16u^5 - R^4 u} \\
&- \frac{4R^2 u^3 H'(u)^3}{(R^2 - 4u^2)(R^2 + 4u^2)} - \frac{8R^2 u^3 (R^4 - 16u^4) H'(u)^3}{256R^4 u^4 H(u)^2 + (R^2 - 4u^2)^4} = 0.
\end{aligned} \tag{3.53}$$

We will also use  $z$ -coordinate which is given by  $z = R/(2u)$ . The equation of motion is

$$\begin{aligned}
H''(z) &- \frac{16z^4 H(z) H'(z)^2}{16z^4 H(z)^2 + (z^2 - 1)^4} - \frac{16(z^2 - 1)^2 H(z)}{(16z^4 H(z)^2 + (z^2 - 1)^4)} \\
&+ \frac{\left(16(z^4 - 4z^2 - 1)z^4 H(z)^2 + (z^2 - 1)^4(3z^4 + 1)\right) H'(z)}{16(z^4 - 1)z^5 H(z)^2 + (z^2 - 1)^5(z^2 + 1)z} \\
&+ \frac{z^3 \left(16z^4 H(z)^2 + (z^2 - 1)^2(3z^4 + 2z^2 + 3)\right) H'(z)^3}{16z^4(z^4 - 1)H(z)^2 + (z^2 + 1)(z^2 - 1)^5} = 0.
\end{aligned} \tag{3.54}$$

We solve the equation (3.53), or alternatively the equation (3.54), by shooting from the AdS centre and read off the value of  $H_{ext}$  at the AdS boundary. The only parameter

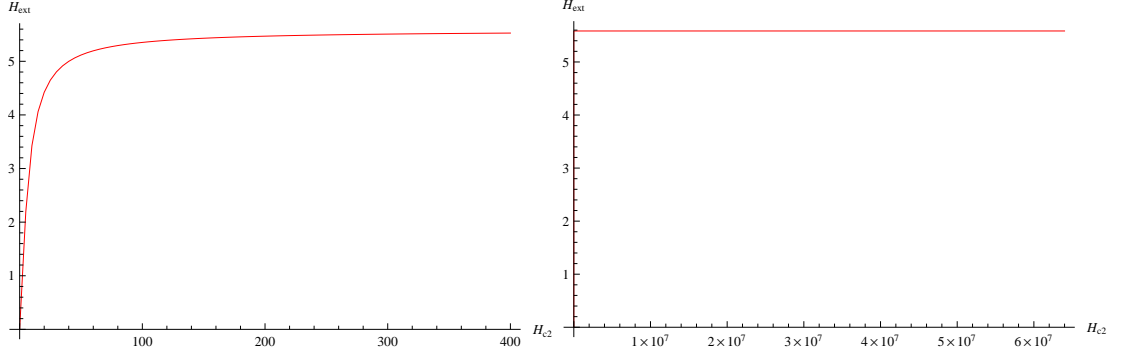


Figure 3.4: The plots of  $H_{ext}$  versus  $H_{c2}$ . In these plots, we use the setting  $u_{ball}/R = 500001/1000000$ ,  $u_{inf}/R = 10000$ . The right plot clearly shows that there is a maximal value of  $H_{ext}$ .

to tune is  $H_{c2}$ . In figure 3.4, we present the results obtained from setting  $u_{ball}/R = 500001/1000000$ ,  $u_{inf}/R = 10000$ , where  $u_{ball}$  and  $u_{inf}$  are numerical values for AdS centre and AdS boundary, respectively. Note that we make  $u_{ball}/R$  to be numerically very close to  $1/2$ . This allows us to study up to high value of  $H_{c2}$  with precision. Numerically, we see that  $H_{ext}$  asymptotically reaches 5.58.

Let us now analytically study the equatorial embedding. We suppose that the non-linearity should already be encoded in the solution to the equation of motion at the first order in  $H(z)$  :

$$H''(z) - \frac{(3z^4 + 1)H'(z)}{(1-z^2)(z^2+1)z} - \frac{16H(z)}{(1-z^2)^2} = 0. \quad (3.55)$$

By requiring  $H(1) = 0$ ,  $H(0) = H_{ext}$ , the solution is given by

$$H(z) = H_{ext} \left( 1 + \frac{8z^2}{(1-z^2)^2} \log\left(\frac{2z}{z^2+1}\right) \right). \quad (3.56)$$

We now study the full equation. Our plan is to expand around the first order result near the AdS centre and near the AdS boundary, then match these results together at the mid-point. We make an assumption that the non-linearity is already given in the solution (3.56). Using the full equation of  $H(z)$  to determine the coefficients, we expand the field  $H(z)$  near the AdS centre ( $z = 1$ ) and near the AdS boundary ( $z = 0$ ) respectively as

$$\begin{aligned} H(z) \Big|_{z \rightarrow 1} &\approx H_0 \left( 1 + \frac{8z^2}{(1-z^2)^2} \log\left(\frac{2z}{z^2+1}\right) \right) + \frac{c}{4}(1-z)^2 + \frac{c}{4}(1-z)^3 \\ &+ \frac{-c^3 - 6c^2H_0 + c(56 - 12H_0^2) - 8H_0^3}{384}(1-z)^4 + \dots + (\dots)(1-z)^8, \end{aligned} \quad (3.57)$$

$$\begin{aligned} H(z) \Big|_{z \rightarrow 0} &\approx H_0 \left( 1 + \frac{8z^2}{(1-z^2)^2} \log\left(\frac{2z}{z^2+1}\right) \right) + a + bz^2 + 8az^2 \log(z) \\ &- 2(4a - b)z^4 + \dots + (\dots)z^6 \log(z), \end{aligned} \quad (3.58)$$

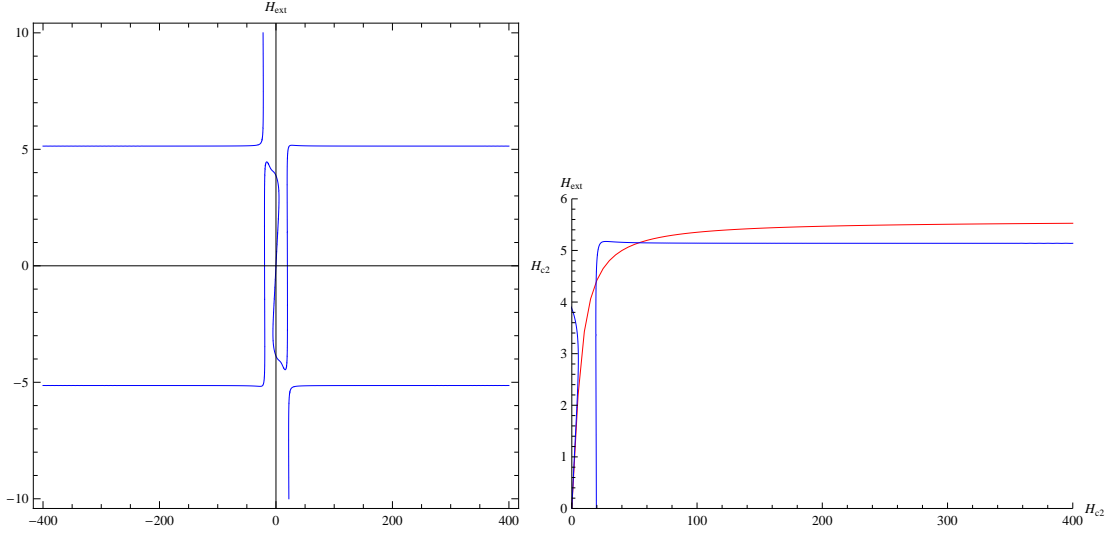


Figure 3.5: Left is the contour plot of the solution to (3.59). Right is the plot from the left with the result from the full numerical solution plotted in red.

where  $H_0, c, a$  and  $b$  are related to  $H_{c2}, H_{ext}$  and  $M_{tz}$ . The first term of each expansion is from the solution (3.56). The orders of the two expansions can be arbitrary and are not directly related to each other, but the higher the orders the more accurate the result. We take  $z = 1/2$  as the meeting point in which the two expansions of  $H(z)$  are approximately equated. The first and second derivatives of them are also approximately equated at that point. After substituting and eliminating the unwanted parameters, we are left with a polynomial equation containing only  $H_{ext}$  and  $H_{c2}$  :

$$\begin{aligned}
& 25H_{c2}^7 (1311465 - 49672H_{ext}^2) + 28H_{c2}^5 (19611320H_{ext}^2 - 504255471) \\
& + 96H_{c2}^3 (11139559023 - 475946168H_{ext}^2) + 37748736H_{c2} (237464H_{ext}^2 - 4951755) \quad (3.59) \\
& - 75497472H_{ext} (3520H_{ext}^4 + 277624H_{ext}^2 - 4951755) = 0.
\end{aligned}$$

The degrees of  $H_{c2}$  and  $H_{ext}$  depend on the orders of the expansions of  $H(z)$  near centre and boundary respectively. The contour plot of this equation is shown in figure 3.5.

From the plot, we choose the curve that include the point  $(H_{c2}, H_{ext}) = (0, 0)$ . Despite the strange behaviour near  $(0, 0)$ , the solution shows that  $H_{ext}$  reaches a constant as  $H_{c2}$  goes to infinity. This qualitatively agrees with the numerical result. This is shown in the right plot of the figure 3.5.

Although our analysis is done perturbatively, this does not necessarily mean that only small values of  $H_{c2}$  can be trusted. In fact our analysis includes the following non-linear considerations

- We do not expand the part

$$H_0 \left( 1 + \frac{8z^2}{(1-z^2)^2} \log \left( \frac{2z}{z^2+1} \right) \right) \quad (3.60)$$

as we expect non-linear behaviour is already presented in the linear equation (3.55). If we expand that term, the asymptotic value of  $H_{ext}$  will not be close to the actual numeric value.

- We make boundary expansion up to the term that gives non-linear relationship between  $H_{ext}$  and  $H_{c2}$ . Expanding fewer term does not capture the non-linearity and hence the result would only be valid for small value of  $H_{c2}$ . On the other hand, we expect that expanding more terms would lead to complications and that no further insights can be gained.

It turns out that our analysis capture the behaviour at small  $H_{c2}$  as well as at large  $H_{c2}$ . For the mid-values of  $H_{c2}$ , more analysis would be required. However, we expect that the graph of  $H_{ext}$  versus  $H_{c2}$  would be monotonically increasing. Therefore, there is a maximal value of  $H_{ext}$ . Indeed, we can extract the maximal value by considering the limit  $H_{c2} \rightarrow \infty$  of equation (3.59) where the equation reduces to

$$25H_{c2}^7 (1311465 - 49672H_{ext}^2) = 0, \quad (3.61)$$

and hence  $H_{ext,max} = 5.14$  (note that the numerical result gives  $H_{ext,max} = 5.58$ ). The equatorial embedding cannot exist for  $H_{ext} > H_{ext,max}$  and hence the branes disappear.

### 3.3.2 Numerical analysis: shooting from the boundary

In this subsection, still with the equatorial embedding, we make another cross check of the numerical result. Here, we consider the shooting method in which the shooting starts from the AdS boundary. In this case, we have to scan the two-dimensional parameter space  $(H_{ext}, M_{tz})$ . Because of the symmetry  $H(u) \leftrightarrow -H(u)$  of the equation of motion (3.53), we can take, without loss of generality,  $H_{ext} \geq 0$ . Given a point in the parameter space  $(H_{ext}, M_{tz})$ , we solve the equation of motion and study the behaviour of  $H(u)$ , and wherever possible we read off the value of  $H(u)$  (called  $H_{c0}$ ) at the AdS centre.

In figure 3.6, we present a scan of  $(H_{ext}, M_{tz})$  parameter space. The blue line and brown dots in the figure are associated with solutions with smooth  $H(u)$ . Points along blue lines are associated with physical solutions because  $H_{c0} = 0$  while brown dots are associated with unphysical solutions in which  $H_{c0} \neq 0$ . There is another kind of unphysical

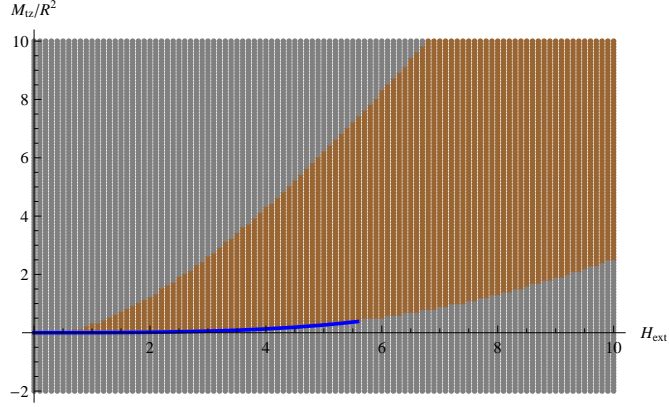


Figure 3.6: The plot shows the  $(H_{ext}, M_{tz})$  parameter space. The blue line is associated with solutions which give B-field vanishing at the AdS centre. Brown dots are associated with solutions which give B-field non-vanishing at the AdS centre. The solutions associated with the blue line and brown dots have smooth profiles  $H(u)$ . Grey dots are associated with solutions that have  $|H'(u_{close})| > 10^{15}$  at some  $u_{close} > R/2$ ; this numerically indicates that  $H'(u)$  blows up at some point.

solutions. They are associated with grey dots in the figure. For these solutions,  $H'(u)$  blow up at some point  $u = u_{close} > R/2$ . Note that the blue line occupies part of the border between the brown and grey regions.

### 3.4 Full check by shooting from the boundary

The cross check from the previous section suggests that our numerical results are likely to be correct. To see if this is really the case, we need to make a further check. In this section, we solve the equations of motion (3.19)-(3.20) by shooting from the AdS boundary, then study the profiles of  $\chi(u)$  and  $H(u)$ . From the boundary expansions (3.40)-(3.41), there are four parameters to tune:  $(m, H_{ext}, c_1, M_{tz})$ . Since the equations of motion (3.19)-(3.20) are symmetric under  $\chi(u) \leftrightarrow -\chi(u), H(u) \leftrightarrow -H(u)$ , we can take, without loss of generality  $m \geq 0, H_{ext} \geq 0$ .

In principle, we need to make the full scan of the four-dimensional parameter space  $(m, H_{ext}, c_1, M_{tz})$ . This means that at each point in the parameter space we have to determine the behaviour of the associated solution. However, the direct analysis will most likely consume a lot of time and computational resources. So our strategy is to start from a given value of  $(m, H_{ext})$ , and then scan the  $(c_1, M_{tz})$  space. Once we have enough insights into the problem, we will, hopefully, be able to make a better algorithm for the full scan

of the four-dimensional parameter space.

There are two kinds of physical solutions: Ball embeddings and Minkowski embeddings. So our algorithms will be to look for the solutions of these types while discarding unphysical solutions in the process. The algorithms are as follows

#### Determining Ball embeddings (“Ball embedding algorithm”)

1. Fix  $(m, H_{ext})$ .
2. Make a rough scan in the  $(c_1, M_{tz})$  space. Initially, we take the sample points:  $-10 \leq c_1/R^3 \leq 10$  with step size 1, and  $-10 \leq M_{tz}/R^2 \leq 10$  with step size 1.
3. At each sample point, read off the value of  $u_{close}$ . Typically, if  $u_{close} > R/2$ , the solution has  $|H'(u_{close})|$  and  $|\chi'(u_{close})|$  blowing up. But if the solution is smooth everywhere, we take  $u_{close} = R/2$ .
4. From these sample points in the  $(c_1, M_{tz})$  space, pick around ten points which give the lowest  $u_{close}$ . Then make a rectangle enclosing these points and make around 400 equally spaced sample points.
5. Repeat steps 3-4 until either of the cases below is realised:
  - (a) The point with  $u_{close} = R/2$  is obtained. Then scan around this point to find other points with  $u_{close} = R/2$ . Repeat until all the important representative points with  $u_{close} = R/2$  are obtained. For these points, read off  $H(u_{close})$ . The points which give  $H(u_{close}) = 0$  are physical while other points are unphysical.
  - (b) Alternatively, if after making a very fine scan there is no point with  $u_{close} = R/2$  can be obtained, then conclude that for this value of  $(m, H_{ext})$ , there is no physical solution associated with Ball embeddings.

#### Determining Minkowski embeddings (“Minkowski embedding algorithm”)

1. Fix  $(m, H_{ext})$ .
2. Make a rough scan in the  $(c_1, M_{tz})$  space. Initially, we take the sample points:  $-10 \leq c_1/R^3 \leq 10$  with step size 1, and  $-10 \leq M_{tz}/R^2 \leq 10$  with step size 1.
3. At each sample point, read off the value of  $\chi(u_{close})$ .

4. From these sample points in the  $(c_1, M_{tz})$  space, pick around ten points which have  $\chi(u_{close})$  closest to 1. Then make a rectangle enclosing these points and make around 400 equally spacing sample points.
5. Repeat steps 3-4 until either of the cases below is realised:
  - (a) There are points in which the profiles of  $\chi(u)$  and  $H(u)$  are smooth from  $u = u_{close}$  to  $u \rightarrow \infty$ . These points are associated to the physical Minkowski embeddings. As a cross check, we also require  $\chi(u_{close}) \approx 1$ .
  - (b) Alternatively, if after making a very fine scan there is no point with  $\chi(u_{close})$  numerically close to 1, then conclude that for this value of  $(m, H_{ext})$ , there is no physical solution associated with Minkowski embeddings.

Given  $(m, H_{ext})$ , the idea is to follow the above algorithms, then determine if there exists physical Minkowski or Ball embeddings. If there are no physical embeddings possible, then this suggests that there is a mass gap. However, we still do not have enough control over this numerical calculation to confirm if there is really a mass gap. Nevertheless, let us simply present our attempts so far. We consider three cases with fix  $m/R = 0.4$  but vary  $H_{ext} = 1, 2.5, 3$ . If the right plot of figure 3.3 is correct, then the first case should give a Ball embedding, the second case gives no physical embedding, and the third case gives a Minkowski embedding.

#### 3.4.1 The case $m/R = 0.4, H_{ext} = 1$

Let us discuss the results for the case  $m/R = 0.4, H_{ext} = 1$ . In figure 3.7, we present the results obtained from the algorithm which tries to determine Ball embeddings. In this figure, we show the contour plot of  $u_{close}/R$  in the  $(c_1, M_{tz})$  parameter space. We also present the points which give  $u_{close}/R = 0.5001$  which is the numerical value for  $u_{close}/R = 0.5$ . These points (shown as black dots) have smooth profiles of  $\chi(u), H(u)$ . So they are potentially associated with physical Ball embeddings. In order to determine if this is really the case, we will have to read off the value of  $H_{c0} \equiv H(R/2)$ . Physical Ball embeddings have smooth profiles of  $\chi(u), H(u)$ , and have  $H_{c0} = 0$ .

In the left plot of the figure 3.8, we make the interpolation of black dots from figure 3.7. We define the affine parameter  $\alpha$  as the distance along the curve from a reference point. We also indicate the point which is taken to have  $\alpha = 0$ . The right plot shows the values of  $H_{c0}$  as a function of  $\alpha$ . The physical Ball embedding has  $H_{c0} = 0$ . However, this

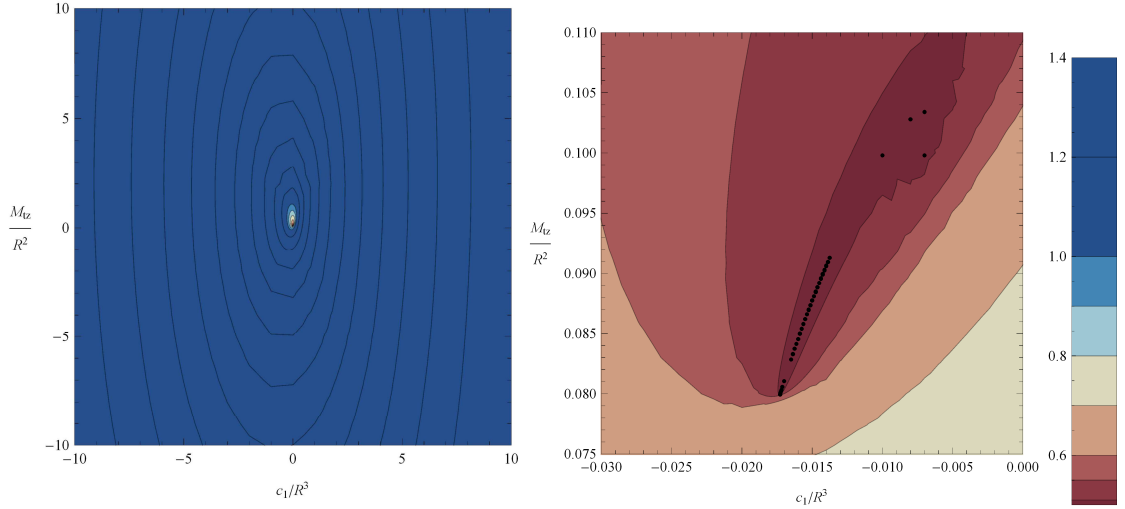


Figure 3.7: The contour plots showing the values of  $u_{close}/R$  in the  $(c_1, M_{tz})$  parameter space with fixed  $(m/R, H_{ext}) = (0.4, 1)$ . The left plot is the interpolation of the contour plot for the full range  $-10 \leq c_1/R^3 \leq 10$ ,  $-10 \leq M_{tz}/R^2 \leq 10$ . The middle plot is the same as the left plot but with a smaller range focusing around the points with  $u_{close} = 0.5001R$  (the numerical value for  $u_{close} = R/2$ ). The sample points with  $u_{close} = 0.5001R$  are shown in black dots. The right plot is the colour bar encoding the values of  $u_{close}/R$ . Note that we use dark blue colour for  $u_{close}/R \geq 1$ .

is not seen from our data. At  $\alpha = 0$ , the value of  $H_{c0}$  is 0.009. As  $\alpha$  increases, the value of  $H_{c0}$  is generically increased. From the curve, it is therefore advisable to study the point around  $\alpha = 0$  more carefully to see if we can have a solution with  $H_{c0} = 0$ .

Let us now discuss the results which are obtained from the algorithm which tries to determine Minkowski embeddings. In figure 3.9 we show the values of  $\chi(u_{close})$  in the  $(c_1, M_{tz})$  parameter space. In order to have a physical Minkowski embedding, we require  $\chi(u_{close}) \approx 1$ . However, the best result obtained from our sample points gives  $\chi(u_{close}) = 0.65$ . We have made a reasonably fine tuned scan. So based on this result and the behaviour of the contour plot, it is highly unlikely that there is a Minkowski embedding for  $(m/R, H_{ext}) = (0.4, 1)$ .

### 3.4.2 The case $m/R = 0.4, H_{ext} = 2.5$

Let us now discuss the results for the case  $m/R = 0.4, H_{ext} = 2.5$ . The discussion is in a similar way as the previous case. We show the results from the Ball embedding algorithm in figures 3.10-3.11. We have made the contour plot of  $u_{close}/R$  in the  $(c_1, M_{tz})$  parameter

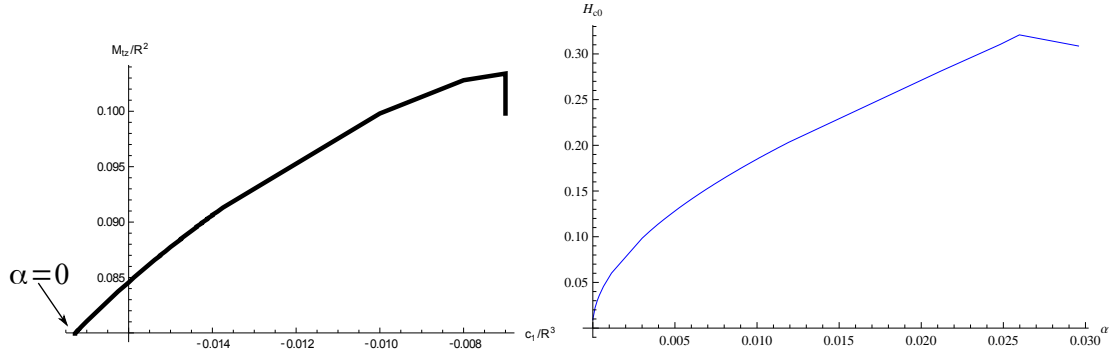


Figure 3.8: The left plot shows the interpolation of black dots from figure 3.7. We define the affine parameter  $\alpha$  as the distance along the curve from a reference point which is shown to have  $\alpha = 0$ . The right plot shows the values of  $H_{c0} \equiv H(R/2)$  as a function of  $\alpha$ . The minimum value of  $|H_{c0}|$  which we found is 0.009 at  $\alpha = 0$ . A further investigation is required to see if we can get the point with  $H_{c0}$  closer to 0.

space, and present the sample values (shown in black dots) which give  $u_{close}/R = 0.5001$ . These values are interpolated and assigned an affine parameter  $\alpha$ . As shown in figure 3.11, the affine parameter  $\alpha$  is taken to be the angle from a reference axis. We then plot the value of  $H_{c0}$  for various  $\alpha$  in the right plot of figure 3.11. This plot suggests that it is unlikely to have the solution with  $H_{c0} = 0$ , and hence there is no physical Ball embedding for  $(m/R, H_{ext}) = (0.4, 2.5)$ .

Let us now discuss the results which are obtained from the Minkowski embedding algorithm. In figure 3.12 we show the values of  $\chi(u_{close})$  in the  $(c_1, M_{tz})$  parameter space. The value of  $\chi(u_{close})$  which is closest to 1 is found to be 0.967. This value is quite close to 1, the value which suggests the physical Minkowski embedding. So we will need a further investigation.

### 3.4.3 The case $m/R = 0.4, H_{ext} = 3$

Let us now discuss the results for the case  $m/R = 0.4, H_{ext} = 3$ . We show the results from the Ball embedding algorithm in figure 3.13. We have made the contour plot of  $u_{close}/R$  in the  $(c_1, M_{tz})$  parameter space. From our sample points, we do not get any point with  $u_{close} = 0.5001R$ . The closest we get is  $0.546R$ . So it is quite unlikely that there is a Ball embedding for  $(m/R, H_{ext}) = (0.4, 2.5)$ .

Let us now discuss the results which are obtained the Minkowski embedding algorithm. From the data presented in figure 3.14 we see that the value of  $\chi(u_{close})$  which is closest

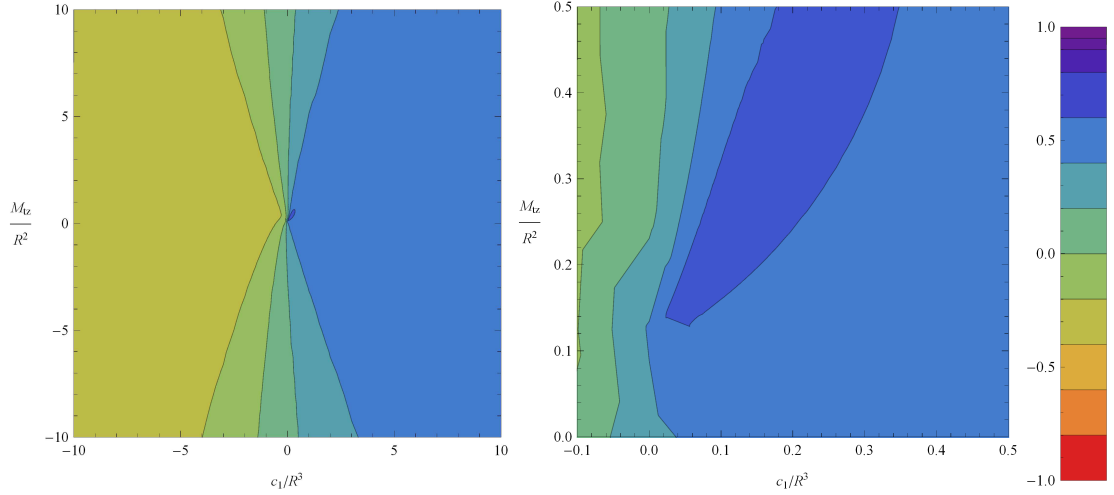


Figure 3.9: The contour plots showing the values of  $\chi(u_{close})$  in the  $(c_1, M_{tz})$  parameter space with fixed  $(m/R, H_{ext}) = (0.4, 1)$ . The left plot is the interpolation of the contour plot for the full range  $-10 \leq c_1/R^3 \leq 10$ ,  $-10 \leq M_{tz}/R^2 \leq 10$ . The middle plot is the same as the left plot but with a smaller range focusing around the points with  $\chi(u_{close})$  closest to 1. The right plot is the colour bar encoding the values of  $\chi(u_{close})$ . The physical Minkowski embedding has  $\chi(u_{close}) \approx 1$ . However, the best result obtained from our sample points gives  $\chi(u_{close}) = 0.65$ . So it is highly unlikely that there is a Minkowski embedding for  $(m/R, H_{ext}) = (0.4, 1)$ .

to 1 is found to be 0.999. This value is very close to 1, so we expect that there is a nearby point in the  $(c_1, M_{tz})$  space which gives  $\chi(u_{close}) \approx 1$  as well as smooth profiles of  $\chi(u), H(u)$  in the range  $u \in [u_{close}, \infty)$ . If this point exists, then we can conclude with a certainty that there is a Minkowski embedding. However, we will have to see if this is really the case.

### 3.5 Summary and discussions

In this chapter, we analyse the finite size effect of external magnetic field on a strongly coupled gauge theory at zero temperature by using the D3/D7 model. This model was studied before by [112]. The external magnetic field is studied by turning on a pure gauge B-field whose form is based on local tetrads. We argue however that this ansatz does not solve the constraint on D7-branes. We propose a new ansatz which is based on vector spherical harmonics. We check that this ansatz indeed satisfies the equations of motion on D7-branes.

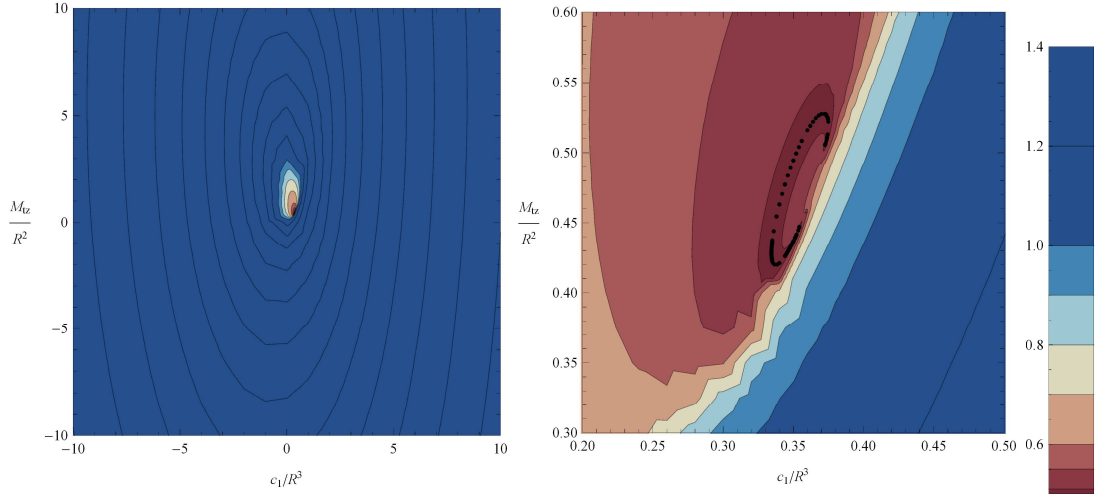


Figure 3.10: The contour plots showing the values of  $u_{close}/R$  in the  $(c_1, M_{tz})$  parameter space with fixed  $(m/R, H_{ext}) = (0.4, 2.5)$ . The left plot is the interpolation of the contour plot for the full range  $-10 \leq c_1/R^3 \leq 10$ ,  $-10 \leq M_{tz}/R^2 \leq 10$ . The middle plot is the same as the left plot but with a smaller range focusing around the points with  $u_{close} = 0.5001R$  (the numerical value for  $u_{close} = R/2$ ). The sample points with  $u_{close} = 0.5001R$  are shown in black dots. The right plot is the colour bar encoding the values of  $u_{close}/R$ .

By analysing the embedding, we find that for some fixed external magnetic field, there is a range of values of quark mass where the system cannot be studied. We call this forbidden region as “mass gap”. One of the reason for its presence is the disappearance of some Ball embeddings. Note that the appearance of the mass gap in the presence of B-field is unusual because the gap is in the middle of the spectrum of the bare parameter space. Therefore, we have to make sure that our finding is not due to a numerical mistake. For this reason, we try several cross checks.

We first make a cross check by analysing the equatorial embedding. The results suggest that the equatorial embedding does disappear for a sufficiently large value of external magnetic field. We have also scanned the whole parameter space to confirm that this is really the case.

Although the above cross check seems to confirm some features of the mass gap, it is still not completely clear. So we make another cross check. This time, we use the shooting method by shooting from the AdS boundary. This requires the full scan of the four-dimensional parameter space  $(m, H_{ext}, c_1, M_{tz})$ . However, we still do not have a full control over this computation, so we study some example points.

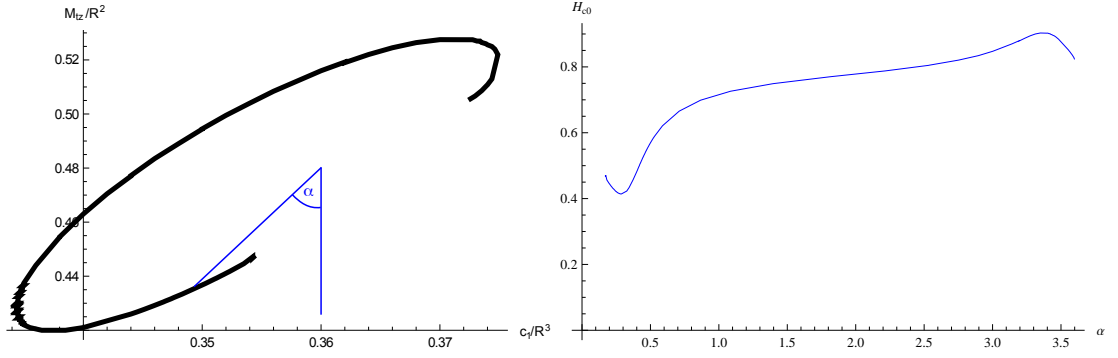


Figure 3.11: The left plot shows the interpolation of black dots from figure 3.10. We define the affine parameter  $\alpha$  as the angle from a reference axis. The right plot shows the values of  $H_{c0} \equiv H(R/2)$  as a function of  $\alpha$ . The interpolation suggests that it is unlikely to have  $H_{c0} = 0$ .

We fix  $(m, H_{ext})$  and scan the resulting  $(c_1, M_{tz})$  space. Typically, there are two kinds of unphysical solutions: either that the profiles  $\chi(u), H(u)$  are non-smooth or that the profiles  $\chi(u), H(u)$  are smooth everywhere but  $H(R/2) \neq 0$ . These solutions occupies most of the  $(c_1, M_{tz})$  space. So we need to be careful to isolate all the physical embeddings from unphysical ones. This is under an investigation.

If, after the investigation, it turns out that the mass gap does really exist, then it is possible that this implies that the ground state we are investigating is not the real ground state. A preliminary result based on scalar fluctuations also suggests that this ground state, which is homogeneous, is not the real ground state. So we will have to find the real, inhomogeneous ground state.

After making sure whether the mass gap exists, it is also interesting to see what happens to the system if we turn on the chemical potential. In particular, we want to see how the full phase diagram involving magnetic field and chemical potential looks like.

### 3.A Gauge symmetry of embedding equations of motion

We consider gauge transformation

$$A_a \rightarrow A_a + \partial_a \lambda, \quad P[B]_{ab} \rightarrow P[B]_{ab} \quad (3.62)$$

or

$$A_a \rightarrow A_a - \frac{1}{2\pi\alpha'} \lambda_a, \quad P[B]_{ab} \rightarrow P[B]_{ab} + \partial_a \lambda_b - \partial_b \lambda_a. \quad (3.63)$$

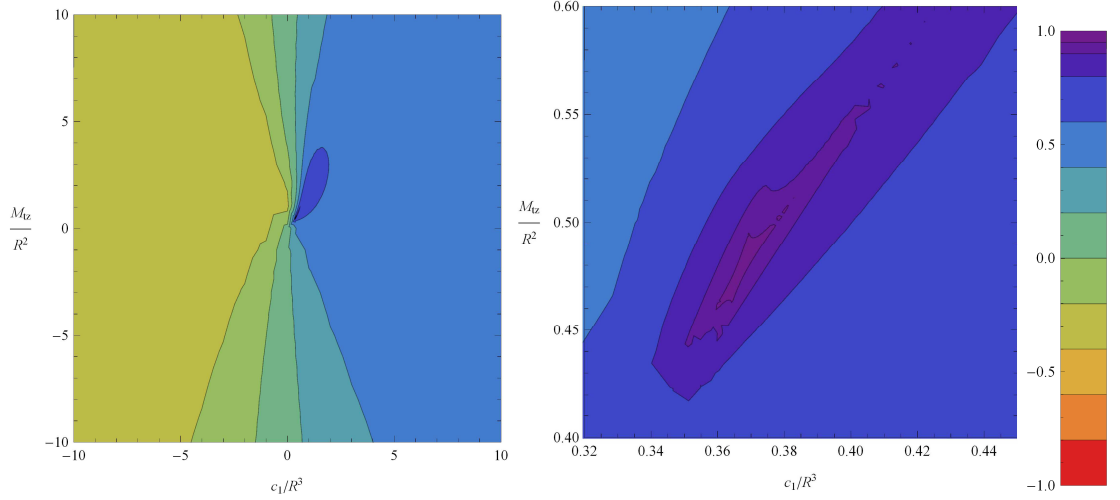


Figure 3.12: The contour plots showing the values of  $\chi(u_{close})$  in the  $(c_1, M_{tz})$  parameter space with fixed  $(m/R, H_{ext}) = (0.4, 2.5)$ . The left plot is the interpolation of the contour plot for the full range  $-10 \leq c_1/R^3 \leq 10$ ,  $-10 \leq M_{tz}/R^2 \leq 10$ . The middle plot is the same as the top left plot but with a smaller range focusing around the points with  $\chi(u_{close})$  closest to 1. The right plot is the colour bar encoding the values of  $\chi(u_{close})$ . The physical Minkowski embedding has  $\chi(u_{close}) \approx 1$ . The best result obtained from our sample points gives  $\chi(u_{close}) = 0.967$ . Since this value is quite close to 1, we need a further investigation to see if there is a physical Minkowski embedding.

It is easy to see that  $\mathcal{E}_{ab}$  is invariant under the above gauge transformations. This implies that equation (3.3) is also invariant under this gauge transformation. For equation (3.2), expanding derivatives in the first two terms gives

$$\begin{aligned} & \partial_b \left( \sqrt{-\mathcal{E}}(\mathcal{E}^{ba} + \mathcal{E}^{ab}) \right) G_{\nu\lambda} \partial_a x^\nu + \partial_b \left( \sqrt{-\mathcal{E}}(\mathcal{E}^{ba} - \mathcal{E}^{ab}) \right) B_{\nu\lambda} \partial_a x^\nu \\ & + \sqrt{-\mathcal{E}} \mathcal{E}^{ba} (E_{\nu\lambda} + E_{\lambda\nu}) \partial_b \partial_a x^\nu + \sqrt{-\mathcal{E}} \mathcal{E}^{ba} (\partial_\mu E_{\lambda\nu} - \partial_\lambda E_{\mu\nu} + \partial_\nu E_{\mu\lambda}) \partial_a x^\mu \partial_b x^\nu = 0. \end{aligned} \quad (3.64)$$

Using equation (3.3), the above equation gives

$$\begin{aligned} & \partial_b \left( \sqrt{-\mathcal{E}}(\mathcal{E}^{ba} + \mathcal{E}^{ab}) \right) G_{\nu\lambda} \partial_a x^\nu \\ & + 2\sqrt{-\mathcal{E}} \mathcal{E}^{ba} \left( G_{\nu\lambda} \partial_b \partial_a x^\nu + \frac{1}{2} (\partial_\mu G_{\lambda\nu} - \partial_\lambda G_{\mu\nu} + \partial_\nu G_{\mu\lambda} + (dB)_{\mu\lambda\nu}) \partial_a x^\mu \partial_b x^\nu \right) = 0, \end{aligned} \quad (3.65)$$

which is manifestly invariant under the gauge transformation.

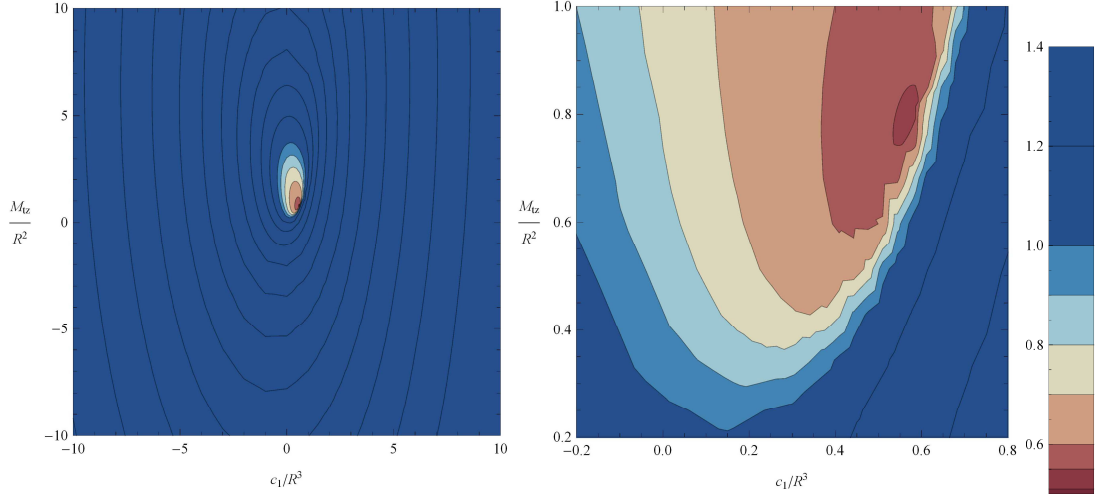


Figure 3.13: The contour plots showing the values of  $u_{close}/R$  in the  $(c_1, M_{tz})$  parameter space with fixed  $(m/R, H_{ext}) = (0.4, 3)$ . The left plot is the interpolation of the contour plot for the full range  $-10 \leq c_1/R^3 \leq 10$ ,  $-10 \leq M_{tz}/R^2 \leq 10$ . The middle plot is the same as the left plot but with a smaller range focusing around the points with values closest to  $u_{close} = 0.5001R$ . From our data, there is no point with  $u_{close} = 0.5001R$ . The closest we get is  $0.546R$ . So it is quite unlikely that there is a Ball embedding.

### 3.B Regularity of B-field

In order for B-field to not change the geometry, we require the B-field to be pure gauge ( $dB = 0$ ). In fact, we also need it to be regular everywhere. Otherwise, the singularity will makes  $dB \neq 0$ .

For the Ball embedding, we consider the metric near AdS centre as this is the potential point where B-field becomes singular. We make a change of a variable

$$u = \frac{R}{2} + \frac{v}{2} \quad (3.66)$$

and expand the metric to the leading order of  $v$ . This gives

$$ds^2 \approx -dt^2 + v^2(d\bar{\theta}^2 + \sin^2 \bar{\theta} d\bar{\phi}^2 + \cos^2 \bar{\theta} d\bar{\psi}^2) + dv^2 + R^2(1 - \chi_{ball}^2)(d\theta^2 + \sin^2 \theta d\phi^2 + \cos^2 \theta d\psi^2). \quad (3.67)$$

That is, the near centre geometry is  $\mathbb{R}^{1,4} \times S^3$ . On the  $\mathbb{R}^{1,4}$  part, we can reparameterise to Cartesian coordinates

$$x = v \sin \bar{\theta} \cos \bar{\phi}, \quad y = v \sin \bar{\theta} \sin \bar{\phi}, \quad z = v \cos \bar{\theta} \cos \bar{\psi}, \quad w = v \cos \bar{\theta} \sin \bar{\psi}. \quad (3.68)$$

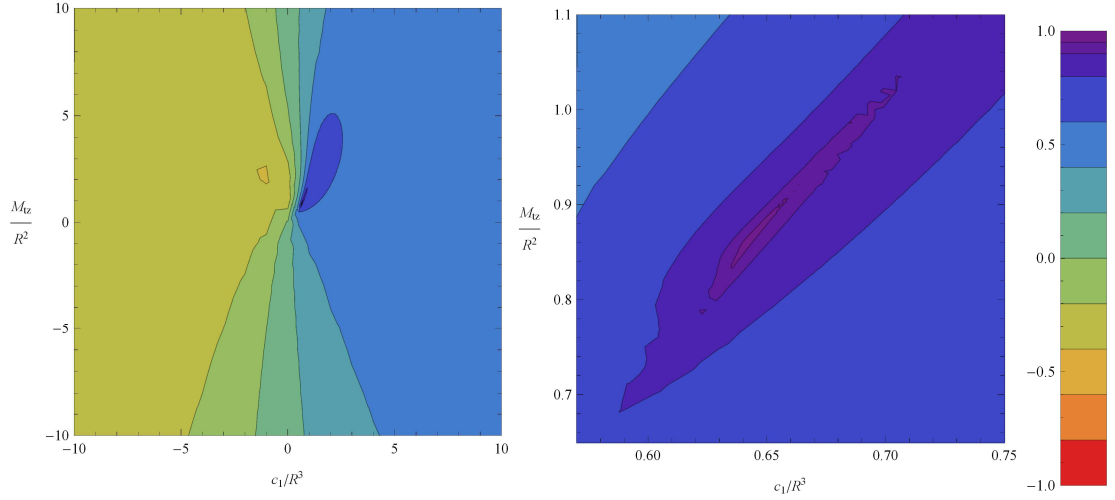


Figure 3.14: The contour plots showing the values of  $\chi(u_{close})$  in the  $(c_1, M_{tz})$  parameter space with fixed  $(m/R, H_{ext}) = (0.4, 3)$ . The left plot is the interpolation of the contour plot for the full range  $-10 \leq c_1/R^3 \leq 10, -10 \leq M_{tz}/R^2 \leq 10$ . The middle plot is the same as the top left plot but with a smaller range focusing around the points with  $\chi(u_{close})$  closest to 1. The right plot is the colour bar encoding the values of  $\chi(u_{close})$ . The physical Minkowski embedding has  $\chi(u_{close}) \approx 1$ . The best result obtained from our sample points gives  $\chi(u_{close}) = 0.999$ . Since this value is very close to 1, it is highly likely that there is a physical Minkowski embedding. However, a further investigation is required to see if a physical Minkowski embedding really does exist.

Then, B-field is

$$\begin{aligned}
 B = R^2 \left( \frac{H(u)}{v^4} - \frac{1}{4} \frac{H'(u)}{v^3} \right) ((x dx + y dy + z dz + w dw)(y dx - x dy + w dz - z dw)) \\
 + \frac{H(u)R^2}{v^2} (dx dy + dz dw).
 \end{aligned} \tag{3.69}$$

Regularity at  $v = 0$  requires  $H(u) = H_0 v^2 + \dots$ . This condition should be imposed only on Ball embedding since in Minkowski embedding, the D7-brane does not reach the centre.

## Chapter 4

# The M5–brane action revisited

This chapter is largely based on [2].

Having discussed an application of gauge/gravity duality, let us now turn to something different. In chapter 1, we have briefly mentioned that a single M5–brane action in a general eleven-dimensional supergravity background is already constructed. In particular, we stated that the covariant action of [75, 76] can be constructed with the help of an auxiliary field. In the case of flat six–dimensional worldvolume, if the auxiliary field is gauge-fixed to lie along one spatial (or temporal) direction of the worldvolume, then Lorentz symmetry is only manifest in five–dimensional subspace. In this way, this action is a  $1 + 5$  splitting of the six dimensions of the M5–brane worldvolume.

The references [66, 78] construct an alternative 5–brane action based on the BLG action. This construction is called Nambu–Poisson (NP) M5–brane model. It is conjectured to be related, via a map [115] analogous to Seiberg–Witten map [116], with the original M5–brane in a constant  $C_3$ –field background. In the NP M5–brane model the manifest  $SO(1, 5)$  6d Lorentz symmetry is naturally broken by the presence of multiple M2–branes and the  $C_3$ –field to  $SO(1, 2) \times SO(3)$ , which corresponds to a  $3 + 3$  splitting.

To see whether the quadratic NP M5–brane would be related to the original M5–brane action, we are motivated to construct a full non-linear M5–brane action with a  $3 + 3$  splitting. Our strategy to achieve this goal is as follows<sup>1</sup>. We will start with the covariant form [119] of the quadratic self–dual action of [66] for a 2–form chiral gauge field in six–dimensions. In addition to the conventional invariance under the gauge transformations of the chiral field, the covariant action possesses two more local symmetries. One of them

---

<sup>1</sup>For analogous procedures of getting manifestly duality–symmetric non–linear actions see e.g. [71, 117, 118].

ensures that the auxiliary fields, which make the action covariant, are non-dynamical and another one guarantees that the self-duality condition on the field strength of the chiral field is the general solution of its equations of motion. We will add to this quadratic action a generic non-linear function of components of the chiral field strength and derive conditions on the form of this function imposed by the two local symmetries. We will then check that the non-linearly self-dual field strength of the superembedding formulation satisfies these conditions and, as a result, will derive an explicit form of the M5-brane action in which the  $6d$  diffeomorphism invariance is subject to 3+3 splitting.

In section 4.1 we introduce main notation and conventions used throughout this chapter. In section 4.2 we review the original action and present the structure of the novel action for the M5-brane. The derivation of the new action is explained in section 4.3. In section 4.4 we show that on-shell values of the two actions are equal and in section 4.5 briefly discuss the dimensional reduction of the novel M5-brane action to that of the M2-brane. The results are summarised in section 4.6, where we also discuss open issues and possible directions of further research. In the appendix 4.A we give more details of the check of the form of the new M5-brane action by comparing the self-duality relations which follow from the action with those obtained in the superembedding description of the M5-brane.

## 4.1 Notation and Conventions

The  $6d$  and the  $D = 11$  Minkowski metrics have the almost plus signature,  $x^\mu$  ( $\mu = 0, 1, \dots, 5$ ) stand for the worldvolume coordinates of the M5-brane which carries the chiral gauge field  $B_2(x) = \frac{1}{2}dx^\mu dx^\nu B_{\nu\mu}(x)$ . The  $D = 11$  bulk superspace is parametrised by  $Z^{\mathcal{M}} = (X^M, \theta)$ , where  $X^M$  are eleven bosonic coordinates and  $\theta$  are 32 real fermionic coordinates. The geometry of the  $D = 11$  supergravity are described by tangent-space vector supervielbeins  $E^A(Z) = dZ^{\mathcal{M}}E_{\mathcal{M}}^A(Z)$  ( $A = 0, 1, \dots, 10$ ) and Majorana-spinor supervielbeins  $E^\alpha(Z) = dZ^{\mathcal{M}}E_{\mathcal{M}}^\alpha(Z)$  ( $\alpha = 1, \dots, 32$ ).

The vector supervielbein satisfies the following essential torsion constraint, which is required for proving the kappa-symmetry of the M5-brane action,

$$T^A = DE^A = dE^A + E^B \Omega_B^A = -iE^\alpha \Gamma_{\alpha\beta}^A E^\beta, \quad (4.1)$$

where  $\Omega_B^A(Z)$  is the one-form spin connection in  $D = 11$ ,  $\Gamma_{\alpha\beta}^A = \Gamma_{\beta\alpha}^A$  are real symmetric gamma-matrices and the external differential acts from the right.

The induced metric on the  $M5$ -brane worldvolume is constructed with the pull-backs of the vector supervielbeins  $E^A(Z)$

$$g_{\mu\nu}(x) = E_\mu^A E_\nu^B \eta_{AB}, \quad E_\mu^A = \partial_\mu Z^N E_N^A(Z(x)). \quad (4.2)$$

The  $M5$ -brane couples to the  $D = 11$  supergravity 3-form gauge superfield  $C_3(Z) = \frac{1}{3!} dZ^{\mathcal{M}_1} dZ^{\mathcal{M}_2} dZ^{\mathcal{M}_3} C_{\mathcal{M}_3 \mathcal{M}_2 \mathcal{M}_1}$  and its  $C_6(Z)$  dual, their field strengths are constrained as follows

$$\begin{aligned} dC_3 &= -\frac{i}{2} E^A E^B E^\alpha E^\beta (\Gamma_{BA})_{\alpha\beta} + \frac{1}{4!} E^A E^B E^C E^D F_{DCBA}^{(4)}(Z), \\ dC_6 - C_3 dC_3 &= \frac{2i}{5!} E^{A_1} \dots E^{A_5} E^\alpha E^\beta (\Gamma_{A_5 \dots A_1})_{\alpha\beta} + \frac{1}{7!} E^{A_1} \dots E^{A_7} F_{A_7 \dots A_1}^{(7)}(Z) \quad (4.3) \\ F^{(7) A_1 \dots A_7} &= \frac{1}{4!} \epsilon^{A_1 \dots A_{11}} F_{A_8 \dots A_{11}}^{(4)}, \quad \epsilon^{0 \dots 10} = -\epsilon_{0 \dots 10} = 1. \end{aligned}$$

The generalised field strengths of  $B_2(x)$  which appears in the  $M5$ -brane action is

$$H_3 = dB_2 + C_3, \quad (4.4)$$

where  $C_3(Z(x))$  is the pullback on the  $M5$ -brane worldvolume of the 3-form gauge field.

## 4.2 M5-brane actions

We start by briefly reviewing the original form of the  $M5$ -brane action and then will present our main result, namely, the alternative worldvolume action for the  $M5$ -brane in a generic  $D = 11$  supergravity background.

### 4.2.1 Original $M5$ -brane action

In this case to ensure the  $6d$  worldvolume covariance of the  $M5$ -brane action one uses a normalised gradient of the auxiliary scalar field  $a(x)$  which can be chosen to be time-like or space-like, e.g.

$$v_\mu(x) = \frac{\partial_\mu a}{\sqrt{\partial_\nu a g^{\nu\lambda}(x) \partial_\lambda a}}, \quad v_\mu v^\mu = 1 \quad (4.5)$$

The both choices are equivalent since in the action  $\partial_\mu a$  appears only in the projector of rank one

$$P_\mu{}^\nu(x) = \frac{\partial_\mu a \partial^\nu a}{(\partial a)^2}, \quad PP = P, \quad (\partial a)^2 \equiv \partial_\nu a g^{\nu\lambda} \partial_\lambda a = \partial_\nu a \partial^\nu a. \quad (4.6)$$

This projector singles out one worldvolume direction from the six, i.e. makes the 1+5 covariant splitting of the  $6d$  worldvolume directions.

The  $M5$ -brane action in a generic  $D = 11$  supergravity superbackground constructed in [74–76] has the following form:

$$S = +2 \int_{\mathcal{M}_6} d^6x \left[ \sqrt{-\det(g_{\mu\nu} + i\tilde{H}_{\mu\nu})} + \frac{\sqrt{-g}}{4(\partial a)^2} \partial_\lambda a \tilde{H}^{\lambda\mu\nu} H_{\mu\nu\rho} \partial^\rho a \right] - \int_{\mathcal{M}_6} (C_6 + H_3 \wedge C_3), \quad (4.7)$$

with

$$\tilde{H}^{\rho\mu\nu} \equiv \frac{1}{6\sqrt{-g}} \epsilon^{\rho\mu\nu\lambda\sigma\tau} H_{\lambda\sigma\tau}, \quad \tilde{H}_{\mu\nu} \equiv \frac{\partial^\rho a}{\sqrt{(\partial a)^2}} \tilde{H}_{\rho\mu\nu}, \quad g = \det g_{\mu\nu}, \quad (4.8)$$

where

$$\epsilon^{0\dots 5} = -\epsilon_{0\dots 5} = 1.$$

In addition to the conventional abelian gauge symmetry for the chiral 2-form, the action (4.7) has also the following two local gauge symmetries :

$$\delta B_{\mu\nu} = 2\partial_{[\mu} a \Phi_{\nu]}(x), \quad \delta a(x) = 0, \quad (4.9)$$

as well as

$$\delta a = \varphi(x), \quad \delta B_{\mu\nu} = \frac{\varphi(x)}{\sqrt{(\partial a)^2}} (H_{\mu\nu} - \mathcal{V}_{\mu\nu}), \quad (4.10)$$

where

$$\mathcal{V}^{\mu\nu}(\tilde{H}) \equiv -2 \frac{\delta \sqrt{\det(\delta_\mu^\nu + i\tilde{H}_\mu{}^\nu)}}{\delta \tilde{H}_{\mu\nu}}, \quad H_{\mu\nu} \equiv H_{\mu\nu\rho} \frac{\partial^\rho a(x)}{\sqrt{(\partial a)^2}}, \quad (4.11)$$

with  $\varphi(x)$  and  $\Phi_\mu(x)$  being arbitrary local functions on the worldvolume. The first symmetry (4.9) ensures that the equation of motion of  $B_2$  reduces to the non-linear self-duality condition

$$H_{\mu\nu} = \mathcal{V}_{\mu\nu}(\tilde{H}), \quad (4.12)$$

while the second symmetry (4.10) is responsible for the auxiliary nature of the scalar field  $a(x)$  and the  $6d$  covariance of the action.

The action (4.7) is also invariant under the local fermionic kappa-symmetry transformations with the parameter  $\kappa^\alpha(x)$  which acts on the pullbacks of the target-space supervielbeins and the  $B_2$  field strength as follows

$$i_\kappa E^\alpha \equiv \delta_\kappa Z^\mathcal{M} E_\mathcal{M}^\alpha = \frac{1}{2} (1 + \bar{\Gamma})^\alpha{}_\beta \kappa^\beta, \quad i_\kappa E^A \equiv \delta_\kappa Z^\mathcal{M} E_\mathcal{M}^A = 0, \quad (4.13)$$

$$\delta_\kappa g_{\mu\nu} = -4i E_{(\mu}^\alpha (\Gamma_{\nu)})_{\alpha\beta} i_\kappa E^\beta, \quad \delta_\kappa H^{(3)} = i_\kappa dC^{(3)}, \quad \delta_\kappa a(x) = 0,$$

where  $(1 + \bar{\Gamma})/2$  is the projector of rank 16 with  $\bar{\Gamma}$  having the following form

$$\sqrt{\det(\delta_\mu^\nu + i\tilde{H}_\mu{}^\nu)} \bar{\Gamma} = \gamma^{(6)} - \frac{1}{2} \Gamma^{\mu\nu\lambda} P_\mu{}^\rho \tilde{H}_{\nu\lambda\rho} - \frac{1}{16\sqrt{-g}} \epsilon^{\mu_1\dots\mu_6} \tilde{H}_{\mu_1\mu_2\lambda} \tilde{H}_{\mu_3\mu_4\rho} P^{\lambda\rho} \Gamma_{\mu_5\mu_6},$$

$$\bar{\Gamma}^2 = 1, \quad \text{tr} \bar{\Gamma} = 0, \quad (4.14)$$

where

$$\Gamma_\mu = E_\mu^A \Gamma_A, \quad \gamma^{(6)} = \frac{1}{6! \sqrt{-g}} \epsilon^{\mu_1 \dots \mu_6} \Gamma_{\mu_1 \dots \mu_6}. \quad (4.15)$$

### 4.2.2 New M5-brane action

For this case, to ensure worldvolume covariance of the construction, instead of the single scalar field we need to introduce a triplet of auxiliary scalar fields  $a^s(x)$  with the index ( $s = 1, 2, 3$ ) labelling a 3-dimensional representation of  $GL(3)$  which is an *internal* global symmetry of the action. The partial derivatives of the scalars are used to construct the projector matrices [119]

$$P_\mu^\nu = \partial_\mu a^r Y_{rs}^{-1} \partial^\nu a^s, \quad \Pi_\mu^\nu = \delta_\mu^\nu - P_\mu^\nu, \quad \Pi_\mu^\nu \partial_\nu a^s = 0 \quad (4.16)$$

with  $Y_{rs}^{-1}$  being the inverse matrix of

$$Y^{rs} \equiv \partial_\lambda a^r \partial_\rho a^s g^{\lambda\rho}. \quad (4.17)$$

The projectors identically satisfy the following differential condition

$$\Pi_{[\rho}^\lambda \Pi_{\kappa]}^\mu D_\lambda P_\mu^\nu = 0 = \Pi_{[\rho}^\lambda \Pi_{\kappa]}^\mu D_\lambda \Pi_\mu^\nu \quad (4.18)$$

where  $D_\mu$  is the worldvolume covariant derivative with respect to the induced metric  $g_{\mu\nu}$ .

Note that the projectors (4.16) have rank 3 and thus effectively split the 6d directions into 3+3 ones orthogonal to each other.

The new M5-brane action coupled to a curved superbackground has the following form

$$S = \int_{\mathcal{M}_6} d^6x \left[ -\frac{\sqrt{-g}}{6} (\tilde{G}^{\mu\nu\rho} G_{\mu\nu\rho} + 3\tilde{F}^{\mu\nu\rho} F_{\mu\nu\rho}) + 2\mathcal{L}_{M5}(F, G) \right] - \int_{\mathcal{M}_6} (C_6 + H \wedge C_3), \quad (4.19)$$

where

$$\begin{aligned} \mathcal{L}_{M5} = & -\frac{1}{36(1+G^2)} \epsilon^{\mu_1 \mu_2 \mu_3 \mu_4 \mu_5 \mu_6} G_{\mu_1 \mu_2 \mu_3} F_{\mu_4 \nu \lambda} F_{\mu_5}^{\lambda \kappa} F_{\mu_6 \kappa}^\nu \\ & + \frac{1}{1+G^2} \sqrt{-\det \left( g_{\mu\nu} + \frac{1}{2} (F+G)_{\mu\rho\sigma} (F+G)_{\nu}{}^{\rho\sigma} \right)} \end{aligned} \quad (4.20)$$

and  $F_{\mu\nu\rho}$  and  $G_{\mu\nu\rho}$  are components of the field strength  $H_{\mu\nu\rho}$  projected as follows

$$F_{\mu\nu\rho} \equiv H_{\tau\sigma\lambda} P_\mu^\tau P_\nu^\sigma P_\rho^\lambda, \quad G_{\mu\nu\rho} \equiv H_{\tau\sigma\lambda} \Pi_\mu^\tau \Pi_\nu^\sigma \Pi_\rho^\lambda, \quad G^2 \equiv \frac{1}{6} H_{\mu\nu\rho} \Pi_\tau^\mu \Pi_\sigma^\nu \Pi_\lambda^\rho H^{\tau\sigma\lambda}, \quad (4.21)$$

$$\tilde{F}_{\mu\nu\rho} \equiv \tilde{H}_{\tau\sigma\lambda} P_\mu^\tau P_\nu^\sigma P_\rho^\lambda, \quad \tilde{G}_{\mu\nu\rho} \equiv \tilde{H}_{\tau\sigma\lambda} \Pi_\mu^\tau \Pi_\nu^\sigma \Pi_\rho^\lambda, \quad (4.22)$$

The action enjoys the following two local gauge symmetries analogous to eqs. (4.9) and (4.10). The first one is

$$\delta B_{\mu\nu} = P_\mu^\rho P_\nu^\sigma \Phi_{\rho\sigma}(x), \quad \delta a^s = 0, \quad (4.23)$$

where  $\Phi_{\rho\sigma}(x)$  are arbitrary parameters. Note that in view of the conditions (4.18) it follows that the projected field strengths (4.21), and hence  $\mathcal{L}_{M5}(G, F)$ , are invariant under this symmetry

$$\delta_{\Phi} G_{\mu\nu\rho} = \delta_{\Phi} F_{\mu\nu\rho} = 0, \quad (4.24)$$

while their dual (4.22) are not.

The second symmetry ensures the triplet of the scalar fields  $a^s(x)$  to be auxiliary

$$\delta a^s = \varphi^s(x), \quad \delta B_{\mu\nu} = \frac{1}{2} \varphi^r Y_{rs}^{-1} \partial^{\rho} a^s \epsilon_{\mu\nu\rho\tau\sigma\lambda} \left( \sqrt{-g} \tilde{F}^{\tau\sigma\lambda} - \frac{\partial \mathcal{L}_{M5}}{\partial F_{\tau\sigma\lambda}} \right), \quad (4.25)$$

where  $\varphi^s(x)$  are local parameters<sup>2</sup>.

This symmetry allows one to gauge fix  $a^s(x)$  to coincide with three world-sheet coordinates, e.g.  $x^a$  ( $a = 0, 1, 2$ ) or  $x^i$  ( $i = 3, 4, 5$ ), thus getting a non-covariant but non-manifestly worldsheet diffeomorphism invariant M5-brane action. For instance, let us impose the gauge fixing condition

$$a^s = \delta_a^s x^a, \quad (4.26)$$

identifying  $a^s$  with  $x^a$ . Then the following combination of the worldvolume diffeomorphism  $\delta x^{\mu} = \xi^{\mu}(x)$  and the local symmetry (4.25) leaves this gauge condition intact

$$\delta a^s(x) = \xi^{\mu}(x) \partial_{\mu} a^s + \varphi^s(x) = \xi^s(x) + \varphi^s(x) = 0, \quad \rightarrow \quad \varphi^s(x) = -\xi^s(x).$$

Under the local transformation combined of the  $6d$  diffeomorphism  $\delta x^{\mu} = \xi^{\mu}(x)$  and the local variation (4.25) with  $\varphi^a(x) = -\xi^a(x)$  the gauge field  $B_{\mu\nu}$  transforms as follows

$$\Delta_{\xi^{\mu}} B_{\mu\nu} = \delta_{\xi^{\mu}} B_{\mu\nu} - \frac{1}{2} \xi^a(x) \epsilon_{a\mu\nu\tau\sigma\lambda} \left( \sqrt{-g} \tilde{F}^{\tau\sigma\lambda} - \frac{\partial \mathcal{L}_{M5}}{\partial F_{\tau\sigma\lambda}} \right),$$

while the other M5-brane fields  $X^M(x)$  and  $\theta^{\alpha}(x)$  being transformed in the conventional way as worldvolume scalars. In the gauge (4.26) the action (4.19), (4.20) is non-manifestly invariant under the modified worldvolume diffeomorphisms of the above form.

Upon tedious computations we have checked that the action is invariant under the kappa-symmetry transformations (4.13) but with a  $\bar{\Gamma}$  projector which has the following

---

<sup>2</sup>In what follows we will use a normalisation of the functional derivative, denoted by  $\frac{\partial \mathcal{L}(F)}{\partial F_{\mu\nu\dots}}$ , which differs from the one defined in (4.11). Namely, by definition the variation of a  $p$ -form  $F_{\mu_1\dots\mu_p}$  and the corresponding functional derivatives are defined as follows  $\delta F_{\mu_1\dots\mu_p} = \delta F_{\nu_1\dots\nu_p} \frac{\delta F_{\mu_1\dots\mu_p}}{\delta F_{\nu_1\dots\nu_p}} = \delta F_{\nu_1\dots\nu_p} \frac{1}{p!} \frac{\partial F_{\mu_1\dots\mu_p}}{\partial F_{\nu_1\dots\nu_p}}$ . So that

$$\frac{\partial \mathcal{L}}{\partial F_{\nu_1\dots\nu_p}} \equiv p! \frac{\delta \mathcal{L}}{\delta F_{\nu_1\dots\nu_p}}.$$

form

$$\begin{aligned}
\frac{1}{1+G^2} \sqrt{\det \left( \delta_\mu^\nu + \frac{1}{2}(F+G)_{\mu\rho\sigma}(F+G)^{\nu\rho\sigma} \right)} \bar{\Gamma} &= \\
&= \gamma^{(6)} + \frac{1}{6} \gamma^{(6)} (3F+G)^{\mu\nu\rho} \Gamma_{\mu\nu\rho} + \frac{1}{2(1+G^2)} \gamma^{(6)} F^{\mu\nu\tau} F^{\rho\lambda}{}_\tau \Gamma_{\mu\nu\rho\lambda} \\
&\quad + \frac{1}{6(1+G^2)} \gamma^{(6)} \Gamma^{\mu\nu\rho} (3(FFG)_{\mu\nu\rho} + (FFF)_{\mu\nu\rho}), \tag{4.27}
\end{aligned}$$

where

$$(FFG)_{\mu\nu\rho} \equiv F_\mu{}^{\tau\sigma} F_{\nu\sigma\lambda} G_\rho{}^\lambda{}_\tau, \quad (FFF)_{\mu\nu\rho} \equiv F_\mu{}^{\tau\sigma} F_{\nu\sigma\lambda} F_\rho{}^\lambda{}_\tau. \tag{4.28}$$

Note that the term multiplying  $\bar{\Gamma}$  on the left hand side of (4.27) is equal (modulo  $\sqrt{-\det g_{\mu\nu}}$ ) to the last term of the non-linear part (4.20) of the M5–brane Lagrangian.

Finally, the non-linear self-duality condition which is obtained from action (4.19) as the consequence of the equations of motion of  $B_2$  (see eq. (4.39) of the next Section) has the following form

$$\tilde{G}^{\mu\nu\rho} = \frac{1}{\sqrt{-g}} \left( \frac{\partial \mathcal{L}_{M5}}{\partial G} \right)^{\mu\nu\rho}, \quad \tilde{F}^{[\mu\nu\rho]} = \frac{1}{\sqrt{-g}} \left( \frac{\partial \mathcal{L}_{M5}}{\partial F} \right)^{[\mu\nu\rho]}. \tag{4.29}$$

As we will show, this self-duality condition is related to eq. (4.12) via the manifestly covariant self-duality relation which comes from the superembedding approach [69].

### 4.3 Derivation of the new M5–brane action

In the previous section, we have shown the new M5–brane action (4.19). In this section, we discuss its derivation. The first step is to start from the covariant form [119] of the quadratic action [66] for the 6d chiral field. It is given by <sup>3</sup>

$$\begin{aligned}
S &= \frac{1}{6} \int d^6x \sqrt{-\det g_{\mu\nu}} (H - \tilde{H})_{\mu\nu\rho} (\Pi_\lambda{}^\mu \Pi_\kappa{}^\nu \Pi_\tau{}^\rho + 3\Pi_\lambda{}^\mu \Pi_\kappa{}^\nu P_\tau{}^\rho) H^{\lambda\kappa\tau} \\
&\equiv \frac{1}{6} \int d^6x \sqrt{-\det g_{\mu\nu}} [(G - \tilde{G})_{\mu\nu\rho} G^{\mu\nu\rho} + 3(F - \tilde{F})_{\mu\nu\rho} F^{\mu\nu\rho}]. \tag{4.30}
\end{aligned}$$

As a consistency check, this action can also be obtained from (4.19) by truncating the latter to the second order in the chiral field strength  $H_3$ . The action (4.30) is invariant under the symmetry (4.23) and under the linearised counterpart of (4.25)

$$\delta a^s = \varphi^s(x), \quad \delta B_{\mu\nu} = \frac{1}{2} \varphi^s Y_{sr}^{-1} \partial^\rho a^r \epsilon_{\mu\nu\rho\tau\sigma\lambda} \sqrt{-g} \left( \tilde{F}^{\tau\sigma\lambda} - F^{\tau\sigma\lambda} \right). \tag{4.31}$$

<sup>3</sup>For simplicity, but without loss of generality, we consider (for a moment) the pullbacks of the 11D gauge fields be zero.

The quadratic action leads to the equation of motion

$$\partial_\rho \left( \sqrt{-g}(G - \tilde{G})^{\mu\nu\rho} + 3\sqrt{-g}(F - \tilde{F})^{[\mu\nu\rho]} \right) = 0. \quad (4.32)$$

One may guess that the general solution is given by

$$\sqrt{-g}(G - \tilde{G})^{\mu\nu\rho} + 3\sqrt{-g}(F - \tilde{F})^{[\mu\nu\rho]} \stackrel{?}{=} \frac{1}{2}\epsilon^{\mu\nu\rho\tau\sigma\lambda}\partial_\tau \left[ \sqrt{-g}\tilde{\Phi}_{\sigma\lambda} \right], \quad (4.33)$$

for some arbitrary integration constant  $\tilde{\Phi}_{\sigma\lambda} = \tilde{\Phi}_{[\sigma\lambda]}$ . However, this solution is not good because it is incompatible after contracted with the projections  $P_\mu^{\mu'} P_\nu^{\nu'} P_\rho^{\rho'}$  and  $\Pi_\mu^{[\mu'} P_\nu^{\nu'} P_\rho^{\rho']}$ ; the LHS does not survive the projection, while the RHS does, which restricts  $\tilde{\Phi}_{\sigma\lambda}$ . So we need to modify the RHS of (4.33) to make it vanish under the projections  $P_\mu^{\mu'} P_\nu^{\nu'} P_\rho^{\rho'}$  and  $\Pi_\mu^{[\mu'} P_\nu^{\nu'} P_\rho^{\rho']}$ . For this purpose, we consider the identity

$$\tilde{\Phi}_{\sigma\lambda} = \tilde{\Phi}_{\eta\xi} (P_\sigma^\eta P_\lambda^\xi + 2P_\sigma^\eta \Pi_\lambda^\xi + \Pi_\sigma^\eta \Pi_\lambda^\xi). \quad (4.34)$$

Since each term is of different projection, we propose that the general solution of the equation of motion (4.32) is of the form

$$\sqrt{-g}(G - \tilde{G})^{\mu\nu\rho} + 3\sqrt{-g}(F - \tilde{F})^{[\mu\nu\rho]} = \frac{1}{2}\epsilon^{\mu\nu\rho\tau\sigma\lambda}\partial_\tau \left[ \sqrt{-g}\tilde{\Phi}_{\eta\xi} (\alpha P_\sigma^\eta P_\lambda^\xi + 2\beta P_\sigma^\eta \Pi_\lambda^\xi + \gamma \Pi_\sigma^\eta \Pi_\lambda^\xi) \right], \quad (4.35)$$

for some numbers  $\alpha, \beta, \gamma$ . The requirement that RHS vanishes under the projections  $P_\mu^{\mu'} P_\nu^{\nu'} P_\rho^{\rho'}$  and  $\Pi_\mu^{[\mu'} P_\nu^{\nu'} P_\rho^{\rho']}$  implies that  $\beta = \gamma = 0$ . Furthermore, without loss of generality, we can take  $\alpha = 1$ . Therefore, the general solution to the equation of motion (4.32) is given by

$$\sqrt{-g}(G - \tilde{G})^{\mu\nu\rho} + 3\sqrt{-g}(F - \tilde{F})^{[\mu\nu\rho]} = \frac{1}{2}\epsilon^{\mu\nu\rho\tau\sigma\lambda}\partial_\tau \left[ \sqrt{-g}\tilde{\Phi}_{\eta\xi} P_\sigma^\eta P_\lambda^\xi \right], \quad (4.36)$$

for some arbitrary integration constant  $\tilde{\Phi}_{\eta\xi}$ . This integration constant can be compensated by a gauge transformation of the equation of motion under (4.23) with gauge parameter  $-\tilde{\Phi}_{\xi\eta}$ . Hence, in view of the definition of the projected components of the field strength (4.21), the solution of the dynamical equation is equivalent to the self-duality conditions

$$(G - \tilde{G})^{\mu\nu\rho} = 0, \quad (F - \tilde{F})^{[\mu\nu\rho]} = 0. \quad (4.37)$$

We are now looking for a non-linear generalisation of the action (4.30) which would respect the both symmetries (4.23) and (4.25). Note that the second symmetry should be deformed by the non-linear terms, since the form of its transformation is associated with the form of the non-linear self-duality condition. In the case of the M5–brane these are (4.10)–(4.12), and (4.25) and (4.29).

Since the field strength components  $F_{\mu\nu\rho}$  and  $G_{\mu\nu\rho}$  are invariant under the transformations (4.23) (see eqs. (4.24)), while their dual (4.22) are not, the non-linear terms in the action should only depend on  $F$  and  $G$ . So the general form of the non-linear action which respects the symmetry (4.23) is obtained by replacing the quadratic terms  $FF$  and  $GG$  in (4.30) by an arbitrary function  $\mathcal{L}(F, G)$

$$S = \int_{\mathcal{M}_6} d^6x \left( -\frac{\sqrt{-g}}{6} (\tilde{G}^{\mu\nu\rho} G_{\mu\nu\rho} + 3\tilde{F}^{\mu\nu\rho} F_{\mu\nu\rho}) + 2\mathcal{L}(F, G) \right). \quad (4.38)$$

The variation of this action with respect to the gauge potential  $B_2$  produces the equations of motion

$$\partial_\rho \left[ \left( \frac{\partial \mathcal{L}}{\partial G} \right)^{\mu\nu\rho} - \sqrt{-g} \tilde{G}^{\mu\nu\rho} + 3 \left( \frac{\partial \mathcal{L}}{\partial F} \right)^{[\mu\nu\rho]} - 3\sqrt{-g} \tilde{F}^{[\mu\nu\rho]} \right] = 0. \quad (4.39)$$

In view of (4.24) and the fact that  $\mathcal{L}$  only depends on  $F$  and  $G$ , we can integrate the above equation of motion with the help of the symmetry (4.23) along the same lines as in free theory. The integration produces the non-linear self-duality relations

$$\tilde{G}^{\mu\nu\rho} = \frac{1}{\sqrt{-g}} \left( \frac{\partial \mathcal{L}}{\partial G} \right)^{\mu\nu\rho}, \quad \tilde{F}^{[\mu\nu\rho]} = \frac{1}{\sqrt{-g}} \left( \frac{\partial \mathcal{L}}{\partial F} \right)^{[\mu\nu\rho]}. \quad (4.40)$$

We should now find conditions on the form of  $\mathcal{L}(F, G)$  imposed by the requirement that the action is invariant under

$$\delta a^s = \varphi^s(x), \quad \delta B_{\mu\nu} = \frac{1}{2} \varphi^s Y_{sr}^{-1} \partial^\rho a^r \epsilon_{\mu\nu\rho\tau\sigma\lambda} \left( \sqrt{-g} \tilde{F}^{\tau\sigma\lambda} - \frac{\partial \mathcal{L}}{\partial F_{\tau\sigma\lambda}} \right). \quad (4.41)$$

Upon somewhat lengthy calculations using, in particular, the properties of the projectors (4.16)–(4.18) and the form of their variation under (4.41)

$$\delta_\varphi P_{\mu\nu} = 2\Pi_{\rho(\mu} \partial^\rho \varphi^r Y_{rs}^{-1} \partial_\nu) a^s \quad (4.42)$$

we get the following condition on  $\mathcal{L}(F, G)$

$$\begin{aligned} \partial_\mu \left[ Y_{rs}^{-1} \partial^\nu a^s \left( \sqrt{-g} \left( \frac{\partial \mathcal{L}}{\partial G} \right)^{\mu\tau\sigma} F_{\nu\tau\sigma} - \sqrt{-g} G^{\mu\tau\sigma} \left( \frac{\partial \mathcal{L}}{\partial F} \right)_{\nu\tau\sigma} \right. \right. \\ \left. \left. - \frac{g}{2} \epsilon_{\nu\tau\sigma\lambda\xi\eta} F^{\lambda\xi\eta} F^{\tau\sigma\mu} - \frac{1}{2} \epsilon_{\nu\tau\sigma\lambda\xi\eta} \left( \frac{\partial \mathcal{L}}{\partial F} \right)^{\lambda\xi\eta} \left( \frac{\partial \mathcal{L}}{\partial F} \right)^{\tau\sigma\mu} \right) \right] = 0. \quad (4.43) \end{aligned}$$

This condition is analogous to those found in other instances of models with non-linear (twisted) self-duality, e.g in  $D = 6$  [71] and  $D = 4$  [117, 118]. It is well known that these conditions may have different solutions leading to different non-linear generalisations of quadratic duality-symmetric actions (see e.g. [71, 117, 118, 120, 121]). We are interested in a particular solution of the above equation, i.e. in the form of  $\mathcal{L}(F, G)$  which describes the

$M5$ –brane. To find this form we assume that, as in the case of the self–duality condition (4.12) obtained from the original  $M5$ –brane action, also the self–duality conditions (4.29) (or (4.40)) should be equivalent to the self–duality conditions appearing in the superembedding formulation of the  $M5$ –brane [69]. Exploring these conditions we shall derive the form (4.20) of the non–linear  $M5$ –brane Lagrangian.

### 4.3.1 Non–linear self–duality of the $M5$ –brane in the superembedding approach

In the superembedding description of the  $M5$ –brane [69, 122] the field strength  $H_3$  of the chiral field  $B_2$  is expressed in terms of a self–dual tensor  $h_3 = *h_3$  as follows<sup>4</sup>

$$\frac{1}{4}H_{\mu\nu\rho} = m_\mu^{-1\lambda}h_{\lambda\nu\rho}, \quad \frac{1}{4}\tilde{H}^{\mu_1\nu_1\rho_1} = \frac{1}{6}\epsilon^{\mu_1\nu_1\rho_1\mu\nu\rho}m_\mu^{-1\lambda}h_{\lambda\nu\rho} = Q^{-1}m^{\mu_1\lambda}h_{\lambda\nu_1\rho_1} \quad (4.44)$$

where  $m_\mu^{-1\lambda}$  is the inverse matrix of

$$m_\mu^\lambda = \delta_\mu^\lambda - 2k_\mu^\lambda, \quad m_\mu^{-1\lambda} = Q^{-1}(2\delta_\mu^\lambda - m_\mu^\lambda), \quad k_\mu^\lambda = h_{\mu\nu\rho}h^{\lambda\nu\rho} \quad (4.45)$$

and

$$Q = 1 - \frac{2}{3}\text{tr} k^2. \quad (4.46)$$

As was shown in [72], by splitting the indices in eqs. (4.44) into 1+5 and expressing components of  $h_3$  in terms of  $\tilde{H}_{\mu\nu 5}$  one gets the duality relation (4.12)<sup>5</sup>.

We shall now carry out a similar procedure, but splitting the 6d indices into 3+3, and upon a somewhat lengthy algebra will arrive at the self–duality condition in the form of (4.29), thus getting the non–linear function  $\mathcal{L}_{M5}(F, G)$  (4.20) which enters the  $M5$ –brane action (4.19).

The 3+3 splitting can be performed with the use of the projectors (4.16), but for computational purposes we have found it more convenient to pass to a local tangent–space frame using  $6d$  vielbeins  $e_\mu^m$  ( $e_\mu^m\eta_{mn}e_\nu^n = g_{\mu\nu}$ ) and to write the 3+3 tangent space indices explicitly. So the three directions singled out by the projector  $P_m^n \equiv e_m^\mu P_\mu^\nu e_\nu^n$ , which we assume to contain the time direction, will be labelled by the indices  $a, b, c$ , and the three spacial directions singled out by  $\Pi_m^n \equiv e_m^\mu \Pi_\mu^\nu e_\nu^n$  will be labeled by  $i, j, k$ :

$$P_m^n \rightarrow \delta_a^b, \quad \Pi_m^n \rightarrow \delta_i^j, \quad a, b, c = 0, 1, 2; \quad i, j, k = 3, 4, 5, \quad (4.47)$$

<sup>4</sup>Our normalisation of the field strength differs from that in [72] by the factor of  $\frac{1}{4}$  in front of  $H_3$ .

<sup>5</sup>This splitting is amount to projecting the tensor fields along the direction of  $\partial_\mu a$  and orthogonal to it.

while the  $6d$  Levi–Civita tensor splits as follows

$$\epsilon^{\mu\nu\rho\lambda\tau\kappa} \Rightarrow \epsilon^{abc}\epsilon^{ijk}, \quad \epsilon^{012} = -\epsilon_{012} = 1, \quad \epsilon^{345} = 1. \quad (4.48)$$

We are now ready to split the indices of  $H_3$  and  $h_3$  in (4.44).

### 3+3 splitting

As  $h_3$  is self–dual, we pick its 10 independent components in the local Lorentz frame as follows

$$h_{ija}, \quad h_{ijk} \quad (4.49)$$

and define<sup>6</sup>

$$f_a^k \equiv \frac{1}{2}\epsilon^{ijk}h_{ija}, \quad g \equiv \frac{1}{6}\epsilon^{ijk}h_{ijk}. \quad (4.50)$$

In view of the self–duality

$$h^{mnp} = \frac{1}{3!}\epsilon^{mnp l_1 l_2 l_3} h_{l_1 l_2 l_3}, \quad (4.51)$$

we have

$$h^{jab} = -\epsilon^{abc}f_c^j, \quad h^{abc} = g\epsilon^{abc}, \quad (4.52)$$

or

$$f_{ic} = \frac{1}{2}\epsilon_{abc}h_i^{ab}, \quad g = -\frac{1}{6}\epsilon_{abc}h^{abc}. \quad (4.53)$$

The corresponding components of  $H_3$  are defined as

$$F_a^k \equiv \frac{1}{2}\epsilon^{ijk}H_{ija}, \quad G \equiv \frac{1}{6}\epsilon^{ijk}H_{ijk}. \quad (4.54)$$

The duals of  $F$  and  $G$  are

$$\tilde{F}_{ic} \equiv \frac{1}{2}\epsilon_{abc}H_i^{ab}, \quad \tilde{G} \equiv -\frac{1}{6}\epsilon_{abc}H^{abc}. \quad (4.55)$$

Note that the tensors (4.54) and (4.55) are counterparts of (4.21) and (4.22) in the local Lorentz frame (4.47).

Our final goal is to write  $\tilde{F}, \tilde{G}$  in terms of  $F, G$  using the relations (4.44). To this end, using (4.44) we first find the expressions for  $F, G, \tilde{F}$  and  $\tilde{G}$  in terms of  $g$  and  $f_i^a$

$$\begin{aligned} \frac{1}{4}F_i^a &= Q^{-1} (f(1 + 4g^2 - 4\text{tr}f^2) + 8f^3 - 8gf^{-1} \det f)_i^a \\ &= Q^{-1} \frac{\partial}{\partial f_a^i} \left( \frac{1}{2}(g^2 + \text{tr}f^2) - \frac{1}{16}Q \right), \end{aligned} \quad (4.56)$$

---

<sup>6</sup>One should not confuse the field  $g(x)$  with the determinant of the induced metric  $g_{\mu\nu}$ .

$$\begin{aligned}\frac{1}{4}G &= Q^{-1} (g + 4g^3 + 4g\text{tr}f^2 - 8\det f) \\ &= Q^{-1} \frac{\partial}{\partial g} \left( \frac{1}{2}(g^2 + \text{tr}f^2) - \frac{1}{16}Q \right),\end{aligned}\quad (4.57)$$

and

$$\begin{aligned}\frac{1}{4}\tilde{F}_i^a &= Q^{-1} (f(1 - 4g^2 + 4\text{tr}f^2) - 8f^3 + 8gf^{-1}\det f)_i^a \\ &= Q^{-1} \frac{\partial}{\partial f_a^i} \left( \frac{1}{2}(g^2 + \text{tr}f^2) + \frac{1}{16}Q \right),\end{aligned}\quad (4.58)$$

$$\begin{aligned}\frac{1}{4}\tilde{G} &= Q^{-1} (g - 4g^3 - 4g\text{tr}f^2 + 8\det f) \\ &= Q^{-1} \frac{\partial}{\partial g} \left( \frac{1}{2}(g^2 + \text{tr}f^2) + \frac{1}{16}Q \right),\end{aligned}\quad (4.59)$$

where

$$Q = 1 - 16g^4 + 16(\text{tr}f^2)^2 - 32g^2\text{tr}f^2 - 32\text{tr}f^4 + 128g\det f, \quad (4.60)$$

$$\text{tr}f^2 \equiv f_i^a f_j^b \delta^{ij} \eta_{ab}, \quad \det f \equiv \frac{1}{6} \epsilon_{ijk} \epsilon^{abc} f_a^i f_b^j f_c^k, \quad (f^{-1})_i^a \det f \equiv \frac{1}{2} \epsilon_{ijk} \epsilon^{abc} f_b^j f_c^k. \quad (4.61)$$

### The M5–brane action in terms of $G$ and $F_a^i$

Let us now present the M5–brane action in the local tangent frame. For the fields (4.54) and (4.55) the M5–brane action (4.19) takes the following form

$$S_{3+3} = - \int d^6x \left( \sqrt{-\det g_{\mu\nu}} (F_a^i \tilde{F}_i^a + G\tilde{G}) - 2\mathcal{L}_{M5} \right) - \int_{\mathcal{M}_6} (C_6 + H \wedge C_3), \quad (4.62)$$

where the term  $\mathcal{L}_{M5}$  is

$$\mathcal{L}_{M5} = \sqrt{-\det g_{\mu\nu}} \left( \frac{G \det F}{1 + G^2} + \frac{\sqrt{\det \left( \delta_i^j (1 + G^2) + F_i^a F_a^j \right)}}{1 + G^2} \right). \quad (4.63)$$

Note that the action (4.62) is equivalent to (4.19), but the former is simply in the local tangent frame.

Let us also present the non–linear self–duality relations (4.29) in the local tangent frame. They are

$$\tilde{G} = \frac{1}{\sqrt{-\det g_{\mu\nu}}} \frac{\partial \mathcal{L}_{M5}}{\partial G}, \quad \tilde{F}_i^a = \frac{1}{\sqrt{-\det g_{\mu\nu}}} \frac{\partial \mathcal{L}_{M5}}{\partial F_a^i}. \quad (4.64)$$

The advantage of the local tangent frame is that it allows us to use Mathematica to check the non–linear self–duality relations. We first check that the non–linear self–duality

relations obtained from the M5–brane action is equivalent to those obtained from the superembedding approach. To give some insights, we first present several special cases, and then proceed to explain the full check. In addition to this check, we also need to check that the condition (4.43) is satisfied.

### Self–duality relations in particular cases

To guess the form (4.63) of the function  $\mathcal{L}_{M5}$  in the M5-brane action we first consider a number of simple cases.

#### $f = 0$ case

The relations (4.56)–(4.60) reduce to

$$F_i^a = \tilde{F}_i^a = 0, \quad Q = 1 - 16g^4,$$

$$\frac{1}{4}G = \frac{g + 4g^3}{1 - 16g^4} = \frac{g}{1 - 4g^2}, \quad (4.65)$$

$$\frac{1}{4}\tilde{G} = \frac{g - 4g^3}{1 - 16g^4} = \frac{g}{1 + 4g^2}. \quad (4.66)$$

We now solve eq. (4.65) for  $g$

$$g = \frac{\pm\sqrt{1 + G^2} - 1}{2G}. \quad (4.67)$$

Since, due to (4.65), in the linear approximation  $G/4 = g$ , we should pick up only the solution with the upper sign. Substituting this solution into (4.66) we get the relation between  $\tilde{G}$  and  $G$

$$\tilde{G} = \frac{G}{\sqrt{1 + G^2}} = \frac{\partial\sqrt{1 + G^2}}{\partial G}. \quad (4.68)$$

We see that eq. (4.68) is exactly the same as (4.64) when in (4.63) we put  $F_i^a = 0 = F_{\mu\nu\rho}$ . This demonstrates how the (square root of) factor  $1 + G^2$  appears in the function  $\mathcal{L}_{M5}(F, G)$  (4.20) or (4.63) of the M5–brane action (4.19).

#### $g = \det f = 0$ case

Now the relations (4.56)–(4.60) reduce to

$$G = \tilde{G} = 0, \quad Q = 1 + 16(\text{tr} f^2)^2 - 32\text{tr} f^4,$$

$$\frac{1}{4}F_i^a = Q^{-1} (f(1 - 4\text{tr}f^2) + 8f^3)_i^a = Q^{-1} \frac{\partial}{\partial f_a^i} \left( \frac{1}{2}\text{tr}f^2 - \frac{1}{16}Q \right), \quad (4.69)$$

$$\frac{1}{4}\tilde{F}_i^a = Q^{-1} (f(1 + 4\text{tr}f^2) - 8f^3)_i^a = Q^{-1} \frac{\partial}{\partial f_a^i} \left( \frac{1}{2}\text{tr}f^2 + \frac{1}{16}Q \right), \quad (4.70)$$

Let us simplify things even further by considering a solution of the non-linear self-duality equation such that the only non-zero components of  $f_i^a$  are  $f_i^1$ . Then the above equations further reduce to

$$G = \tilde{G} = 0, \quad Q = 1 - 16(f^2)^2, \quad f^2 \equiv f_i^1 f_i^1,$$

$$\frac{1}{4}F_i^1 = Q^{-1} (1 + 4f^2) f_i^1 = \frac{f_i^1}{1 - 4f^2}, \quad (4.71)$$

$$\frac{1}{4}\tilde{F}_i^1 = \frac{f_i^1}{1 + 4f^2}, \quad (4.72)$$

From these equations we find that

$$1 - 4f^2 = -\frac{2(1 \mp \sqrt{1 + F^2})}{F^2}, \quad 1 + 4f^2 = \frac{2\sqrt{1 + F^2}}{F^2} (\sqrt{1 + F^2} \mp 1),$$

$$f_i^1 = \frac{F_i^1}{2F^2} (\pm \sqrt{1 + F^2} - 1).$$

Since, due to (4.71), in the linear approximation  $F_i^a/4 = f_i^a$ , in the above relation we should pick the upper sign and upon substituting it into (4.70) we get the duality relation

$$\tilde{F}_i^1 = \frac{F_i^1}{\sqrt{1 + F^2}} = \frac{\partial \sqrt{1 + F^2}}{\partial F_1^i}. \quad (4.73)$$

We see that this relation coincides with (4.64) for  $G = 0$  and  $F_i^a$  having only the non-zero components  $F_i^1$ .

### Self-dual string soliton ( $g \neq 0, \det f = 0$ case)

Let us now consider a more complicated particular case of a string soliton solution of [71]. A similar consideration is applicable to the BPS self-dual string of [123]. For the string aligned along the  $x^2$ -coordinate, in terms of fields (4.54) and (4.55) the string soliton solution of [71] has the following form:

$$G = -\frac{\beta x^1}{\rho^4}, \quad F_1^k = -\frac{\beta x^k}{\rho^4}, \quad (4.74)$$

$$\tilde{G} = -\frac{\alpha' x^1}{\rho}, \quad \tilde{F}_1^k = -\frac{\alpha' x^k}{\rho}. \quad (4.75)$$

where  $k = 3, 4, 5$ ,  $\rho := \sqrt{x_1^2 + x_3^2 + x_4^2 + x_5^2}$ ,  $\beta$  is a constant and

$$\alpha'(\rho) = \frac{\beta}{\sqrt{\beta^2 + \rho^6}}. \quad (4.76)$$

In this form the string soliton solution was considered in [3]. It naturally splits the 6d worldvolume into 3+3 directions.

The form (4.74) of  $G$  and  $F$  suggests that in (4.56) and (4.57)  $g \neq 0$  and the non-zero components of  $f_i^a$  are  $f_i^1$ . So the equations (4.56)–(4.60) reduce to

$$Q = 1 - 16(g^2 + f^2)^2. \quad (4.77)$$

$$\frac{1}{4}F_i^1 = \frac{f_i^1}{1 - 4(g^2 + f^2)}, \quad \frac{1}{4}G = \frac{g}{1 - 4(g^2 + f^2)}, \quad (4.78)$$

and

$$\frac{1}{4}\tilde{F}_i^1 = \frac{f_i^1}{1 + 4(g^2 + f^2)}, \quad \frac{1}{4}\tilde{G} = \frac{g}{1 + 4(g^2 + f^2)}. \quad (4.79)$$

Carrying out the same analysis as in the previous examples, from (4.77)–(4.79) we get the duality relations

$$\tilde{F}_i^1 = \frac{F_i^1}{\sqrt{1 + G^2 + F^2}} = \frac{\partial\sqrt{1 + G^2 + F^2}}{\partial F_1^i}, \quad \tilde{G} = \frac{G}{\sqrt{1 + G^2 + F^2}} = \frac{\partial\sqrt{1 + G^2 + F^2}}{\partial G} \quad (4.80)$$

which are again a particular case of (4.64). One can then guess that in the manifestly covariant formulation the expression under the square root combines into the determinant of the matrix formed by the bilinear combinations of  $G_{\mu\nu\rho}$  and  $F_{\mu\nu\rho}$  as in eq. (4.20) or (4.63).

To see that this is indeed so and that (4.63) should also contain the term  $G \det F$  let us consider the case in which  $G = 0$  while  $F_i^a$  is (otherwise) generic.

**$G = 0$  case**

We have

$$G = 0 = (g + 4g^3 + 4g\text{tr}f^2 - 8\det f), \quad (4.81)$$

$$\frac{1}{4}\tilde{G} = 2Q^{-1}g, \quad (4.82)$$

$$\begin{aligned} Q &= 1 - 16g^4 + 16(\text{tr}f^2)^2 - 32g^2\text{tr}f^2 - 32\text{tr}f^4 + 128g\det f \\ &= 1 + 16g^2 + 16(\text{tr}f^2)^2 + 48g^4 + 32g^2\text{tr}f^2 - 32\text{tr}f^4, \end{aligned} \quad (4.83)$$

$$\frac{1}{4}F_i^a = Q^{-1} (f(1 + 4g^2 - 4\text{tr}f^2) + 8f^3 - 8gf^{-1}\det f)_i^a \quad (4.84)$$

and

$$\frac{1}{4}\tilde{F}_i^a = Q^{-1} (f(1 - 4g^2 + 4\text{tr}f^2) - 8f^3 + 8gf^{-1} \det f)_i^a. \quad (4.85)$$

Now, the direct computation of  $\det F$  using (4.84) and (4.81) gives (see also eq. (4.107) of the Appendix)

$$\det F = 8Q^{-1}g. \quad (4.86)$$

Comparing this equation with (4.82) we get

$$\tilde{G} = \det F, \quad (4.87)$$

which is exactly the relation that we get by varying the term (4.63) of the M5-brane action (4.19) or (4.62) with respect to  $G$  and setting  $G = 0$  afterwards. This explains the appearance of the term  $G \det F$  in the M5–brane action.

On the other hand, upon expressing the right–hand side of (4.85) in terms of  $F_i^a$  and performing somewhat lengthy computations using Mathematica one gets the duality relation for  $\tilde{F}$  which coincides with eq. (4.64) evaluated at  $G = 0$ .

Finally, by a direct check using Mathematica one can verify that also in the generic case the components  $F$ ,  $\tilde{F}$ ,  $G$  and  $\tilde{G}$  of the field strength  $H_3$  determined by the superembedding relations (4.56)–(4.60) satisfy the non–linear duality relations (4.64) which follow from the M5–brane action (4.19). Main steps of the calculation are described in the Appendix.

The last point that one should check is that the function (4.20) satisfies eq. (4.43) which insures the invariance of the M5–brane action under the local transformations (4.25). The direct calculation shows that this is indeed so. Actually, (4.20) satisfies even stronger relation, namely, it makes to vanish the expression under the derivative in (4.43).

## 4.4 Comparison of the two M5–brane actions

As was discussed in [119] duality symmetric actions corresponding to different splittings of space–time differ from each other by terms that vanish on–shell, *i.e.* when (an appropriate part of) the self–duality relations is satisfied. In [119] this was discussed for the free chiral 2–form in  $6d$ .

We shall now confront the two M5–brane actions (4.7) and (4.19) by comparing their values for the 3–form field strength satisfying the non–linear self–duality equation. As we have seen, the non–linear self–duality relations that follow from these actions are similar and are equivalent to the self–duality condition that follows from the superembedding

formulation. Therefore, to compute the on-shell values of the  $M5$ -brane actions we will substitute into them the expressions of the components of  $H_3$  and  $\tilde{H}_3$  in terms of the components of the self-dual tensor  $h_3$ .

In the case of the novel action these are eqs. (4.56)–(4.59). Substituting them into the action (4.19) (or (4.62)) and using Mathematica we find that the on-shell value of the self-dual  $M5$ -brane action is

$$S_{M5}^{\text{on-shell}} = 4 \int d^6x \sqrt{-\det g_{\mu\nu}} Q^{-1} - \int_{\mathcal{M}_6} (C_6 + H \wedge C_3). \quad (4.88)$$

Notice that the Lagrangian of this action is the functional of  $Q(h)$  defined in (4.46). We thus see that the on-shell action is manifestly  $6d$  covariant and does not depend on the auxiliary fields  $a^r(x)$  (4.16).

To compute the corresponding on-shell value of the original  $M5$ -brane action (4.7) we perform the  $1+5$  splitting of the duality relations (4.44) which take the following form

$$\tilde{H}_{\hat{a}\hat{b}\hat{5}} = 4Q^{-1} \left( (1 - 2\text{tr}\bar{f}^2)\bar{f} + 8\bar{f}^3 \right)_{\hat{a}\hat{b}\hat{5}}, \quad H_{\hat{a}\hat{b}\hat{5}} = 4Q^{-1} \left( (1 + 2\text{tr}\bar{f}^2)\bar{f} - 8\bar{f}^3 \right)_{\hat{a}\hat{b}\hat{5}},$$

where  $\bar{f}_{\hat{a}\hat{b}} = h_{\hat{a}\hat{b}\hat{5}}$  and  $\hat{a}, \hat{b} = 0, 1, 2, 3, 4$ . Upon substituting the above expressions into the action (4.7) we find that its value is again given by eq. (4.88). Thus the two forms of the  $M5$ -brane action give rise to the same equations of motion and their on-shell values are equal and are given by the superembedding scalar function  $Q(h)$ . For the self-dual string soliton considered in Section 4.3.1, the value of the action determines the tension of the string, as was discussed in [71].

An interesting open problem that may have important consequences for the issue of quantisation of the self-dual fields is the understanding of the off-shell relationship between the different self-dual actions.

## 4.5 Relation to $M2$ -branes

The new form of the  $M5$ -brane action can be useful for studying its relation to the Nambu–Poisson description of the  $M5$ -brane in a constant  $C_3$  field originated from the  $3d$  BLG model with the gauge group of volume preserving diffeomorphisms [66,78]. The BLG model invariant under the volume preserving diffeomorphisms describes a condensate of  $M2$ -branes which via a Myers effect may grow into an  $M5$ -brane. In [66,78] it was conjectured that the Nambu–Poisson  $M5$ -brane model is related to the conventional description of the  $M5$ -brane in a constant  $C$ -field background through a transformation analogous to the Seiberg–Witten map [116]. Such a map between the fields and gauge transformations of

the two models was constructed in [115], however the relation between the two actions still remains to be established. We leave the study of this issue for future and will only show that in a flat background without C–field the worldvolume dimensional reduction of the bosonic M5–brane action (4.19) (or (4.62)) directly results in the membrane action. To this end we fix the  $6d$  worldvolume diffeomorphisms by imposing the static gauge

$$x^\mu = X^\mu, \quad X^I(x^\mu) \quad I = 6, 7, 8, 9, 10$$

where  $X^I(x)$  are five physical scalar fields corresponding to the target–space directions transversal to the M5–brane worldvolume. We perform the dimensional reduction of three worldvolume directions  $x^i$  ( $i = 3, 4, 5$ ) assuming that the scalar fields  $X^I$  and the chiral tensor field  $B_{\mu\nu}$  only depend on the three un–compactified coordinates  $x^a$  and not on  $x^i$ . Then the induced worldvolume metric takes the form

$$g_{\mu\nu} = (\eta_{ab} + \partial_a X^I \partial_b X^I, \delta_{ij}), \quad g_{ai} = 0. \quad (4.89)$$

We use the local gauge symmetry (4.25) to fix the values of the three auxiliary scalars  $a^r(x)$  in such a way that the projectors (4.16) take the form

$$P_\mu{}^\nu = \delta_\mu^a \delta_a^\nu, \quad \Pi_\mu{}^\nu = \delta_\mu^i \delta_i^\nu. \quad (4.90)$$

Then the components  $G_{\mu\nu\rho}$  (4.21) of the gauge field strength vanish and  $F_{\mu\nu\rho}$  reduce to

$$F_{aij} = \partial_a B_{ij} \quad \Rightarrow \quad F_a^i = \frac{1}{2} \epsilon^{ijk} F_{ajk} = \partial_a \tilde{X}^i, \quad (4.91)$$

where the dualised components of the gauge field  $B_{ij}(x^a)$

$$\tilde{X}^i \equiv \frac{1}{2} \epsilon^{ijk} B_{jk}$$

play the role of the additional three scalar fluctuations of the membrane associated with  $D = 11$  target–space directions orthogonal to the membrane worldvolume. Indeed, upon the dimensional reduction the M5 brane action (4.62) becomes

$$S_{M2} = \int d^3x \sqrt{-\det(\eta_{ab} + \partial_a X^I \partial_b X^I + \partial_a \tilde{X}^i \partial_b \tilde{X}^i)}, \quad (4.92)$$

which is the action for a membrane in flat  $D = 11$  space–time in the static gauge.

## 4.6 Discussions

Using the non–linear self–duality equation for the 3–form gauge field strength arising in the superembedding description of the M5–brane we have derived a novel form of the kappa–symmetric M5–brane action with a covariant 3+3 splitting of its  $6d$  worldvolume.

The value of this action on the mass–shell of the non–linear self–dual gauge field coincides with the on–shell value of the original M5–brane action expressed in terms of the  $6d$  scalar function  $Q$  of the self–dual chiral field  $h_3$  appearing in the superembedding description of the M5–brane. It would be interesting and important to better understand the off–shell relation between the two actions.

Having at hand the M5–brane action in the form (4.19), (4.20) one can repeat the steps of [124] towards understanding the link of this action to the Nambu–Poisson 5–brane of [66, 78] by restricting the worldvolume pullback of the 11D gauge field  $C_3$  to be constant and by partial gauge fixing local symmetries of (4.19), (4.20) to a group of  $3d$  volume preserving diffeomorphisms. The Seiberg–Witten–like map constructed in [115] may be need to relate the fields of the two models. It would be also of interest to relate our construction to a noncommutative M5–brane of [125].

The novel form of the action is also naturally suitable for studying the effective theory of the M5–brane wrapping a  $3d$  compact Riemann–manifold.

As another direction of study, one may try, using the superembedding form of the self–duality relation, to construct an M5–brane action in the form which exhibits 2+4 splitting of the  $6d$  worldvolume which may be useful for studying  $M5$ –branes wrapping  $2d$  and  $4d$  manifolds, and M5–brane instantons wrapping  $4d$  divisors of Calabi–Yau 4–folds in  $M_3 \times CY_4$  compactifications of M–theory as discussed e.g. in [126–131].

## **4.A Exact check of the M5–brane action non–linear self–duality from superembedding**

To check the form of (4.20) (or, equivalently, (4.63)), using the superembedding relations (4.56)–(4.59) we should verify that

$$\tilde{G}(f, g) = 4Q^{-1} (g - 4g^3 - 4g\text{tr}f^2 + 8 \det f) = \frac{1}{\sqrt{-\det g_{\mu\nu}}} \frac{\partial \mathcal{L}_{M5}}{\partial G} (F(f, g), G(f, g)), \quad (4.93)$$

and

$$\begin{aligned} \tilde{F}(f, g) &= 4Q^{-1} (f(1 - 4g^2 + 4\text{tr}f^2) - 8f^3 + 8gf^{-1} \det f) \\ &= \frac{1}{\sqrt{-\det g_{\mu\nu}}} \frac{\partial \mathcal{L}_{M5}}{\partial F} (F(f, g), G(f, g)). \end{aligned} \quad (4.94)$$

To verify the above relations, on their right hand sides we should take  $G$ – and  $F$ –derivatives of  $\mathcal{L}_{M5}$  in the form (4.63), substitute into the results the expressions (4.56) and (4.57) for  $F$  and  $G$  in terms of  $f$  and  $g$ , and to see that they coincide with the left hand sides of

(4.93) and (4.94), i.e. with  $\tilde{G}$  and  $\tilde{F}$  expressed in terms of  $f$  and  $g$ . In particular, we will need to express  $\text{tr}(F^2)$ ,  $\text{tr}(F^4)$  and  $\det(F)$  in terms of  $f$  and  $g$ .

The algebra is very involved but it is manageable systematically by Mathematica. To this end we used NCAAlgebra package which is found in <http://math.ucsd.edu/~ncalg/>.

#### 4.A.1 Matrix Notation

To use Mathematica we should properly define the matrices we deal with. Let  $F_a^i$  be the components of the matrix  $F$ ,  $\eta_{ab}$  or  $\eta^{ab}$  be the components of the matrix  $\eta$  and  $\delta_{ij}$  or  $\delta^{ij}$  be the component of the matrix  $\delta$ . It will be clear from the context whether the indices of  $\eta$  and  $\delta$  are up or down. To simplify the notation, we drop  $\delta$  from all the matrix expressions.

For example,  $F_a^j \delta_{jk} F_b^k \eta^{bc} F_c^i$  is denoted as  $F \delta F^T \eta F$  or just  $F F^T \eta F$ . This expression is what in previous sections we simply referred to as  $F^3$ .

The inverse matrix  $F^{-1}$  has the components  $(F^{-1})_i^a$ . We will, actually, encounter the adjugate matrix  $\text{adj}(F)$  and the cofactor matrix  $\text{co}(F) \equiv \text{adj}(F)^T$  more often than  $F^{-1}$  and  $(F^{-1})^T$ . The definition of  $\text{adj}(F)$  is

$$\text{adj}(F)_i^a \equiv (F^{-1})_i^a \det F = \frac{1}{2} \epsilon_{ijk} \epsilon^{abc} F_b^j F_c^k, \quad (4.95)$$

where

$$\det F \equiv \frac{1}{6} \epsilon_{ijk} \epsilon^{abc} F_a^i F_b^j F_c^k. \quad (4.96)$$

In the matrix form, the equation (4.56) reads

$$F = 4Q^{-1} (f(1 + 4g^2 - 4\text{tr}(f^T \eta f)) + 8ff^T \eta f - 8g \eta \text{co}(f)) \quad (4.97)$$

its transpose is given by

$$F^T = 4Q^{-1} (f^T(1 + 4g^2 - 4\text{tr}(f^T \eta f)) + 8f^T \eta f f^T - 8g \text{adj}(f) \eta). \quad (4.98)$$

and

$$Q = 1 - 16g^4 + 128g \det(f) - 32g^2 \text{tr}(f^T \eta f) + 16(\text{tr}(f^T \eta f))^2 - 32\text{tr}(f^T \eta f f^T \eta f). \quad (4.99)$$

We are ready to discuss the computation of the expressions  $\text{tr}(F^2) \equiv \text{tr} F^T \eta F$ ,  $\text{tr}(F^4) \equiv \text{tr} F^T \eta F F^T \eta F$  and  $\det(F)$  in terms of  $f$  and  $g$ .

#### 4.A.2 Outline of computation

To compute  $F^T \eta F$ , the following identities are useful to simplify the results:

$$\eta^2 = 1, \quad (4.100)$$

$$f \operatorname{adj}(f) = \operatorname{adj}(f)f = \det f, \quad f^T \operatorname{co}(f) = \operatorname{co}(f)f^T = \det f, \quad (4.101)$$

$$\begin{aligned} \operatorname{adj}(f)\eta\operatorname{co}(f) &= -(f^T\eta f)^{-1} \det(f^T\eta f) = -\operatorname{adj}(f^T\eta f) \\ &= -(f^T\eta f)^2 + \operatorname{tr}(f^T\eta f)f^T\eta f - \frac{1}{2}[(\operatorname{tr}(f^T\eta f))^2 - \operatorname{tr}((f^T\eta f)^2)], \end{aligned} \quad (4.102)$$

where in the last equality we used the Cayley–Hamilton formula for  $3 \times 3$  matrices. We also need the Cayley-Hamilton formula of the form

$$(f^T\eta f)^3 = \operatorname{tr}(f^T\eta f)(f^T\eta f)^2 - \frac{1}{2}[(\operatorname{tr}(f^T\eta f))^2 - \operatorname{tr}((f^T\eta f)^2)]f^T\eta f - (\det f)^2. \quad (4.103)$$

Using these formulas one can see that each term in the expression for  $F^T\eta F$  is proportional to either

$$1, \quad \text{or} \quad f^T\eta f, \quad \text{or} \quad (f^T\eta f)^2. \quad (4.104)$$

Therefore,

$$\begin{aligned} \frac{\operatorname{tr}(F^2)}{16Q^{-2}} &= \operatorname{tr}(f^2) + \left( -48g \det(f) + 16\operatorname{tr}(f^4) + 8g^2\operatorname{tr}(f^2) - 8(\operatorname{tr}f^2)^2 \right) \\ &\quad + \left( 64g \det(f)\operatorname{tr}(f^2) - 192g^3 \det(f) - 192(\det f)^2 + 96g^2\operatorname{tr}(f^4) + 16g^4\operatorname{tr}(f^2) \right. \\ &\quad \left. - 64g^2(\operatorname{tr}f^2)^2 - 16(\operatorname{tr}f^2)^3 + 32\operatorname{tr}(f^2)\operatorname{tr}(f^4) \right), \end{aligned} \quad (4.105)$$

where  $\operatorname{tr}(f^2)$  and  $\operatorname{tr}(f^4)$  are shorthand for  $\operatorname{tr}(f^T\eta f)$  and  $\operatorname{tr}((f^T\eta f)^2)$ .

We compute  $\operatorname{tr}(F^4)$  and  $\operatorname{tr}(F^6) \equiv \operatorname{tr}((F^T\eta F)^3)$  using the same method. We finally trade  $\operatorname{tr}(F^6)$  with  $\det F$  using the Cayley–Hamilton formula

$$\det F = \sqrt{-\frac{1}{6}(\operatorname{tr}(F^2)^3 - 3\operatorname{tr}(F^4)\operatorname{tr}(F^2) + 2\operatorname{tr}(F^6))} \quad (4.106)$$

The explicit expression for  $\det F$  in terms of  $f$  and  $g$  looks as follows

$$\begin{aligned} \frac{1}{64}Q^3 \det(F) &= \det(f) + 12g^2 \det(f) + 48g^4 \det(f) + 64g^6 \det(f) + 192g \det(f)^2 \\ &\quad + 1280g^3 \det(f)^2 - 512 \det(f)^3 - 4 \det(f)\operatorname{tr}(f^2) - 96g^2 \det(f)\operatorname{tr}(f^2) \\ &\quad - 320g^4 \det(f)\operatorname{tr}(f^2) + 256g \det(f)^2\operatorname{tr}(f^2) + 4g(\operatorname{tr}f^2)^2 + 32g^3(\operatorname{tr}f^2)^2 \\ &\quad + 64g^5(\operatorname{tr}f^2)^2 + 16 \det(f)(\operatorname{tr}f^2)^2 + 320g^2 \det(f)(\operatorname{tr}f^2)^2 - 64 \det(f)(\operatorname{tr}f^2)^3 \\ &\quad + 64g(\operatorname{tr}f^2)^4 - 4g\operatorname{tr}(f^4) - 32g^3\operatorname{tr}(f^4) - 64g^5\operatorname{tr}(f^4) - 32 \det(f)\operatorname{tr}(f^4) \\ &\quad - 640g^2 \det(f)\operatorname{tr}(f^4) + 128 \det(f)\operatorname{tr}(f^2)\operatorname{tr}(f^4) - 192g(\operatorname{tr}f^2)^2\operatorname{tr}(f^4) \\ &\quad + 128g(\operatorname{tr}f^4)^2, \end{aligned} \quad (4.107)$$

We can now compute the expression in terms of  $f$  and  $g$  of the term in (4.63) containing the square root

$$\begin{aligned} & \sqrt{1 - \frac{\det(F^2)}{(1+G^2)^2} + (G^2 + \text{tr}(F^2)) + \frac{1}{2} \frac{((\text{tr}F^2)^2 - \text{tr}(F^4))}{1+G^2}} \\ &= Q^{-3}(1+G^2)^{-1} \sqrt{\left(\sum_{n=0}^{12} a_n(f)g^n\right)^2}, \end{aligned} \quad (4.108)$$

where the argument of the square root in the last line, which turns out to form a perfect square, is a polynomial in  $g$  with coefficients  $a_n(f)$  depending on  $\text{tr}(f^2)$ ,  $\text{tr}(f^4)$  and  $\det(f)$ . The form of these coefficients is rather cumbersome, and we do not give it here. Using the above expressions we can then check that (4.93) indeed holds.

We now pass to the check of (4.94). In the matrix form it reads

$$\tilde{F} = 4Q^{-1} (f(1 - 4g^2 + 4\text{tr}f^2) - 8ff^T\eta f + 8g\eta \text{co}(f)) = \frac{1}{\sqrt{-\det g_{\mu\nu}}} \eta \frac{\partial \mathcal{L}_{M5}}{\partial F^T}. \quad (4.109)$$

This is a matrix equation, and we need to compute  $F$ ,  $FF^T\eta F$ , and  $\eta \text{co}(F)$ . To do this, we proceed as above and compute  $F$ ,  $FF^T\eta F$  and  $FF^T\eta FF^T\eta F$  and then trade  $FF^T\eta FF^T\eta F$  with  $\eta \text{co}(F)$  using the relation

$$\eta \text{co}(F) = - \frac{(FF^T\eta FF^T\eta F + \frac{1}{2}F((\text{tr}F^2)^2 - \text{tr}(F^4)) - \text{tr}(F^2)FF^T\eta F)}{\det F}. \quad (4.110)$$

In the final result, the matrices  $F$ ,  $FF^T\eta F$  and  $\eta \text{co}(F)$  are expressed in terms of  $g$ ,  $f$ ,  $ff^T\eta f$ , and  $\eta \text{co}(f)$ . We can then substitute these into  $\partial \mathcal{L}_{M5}/(\sqrt{-\det g_{\mu\nu}}\partial F)$  which is given by

$$\frac{1}{\sqrt{-\det g_{\mu\nu}}} \eta \frac{\partial \mathcal{L}_{M5}}{\partial F^T} = \frac{G\eta \text{co}(F)}{(1+G^2)} + \frac{-\frac{\det(F)\eta \text{co}(F)}{(1+G^2)^2} + \frac{(F\text{tr}(F^2) - FF^T\eta F)}{1+G^2} + F}{\sqrt{1 - \frac{\det(F^2)}{(1+G^2)^2} + (G^2 + \text{tr}(F^2)) + \frac{1}{2} \frac{((\text{tr}F^2)^2 - \text{tr}(F^4))}{1+G^2}}}, \quad (4.111)$$

and check that eq. (4.94) does hold.

## Chapter 5

# Non-Abelian Self-Dual String Solutions

This chapter is mostly based on [3, 4]

In this final topic, we discuss a solution of coincident M5-branes. Although, as discussed in the introduction, there is still no complete description of coincident M5-branes, we can still analyse BPS solutions of the model; in order to obtain BPS equations, we do not need to know the complete model.

Motivated by the analysis in [132, 133], a theory of non-abelian chiral 2-form in 6-dimensions was constructed [87]. The theory admits a self-duality equation on the field strength as the equation of motion. It has a modified 6d Lorentz symmetry. On dimensional reduction on a circle, the action gives the standard 5d Yang-Mills action plus higher order corrections. Based on these properties, it was proposed that the theory describes the gauge sector of multiple M5-branes in flat space. In this theory the self-interaction of the two-form gauge field is mediated by a set of five-dimensional non-propagating Yang-Mills gauge field. In the Abelian case, the 1-form gauge field is free and simply decouples.

We give a further support of this proposal by constructing the non-abelian self-dual strings to the equation of motion of the non-abelian theory [132]. We first observe that an auxiliary 1-form gauge field of the Perry-Schwarz solution [71] is based on a Dirac monopole. This suggests that the non-abelian self-dual string solution may be constructed by taking the auxiliary Yang-Mills gauge field to be given by a non-abelian monopole. Indeed, we are able to construct an  $SU(2)$  self-dual string solution both for uncompactified six dimensions as well as with one dimension compactified. Our solution is obtained by replacing the Dirac monopole in the Perry-Schwarz string, in the uncompactified case to

the non-abelian Wu-Yang monopole; and in the compactified case to the 't Hooft-Polyakov monopole. Our solutions can be interpreted as two M5-branes intersecting with a single M2-brane.

We then consider the case of an arbitrary number  $N_5$  of M5-branes and construct a self-dual string solution with  $N_2$  unit of self-dual charges. This solution is supported by an auxiliary Yang-Mills gauge field which is a charge  $N_2$  monopole solution. We will work out the dependence on  $N_2$  and  $N_5$  in the radius-transverse distance relation describing the M2-branes spike, and show that it agrees with the supergravity description of an intersecting M2-M5 branes system. Therefore our results provide further support of the model of [87].

In section 5.1, we review the non-abelian 5-brane theory of [87]. In section 5.2, after reviewing the original Perry-Schwarz self-dual string solution, we present a new abelian self-dual string solution which is orientated in a different direction. The existence of the latter solution is guaranteed by the Lorentz symmetry of the Perry-Schwarz theory. Then we solve the non-abelian equation of motion of [87] and obtain an exact solution describing a string. We then discuss how this solution can be lifted as a solution of the (2,0) supersymmetric theory. The resulting solution describes a non-abelian string with self-dual charges. In section 5.3, we consider the compactified case and construct the corresponding self-dual string solution. In section 5.4, we discuss the case of an arbitrary number of M5-branes with self-dual string of arbitrary charge. This chapter is concluded with some further comments and discussions in section 5.5.

## 5.1 Review of the Non-Abelian Multiple 5-brane Theory

In [87], an action for non-abelian chiral 2-form in 6-dimensions was constructed as a generalisation of the linear theory of Perry-Schwarz. As in Perry-Schwarz, manifest 6d Lorentz symmetry was given up and the self-dual tensor gauge field is represented by a  $5 \times 5$  antisymmetric field  $B_{\mu\nu}$ ,  $\mu, \nu = 0, \dots, 4$ . Throughout this chapter we use the convention that the 5d and 6d coordinates are denoted by  $x^\mu = (x^0, x^1, \dots, x^4)$  and  $x^M = (x^\mu, x^5)$ . We use  $\eta^{MN} = (-++++)$  for the metric and  $\epsilon^{01234} = -\epsilon_{01234} = 1$ ,  $\epsilon^{012345} = -\epsilon_{012345} = 1$  for the antisymmetric tensors. The Hodge dual of a 3-form  $G_{MNP}$  is defined by

$$\tilde{G}_{MNP} := -\frac{1}{6}\epsilon_{MNPQRS}G^{QRS}. \quad (5.1)$$

Motivated by the consideration in [133], a set of 5d 1-form gauge fields  $A_\mu^a$  was introduced for a gauge group  $G$ . The proposed action is

$$S = S_0 + S_E \quad (5.2)$$

with  $S_0$  a non-abelian generalisation of the Perry-Schwarz action,

$$S_0 = \frac{1}{2} \int d^6x \operatorname{tr} \left( -\tilde{H}^{\mu\nu} \tilde{H}_{\mu\nu} + \tilde{H}^{\mu\nu} \partial_5 B_{\mu\nu} \right) \quad (5.3)$$

where  $H_{\mu\nu\lambda} = 3D_{[\mu} B_{\nu\lambda]} = 3[\partial_{[\mu} + A_{[\mu}, B_{\nu\lambda]}]$ ; and with  $S_E$

$$S_E = \int d^5x \operatorname{tr} \left( (F_{\mu\nu} - c \int dx_5 \tilde{H}_{\mu\nu}) E^{\mu\nu} \right), \quad (5.4)$$

where  $E_{\mu\nu}(x^\lambda)$  is a 5d auxiliary field, providing a constraint such that  $A_\mu$  carries no extra degrees of freedom. Here  $c$  is a constant and it was taken to be 1 in [87]. Actually one can take any nonzero value of  $c$  and this makes no change to all the symmetries discussed in [87]. The only modification is the relation of the Yang-Mills coupling to the compactification radius,  $g_{YM}^2 = \pi R c^2$ . In the following we will show how the value of  $c$  is fixed by the requirement of charge quantisation of our self-dual string solution.

Besides the Yang-Mills gauge symmetry,

$$\delta A_\mu = \partial_\mu \Lambda + [A_\mu, \Lambda], \quad \delta B_{\mu\nu} = [B_{\mu\nu}, \Lambda], \quad \delta E_{\mu\nu} = [E_{\mu\nu}, \Lambda] \quad (5.5)$$

for arbitrary  $\Lambda = \Lambda(x^\lambda)$ , the action has the tensor gauge symmetry

$$\delta_T A_\mu = 0, \quad \delta_T B_{\mu\nu} = \Sigma_{\mu\nu}, \quad \delta_T E_{\mu\nu} = 0, \quad (5.6)$$

for  $\Sigma_{\mu\nu}(x^M)$  satisfying  $D_{[\lambda} \Sigma_{\mu\nu]} = 0$ . This form of symmetry first appears in [85]. As demonstrated in [87], the theory has manifest 5d Lorentz symmetry and a modified 6d Lorentz symmetry. To establish those symmetries of the action, one takes the field configuration satisfying the boundary conditions:

$$D_\lambda B_{\mu\nu}, \quad \partial_5 B_{\mu\nu} \rightarrow 0 \quad \text{as } |x^M| \rightarrow \infty. \quad (5.7)$$

With an appropriate fixing of this tensor gauge symmetry, one can turn the equation of motion of  $B_{\mu\nu}$  into a first order self-duality condition:

$$\tilde{H}_{\mu\nu} = \partial_5 B_{\mu\nu}. \quad (5.8)$$

The gauge field is auxiliary and is determined by the equation:

$$F_{\mu\nu} = c \int dx_5 \tilde{H}_{\mu\nu}. \quad (5.9)$$

This constraint was inspired from the analysis of the dimensional reduction, in which one gets multiple D4-branes plus higher derivative correction terms. Notice that, on mass-shell, the constraint (5.9) simply says that  $F_{\mu\nu}$  is given by the boundary values of  $B_{\mu\nu}$  for the uncompactified case:

$$F_{\mu\nu} = c(B_{\mu\nu}(x_5 = \infty) - B_{\mu\nu}(x_5 = -\infty)), \quad (5.10)$$

and

$$F_{\mu\nu} = 2\pi R c \tilde{H}_{\mu\nu}^{(0)}, \quad (5.11)$$

when  $x^5$  is compactified on a circle of radius  $R$ . Here  $\tilde{H}_{\mu\nu}^{(0)}$  is the zero mode part of the field strength.

## 5.2 Non-Abelian Self-Dual String Solution: Uncompactified Case

In this section, we construct self-dual string solution that satisfies both (5.8) and (5.10). As mentioned above, a direct observation on the constraint (5.10) shows that the solution cannot be aligned in the  $x^5$  direction since this would imply  $F_{\mu\nu} = 0$  which is trivial. This does not imply the non-existence of a string solution in other directions, because the self-duality equation (5.8) has only 5d Lorentz symmetry as it's a gauge fixed equation of motion [87]. Therefore, as a preparation to constructing the more general non-abelian self-dual string solution, we will first construct an abelian self-dual string solution aligning in the  $x^4$  direction and we will start by reviewing the original abelian self-dual string solution of Perry and Schwarz.

### 5.2.1 Self-dual string solution in the Perry-Schwarz Theory

In [71], a nonlinear theory of chiral 2-form gauge field which results in the Born-Infeld action for a  $U(1)$  gauge field when reduced to 5 dimensions was constructed. The Perry-Schwarz non-linear field equation is given by

$$\tilde{H}_{\mu\nu} = \frac{(1 - y_1)H_{\mu\nu 5} + H_{\mu\rho 5}H^{\rho\sigma 5}H_{\sigma\nu 5}}{\sqrt{1 - y_1 + \frac{1}{2}y_1^2 - y_2}}, \quad (5.12)$$

where

$$y_1 := -\frac{1}{2}H_{\mu\nu 5}H^{\mu\nu 5}, \quad y_2 := \frac{1}{4}H_{\mu\nu 5}H^{\nu\rho 5}H_{\rho\sigma 5}H^{\sigma\mu 5}. \quad (5.13)$$

As they demonstrated, the equation of motion (5.12) admits a solution describing a self-dual string soliton with finite tension aligning in the direction  $x^5$ . Since (5.12) is (non-manifest) 6d Lorentz covariant, it means there must also exist self-dual string solution aligned in other directions. In the following, we review their construction. Then we construct new self-dual string solution aligned in a different direction.

**Self-dual string in the  $x^5$  direction**

The ansatz Perry and Schwarz considered for their self-dual string solution is

$$B = \alpha(\rho) dt dx^5 + \frac{\beta}{8} (\pm 1 - \cos \tilde{\theta}) d\tilde{\phi} d\tilde{\psi}, \quad (5.14)$$

where the 6d metric is

$$ds^2 = -dt^2 + (dx^5)^2 + d\rho^2 + \rho^2 d\Omega_3^2, \quad (5.15)$$

with the three-sphere given in Euler coordinates

$$d\Omega_3^2 = \frac{1}{4} [(d\tilde{\psi} + \cos \tilde{\theta} d\tilde{\phi})^2 + (d\tilde{\theta}^2 + \sin^2 \tilde{\theta} d\tilde{\phi}^2)], \quad (5.16)$$

where  $0 \leq \tilde{\theta} \leq \pi$ ,  $0 \leq \tilde{\phi} \leq 2\pi$ ,  $0 \leq \tilde{\psi} \leq 4\pi$ . For this ansatz, it is  $y_1 = \alpha'^2$ ,  $y_2 = \alpha'^4/2$  and the non-linear field equation (5.12) reads

$$\alpha'(\rho) = \frac{\beta}{\sqrt{\beta^2 + \rho^6}}. \quad (5.17)$$

This can be solved easily in terms of a hyper-geometric function. The solution is regular everywhere where  $\alpha \sim \rho$  as  $\rho \rightarrow 0$ , while  $\alpha \sim -\frac{\beta}{2\rho^2} + \text{const.}$  as  $\rho \rightarrow \infty$ . Note that the same ansatz also solves the linear self-duality equation, where in this case we have,

$$\alpha'(\rho) = \frac{\beta}{\rho^3} \quad (5.18)$$

and the solution is singular at  $\rho = 0$ . In other words, the non-linear terms in the field equation has smoothen out the singularity at  $\rho = 0$ .

The magnetic charge  $P$  and electric charge  $Q$  per unit length of the string are given by

$$P = \int_{S^3} H, \quad Q = \int_{S^3} *H, \quad (5.19)$$

where  $*$  denotes the Hodge dual operation and  $S^3$  is a three sphere surrounding the string. It is straightforward to obtain that

$$P = 2\pi^2\beta, \quad \text{and} \quad Q = 2\pi^2\rho^3\alpha'(\rho)|_{\rho \rightarrow \infty} = 2\pi^2\beta, \quad (5.20)$$

hence the string is self-dual. This holds for both the nonlinear and the linear cases. Note that our answer is  $1/8$  of those in [71] as we have introduced the factor of  $1/4$  into the metric (5.16) in order to reproduce the correct volume  $2\pi^2$  for a unit three sphere.

The charge quantisation condition [27, 28]

$$PQ' + QP' \in 2\pi\mathbf{Z} \quad (5.21)$$

for the self-dual string gives

$$\beta = \pm n \sqrt{\frac{1}{4\pi^3}}, \quad (5.22)$$

i.e.

$$P = Q = \pm n \sqrt{\pi}, \quad (5.23)$$

where  $n$  is a positive integer. Note that the charge quantisation condition we used is different from the Dirac-Teitelboim-Nepomechie charge quantisation condition [24–26] Perry and Schwarz used. The condition (5.21) is obtained with a self-dual string probing another self-dual string and the positive sign in the charge quantisation condition is appropriate for dyonic branes in  $D = 4k + 2$  spacetime dimensions [27, 28].

Perry and Schwarz have also computed the tension of their string solution. Since the solution is static, the energy can be identified with the Lagrangian and the energy per unit length is found to be

$$T = \tilde{c} \beta^{4/3}, \quad (5.24)$$

where  $\tilde{c}$  is a known numerical coefficient. We remark that for the self-dual string solution of the linearised theory, the tension is

$$T = 0 \quad (5.25)$$

since obviously the action vanishes on-shell. Since the charges and tension are well defined, it appears that the singularity at  $\rho = 0$  is not harmful.

We also remark that the Perry-Schwarz self-dual string solution is non-BPS as there is no other matter field turned on to cancel the tensor field force. In the literature, there is also the 1/2 BPS self-dual string of Howe, Lambert and West [123]. In fact the Perry-Schwarz self-duality equation of motion can be embedded in the fully supersymmetric five-brane equation of motion of [69, 122] by setting all the matter fields to zero and hence the Perry-Schwarz self-dual string solution can be lifted to be a solution of the full five-brane equation of motion, albeit a nonsupersymmetric one. Unlike the nonlinear Perry-Schwarz self-dual string solution, the Howe-Lambert-West self-dual string solution is singular at the location of the string. In fact  $B \sim 1/\rho^2$  near the string, which is exactly as in linearised Perry-Schwarz self-dual string solution.

### Self-dual string soliton in the $x^4$ direction

The Perry-Schwarz solution is translationally invariant along  $x^5$ . One may want to generalise this solution directly and construct a non-Abelian self-dual string solution which is

translationally invariant along  $x^5$  but this is not possible. As reviewed above, the gauge field strength in the non-abelian theory is given on-shell by the boundary value of  $B$ -field as (5.10). Therefore, if the non-Abelian solution is translationally invariant along  $x^5$ , then  $F_{\mu\nu} = 0$  which is trivial.

To get a non-trivial solution, we need to base our construction on Perry-Schwarz solitons which are translationally invariant along other direction, say  $x^4$ . Such a solution can be easily obtained by rotating the original Perry-Schwarz solution as Perry and Schwarz has proved that their theory and the non-linear equation (5.12) respect Lorentz symmetry. Therefore, a simple Lorentz transformation which swap  $(x_4, x_5) \rightarrow (-x_5, x_4)$  can be applied on the original Perry-Schwarz solution (the minus sign is needed to preserve the orientation of spacetime) to obtain the desired solution.

To facilitate the discussion, it is more convenient to use the spherical polar coordinates which is related to the Euler coordinates by the change of coordinates

$$\tilde{\theta} = 2\theta, \quad \tilde{\phi} = \psi - \phi, \quad \tilde{\psi} = \psi + \phi. \quad (5.26)$$

With this coordinates, the three-sphere metric is given by

$$d\Omega_3^2 = d\theta^2 + \sin^2 \theta d\phi^2 + \cos^2 \theta d\psi^2 \quad (5.27)$$

with the ranges  $0 \leq \theta \leq \pi/2, 0 \leq \phi, \psi \leq 2\pi$ , and the Perry-Schwarz ansatz (5.14) becomes

$$B = \alpha(\rho) dt dx^5 + \beta \left( \frac{1}{4} \pm \frac{1}{4} - \frac{1}{2} \cos^2 \theta \right) d\phi d\psi. \quad (5.28)$$

Next change to Cartesian coordinates

$$x = \rho \sin \theta \cos \phi, \quad y = \rho \sin \theta \sin \phi, \quad z = \rho \cos \theta \cos \psi, \quad w = \rho \cos \theta \sin \psi, \quad (5.29)$$

where we have denoted  $(x^1, x^2, x^3, x^4) = (x, y, z, w)$ . The metric becomes

$$ds^2 = -dt^2 + dx^2 + dy^2 + dz^2 + dw^2 + d(x^5)^2, \quad (5.30)$$

and the Perry-Schwarz ansatz reads

$$B = \alpha(\rho) dt dx^5 + \beta \frac{\frac{1}{4} \pm \frac{1}{4} - \frac{1}{2} \frac{w^2 + z^2}{\rho^2}}{(x^2 + y^2)(z^2 + w^2)} (xz dy dw - xw dy dz - yz dx dw + yw dx dz). \quad (5.31)$$

Keeping the orientation, we swap  $(x_4, x_5) \rightarrow (-x_5, x_4)$  and obtain our ansatz for a string solution along the  $x^4$  direction,

$$B = \alpha(\rho) dt dw - \beta \frac{\frac{1}{4} \pm \frac{1}{4} - \frac{1}{2} \frac{(x^5)^2 + z^2}{\rho^2}}{(x^2 + y^2)(z^2 + (x^5)^2)} (xz dy dx^5 - x x^5 dy dz - yz dx dx^5 + y x^5 dx dz) \quad (5.32)$$

where now

$$\rho = \sqrt{(x^5)^2 + r^2}, \quad r := \sqrt{x^2 + y^2 + z^2}. \quad (5.33)$$

It follows that

$$H = \frac{\alpha'}{\rho} dt dw (x dx + y dy + z dz + x^5 dx^5) + \frac{\beta}{\rho^4} (x^5 dx dy dz - x dy dz dx^5 + z dy dx dx^5 - y dz dx dx^5), \quad (5.34)$$

$$*H = \frac{\alpha'}{\rho} (x^5 dx dy dz - x dy dz dx^5 + z dy dx dx^5 - y dz dx dx^5) + \frac{\beta}{\rho^4} dt dw (x dx + y dy + z dz + x^5 dx^5), \quad (5.35)$$

and

$$y_1 = \frac{(\alpha')^2 (x^5)^2}{\rho^2} - \frac{\beta^2 r^2}{\rho^8}, \quad y_2 = \frac{\beta^4 r^4}{2\rho^{16}} + \frac{(\alpha')^4 (x^5)^4}{2\rho^4}. \quad (5.36)$$

Then the field equation (5.12) gives

$$\frac{\beta}{\rho^4} x^5 dt dw + \frac{\alpha'}{\rho} (-x dy dz + z dy dx - y dz dx) = \frac{\alpha' x^5}{\rho} G dt dw + \frac{1}{G} \frac{\beta}{\rho^4} (-x dy dz + z dy dx - y dz dx), \quad (5.37)$$

where

$$G = \sqrt{\frac{1 + \beta^2 r^2 \rho^{-8}}{1 - \alpha'^2 (x^5)^2 \rho^{-2}}}. \quad (5.38)$$

The equation (5.37) is equivalent to

$$\alpha' = \frac{\beta}{\sqrt{\beta^2 + \rho^6}}, \quad (5.39)$$

which is the same equation as before. As a consistency check, we integrate over the  $S^3$  transverse to  $x^4$  and obtain the same charges

$$P = Q = 2\pi^2 \beta. \quad (5.40)$$

For the linearised case,  $\alpha' = \beta/\rho^3$ .

### Self-dual string soliton in the $x^4$ direction in the $B_{\mu 5} = 0$ gauge

The potential  $B_{MN}$  in the solution (5.31) or (5.32) does not satisfy the condition  $B_{\mu 5} = 0$  as needed in [71, 87]. However this is not a problem as they are indeed gauge equivalent to one which does. Instead of giving the gauge transformation, it is more instructive to construct directly the linearised self-dual string soliton in the  $x^4$  direction in this gauge.

The starting point is (5.34) with  $\alpha' = \beta/\rho^3$ . Our strategy is to integrate the self-duality equation of motion

$$H_{\mu\nu 5} = \partial_5 B_{\mu\nu} \quad (5.41)$$

to get  $B_{\mu\nu}$ . Then we use  $B_{\mu\nu}$  to compute the whole  $H_{MNP}$  and check its consistency with our ansatz. The components of  $H$  are

$$H_{twi} = \frac{\beta x^i}{\rho^4}, \quad H_{ijk} = \frac{\epsilon_{ijk} \beta x^5}{\rho^4}, \quad (5.42)$$

$$H_{tw5} = \frac{\beta x^5}{\rho^4}, \quad H_{ij5} = -\frac{\epsilon_{ijk} \beta x^k}{\rho^4}. \quad (5.43)$$

Integrating (5.43), we get the following components of  $B_{\mu\nu}$  :

$$B_{ij} = -\frac{1}{2} \frac{\beta \epsilon_{ijk} x_k}{r^3} \left( \frac{x^5 r}{\rho^2} + \tan^{-1}(x^5/r) \right), \quad B_{tw} = -\frac{\beta}{2\rho^2}, \quad (5.44)$$

In principle,  $x^5$  independent constants of integration can be added but we will not need them. It is now easy to check a consistent solution is obtained by setting all the other independent components of  $B_{\mu\nu}$  to be zero.

Three remarks are in order:

1. We remark that if we apply the condition (5.9) to the Perry-Schwarz self-dual string solution, we obtain

$$F_{ij} = -\frac{c\beta\pi}{2} \frac{\epsilon_{ijk} x_k}{r^3}, \quad F_{tw} = 0 \quad (5.45)$$

for the auxiliary gauge field. Certainly this  $U(1)$  field decouples and play no role in the abelian case. However it is interesting to note that this is precisely the field strength of a Dirac monopole in the  $(x, y, z)$  subspace! The presence of a Dirac monopole was already apparent in the original solution of [71]. Here, we reveal that the same monopole configuration also appears as the auxiliary gauge field. It turns out the use of an non-abelian monopole in place of the Dirac monopole is precisely what is needed to construct the non-abelian self-dual string solution.

2. The solution in the form (5.44) will be our basis for the construction of the non-abelian self-dual string in the next subsection. We remark that it is also quite interesting that this form of the solution provides a link between linearised Perry-Schwarz self-dual string and Howe-Lambert-West self-dual string [123]. To explain this, let us first give a brief review on the key construction of Howe-Lambert-West self-dual string. In the superembedding approach of (2,0) supersymmetric theory, there are two non-linearly related 3-form field strengths which are called  $H$  and  $h$ . The 3-form  $H$  is exact but not necessarily self-dual while the 3-form  $h$  is self-dual but not necessarily exact. When constructing self-dual string, one of the scalar fields is also turned on. The equation of motion is non-linear. However, with an

appropriate ansatz, it is possible to impose a BPS condition which eventually gives a linear differential relation between  $H$  and the scalar field. Writing in our notation, the BPS equations of motion read

$$H_{twi} = \partial_i \phi, \quad H_{tw5} = \partial_5 \phi, \quad (5.46)$$

$$H_{ijk} = \epsilon_{ijk} \partial_5 \phi, \quad H_{ij5} = -\epsilon_{ijk} \partial_k \phi, \quad (5.47)$$

where we have rescaled the scalar to absorb an inessential numerical factor. These conditions ensure the self-duality of  $H$ . Furthermore, they agree precisely with the Perry-Schwarz's equations of motion (5.41) if one identifies  $B_{tw} = \phi$ . In other words, the linearised Perry-Schwarz self-dual string solution could be lifted to a 1/2 BPS solution in the (2,0) supersymmetric theory by adding a scalar field that satisfies the 'BPS' condition (5.47) (due to self-duality, the condition (5.46) is not needed).

3. Substituting equation (5.44) into the BPS condition (5.47), we obtain

$$\phi = -\frac{\beta}{2\rho^2}. \quad (5.48)$$

Since the scalar field describes a transverse direction of the M5-brane, we rescale it to give a length dimension:

$$X := 2\sqrt{2} \frac{\phi}{\sqrt{T_{M5}}}, \quad (5.49)$$

where  $T_{M5} = (2\pi)^{-5} l_p^{-6}$  is the tension of the M5-brane, and  $l_p$  is Planck's length. The numerical factor  $2\sqrt{2}$  is introduced in order for the energy to be correctly scaled. We now compute the energy of the self-dual string with an excited scalar field. As mentioned above, the gauge sector does not contribute to the string tension (and hence energy), we only consider the scalar sector of an M5-brane action. By considering an M5-brane action (see chapter 4 for complete actions) up to a quadratic term in scalar field, the relevant part of the action is

$$S_{\text{quad,scalar}} = -T_{M5} \int d^6 x \frac{1}{2} \partial_\mu X \partial^\mu X. \quad (5.50)$$

The energy of the self-dual string is then given by

$$\begin{aligned} E &= T_{M5} \int dwd\rho d\Omega_3 \rho^3 \frac{4}{T_{M5}} (\partial_i \phi \partial_i \phi + \partial_5 \phi \partial_5 \phi) \\ &= 8\pi^2 \beta^2 \int dwd\rho \frac{1}{\rho^3} \\ &= \frac{4\pi^2}{\sqrt{2}} \beta \sqrt{T_{M5}} \int dwdX \\ &= n \frac{1}{(2\pi)^2 l_p^3} \int dwdX. \end{aligned} \quad (5.51)$$

In the final step, we used the equation (5.22). Note that  $(2\pi)^{-2}l_p^{-3}$  is a tension  $T_{M2}$  of an M2-brane. We see that the energy we obtained can be identified with the energy of a stack of  $n$  coincident M2-branes.

### 5.2.2 Non-abelian Wu-Yang string solution

Now we are ready for the non-abelian case. As noted above of the roles played by the Dirac monopole in the abelian Perry-Schwarz solution, it is natural to consider the non-abelian generalisations of the Dirac monopole in the construction of the non-abelian self-dual strings. Here we have two candidates: the Wu-Yang monopole and the 't Hooft-Polyakov monopole where the latter involves a Higgs scalar field while the former does not. See, for example, [134] for a review of these solutions. We will use these non-abelian configurations to construct non-abelian self-dual string solutions for both the uncompactified case (where the Wu-Yang solution will be used) and compactified case (where the 't Hooft-Polyakov monopole will be used).

Let us first briefly review the non-abelian Wu-Yang monopole. Without loss of generality, we will consider  $SU(2)$  gauge group with Hermitian generators  $T^a = \frac{\sigma^a}{2}$  satisfying

$$[T^a, T^b] = i\epsilon^{abc}T^c, \quad a, b, c = 1, 2, 3. \quad (5.52)$$

This corresponds to the relative gauge symmetry of a system of two five-branes. Our convention for the Lie algebra valued fields are:  $F_{\mu\nu} = iF_{\mu\nu}^a T^a$ ,  $A_\mu = iA_\mu^a T^a$  and  $F_{\mu\nu}^a = \partial_\mu A_\nu^a - \partial_\nu A_\mu^a - \epsilon^{abc} A_\mu^b A_\nu^c$ .

The non-abelian Wu-Yang monopole is given by

$$A_i^a = -\epsilon_{aik} \frac{x_k}{r^2}, \quad F_{ij}^a = \epsilon_{ijm} \frac{x_m x_a}{r^4}, \quad (5.53)$$

where  $i, j = 1, 2, 3$  and Note that the field strength for the Wu-Yang solution is related to the field strength  $F_{ij}^{(\text{Dirac})} = \epsilon_{ijm} x_m / r^3$  of the Dirac monopole by a simple relation:

$$F_{ij}^a = F_{ij}^{(\text{Dirac})} \frac{x_a}{r}. \quad (5.54)$$

In fact by performing a (singular) gauge transformation

$$U = e^{i\sigma_3\varphi/2} e^{i\sigma_2\theta/2} e^{-i\sigma_3\varphi/2}, \quad (5.55)$$

one can go to an Abelian gauge where only the 3rd component of the gauge field survives.

In this gauge

$$A_i^a = \delta_3^a A_i^{(\text{Dirac})}. \quad (5.56)$$

Despite its close connection with the Dirac monopole, the Wu-Yang solution is not a monopole since it does not source the non-abelian magnetic field. In fact the colour magnetic charge vanishes

$$\int_{S^2} F^a = 0. \quad (5.57)$$

Nevertheless the Wu-Yang solution is a useful prototype for constructing a non-abelian monopole and we will follow the common practice of the literature to refer to it as the Wu-Yang monopole. In particular, a magnetic charge can be defined if there is also in presence a Higgs scalar field as in the 't Hooft-Polyakov monopole.

Inspired by the relation (5.54) of the Wu-Yang solution, we will try to solve the non-abelian self-duality equation (5.8) by adopting the following ansatz for the field strength,

$$H_{\mu\nu\lambda}^a = H_{\mu\nu\lambda}^{(\text{PS})} \frac{x^a}{r} \quad (5.58)$$

Here  $r = \sqrt{x^2 + y^2 + z^2}$  and

$$H^{(\text{PS})} := \frac{\beta}{\rho^4} \left[ dt dw (x dx + y dy + z dz + x^5 dx^5) \right. \\ \left. + x^5 dx dy dz - z dx dy dx^5 - y dz dx dx^5 - x dy dz dx^5 \right] \quad (5.59)$$

is the field strength for the linearised Perry-Schwarz solution in the  $x^4$  direction (5.34). The self-duality of (5.58) follows immediately from the self-duality of the Perry-Schwarz solution. For the moment, we will allow  $\beta$  to be a free parameter.

Our strategy is again to integrate  $H_{\mu\nu 5} = \partial_5 B_{\mu\nu}$  to get  $B_{\mu\nu}$ . Then we obtain  $F_{\mu\nu}$  and  $A_\mu$  from the boundary value of  $B_{\mu\nu}$ . Finally, we use  $B_{\mu\nu}$  and  $A_\mu$  to compute the whole  $H_{MNP}$  and check its consistency with our ansatz. Now the components of our ansatz are:

$$H_{twi}^a = \frac{\beta x^i x^a}{r \rho^4}, \quad H_{ijk}^a = \frac{\epsilon_{ijk} \beta x^5 x^a}{r \rho^4}, \quad (5.60)$$

$$H_{tw5}^a = \frac{\beta x^5 x^a}{r \rho^4}, \quad H_{ij5}^a = -\frac{\epsilon_{ijk} \beta x^k x^a}{r \rho^4}. \quad (5.61)$$

Integrating (5.61), we get the following components of  $B_{\mu\nu}$  :

$$B_{\mu\nu}^a = B_{\mu\nu}^{(\text{PS})} \frac{x^a}{r}, \quad \mu\nu = ij \text{ or } tw, \quad (5.62)$$

where  $B_{ij}^{(\text{PS})}, B_{tw}^{(\text{PS})}$  are the  $B$ -field components (5.44) for the Perry-Schwarz solution. In principle,  $x^5$  independent constants of integration can be added but we will not need them.

A consistent solution can be obtained by setting all the other independent components of  $B_{\mu\nu}$  to be zero. To see this, let us compute  $F_{\mu\nu}$  from (5.10). It is remarkable that

$$F_{ij}^a = -\frac{c\beta\pi}{2} \frac{\epsilon_{ijm} x_m x_a}{r^4}, \quad F_{tw}^a = 0, \quad (5.63)$$

which is precisely the form (5.53) of the Wu-Yang monopole if we take

$$c\beta = -\frac{2}{\pi}. \quad (5.64)$$

As a result, the non-vanishing component of the gauge field is given by

$$A_i^a = -\epsilon_{aik} \frac{x_k}{r^2}. \quad (5.65)$$

So far we have used only the field strength components  $H_{ij5}, H_{tw5}$  of (5.61). However since  $D_\mu(x^a T^a/r) = 0$  for the Wu-Yang gauge field, therefore (5.60) is reproduced immediately and (5.58) is indeed satisfied.

Like the Wu-Yang monopole, the colour magnetic charge of our Wu-Yang string solution vanishes. This is not a problem as we should not forget about the scalar fields as our ultimate aim is to construct the non-abelian self-dual string solution in the multiple M5-branes theory and so the inclusion of scalar fields is natural from the point of view of (2,0) supersymmetry. Although we do not have the full (2,0) supersymmetric theory, one can argue that the self-duality equation of motion (5.8) is not modified by the presence of the scalar fields. This can be seen by a simple dimensional analysis since the dimension of a canonically normalised scalar field is two, and there is no local polynomial term one can write down which is consistent with conformal symmetry. That the self-duality equation is not modified by the scalar fields is also the case in the other proposed constructions [80, 135, 136]. As for the scalar field, first it is clear that due to R-symmetry, the self-interacting potential vanishes if there is only one scalar field turned on. As a result, the equation of motion of the scalar field is

$$D_M^2 \phi = 0. \quad (5.66)$$

This is the general situation but for special cases, for example when a BPS condition is satisfied, the second order equation could be reduced to a first order equation. A reasonable form of the BPS equation is the non-abelian generalisation of the BPS equation (5.46), (5.47)

$$H_{ijk} = \epsilon_{ijk} \partial_5 \phi, \quad H_{ij5} = -\epsilon_{ijk} D_k \phi. \quad (5.67)$$

We conjecture that (5.67) is indeed a BPS equation of the non-abelian (2,0) theory since first of all it implies the equation of motion (5.66). Moreover (5.67) would follow immediately from the supersymmetry transformation ( $\Gamma^{012345} \epsilon = \epsilon$ ,  $\Gamma^{012345} \psi = -\psi$ )

$$\delta\psi = (\Gamma^M \Gamma^I D_M \phi^I + \frac{1}{3!2} \Gamma^{MNP} H_{MNP}) \epsilon \quad (5.68)$$

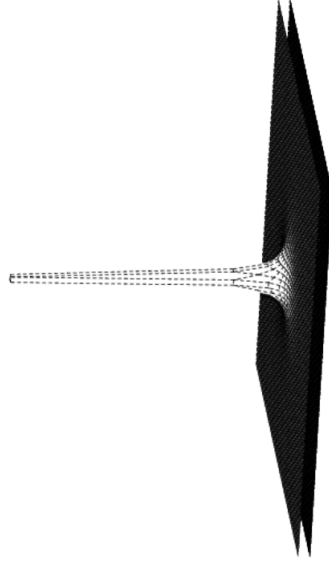


Figure 5.1: An M2 brane ending on a system of two parallel M5-branes separated by a distance.

(which is the most natural non-abelian generalisation of the abelian (2,0) supersymmetry transformation) and the 1/2 BPS condition

$$\Gamma^{046}\epsilon = -\epsilon, \quad (5.69)$$

together with the condition that  $\phi^6 := \phi = \phi(x^a)$ ,  $a = 1, 2, 3, 5$ .

We note that (5.67) is compatible with the self-duality equation if the scalar field is equal to the  $B_{tw}$  component:

$$\phi^a = B_{tw}^a = -\frac{\beta}{2\rho^2} \frac{x^a}{r}, \quad (5.70)$$

or more generally,

$$\phi^a = -\left(u + \frac{\beta}{2\rho^2}\right) \frac{x^a}{r}, \quad (5.71)$$

where  $u$  is a constant. To see the physical meaning of this solution, let us consider the transverse distance  $|\phi|$  defined by  $|\phi|^2 = \phi^a \phi^a$ . This gives

$$|\phi| = \left|u + \frac{\beta}{2\rho^2}\right|. \quad (5.72)$$

We will choose the constant  $u$  to be of the same sign as  $\beta$  so that  $|\phi|$  is never zero. This describes a system of M5-branes with a spike at  $\rho = 0$  and level off to  $u$  as  $\rho \rightarrow \infty$ . Hence the physical interpretation of our self-dual string is that two M5-branes are separating by a distance  $u$  and with an M2-brane ending on them. With this interpretation, there is a

symmetry breaking and one can identify an  $U(1)$   $B$ -field at the large distance  $\rho$ :

$$\mathcal{B}_{\mu\nu} \equiv \hat{\phi}^a B_{\mu\nu}^a = \pm B_{\mu\nu}^{(\text{PS})} \quad (5.73)$$

where  $\hat{\phi}^a := \phi^a/|\phi|$  and the  $+$  ( $-$ ) sign in the second equation above corresponds to the case  $c > 0$  ( $c < 0$ ). Since the field configuration approaches that of the abelian self-dual string at large distance, we immediately obtain the charges

$$P = Q = -2\pi^2|\beta| = -\frac{4\pi}{|c|}. \quad (5.74)$$

and charge quantisation determines that

$$\beta = \mp n \sqrt{\frac{1}{4\pi^3}}, \quad c = \pm 4 \frac{\sqrt{\pi}}{n} \quad (5.75)$$

and  $P = Q = -n\sqrt{\pi}$ . We require that the theory should admit solution with the minimal unit of charge and so the possible values of the constant  $c$  in the non-abelian action (5.4) is:

$$c = \pm 4\sqrt{\pi} \quad (5.76)$$

and the charges of our solution are  $P = Q = -\sqrt{\pi}$ .

Just as in the abelian case, the action for the gauge fields vanish on shell. Therefore the string gets its energy solely from the scalar field. We may try to compute the energy by following the discussion of the abelian case. However, we postpone the computation of energy until we discuss a more general case in section 5.4.

### 5.3 Non-Abelian Self-Dual String Solution: Compactified Case

In this section, we consider the theory with  $x^5$  compactified on a circle with radius  $R$  and construct the self-dual string solution. The constraint that the gauge field has to satisfy is now (5.11). Without loss of generality, let us assume that the string aligns in the  $w = x^4$  direction.

In the compactified theory, the field strength can be expanded in terms of Fourier modes,

$$H_{MNP} = \sum_n e^{inx^5/R} H_{MNP}^{(n)}(r). \quad (5.77)$$

The gauge field  $B_{\mu\nu}$  can be then obtained by integrating over the equation of motion  $H_{\mu\nu 5} = \partial_5 B_{\mu\nu}$ . It is

$$B_{\mu\nu} = \frac{x^5}{2\pi Rc} F_{\mu\nu}(r) + \sum_{n=-\infty}^{\infty} e^{inx^5/R} B_{\mu\nu}^{(n)}(r), \quad (5.78)$$

where we have used the boundary condition (5.11) to determine the first term and  $B_{\mu\nu}^{(0)}(r)$  is an integration constant. The higher modes  $B_{\mu\nu}^{(n\neq 0)}$  are given by:

$$H_{\mu\nu 5}^{(n\neq 0)}(r) = \frac{in}{R} B_{\mu\nu}^{(n\neq 0)}(r). \quad (5.79)$$

Notice that the first term on the right hand side has no contribution to  $H_{\mu\nu\lambda}$  because of Bianchi identity and hence

$$H_{\mu\nu\lambda}^{(n)} = D_{[\lambda} B_{\mu\nu]}^{(n)} \quad (5.80)$$

for all  $n$ .

Let us consider an ansatz with the only nonzero components of gauge potential being  $B_{tw}$  and  $B_{ij}$ . The self-duality condition reads

$$H_{ijk} = \epsilon_{ijk} H_{tw5}, \quad H_{twk} = -\frac{1}{2} \epsilon_{ijk} H_{ij5}, \quad (5.81)$$

or, written in terms of modes,

$$D_{[i} B_{jk]}^{(0)} = \epsilon_{ijk} \frac{F_{tw}}{2\pi R c}, \quad D_k B_{tw}^{(0)} = -\frac{f_k}{2\pi R c} \quad (5.82)$$

$$D_k b_k^{(n)} = \frac{in}{R} B_{tw}^{(n)}, \quad D_k B_{tw}^{(n)} = -b_k^{(n)} \frac{in}{R}, \quad n \neq 0, \quad (5.83)$$

where we have denoted

$$f_k(r) := \frac{1}{2} \epsilon_{ijk} F_{ij} \quad \text{and} \quad b_k^{(n)}(r) := \frac{1}{2} \epsilon_{ijk} B_{ij}^{(n)} \quad \text{for } n \neq 0. \quad (5.84)$$

Notice that the 2nd equation of (5.82) takes exactly the same form as the BPS equation for the 't Hooft-Polyakov magnetic monopole if we identify  $-2\pi R c B_{tw}^{(0)}$  as the scalar field there. Indeed in the BPS limit, the equation of motion for the 't Hooft-Polyakov monopole reads

$$\frac{1}{2} \epsilon_{ijk} F_{ij} = D_k \phi, \quad (5.85)$$

where  $\phi$  is an adjoint Higgs scalar field. The solution is given by

$$A_i^a = -\epsilon_{aik} \frac{x^k}{r^2} (1 - k_v(r)), \quad \phi^a = \frac{v x^a}{r} h_v(r), \quad (5.86)$$

where

$$k_v(r) := \frac{vr}{\sinh(vr)}, \quad h_v(r) := \coth(vr) - \frac{1}{vr}. \quad (5.87)$$

Asymptotically  $r \rightarrow \infty$ , we have

$$A_i^a \rightarrow -\epsilon_{aik} \frac{x^k}{r^2}, \quad \phi^a \rightarrow \frac{|v|x^a}{r} := \phi_\infty, \quad (5.88)$$

which coincides with Wu-Yang monopole. Note that the gauge symmetry is broken at infinity to  $U(1)$ , the little group of  $\phi_\infty$ . This may be identified as the electromagnetic gauge group and one could use this to define the magnetic monopole charge [137, 138].

The electromagnetic field strength can be defined as

$$\mathcal{F}_{ij} = F_{ij}^a \frac{\phi^a}{|v|} = \epsilon_{ijk} \frac{x^k}{r^3}, \quad \text{for large } r. \quad (5.89)$$

The magnetic charge is given by  $p = \int_{S^2} \mathcal{F} = 4\pi$ , which corresponds to a magnetic monopole of unit charge. Note that at the core  $r \rightarrow 0$ , we have

$$A_i \rightarrow 0, \quad \phi \rightarrow 0 \quad (5.90)$$

and hence the  $SU(2)$  symmetry is unbroken at the monopole core.

The resemblance of our equation with the BPS equation of the 't Hooft-Polyakov monopole motivates us to take for  $A_\mu$  the same ansatz as in the 't Hooft-Polyakov monopole,

$$A_i^a = -\epsilon_{aik} \frac{x^k}{r^2} (1 - k_v(r)), \quad (5.91)$$

This implies  $F_{tw} = 0$  and hence the 1st equation of (5.82) can be solved with

$$B_{ij}^{(0)} = c_0 F_{ij}, \quad (5.92)$$

where  $c_0$  is an arbitrary constant. On the other hand, (5.83) gives

$$D_k D_k B_{tw}^{(n \neq 0)} = \frac{n^2}{R^2} B_{tw}^{(n \neq 0)}. \quad (5.93)$$

For zero mode, we have  $D_k D_k B_{tw}^{(0)} = 0$ , combine them together we can write

$$D_k D_k B_{tw}^{(n)} = \frac{n^2}{R^2} B_{tw}^{(n)}. \quad (5.94)$$

We take the ansatz for  $B_{tw}^{(n)}$  as

$$B_{tw}^{(n)a} = a_n(r) \frac{v x^a}{r} \quad (5.95)$$

then the equation (5.94) is equivalent to

$$\frac{\partial_r(r^2 \partial_r a_n(r))}{r^2} - \frac{2k_v(r)^2}{r^2} a_n(r) = \frac{n^2}{R^2} a_n(r). \quad (5.96)$$

The well-behaved physical solution is

$$a_0 = \alpha_0 h_v(r), \quad (5.97)$$

$$a_{n \neq 0}(r) = \alpha_n \frac{e^{-|n|r/R}}{vr} \left( 1 + \frac{vR}{|n|} \coth(vr) \right), \quad (5.98)$$

where  $\alpha_n$  are arbitrary constants. Here we have dropped the independent solutions which are exponentially increasing at large distance and hence not physical. As a result, we obtain for the gauge fields

$$B_{tw}^a = -\frac{h_v(r)}{2\pi Rc} \frac{vx^a}{r} + \sum_{n \neq 0} \alpha_n e^{inx^5/R} \frac{e^{-|n|r/R}}{vr} \left(1 + \frac{vR}{|n|} \coth(vr)\right) \frac{vx^a}{r}, \quad (5.99)$$

$$B_{ij}^a = \frac{x^5}{2\pi Rc} F_{ij}^a(r) + c_0 F_{ij}^a(r) + \sum_{n \neq 0} e^{inx^5/R} B_{ij}^{a(n)}(r). \quad (5.100)$$

where

$$b_k^{(n)a} = -v^3 \frac{R}{in} (ra'_n - k_v(r)a_n) \frac{x^k x^a}{r} - \delta_k^a \frac{vR}{in} a_n k_v(r) \frac{1}{r}, \quad n \neq 0. \quad (5.101)$$

The proportionality factor for  $a_0$  is determined by recalling that  $-2\pi Rc B_{tw}^{(0)}$  is the scalar of the 't Hooft-Polyakov monopole, while  $\alpha_{n \neq 0}$  are left undetermined. Physically this corresponds to different excitations over the fundamental solution with all  $\alpha_{n \neq 0} = 0$ . Note that there is a “winding mode” in  $B_{ij}$ , while there is no such mode in  $B_{tw}$  because  $F_{tw} = 0$ . Although this has no effect classically, we expect that this is observable quantum mechanically like the Berry phase. See, for example, [139–141] for a discussion of Berry phase associated with branes in string theory.

Next let us include a (2,0) scalar field  $\phi$ . As above we assume that it satisfies the BPS equation (5.47), then the BPS equation is satisfied automatically if we identify  $\phi^{(0)} = B_{tw}^{(0)}$ . As a result, we have

$$\phi^{(0)a} = -u \left( \coth(vr) - \frac{1}{vr} \right) \frac{x^a}{r}. \quad (5.102)$$

where

$$u := \frac{v}{2\pi Rc} \quad (5.103)$$

set the scale of the vev of  $\phi^{(0)}$  at large  $r$  since we can say  $\phi^{(0)} \rightarrow -\frac{|v|}{2\pi Rc} x^a T^a / r$  as  $r \rightarrow \infty$ . In addition, one can define a  $U(1)$  projection onto  $\phi^{(0)}$ . This allows us to define the charges

$$\begin{aligned} P = Q &= \int_{S^1 \times S^2} H^a \hat{\phi}^a \\ &= \mp \int dx^5 dS_k \frac{1}{2} \epsilon_{ijk} \left( \frac{1}{2\pi Rc} F_{ij}^a \frac{x^a}{r} + (\text{KK}) \right) \\ &= -\frac{4\pi}{|c|}, \end{aligned} \quad (5.104)$$

where the  $- (+)$  sign in the second equation above corresponds to the case  $c > 0$  ( $c < 0$ ); and the term (KK) stands for the KK modes and their contribution to the charges is zero. Substituting (5.76), we find that the solution is self-dual and carries the charges

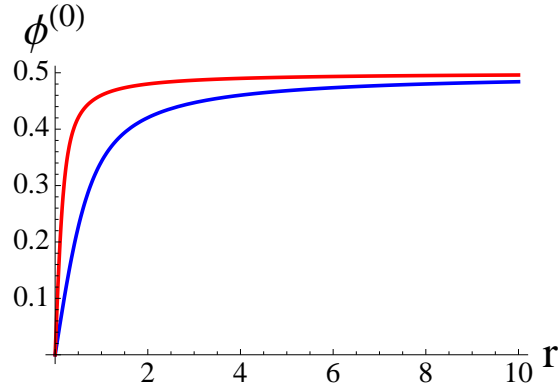


Figure 5.2: Scalar Profile. The red curve corresponds to  $R = 4$  and the blue one to  $R = 1$

$P = Q = -\sqrt{\pi}$ . Physically one can identify this self-dual string with the uncompactified one obtained in the previous section and so they carry the same charges.

The scalar profile of (5.102) is plotted in figure 5.2, for two compactification radius  $R = 1$  and  $R = 4$  and a fixed vev  $u = -0.5$ . One may compare our results to the scalar profile in [142]. In this work, a modified Nahm's equation for the scalar field was conjectured. However unlike the ordinary Nahm's equation where one can obtain the non-abelian Yang-Mills gauge field at the same time, it is not clear how one might obtain the corresponding non-abelian tensor gauge field from the modified Nahm's equation and the proposal still needed to be completed. Nevertheless, qualitatively their scalar profile is similar to ours.

## 5.4 Non-Abelian $SU(N_5)$ Self-Dual String Solution

### 5.4.1 Generalised non-abelian Wu-Yang monopole

Our construction of the self-dual string solution in the  $SU(N_5)$  theory will be based on a generalisation of the  $SU(2)$  charge one Wu-Yang monopole solution to one with arbitrary charge  $n$ . Let us start with a review of the generalised Wu-Yang monopole.

Consider an  $SU(2)$  gauge theory, and for reasons which will become clear later, let us denote the Lie algebra generators by  $\alpha^a$  with

$$[\alpha^a, \alpha^b] = i\epsilon^{abc}\alpha^c. \quad (5.105)$$

The generalised Wu-Yang monopole is given by the following field configuration [134]

$$A_k = iA_k^a\alpha^a = -\frac{i}{2r}(\tau_\varphi^{(n)}\hat{\theta}_k - n\tau_\theta^{(n)}\hat{\varphi}_k), \quad (5.106)$$

i.e.

$$A_\theta = -\frac{i}{2r}\tau_\varphi^{(n)}, \quad A_\varphi = \frac{in}{2r}\tau_\theta^{(n)}. \quad (5.107)$$

Here

$$\begin{aligned} \hat{\theta}_k dx^k &:= \cos\theta \cos\varphi dx^1 + \cos\theta \sin\varphi dx^2 - \sin\theta dx^3, \\ \hat{\varphi}_k dx^k &:= -\sin\varphi dx^1 + \cos\varphi dx^2, \end{aligned} \quad (5.108)$$

$$x^1 = r \sin\theta \cos\varphi, \quad x^2 = r \sin\theta \sin\varphi, \quad x^3 = r \cos\theta, \quad (5.109)$$

$$\begin{aligned} \hat{r}^{(n)} &:= (\sin\theta \cos(n\varphi), \sin\theta \sin(n\varphi), \cos\theta), \\ \hat{\theta}^{(n)} &:= (\cos\theta \cos(n\varphi), \cos\theta \sin(n\varphi), -\sin\theta) = \frac{\partial \hat{r}^{(n)}}{\partial \theta}, \\ \hat{\varphi}^{(n)} &:= (-\sin(n\varphi), \cos(n\varphi), 0) = \frac{1}{n \sin\theta} \frac{\partial \hat{r}^{(n)}}{\partial \varphi} \end{aligned} \quad (5.110)$$

and

$$\tau_r^{(n)} = \hat{r}^{(n)} \cdot \vec{\alpha}, \quad \tau_\theta^{(n)} = \hat{\theta}^{(n)} \cdot \vec{\alpha}, \quad \tau_\varphi^{(n)} = \hat{\varphi}^{(n)} \cdot \vec{\alpha}, \quad (5.111)$$

The Wu-Yang monopole configuration considered in section 5.2 is given by the case  $n = 1$ .

It is useful to note that

$$A_k = U \bar{A}_k U^{-1} + U \partial_k U^{-1}, \quad (5.112)$$

with

$$U = e^{-i\vec{\alpha} \cdot \hat{\varphi}^{(n)}} \quad (5.113)$$

and

$$\bar{A}_k = \frac{n}{r} \frac{1 - \cos\theta}{\sin\theta} \hat{\varphi}_k \times i\alpha^3, \quad (5.114)$$

As a result,

$$F_{ij} = U \bar{F}_{ij} U^{-1}, \quad (5.115)$$

where

$$\bar{F}_{ij} = \partial_i \bar{A}_j - \partial_j \bar{A}_i = n \epsilon_{ijk} \frac{x^k}{r^3} \times i\alpha_3. \quad (5.116)$$

Since

$$U \alpha^3 U^{-1} = \hat{r}_a^{(n)} \alpha^a, \quad (5.117)$$

we obtain

$$F_{ij} = n \epsilon_{ijk} \frac{x^k}{r^3} i \hat{r}_a^{(n)} \alpha^a. \quad (5.118)$$

Therefore (5.106), (5.118) provide a generalisation of the Wu-Yang monopole solution to “charge”  $n$ .

We also note that

$$D_i \left( \hat{r}_a^{(n)} \alpha^a \right) = 0 \quad (5.119)$$

holds for the generalised Wu-Yang monopole. This is a generalisation of  $D_i(x^a \alpha^a / r) = 0$  for the charge one case.

#### 5.4.2 Non-abelian self-dual string and the distance-radius relation

In this subsection we construct a self-dual string solution where the tensor gauge field is embedded in an  $SU(2)$  sub-algebra of  $SU(N_5)$ . Let us denote the generators of the  $SU(2)$  factor by  $\alpha^a$ :

$$[\alpha^a, \alpha^b] = i\epsilon^{abc} \alpha^c. \quad (5.120)$$

We embed the Pauli spin matrix into an upper left corner of  $N_5 \times N_5$  matrices of  $SU(N_5)$  :

$$\alpha^a = \frac{\sigma^a}{2} \oplus 0_{N_5-2}, \quad (5.121)$$

where  $0_{N_5-2}$  is an  $(N_5 - 2) \times (N_5 - 2)$  zero matrix. The trace is then given by

$$\text{tr}(\alpha^a \alpha^b) = \frac{1}{2} \delta^{ab}. \quad (5.122)$$

Consider an ansatz of the field strength

$$H_{\mu\nu\lambda} = H_{\mu\nu\lambda}^{(\text{PS})} i\hat{r}_a^{(n)} \alpha^a, \quad (5.123)$$

Obviously the field strength is self-dual. Since  $\hat{r}_a^{(n)}$  is independent of  $x_5$ , we can immediately integrate  $H_{045}$ ,  $H_{ij5}$  over  $x_5$  and obtain

$$B_{\mu\nu} = B_{\mu\nu}^{(\text{PS})} i\hat{r}_a^{(n)} \alpha^a, \quad \mu\nu = ij \text{ or } tw. \quad (5.124)$$

One still need to check that this  $B$ -field reproduces correctly the other components  $H_{ijk}$ . To check this, we note that the constraint (5.9) gives

$$F_{ij} = -c\beta \frac{\pi}{2} \epsilon_{ijm} \frac{x^m}{r} i\hat{r}_a^{(n)} \alpha^a \quad F_{tw} = 0. \quad (5.125)$$

Therefore if we take

$$\beta = -\frac{2n}{c\pi}, \quad (5.126)$$

for an integer  $n$ , then the auxiliary gauge field is given by the generalised Wu-Yang monopole. As a result of (5.119), we have

$$D_{[\lambda} B_{\mu\nu]} = \partial_{[\lambda} B_{\mu\nu]}^{(\text{PS})} i\hat{r}_a^{(n)} \alpha^a \quad (5.127)$$

and the result agrees with (5.123).

To obtain a self-dual string solution, we observe that the BPS equation (5.67) can be solved with

$$\phi = - \left( u + \frac{\beta}{2\rho^2} \right) i\hat{r}_a^{(n)} \alpha^a. \quad (5.128)$$

This leaves an unbroken  $U(1)$  generated by

$$\hat{\phi} := \phi/|\phi| = \mp i\hat{r}_a^{(n)} \alpha^a \quad (5.129)$$

at  $\rho \rightarrow \infty$ . Here  $|\phi|^2 := \phi^a \phi^a$  and the  $-(+)$  sign is chosen for  $u > 0 (u < 0)$ . Without loss of generality, we take  $u > 0$  below. The asymptotic  $U(1)$  fields are identified by a projection

$$H_{\mu\nu\lambda}^{U(1)} := H_{\mu\nu\lambda}^a \hat{\phi}^a, \quad B_{\mu\nu}^{U(1)} := B_{\mu\nu}^a \hat{\phi}^a, \quad (5.130)$$

then

$$H_{\mu\nu\lambda}^{U(1)} = H_{\mu\nu\lambda}^{(PS)}, \quad B_{\mu\nu}^{U(1)} = B_{\mu\nu}^{(PS)}. \quad (5.131)$$

The  $U(1)$  magnetic and electric charges (per unit length) are defined by

$$P = \int_{S^3} H^{U(1)}, \quad Q = \int_{S^3} *H^{U(1)}. \quad (5.132)$$

This gives the  $U(1)$  charges,

$$P = Q = 2\pi^2\beta \quad (5.133)$$

The charge quantisation condition is modified due to the existence of a non-trivial centre in the residual gauge group of the non-abelian theory. In fact, in a non-abelian Yang-Mills gauge theory with an unbroken gauge group of the form

$$H = U(1) \times K, \quad (5.134)$$

where the  $U(1)$  factor allows one to define the electric and magnetic charges, and  $K$  is any residual gauge group, Corrigan and Olive have shown [143] that the charge quantisation takes the form <sup>1</sup>

$$e^{4\pi i q g} = k, \quad (5.135)$$

where  $k$  is an element in  $C(K)$ , the centre of  $K$ . For example, if  $K = SU(N)$ , then  $C(K) = Z_N$ ,

$$k = e^{2\pi i n/N} \mathbf{1}_N, \quad n = \text{integers} \quad (5.136)$$

---

<sup>1</sup>The normalisation of the magnetic charge was taken as  $\nabla \cdot \vec{B} = 4\pi g \delta^{(3)}(x)$  in [143].

and the charge quantisation condition for the monopoles reads

$$qg = \frac{n}{2N}. \quad (5.137)$$

For us, since the symmetry is broken down by the scalar field as  $SU(N_5) \rightarrow U(1) \times SU(N_5 - 1)$  and since (2,0) supersymmetry demands that all fields in theory to be in the adjoint representation, this means the centre of the residual gauge symmetry is given by  $Z_{N_5-1}$ . The same argument as Corrigan and Olive then gives

$$PQ' + QP' = \frac{2\pi}{N_5 - 1} \mathbf{Z}. \quad (5.138)$$

We can now use the charge quantisation condition (5.138) to fix the value of  $\beta$ . Let us consider the situation where the self-dual string configuration arises as the intersection of a number  $N_2$  of coincident M2-branes ending perpendicularly on our system of M5-branes. In this case, the charges  $P, Q$  should be proportional to  $N_2$ . Substituting (5.133), we obtain

$$P = Q = 2\pi^2\beta = \frac{N_2}{\sqrt{N_5 - 1}}\sqrt{\pi}. \quad (5.139)$$

From the field theory point of view, the geometrical shape of the M2-branes spike is described by the scalar field  $X = 4\phi/\sqrt{T_{M5}}$ . Note that the normalisation factor of 4 is differed from the normalisation factor of  $2\sqrt{2}$  used in the abelian case discussed above. Again, the normalisation factor is introduced in such a way that it gives the correct energy. It is convenient to introduce the root-mean-square distance (setting  $l_p = 1$ )

$$D := \sqrt{\frac{1}{N_5 T_{M5}} |\text{tr}(4\phi)^2|} \quad (5.140)$$

as a measure of the transverse distance of the M2-branes spike from the system of M5-branes. The cross section of the M2-branes spike is an  $S^3$  and the radius  $\rho$  is governed by the transverse distance-radius relation

$$D = D_0 + \frac{4\pi N_2}{\sqrt{N_5(N_5 - 1)}\rho^2} \quad (5.141)$$

where

$$D_0 := \frac{2\sqrt{2}u}{\sqrt{N_5 T_{M5}}} \quad (5.142)$$

is a constant. For large  $N_5$ , the energy of the spike is given by

$$E = \frac{T_{M5}}{2} \int d^5x \text{tr}(D_\mu X D^\mu X) = N_2 T_{M2} \int dwdD, \quad (5.143)$$

which is identified as an energy of a stack of  $N_2$  coincident M2-branes.

In addition to the worldvolume description, the system of intersecting M2-M5 branes also admits a supergravity description from which one can extract the transverse distance-radius relation and compare with our field theory result. However, the supergravity solution, beyond the brane probe approximation, for a system of M2-branes intersecting on a system of separated M5-branes where  $(N_5 - 1)$  of them are in coincidence and another single M5-brane is separated at a finite distance away from the main group is not known. The closest system which admits a supergravity solution is the system of  $N_2$  M2-branes intersecting a system of  $N_5$  coincident M5-branes [144]. In this reference the technique of blackfold is applied and the transverse distance-radius relation

$$D = \frac{2\pi N_2}{N_5} \frac{1}{\rho^2} \quad (5.144)$$

is obtained. At distance  $D$  large enough compared with the separation so that one cannot resolve the details of the separation, one can expect the supergravity solution for our system can be approximated by the supergravity solution of this system. In this case, one can ignore the first term in our field theory result (5.141) and our transverse distance-radius relation

$$D = 2 \frac{2\pi N_2}{N_5} \frac{1}{\rho^2} \quad (5.145)$$

agrees with that of supergravity on their  $N_2$  and  $N_5$  dependence. Note that, however, (5.144) and (5.145) differs by an overall scale factor of 2. This is presumably due to a subtlety in the scaling of the M5-branes model.

We remark that the field theory description and the supergravity description are good only in their respective regime of validity. To confirm the validity of the agreement we found above, one need to check that there indeed exists an overlapping regime where one can trust both descriptions and hence compare the results sensibly. To check this, we note that our description of the M2-branes spike as a worldvolume soliton of the M5-branes is good provided that higher derivative corrections to our non-abelian action is small:  $l_p |\partial^2 \Phi| \ll |\partial \Phi|$ . This translates to

$$\rho \gg l_p. \quad (5.146)$$

On the other hand, the validity of the blackfold description [144] was discussed in [145]. It was found there that for zero angular velocity which is our case, one needs

$$\rho \gg \max(l_p, \rho_c), \quad (5.147)$$

where  $\rho_c := N_5^{1/3} (1 + \sqrt{1 + 64N_2^2/N_5^4})^{1/6} l_p$ . Therefore in the region (5.147), both the supergravity description and the M5-branes worldvolume description are valid. Now in

order for the field theory result (5.141) to reduce to the form (5.144), it is required that

$$\rho \ll \left(\frac{3}{4\pi^3}\right)^{1/4} \left(\frac{N_2}{uN_5^2}\right)^{1/2}. \quad (5.148)$$

Thus, by arranging the parameters  $N_2$ ,  $N_5$  and  $u$  (for example a scaling limit involving large  $N_2$ ,  $N_5$  and small  $ul_p^2$ ), a non-empty region of  $\rho$  satisfying both (5.147) and (5.148) can always be achieved, and so the agreement we found is justified.

## 5.5 Discussions

In this chapter we have constructed the non-abelian string solutions of the non-abelian 5-brane theory constructed in [87], for both uncompactified and compactified spacetime. The string solution in non-compact spacetime is supported by a non-abelian Wu-Yang monopole, while the string solution in compact spacetime is supported by a non-abelian 't Hooft-Polyakov monopole. We showed how these solutions can be embedded in the (2,0) supersymmetric theory by including a single scalar field obeying a first order BPS equation. Although we don't have the full (2,0) supersymmetric construction yet, we argued that it is the correct BPS equation of the (2,0) theory since it solves the equation of motion, and moreover it can be derived from the most natural form of the supersymmetry transformation law in the non-abelian (2,0) theory. These string solutions carry self-dual charges and has infinite tension arising from the scalar profile which corresponds to having a M2-brane spike on the M5-branes system. These properties are consistent with what one expects for the non-abelian self-dual strings living on a system of two M5-branes.

We have also constructed a self-dual string solution in the  $SU(N_5)$  non-abelian theory of five-branes. Our solution carries an arbitrary  $N_2$  unit of self-dual charge and obtains its charge through the generalised non-abelian Wu-Yang monopole configuration carried by the auxiliary one-form gauge field. We have also shown that the radius-transverse distance relation describing the M2-branes spike agrees with the supergravity description of the intersecting M2-M5 branes system. Our results therefore provide further evidence that the non-abelian theory [87] does give a description for a system of multiple M5-branes.

This solution was obtained for a special symmetry breaking where there is a residual  $SU(N_5 - 1)$  gauge symmetry. For a more general configurations of the Higgs field, the residual symmetry at infinity could be smaller and the self-dual string would be characterised by more number of charges. The discussion is similar to that of non-abelian monopole [114]. It will be interesting to construct these other kinds of self-dual strings and understand their dual description in supergravity and M-theory.

With the solutions at hand, one may perform a small fluctuation analysis of the solutions and use it to learn more about the dynamics of non-abelian self-dual string. It would also be interesting to include couplings to a background  $C$ -field. In [146,147], the quantum Nambu geometry has been obtained as the quantum geometry for M5-branes in a large constant background  $C$ -field. One should be able to construct the star-product for this geometry and use it to derive the “Seiberg-Witten” map for the non-abelian M5-branes theory in a background  $C$ -field.

We note that our field theory description is not good near the spike region ( $\rho \simeq 0$ ). Apparently, unlike the non-abelian BPS monopole, the non-abelian interaction here is not sufficient to remove the spike singularity. Nevertheless one can expect it to be smoothen out only in the complete description of M-theory with all higher derivative corrections included [71].

It is hoped that the self-dual string solution constructed here could provide further insights into the understanding of the  $N^3$  entropy growth of the multiple M5-branes system [148]. Recent progress on this problem has been achieved in [149–151].

## Chapter 6

# Conclusion

In this thesis, we have shown an aspects of developments of branes in string and M-theory. We started with an application of gauge/gravity duality. We then moved on to M-theory where there are still a lot to be done in constructing M-branes worldvolume actions.

In chapter 2, we used a D3/D7 model to describe meson condensation at finite isospin chemical potential in an  $\mathcal{N} = 2$   $SU(N_c)$  strongly coupled gauge theory with  $N_f = 2$  sets of hypermultiplets. We focused on the case where the gauge theory lives on  $\mathbb{R} \times S^3$ . The study was done by considering two coincident D7-branes embedded in global  $AdS_5 \times S^5$  background with or without black hole. The background also includes a 5-form flux and a constant dilaton. AdS boundary expansion of a field on D7-branes gives, via gauge/gravity duality, source and vacuum expectation value of the corresponding operator. We first studied a ground state without meson condensate in a presence of finite isospin chemical potential. At a critical value of isospin chemical potential, this ground state is unstable under mesonic fluctuations. So there is a phase transition. We found that the new ground state is described by scalar meson condensate which breaks a global  $SO(4)$  symmetry. This is the case for both zero and finite temperature cases. We have focused on the case of massless hypermultiplets. So it would be interesting to see if, for the case of massive hypermultiplets, the new ground state would be of the same type.

In chapter 3, we also used a D3/D7 model to study a strongly coupled system with massless or massive hypermultiplets. We studied a finite size effect of an external magnetic field on this system at zero temperature. In order to describe an external magnetic field, we turned on B-field with components on  $S^3 \subset AdS_5$ . Exactly the same system was studied before by [112]. However, B-field used in this reference does not solve the constraint imposed by D7-branes. We corrected this by constructing B-field with the help of vector

spherical harmonics. We found that there is a forbidden region, which forbids us to construct any embedding configuration for some given values of hypermultiplets mass and external magnetic field. We are currently making a cross check to see if our results are correct.

We then changed our consideration to M-theory. A worldvolume theory of M5-brane embedded in a general eleven-dimensional background had been computed before by [75, 76]. In chapter 4, we revisited this system by constructing an alternative action which describes exactly the same system. Our construction is called 3+3 splitting. In order to have a covariant action, we need to introduce 3 auxiliary fields. Additionally, our action is supersymmetric, and kappa symmetric. There are also additional symmetries to ensure that we get the desired equations of motion. With the form of our action, we ultimately expect that our action will be used to understand the conjectured relationship between multiple M2-branes and a single M5-brane.

In chapter 5, we considered a model [87] which will ultimately be extended to a complete worldvolume theory of multiple M5-branes. Although this model originally only described a tensor gauge sector of multiple M5-branes, with additional arguments based on supersymmetry and conformal symmetry, we could use this model to construct self-dual strings. The self-dual strings are important because they describe M2/M5 intersection from M5-branes point of view. Most notably, we have found that radius-transverse distance relationship of the self-dual string exactly agrees with the relationship derived from black-fold approach [144, 145]. This finding gives us a more confidence in the model [87]. To better understand multiple M5-branes, it would be advisable to use this model to construct other solitonic solutions. Some works in this direction has been carried out in literatures [97, 152].

Branes are important objects in string and M-theory. We have discussed examples which show the importance of branes in string and M-theory. We have shown how to apply a D3/D7 model to describe physical systems. We have shown the construction of an M5-brane model with 3+3 splitting. We have found solutions of a multiple M5-branes model describing M2/M5 brane intersection.

# Bibliography

- [1] S. Chunlen, K. Peeters, P. Vanichchamongjaroen, and M. Zamaklar, “Instability of  $N=2$  gauge theory in compact space with an isospin chemical potential,” *JHEP* **1301** (2013) 035, [arXiv:1210.6188 \[hep-th\]](#).
- [2] S.-L. Ko, D. Sorokin, and P. Vanichchamongjaroen, “The M5-brane action revisited,” [arXiv:1308.2231 \[hep-th\]](#).
- [3] C.-S. Chu, S.-L. Ko, and P. Vanichchamongjaroen, “Non-Abelian Self-Dual String Solutions,” *JHEP* **1209** (2012) 018, [arXiv:1207.1095 \[hep-th\]](#).
- [4] C.-S. Chu and P. Vanichchamongjaroen, “Non-abelian Self-Dual String and M2-M5 Branes Intersection in Supergravity,” *JHEP* **1306** (2013) 028, [arXiv:1304.4322 \[hep-th\]](#).
- [5] C. A. Bayona and N. R. Braga, “Anti-de Sitter boundary in Poincare coordinates,” *Gen.Rel.Grav.* **39** (2007) 1367–1379, [arXiv:hep-th/0512182 \[hep-th\]](#).
- [6] J. Erdmenger, N. Evans, I. Kirsch, and E. Threlfall, “Mesons in Gauge/Gravity Duals - A Review,” *Eur.Phys.J.* **A35** (2008) 81–133, [arXiv:0711.4467 \[hep-th\]](#).
- [7] J. Erdmenger and V. Filev, “Mesons from global Anti-de Sitter space,” *JHEP* **1101** (2011) 119, [arXiv:1012.0496 \[hep-th\]](#).
- [8] A. Karch, A. O’Bannon, and L. G. Yaffe, “Critical Exponents from AdS/CFT with Flavor,” *JHEP* **0909** (2009) 042, [arXiv:0906.4959 \[hep-th\]](#).
- [9] B. Zwiebach, *A First Course in String Theory*. Cambridge University Press, 2nd ed., 2009.
- [10] K. Becker, M. Becker, and J. Schwarz, *STRING THEORY AND M-THEORY: A Modern Introduction*. Cambridge University Press, 2007.

- [11] P. West, *Introduction to Strings and Branes*. Cambridge University Press, 2012.
- [12] J. Terning, *Modern Supersymmetry: Dynamics and duality*. Oxford University Press, 2006.
- [13] J. Simon, “Brane Effective Actions, Kappa-Symmetry and Applications,” *Living Rev.Rel.* **15** (2012) 3, [arXiv:1110.2422 \[hep-th\]](#).
- [14] D. S. Berman, “M-theory branes and their interactions,” *Phys.Rept.* **456** (2008) 89–126, [arXiv:0710.1707 \[hep-th\]](#).
- [15] D. P. Sorokin, “Superbranes and superembeddings,” *Phys.Rept.* **329** (2000) 1–101, [arXiv:hep-th/9906142 \[hep-th\]](#).
- [16] J. Casalderrey-Solana, H. Liu, D. Mateos, K. Rajagopal, and U. A. Wiedemann, “Gauge/String Duality, Hot QCD and Heavy Ion Collisions,” [arXiv:1101.0618 \[hep-th\]](#).
- [17] P. Ramond, “Dual Theory for Free Fermions,” *Phys.Rev.* **D3** (1971) 2415–2418.
- [18] A. Neveu and J. Schwarz, “Factorizable dual model of pions,” *Nucl.Phys.* **B31** (1971) 86–112.
- [19] F. Gliozzi, J. Scherk, and D. I. Olive, “Supersymmetry, Supergravity Theories and the Dual Spinor Model,” *Nucl.Phys.* **B122** (1977) 253–290.
- [20] M. B. Green and J. H. Schwarz, “Covariant Description of Superstrings,” *Phys.Lett.* **B136** (1984) 367–370.
- [21] W. Siegel, “Hidden Local Supersymmetry in the Supersymmetric Particle Action,” *Phys.Lett.* **B128** (1983) 397.
- [22] E. Bergshoeff, E. Sezgin, and P. Townsend, “Superstring Actions in  $D = 3, 4, 6, 10$  Curved Superspace,” *Phys.Lett.* **B169** (1986) 191.
- [23] I. A. Bandos, D. P. Sorokin, M. Tonin, P. Pasti, and D. V. Volkov, “Superstrings and supermembranes in the doubly supersymmetric geometrical approach,” *Nucl.Phys.* **B446** (1995) 79–118, [arXiv:hep-th/9501113 \[hep-th\]](#).
- [24] P. A. Dirac, “Quantized Singularities in the Electromagnetic Field,” *Proc.Roy.Soc.Lond.* **A133** (1931) 60–72.

- [25] C. Teitelboim, “Gauge Invariance for Extended Objects,” *Phys.Lett.* **B167** (1986) 63.
- [26] R. I. Nepomechie, “Magnetic Monopoles from Antisymmetric Tensor Gauge Fields,” *Phys.Rev.* **D31** (1985) 1921.
- [27] S. Deser, A. Gomberoff, M. Henneaux, and C. Teitelboim, “Duality, selfduality, sources and charge quantization in Abelian N form theories,” *Phys.Lett.* **B400** (1997) 80–86, [arXiv:hep-th/9702184](#) [hep-th].
- [28] S. Deser, A. Gomberoff, M. Henneaux, and C. Teitelboim, “P-brane dyons and electric magnetic duality,” *Nucl.Phys.* **B520** (1998) 179–204, [arXiv:hep-th/9712189](#) [hep-th].
- [29] M. Aganagic, C. Popescu, and J. H. Schwarz, “D-brane actions with local kappa symmetry,” *Phys.Lett.* **B393** (1997) 311–315, [arXiv:hep-th/9610249](#) [hep-th].
- [30] M. Cederwall, A. von Gussich, B. E. Nilsson, P. Sundell, and A. Westerberg, “The Dirichlet super p-branes in ten-dimensional type IIA and IIB supergravity,” *Nucl.Phys.* **B490** (1997) 179–201, [arXiv:hep-th/9611159](#) [hep-th].
- [31] M. Aganagic, C. Popescu, and J. H. Schwarz, “Gauge invariant and gauge fixed D-brane actions,” *Nucl.Phys.* **B495** (1997) 99–126, [arXiv:hep-th/9612080](#) [hep-th].
- [32] M. Born and L. Infeld, “Foundations of the new field theory,” *Proc.Roy.Soc.Lond.* **A144** (1934) 425–451.
- [33] P. A. Dirac, “An Extensible model of the electron,” *Proc.Roy.Soc.Lond.* **A268** (1962) 57–67.
- [34] A. A. Tseytlin, “On nonAbelian generalization of Born-Infeld action in string theory,” *Nucl.Phys.* **B501** (1997) 41–52, [arXiv:hep-th/9701125](#) [hep-th].
- [35] A. A. Tseytlin, “Born-Infeld action, supersymmetry and string theory,” [arXiv:hep-th/9908105](#) [hep-th].
- [36] R. C. Myers, “Dielectric branes,” *JHEP* **9912** (1999) 022, [arXiv:hep-th/9910053](#) [hep-th].

- [37] A. Hashimoto and W. Taylor, “Fluctuation spectra of tilted and intersecting D-branes from the Born-Infeld action,” *Nucl.Phys.* **B503** (1997) 193–219, [arXiv:hep-th/9703217](#) [hep-th].
- [38] F. Denef, A. Sevrin, and J. Troost, “NonAbelian Born-Infeld versus string theory,” *Nucl.Phys.* **B581** (2000) 135–155, [arXiv:hep-th/0002180](#) [hep-th].
- [39] A. Sevrin, J. Troost, and W. Troost, “The nonAbelian Born-Infeld action at order  $F^6$ ,” *Nucl.Phys.* **B603** (2001) 389–412, [arXiv:hep-th/0101192](#) [hep-th].
- [40] P. Koerber and A. Sevrin, “The NonAbelian D-brane effective action through order  $\alpha'^4$ ,” *JHEP* **0210** (2002) 046, [arXiv:hep-th/0208044](#) [hep-th].
- [41] G. T. Horowitz and A. Strominger, “Black strings and P-branes,” *Nucl.Phys.* **B360** (1991) 197–209.
- [42] O. Aharony, S. S. Gubser, J. M. Maldacena, H. Ooguri, and Y. Oz, “Large N field theories, string theory and gravity,” *Phys.Rept.* **323** (2000) 183–386, [arXiv:hep-th/9905111](#) [hep-th].
- [43] S. Gubser, I. R. Klebanov, and A. Peet, “Entropy and temperature of black 3-branes,” *Phys.Rev.* **D54** (1996) 3915–3919, [arXiv:hep-th/9602135](#) [hep-th].
- [44] J. M. Maldacena, “The Large N limit of superconformal field theories and supergravity,” *Adv.Theor.Math.Phys.* **2** (1998) 231–252, [arXiv:hep-th/9711200](#) [hep-th].
- [45] S. Gubser, I. R. Klebanov, and A. M. Polyakov, “Gauge theory correlators from noncritical string theory,” *Phys.Lett.* **B428** (1998) 105–114, [arXiv:hep-th/9802109](#) [hep-th].
- [46] E. Witten, “Anti-de Sitter space and holography,” *Adv.Theor.Math.Phys.* **2** (1998) 253–291, [arXiv:hep-th/9802150](#) [hep-th].
- [47] P. Breitenlohner and D. Z. Freedman, “Positive Energy in anti-De Sitter Backgrounds and Gauged Extended Supergravity,” *Phys.Lett.* **B115** (1982) 197.
- [48] P. Breitenlohner and D. Z. Freedman, “Stability in Gauged Extended Supergravity,” *Annals Phys.* **144** (1982) 249.

- [49] E. Witten, “Anti-de Sitter space, thermal phase transition, and confinement in gauge theories,” *Adv.Theor.Math.Phys.* **2** (1998) 505–532, arXiv:hep-th/9803131 [hep-th].
- [50] G. Policastro, D. T. Son, and A. O. Starinets, “From AdS / CFT correspondence to hydrodynamics,” *JHEP* **0209** (2002) 043, arXiv:hep-th/0205052 [hep-th].
- [51] K.-j. Hamada and S. Horata, “Conformal algebra and physical states in noncritical three-brane on  $R \times S^{*3}$ ,” *Prog.Theor.Phys.* **110** (2004) 1169–1210, arXiv:hep-th/0307008 [hep-th].
- [52] T. Sakai and S. Sugimoto, “Low energy hadron physics in holographic QCD,” *Prog.Theor.Phys.* **113** (2005) 843–882, arXiv:hep-th/0412141 [hep-th].
- [53] T. Sakai and S. Sugimoto, “More on a holographic dual of QCD,” *Prog.Theor.Phys.* **114** (2005) 1083–1118, arXiv:hep-th/0507073 [hep-th].
- [54] A. Karch, A. O’Bannon, and K. Skenderis, “Holographic renormalization of probe D-branes in AdS/CFT,” *JHEP* **0604** (2006) 015, arXiv:hep-th/0512125 [hep-th].
- [55] A. Karch and A. O’Bannon, “Chiral transition of  $N=4$  super Yang-Mills with flavor on a 3-sphere,” *Phys.Rev.* **D74** (2006) 085033, arXiv:hep-th/0605120 [hep-th].
- [56] E. Witten, “String theory dynamics in various dimensions,” *Nucl.Phys.* **B443** (1995) 85–126, arXiv:hep-th/9503124 [hep-th].
- [57] W. Nahm, “Supersymmetries and their Representations,” *Nucl.Phys.* **B135** (1978) 149.
- [58] E. Cremmer, B. Julia, and J. Scherk, “Supergravity Theory in Eleven-Dimensions,” *Phys.Lett.* **B76** (1978) 409–412.
- [59] E. Bergshoeff, E. Sezgin, and P. Townsend, “Properties of the Eleven-Dimensional Super Membrane Theory,” *Annals Phys.* **185** (1988) 330.
- [60] J. Bagger and N. Lambert, “Modeling Multiple M2’s,” *Phys.Rev.* **D75** (2007) 045020, arXiv:hep-th/0611108 [hep-th].
- [61] J. Bagger and N. Lambert, “Gauge Symmetry and Supersymmetry of Multiple M2-Branes,” *Phys. Rev.* **D77** (2008) 065008, arXiv:0711.0955 [hep-th].

- [62] A. Gustavsson, “Algebraic structures on parallel M2-branes,” *Nucl.Phys.* **B811** (2009) 66–76, [arXiv:0709.1260 \[hep-th\]](#).
- [63] J. Bagger and N. Lambert, “Comments on multiple M2-branes,” *JHEP* **0802** (2008) 105, [arXiv:0712.3738 \[hep-th\]](#).
- [64] G. Papadopoulos, “M2-branes, 3-Lie Algebras and Plucker relations,” *JHEP* **0805** (2008) 054, [arXiv:0804.2662 \[hep-th\]](#).
- [65] J. P. Gauntlett and J. B. Gutowski, “Constraining Maximally Supersymmetric Membrane Actions,” *JHEP* **0806** (2008) 053, [arXiv:0804.3078 \[hep-th\]](#).
- [66] P.-M. Ho and Y. Matsuo, “M5 from M2,” *JHEP* **0806** (2008) 105, [arXiv:0804.3629 \[hep-th\]](#).
- [67] O. Aharony, O. Bergman, D. L. Jafferis, and J. Maldacena, “N=6 superconformal Chern-Simons-matter theories, M2-branes and their gravity duals,” *JHEP* **0810** (2008) 091, [arXiv:0806.1218 \[hep-th\]](#).
- [68] N. Drukker, M. Marino, and P. Putrov, “From weak to strong coupling in ABJM theory,” *Commun.Math.Phys.* **306** (2011) 511–563, [arXiv:1007.3837 \[hep-th\]](#).
- [69] P. S. Howe and E. Sezgin, “D = 11, p = 5,” *Phys.Lett.* **B394** (1997) 62–66, [arXiv:hep-th/9611008 \[hep-th\]](#).
- [70] M. Henneaux and C. Teitelboim, “Dynamics of Chiral (Selfdual) P Forms,” *Phys.Lett.* **B206** (1988) 650.
- [71] M. Perry and J. H. Schwarz, “Interacting chiral gauge fields in six-dimensions and Born-Infeld theory,” *Nucl.Phys.* **B489** (1997) 47–64, [arXiv:hep-th/9611065 \[hep-th\]](#).
- [72] P. S. Howe, E. Sezgin, and P. C. West, “The Six-dimensional selfdual tensor,” *Phys.Lett.* **B400** (1997) 255–259, [arXiv:hep-th/9702111 \[hep-th\]](#).
- [73] J. H. Schwarz, “Coupling a selfdual tensor to gravity in six-dimensions,” *Phys.Lett.* **B395** (1997) 191–195, [arXiv:hep-th/9701008 \[hep-th\]](#).
- [74] M. Aganagic, J. Park, C. Popescu, and J. H. Schwarz, “World volume action of the M theory five-brane,” *Nucl.Phys.* **B496** (1997) 191–214, [arXiv:hep-th/9701166 \[hep-th\]](#).

- [75] P. Pasti, D. P. Sorokin, and M. Tonin, “Covariant action for a  $D = 11$  five-brane with the chiral field,” *Phys.Lett.* **B398** (1997) 41–46, [arXiv:hep-th/9701037](#) [[hep-th](#)].
- [76] I. A. Bandos, K. Lechner, A. Nurmagambetov, P. Pasti, D. P. Sorokin, *et al.*, “Covariant action for the superfive-brane of M theory,” *Phys.Rev.Lett.* **78** (1997) 4332–4334, [arXiv:hep-th/9701149](#) [[hep-th](#)].
- [77] P. Pasti, D. P. Sorokin, and M. Tonin, “On Lorentz invariant actions for chiral p forms,” *Phys.Rev.* **D55** (1997) 6292–6298, [arXiv:hep-th/9611100](#) [[hep-th](#)].
- [78] P.-M. Ho, Y. Imamura, Y. Matsuo, and S. Shiba, “M5-brane in three-form flux and multiple M2-branes,” *JHEP* **0808** (2008) 014, [arXiv:0805.2898](#) [[hep-th](#)].
- [79] N. Lambert and C. Papageorgakis, “Nonabelian (2,0) Tensor Multiplets and 3-algebras,” *JHEP* **1008** (2010) 083, [arXiv:1007.2982](#) [[hep-th](#)].
- [80] N. Lambert, C. Papageorgakis, and M. Schmidt-Sommerfeld, “M5-Branes, D4-Branes and Quantum 5D super-Yang-Mills,” *JHEP* **1101** (2011) 083, [arXiv:1012.2882](#) [[hep-th](#)].
- [81] M. R. Douglas, “On  $D=5$  super Yang-Mills theory and (2,0) theory,” *JHEP* **1102** (2011) 011, [arXiv:1012.2880](#) [[hep-th](#)].
- [82] H. Singh, “Super-Yang-Mills and M5-branes,” *JHEP* **1108** (2011) 136, [arXiv:1107.3408](#) [[hep-th](#)].
- [83] N. Lambert and P. Richmond, “(2,0) Supersymmetry and the Light-Cone Description of M5-branes,” *JHEP* **1202** (2012) 013, [arXiv:1109.6454](#) [[hep-th](#)].
- [84] N. Lambert, C. Papageorgakis, and M. Schmidt-Sommerfeld, “Deconstructing (2,0) Proposals,” *Phys.Rev.* **D88** (2013) 026007, [arXiv:1212.3337](#).
- [85] P.-M. Ho, K.-W. Huang, and Y. Matsuo, “A Non-Abelian Self-Dual Gauge Theory in 5+1 Dimensions,” *JHEP* **1107** (2011) 021, [arXiv:1104.4040](#) [[hep-th](#)].
- [86] K.-W. Huang, “Non-Abelian Chiral 2-Form and M5-Branes,” [arXiv:1206.3983](#) [[hep-th](#)].
- [87] C.-S. Chu and S.-L. Ko, “Non-abelian Action for Multiple Five-Branes with Self-Dual Tensors,” *JHEP* **1205** (2012) 028, [arXiv:1203.4224](#) [[hep-th](#)].

- [88] F. Bonetti, T. W. Grimm, and S. Hohenegger, “A Kaluza-Klein inspired action for chiral p-forms and their anomalies,” *Phys.Lett.* **B720** (2013) 424–427, [arXiv:1206.1600 \[hep-th\]](#).
- [89] F. Bonetti, T. W. Grimm, and S. Hohenegger, “Non-Abelian Tensor Towers and (2,0) Superconformal Theories,” *JHEP* **1305** (2013) 129, [arXiv:1209.3017 \[hep-th\]](#).
- [90] H. Singh, “The Yang-Mills and chiral fields in six dimensions,” *JHEP* **1302** (2013) 056, [arXiv:1211.3281 \[hep-th\]](#).
- [91] H.-C. Kim and K. Lee, “Supersymmetric M5 Brane Theories on  $R \times CP^2$ ,” *JHEP* **1307** (2013) 072, [arXiv:1210.0853 \[hep-th\]](#).
- [92] D. Fiorenza, H. Sati, and U. Schreiber, “Multiple M5-branes, String 2-connections, and 7d nonabelian Chern-Simons theory,” [arXiv:1201.5277 \[hep-th\]](#).
- [93] C. Saemann and M. Wolf, “Non-Abelian Tensor Multiplet Equations from Twistor Space,” [arXiv:1205.3108 \[hep-th\]](#).
- [94] C. Saemann, “M-Brane Models and Loop Spaces,” *Mod.Phys.Lett.* **A27** (2012) 1230019, [arXiv:1206.0432 \[hep-th\]](#).
- [95] S. Palmer and C. Saemann, “M-brane Models from Non-Abelian Gerbes,” *JHEP* **1207** (2012) 010, [arXiv:1203.5757 \[hep-th\]](#).
- [96] C. Saemann and M. Wolf, “Six-Dimensional Superconformal Field Theories from Principal 3-Bundles over Twistor Space,” [arXiv:1305.4870 \[hep-th\]](#).
- [97] C.-S. Chu and H. Isono, “Instanton String and M-Wave in Multiple M5-Branes System,” [arXiv:1305.6808 \[hep-th\]](#).
- [98] O. Aharony, K. Peeters, J. Sonnenschein, and M. Zamaklar, “Rho meson condensation at finite isospin chemical potential in a holographic model for QCD,” *JHEP* **0802** (2008) 071, [arXiv:0709.3948 \[hep-th\]](#).
- [99] S. P. Kumar, “Spinning flavour branes and fermion pairing instabilities,” *Phys.Rev.* **D84** (2011) 026003, [arXiv:1104.1405 \[hep-th\]](#).
- [100] S. Kobayashi, D. Mateos, S. Matsuura, R. C. Myers, and R. M. Thomson, “Holographic phase transitions at finite baryon density,” *JHEP* **0702** (2007) 016, [arXiv:hep-th/0611099 \[hep-th\]](#).

- [101] M. Ammon, J. Erdmenger, M. Kaminski, and P. Kerner, “Flavor Superconductivity from Gauge/Gravity Duality,” *JHEP* **0910** (2009) 067, [arXiv:0903.1864 \[hep-th\]](#).
- [102] M. Kruczenski, D. Mateos, R. C. Myers, and D. J. Winters, “Meson spectroscopy in AdS / CFT with flavor,” *JHEP* **0307** (2003) 049, [arXiv:hep-th/0304032 \[hep-th\]](#).
- [103] M. Ammon, J. Erdmenger, M. Kaminski, and P. Kerner, “Superconductivity from gauge/gravity duality with flavor,” *Phys.Lett.* **B680** (2009) 516–520, [arXiv:0810.2316 \[hep-th\]](#).
- [104] J. Erdmenger, M. Kaminski, P. Kerner, and F. Rust, “Finite baryon and isospin chemical potential in AdS/CFT with flavor,” *JHEP* **0811** (2008) 031, [arXiv:0807.2663 \[hep-th\]](#).
- [105] K. Peeters, J. Powell, and M. Zamaklar, “Exploring colourful holographic superconductors,” *JHEP* **0909** (2009) 101, [arXiv:0907.1508 \[hep-th\]](#).
- [106] S. A. Hartnoll, C. P. Herzog, and G. T. Horowitz, “Building a Holographic Superconductor,” *Phys.Rev.Lett.* **101** (2008) 031601, [arXiv:0803.3295 \[hep-th\]](#).
- [107] I. Amado, D. Arean, A. Jimenez-Alba, K. Landsteiner, L. Melgar, *et al.*, “Holographic Type II Goldstone bosons,” *JHEP* **1307** (2013) 108, [arXiv:1302.5641 \[hep-th\]](#).
- [108] V. Gusynin, V. Miransky, and I. Shovkovy, “Catalysis of dynamical flavor symmetry breaking by a magnetic field in (2+1)-dimensions,” *Phys.Rev.Lett.* **73** (1994) 3499–3502, [arXiv:hep-ph/9405262 \[hep-ph\]](#).
- [109] V. Gusynin, V. Miransky, and I. Shovkovy, “Dimensional reduction and dynamical chiral symmetry breaking by a magnetic field in (3+1)-dimensions,” *Phys.Lett.* **B349** (1995) 477–483, [arXiv:hep-ph/9412257 \[hep-ph\]](#).
- [110] I. A. Shovkovy, “Magnetic Catalysis: A Review,” *Lect.Notes Phys.* **871** (2013) 13–49, [arXiv:1207.5081 \[hep-ph\]](#).
- [111] V. G. Filev, C. V. Johnson, R. Rashkov, and K. Viswanathan, “Flavoured large N gauge theory in an external magnetic field,” *JHEP* **0710** (2007) 019, [arXiv:hep-th/0701001 \[hep-th\]](#).

- [112] V. G. Filev and M. Ihl, “Flavoured Large N Gauge Theory on a Compact Space with an External Magnetic Field,” *JHEP* **1301** (2013) 130, [arXiv:1211.1164](#) [[hep-th](#)].
- [113] K. Skenderis and M. Taylor, “Branes in AdS and p p wave space-times,” *JHEP* **0206** (2002) 025, [arXiv:hep-th/0204054](#) [[hep-th](#)].
- [114] N. Manton and P. Sutcliffe, *Topological solitons*. Cambridge University Press, 2004.
- [115] C.-H. Chen, K. Furuuchi, P.-M. Ho, and T. Takimi, “More on the Nambu-Poisson M5-brane Theory: Scaling limit, background independence and an all order solution to the Seiberg-Witten map,” *JHEP* **1010** (2010) 100, [arXiv:1006.5291](#) [[hep-th](#)].
- [116] N. Seiberg and E. Witten, “String theory and noncommutative geometry,” *JHEP* **9909** (1999) 032, [arXiv:hep-th/9908142](#) [[hep-th](#)].
- [117] G. Bossard and H. Nicolai, “Counterterms vs. Dualities,” *JHEP* **1108** (2011) 074, [arXiv:1105.1273](#) [[hep-th](#)].
- [118] P. Pasti, D. Sorokin, and M. Tonin, “Covariant actions for models with non-linear twisted self-duality,” *Phys.Rev.* **D86** (2012) 045013, [arXiv:1205.4243](#) [[hep-th](#)].
- [119] P. Pasti, I. Samsonov, D. Sorokin, and M. Tonin, “BLG-motivated Lagrangian formulation for the chiral two-form gauge field in D=6 and M5-branes,” *Phys.Rev.* **D80** (2009) 086008, [arXiv:0907.4596](#) [[hep-th](#)].
- [120] M. K. Gaillard and B. Zumino, “Duality Rotations for Interacting Fields,” *Nucl.Phys.* **B193** (1981) 221.
- [121] G. Gibbons and D. Rasheed, “Electric - magnetic duality rotations in nonlinear electrodynamics,” *Nucl.Phys.* **B454** (1995) 185–206, [arXiv:hep-th/9506035](#) [[hep-th](#)].
- [122] P. S. Howe, E. Sezgin, and P. C. West, “Covariant field equations of the M theory five-brane,” *Phys.Lett.* **B399** (1997) 49–59, [arXiv:hep-th/9702008](#) [[hep-th](#)].
- [123] P. S. Howe, N. Lambert, and P. C. West, “The Selfdual string soliton,” *Nucl.Phys.* **B515** (1998) 203–216, [arXiv:hep-th/9709014](#) [[hep-th](#)].

- [124] I. A. Bandos and P. K. Townsend, “Light-cone M5 and multiple M2-branes,” *Class.Quant.Grav.* **25** (2008) 245003, arXiv:0806.4777 [hep-th].
- [125] E. Bergshoeff, D. Berman, J. van der Schaar, and P. Sundell, “A Noncommutative M theory five-brane,” *Nucl.Phys.* **B590** (2000) 173–197, arXiv:hep-th/0005026 [hep-th].
- [126] E. Witten, “Nonperturbative superpotentials in string theory,” *Nucl.Phys.* **B474** (1996) 343–360, arXiv:hep-th/9604030 [hep-th].
- [127] R. Kallosh and D. Sorokin, “Dirac action on M5 and M2 branes with bulk fluxes,” *JHEP* **0505** (2005) 005, arXiv:hep-th/0501081 [hep-th].
- [128] L. Anguelova and K. Zoubos, “Five-brane Instantons vs Flux-induced Gauging of Isometries,” *JHEP* **0610** (2006) 071, arXiv:hep-th/0606271 [hep-th].
- [129] D. Tsimpis, “Fivebrane instantons and Calabi-Yau fourfolds with flux,” *JHEP* **0703** (2007) 099, arXiv:hep-th/0701287 [hep-th].
- [130] M. Kerstan and T. Weigand, “Fluxed M5-instantons in F-theory,” *Nucl.Phys.* **B864** (2012) 597–639, arXiv:1205.4720 [hep-th].
- [131] M. Bianchi, G. Inverso, and L. Martucci, “Brane instantons and fluxes in F-theory,” *JHEP* **1307** (2013) 037, arXiv:1212.0024 [hep-th].
- [132] C.-S. Chu and D. J. Smith, “Multiple Self-Dual Strings on M5-Branes,” *JHEP* **1001** (2010) 001, arXiv:0909.2333 [hep-th].
- [133] C.-S. Chu, “A Theory of Non-Abelian Tensor Gauge Field with Non-Abelian Gauge Symmetry  $G \times G$ ,” arXiv:1108.5131 [hep-th].
- [134] Y. M. Shnir, *Magnetic Monopoles*. Springer, 2005.
- [135] H. Samtleben, E. Sezgin, and R. Wimmer, “(1,0) superconformal models in six dimensions,” *JHEP* **1112** (2011) 062, arXiv:1108.4060 [hep-th].
- [136] H. Samtleben, E. Sezgin, R. Wimmer, and L. Wulff, “New superconformal models in six dimensions: Gauge group and representation structure,” *PoS CORFU2011* (2011) 071, arXiv:1204.0542 [hep-th].
- [137] G. ’t Hooft, “Magnetic Monopoles in Unified Gauge Theories,” *Nucl.Phys.* **B79** (1974) 276–284.

- [138] A. M. Polyakov, “Particle Spectrum in the Quantum Field Theory,” *JETP Lett.* **20** (1974) 194–195.
- [139] B. Chen, H. Itoyama, and H. Kihara, “NonAbelian Berry phase, Yang-Mills instanton and  $USp(2k)$  matrix model,” *Mod.Phys.Lett.* **A14** (1999) 869–879, [arXiv:hep-th/9810237](#) [hep-th].
- [140] B. Chen, H. Itoyama, and H. Kihara, “NonAbelian monopoles from matrices: Seeds of the space-time structure,” *Nucl.Phys.* **B577** (2000) 23–46, [arXiv:hep-th/9909075](#) [hep-th].
- [141] C. Pedder, J. Sonner, and D. Tong, “The Geometric Phase and Gravitational Precession of D-Branes,” *Phys.Rev.* **D76** (2007) 126014, [arXiv:0709.2136](#) [hep-th].
- [142] V. L. Campos, G. Ferretti, and P. Salomonson, “The NonAbelian self dual string on the light cone,” *JHEP* **0012** (2000) 011, [arXiv:hep-th/0011271](#) [hep-th].
- [143] E. Corrigan and D. I. Olive, “Color and Magnetic Monopoles,” *Nucl.Phys.* **B110** (1976) 237.
- [144] V. Niarchos and K. Siampos, “M2-M5 blackfold funnels,” *JHEP* **1206** (2012) 175, [arXiv:1205.1535](#) [hep-th].
- [145] V. Niarchos and K. Siampos, “The black M2-M5 ring intersection spins,” *PoS Corfu2012* (2013) 088, [arXiv:1302.0854](#) [hep-th].
- [146] C.-S. Chu and D. J. Smith, “Towards the Quantum Geometry of the M5-brane in a Constant C-Field from Multiple Membranes,” *JHEP* **0904** (2009) 097, [arXiv:0901.1847](#) [hep-th].
- [147] C.-S. Chu and G. S. Sehmbi, “D1-Strings in Large RR 3-Form Flux, Quantum Nambu Geometry and M5-Branes in C-Field,” *J.Phys.* **A45** (2012) 055401, [arXiv:1110.2687](#) [hep-th].
- [148] I. R. Klebanov and A. A. Tseytlin, “Entropy of near extremal black p-branes,” *Nucl.Phys.* **B475** (1996) 164–178, [arXiv:hep-th/9604089](#) [hep-th].
- [149] S. Bolognesi and K. Lee, “1/4 BPS String Junctions and  $N^3$  Problem in 6-dim (2,0) Superconformal Theories,” *Phys.Rev.* **D84** (2011) 126018, [arXiv:1105.5073](#) [hep-th].

- 
- [150] H.-C. Kim, S. Kim, E. Koh, K. Lee, and S. Lee, “On instantons as Kaluza-Klein modes of M5-branes,” *JHEP* **1112** (2011) 031, [arXiv:1110.2175 \[hep-th\]](#).
- [151] T. Maxfield and S. Sethi, “The Conformal Anomaly of M5-Branes,” *JHEP* **1206** (2012) 075, [arXiv:1204.2002 \[hep-th\]](#).
- [152] C.-S. Chu, “Non-Abelian Self-Dual Strings in Six Dimensions from Four Dimensional 1/2-BPS Monopoles,” [arXiv:1310.7710 \[hep-th\]](#).